

**The role of ligand processing in
neuromedin U receptor signalling and
regulation.**

Thesis submitted for the degree of Doctor of Philosophy

At the University of Leicester

By

Omar Bahattab

Department of Cell Physiology and Pharmacology

University of Leicester

September 2015

The role of ligand processing in neuromedin U receptor signalling and regulation

The neuromedin U (NmU) and neuromedin S (NmS), neuropeptides, from various species share the greatest homology in their C-terminal regions. Both NmU and NmS share the seven residues located in the C terminus of their sequence, including the amidation of the C-terminal amino acids. Two family A G protein-coupled receptors have been identified for these peptides; NMU1 and NMU2. Both receptors have high affinity for both ligands but the differential expression of receptors and ligands may dictate what they do. Both receptors can signal through $G\alpha_{q/11}$ and $G\alpha_{i/o}$, leading to increases in intracellular $[Ca^{2+}]_i$ and pertussis toxin-sensitive inhibition of adenylyl cyclase activity, respectively. Data presented here demonstrate that following desensitisation of NMU2, re-sensitisation is dependent on receptor internalisation, endosomal acidification and receptor recycling. Re-sensitisation is also dependent on endothelin converting enzyme-1 (ECE-1) activity, most likely through proteolysis of NmU in endosomes, which may facilitate disassociation of receptor- β -arrestin complexes resulting in NMU2 recycling and re-sensitisation. In addition to Ca^{2+} release, NMUs activate extracellular signal-regulated kinase (ERK) and it is possible that this may involve a number of different mechanisms. This study shows that human (h) NmU-25 and hNmS-33 evoke time- and concentration-dependent activation of ERK by NMU2. In experiments in which the free ligand was removed following a 5 minute stimulation, hNmS-33 provoked prolonged activation of ERK whereas ERK activation returned to basal level following hNmU-25. In these experiments, the ECE-1 inhibitor, SM19712, prolonged ERK activation following hNmU. Knockdown of either β -arrestin-1 or -2 with siRNA and, in particular, combined isoformic knockdown reduced re-sensitisation of Ca^{2+} signalling by NMU2 following desensitisation with either ligand. Knockdown of β -arrestins-1 and -2 individually or in combination significantly enhanced and extended the duration of NmU-mediated ERK activation, but had a much more limited impact on hNmS-33-mediated ERK activation. The current study indicates that ERK is likely regulated by G-protein-dependent mechanisms, mainly through $G\alpha_q$, with little evidence for a role for G-protein-independent mechanisms.

ACKNOWLEDGEMENTS

I would like to express my special appreciation and thanks to my supervisor **Dr. Gary Willars**, you have been a tremendous mentor for me. I would like to thank you for encouraging my research and for allowing me to grow as a research scientist. Your advice on research has been invaluable. I would also like to thank my second supervisor, **Professor John Challiss**. I also want to thank you for letting my defence be enjoyable, and for your brilliant comments and suggestions, thanks to you.

A special thanks to my committee member, **Dr John Mitcheson** for serving as my committee member even in hardship. I would especially like to thank the technical support and other support staff at the University of Leicester. All of you have been there to support me during my research. Also, thanks to the Protein Nucleic Acid Chemistry Laboratory (PNACL) mass spectrometry facility at the University of Leicester, in particular **Dr. Andrew Bottrill & Sharad Mistry**. I am also very grateful for the support of the Advanced Imaging Facility from **Dr. Kees Straatman** (Centre for Core Biotechnology Services, University of Leicester).

A special thanks to my family. Words cannot express how grateful I am to my father, wife, daughters, brothers and sisters for all of the sacrifices that you have made on my behalf. Your prayer for me was what sustained me thus far. Thank you for supporting me for everything, and especially I cannot thank you enough for encouraging me throughout this experience. To my beloved daughters **Jana** and **Nour**, I would like to express my thanks for being such good girls and always cheering me up.

I would also like to extend my thanks to **Dr. Khaled Alhosaini** and **Dr. Jing Lu** for their support during my journey.

*This thesis is
dedicated to my
mother's soul.*

Omar

ABBREVIATIONS

[Ca²⁺]_i	Intracellular calcium concentration
7TM	Seven transmembrane
7TMRs	Seven transmembrane receptors
AC	Adenylyl cyclase
ACTH	Adrenocorticotrophic hormone
ADAM	A disintegrin and metalloproteinase domain-containing protein
ALL	Acute lymphatic leukaemia
AML	Acute myeloid leukaemia
AP-2	Adaptor protein-2
APS	Ammonium persulphate
ARC	Arcuate nucleus
ATP	Adenosine triphosphate
BBB	Blood-brain-barrier
BiFC	Bimolecular fluorescence complementation
BRET	Bioluminescence resonance energy transfer
BSA	Bovine serum albumin
cAMP	Adenosine cyclic-3',5'-monophosphate
CCE	Capacitative Ca ²⁺ entry
Cch	Carbachol
CCK4	Cholecystokinin tetrapeptide
CCPs	Clathrin-coated pits
CCVs	Clathrin-coated vesicles
CCX-CKR	High affinity receptor for the chemokines
cDNA	Complementary DNA
CHO	Chinese hamster ovary
cNmU-25	Chicken NmU-25
cNmU-9	Chicken NmU-9
CNS	Central nervous system
CRAC	Ca ²⁺ release-activating Ca ²⁺ channel
CRH	Corticotrophin-releasing hormone
C-terminal	Carboxy-terminal
Cy3B-pNmU-8	pNmU-8 fluorescently-tagged at <i>N</i> -terminal with Cy3B
DAG	Diacylglycerol
ddH₂O	Double-distilled water
DGK	Diacylglycerol kinase
DIO	Diet-induced obesity
DMEM	Dulbecco's modified Eagle's medium
DMSO	Dimethyl sulphoxide

DNA	Deoxyribonucleic acid
dNmU-25	Dog NmU-25
dNmU-8	Dog NmU-8
dNTPs	Deoxyribonucleotide triphosphate
D-PBS	Dulbecco`s phosphate-buffered saline
DTT	Dithiothreitol
EC₅₀	Concentration given 50% of the maximal response
ECE-1	Endothelin-converting enzyme 1
ECL	Enhanced chemiluminescence
ECL	Electrochemiluminescent
EDTA	Ethylenediaminetetraacetic acid
EFC	Enzyme fragment complementation
EGF	Epidermal growth factor
eGFP	Enhanced green fluorescent protein
EGFR	Epidermal growth factor receptor
EPAC	Exchange protein activated by cAMP
ERK	Extracellular signal-regulated kinase
ET_A	Endothelin A receptor
FBS	Fetal bovine serum
Fluo-4-AM	Fluo-4-acetoxymethylester
FM-3	Previous name of neuromedin U receptor type-1
FM-4	Previous name of neuromedin U receptor type-2
Fmoc	Fluorenylmethyloxycarbonyl
fNmU-17	Frog NmU-17
fNmU-23	Frog NmU-23
fNmU-25	Frog NmU-25
G protein	Heterotrimeric guanine nucleotide-binding protein
GABA_B	Gamma-aminobutyric acid receptor type B
GAP	GTPase-activating protein
GDP	Guanosine diphosphate
GEF	Guanine-nucleotide exchange factor
gfNmU-21	Goldfish NmU-21
gfNmU-25	Goldfish NmU-25
gfNmU-38	Goldfish NmU-38
GIT	Gastrointestinal tract
GLP-1	Glucagon-like peptide 1
GPCR	G protein-coupled receptor
gpNmU-9	Guinea pig NmU-9
GRK	G protein-coupled receptor kinase
GTP	Guanosine triphosphate
H2r	Histamine H2 receptor
HB-EGF	Heparin-binding EGF-like growth factor
HEK293	Human embryonic kidney 293 cell lines
HEK-NMU1	HEK 293 cells stably expressing NMU1
HEK-NMU1-eGFP	HEK 293 cells stably expressing C-terminal eGFP-tagged NMU1
HEK-NMU2	HEK 293 cells stably expressing NMU2

HEK-NMU2-eGFP	HEK 293 cells stably expressing C-terminal eGFP-tagged NMU2
hNmS-33	Human NmS-33
hNmU-25	Human NmU-25
HPLC	High-performance liquid chromatography
HRP	Horseradish peroxidase
I3	Third intracellular loop
IBMX	Isobutylmethylxanthine
ICC	Immunocytochemistry
ICV	Intracerebroventricular
IL	Interleukin
InsP_x	Inositol (poly)phosphate
IP₃	Inositol 1,4,5-trisphosphate
IV	Intravenous
JqNmU-25	Japanese quail NmU-25
K_d	Dissociation constant
KHB	Krebs-HEPES buffer
KIR2DL1	Killer cell immunoglobulin-like receptor 2DL1
KO	Knockout
LPARs	Lysophosphatidic acid receptors
MAPK	Mitogen-activated protein kinase
MEM	Minimum essential medium
MES	2-(<i>N</i> -morpholino) ethane sulfonic acid
mNmS-36	Mouse NmS-36
mRNA	Messenger RNA
NGF	Nerve growth factor
NK cells	Natural killer cells
NK1	Neurokinin 1 receptor
NmS	Neuromedin S
NmU	Neuromedin U
NMU1	Neuromedin U receptor subtype-1
NMU1-eGFP	Neuromedin U receptor subtype-1 C-terminus tagged with eGFP
NMU2	Neuromedin U receptor subtype-2
NMU2-eGFP	Neuromedin U receptor subtype-2 C-terminus tagged with eGFP
NmU-LI	NmU-like immunoreactivity
NMUR1	NMU1 gene
NMUR2	NMU2 gene
NSCLC cells	Non-small lung cancer cells
<i>N</i>-terminal	Amino-terminal
NTS	Nucleus tractus solitarius
OA	Okadaic acid
PAGE	Polyacrylamide gel electrophoresis
PC	Prostate cancer
PDBu	Phorbol 12,13-dibutyrate
PDGFR	Platelet-derived growth factor receptors

pEC₅₀	Negative logarithm of the concentration given 50% of the maximal response
pERK	Phosphorylated extracellular signal-regulated kinase
PIP₂	Phosphatidylinositol-4,5-bisphosphate
PKA	Protein kinase A
PKC	Protein kinase C
PLC	Phospholipase C
PLCβ	Phospholipase Cβ
pNmU-25	Porcine NmU-25
pNmU-8	Porcine NmU-8
PP	Protein phosphatase
PP2A	Protein phosphatase type 2A
PTH	Parathyroid hormone
PTH1R	Parathyroid hormone receptor, subtype 1
PTX	Pertussis toxin
PVDF	Polyvinylidene difluoride
PVN	Paraventricular nucleus
PYK2	Protein kinase tyrosine
RAMP1	Receptor activity-modifying protein 1
rbNmU-25	Rabbit NmU-25
RER	Rough endoplasmic reticulum
RLU	Relative light unit
RNA	Ribonucleic acid
rNmS-36	Rat NmS-36
rNmU-23	Rat NmU-23
ROCK	Rho-kinase
R-PSOP	(R)5'(phenylaminocarbonylamino)spiro[1-azabicyclo[2.2.2]octane-3,2'(3'H)-furo[2,3-b]pyridine]
RT	Room temperature
S1P1	Sphingosine-1-phosphate receptor 1
S6	Ribosomal Protein S6
SAR	Structure-activity relationship
SCN	Suprachiasmatic nucleus
SDS	Sodium dodecyl sulfate
SERCA	Sarcoplasmic/endoplasmic reticulum Ca ²⁺ -ATPase
siRNA	Small/short interfering RNA
SM-19712	Selective ECE-1 inhibitor v(4-chloro-N-[(4-cyano-3methyl-1-phenyl-1H-pyrazol-5-yl)amino]carbonyl] benzensulfateonamide, monosodium salt)
SOS	Son of Sevenless
SPPS	Solid-phase peptide synthesis
STIM1	Stromal interaction molecule 1
TBST	Tris buffered saline with Tween 20
TCA	Trichloroacetic acid
TEMED	N, N, N', N'-tetramethylethylenediamine
tERK	Total extracellular signal-regulated kinase
tNmS-17	Toad NmS-17

tNmS-33	Toad NmS-33
TRPC	Transient receptor potential cation channels
TSHR	Thyrotropin receptor
UTP	Uridine-5`-triphopshate
V2R	Vasopressin V2 receptor

PRESENTATIONS AND PUBLICATIONS

Bahattab, O., Al-Hosaini K, Challiss RAJ., and Willars, G.B. Ligand-dependent temporal patterns of ERK activation and re-sensitisation of Ca²⁺ signalling at the type 2 neuromedin U (NMU2) receptor. 5th BPS Focused Meeting on Cell Signalling, 28 – 29 April 2014, University of Leicester, UK. Poster presentation.

Bahattab, O., Al-Hosaini K, Challiss RAJ., and Willars, G.B. Role of β -arrestins 1&2 in the re-sensitisation and ERK signalling of NMU2. Gordon Research Conference on Molecular Pharmacology, February 1-6, 2015, Ventura, CA, USA. Poster presentation.

Micewicz ED, **Bahattab OS**, Willars GB, Waring AJ, Navab M, Whitelegge JP, *et al.* (2015). Small lipidated anti-obesity compounds derived from neuromedin U. *European Journal of Medicinal Chemistry* 101: 616-626.

Table of contents

ABSTRACT	i
ACKNOWLEDGEMENTS	ii
ABBREVIATIONS	iv
PRESENTATIONS AND PUBLICATIONS	ix
Table of contents	x
CHAPTER 1	1
1.1 Neuropeptides and neurotransmitters	1
1.2 Neuromedins	3
1.2.1 Introduction	3
1.2.2 Structure and functions	4
1.2.3 NmU and NmS distribution	6
1.2.4 Physiological roles of neuromedin U and S.....	8
1.3 Discovery and characterisation of receptors for NmU	12
1.3.1 Background	12
1.3.2 Structural characteristics of NMUs	13
1.3.3 The distribution of NMUs.....	17
1.4 G protein-coupled receptors (GPCRs)	20
1.4.1 Activation and termination of signalling by G proteins	21
1.4.2 Phosphorylation and desensitization of GPCR.....	26
1.4.3 Internalization and trafficking of GPCR.....	28
1.4.4 The role of β -arrestins in the termination and transduction of GPCRs signals.....	29
1.4.5 GPCRs dephosphorylation.....	32
1.5 Ligand-receptor pseudo-irreversible binding and dual coupling of NMUs in recombinant systems	34
1.6 Endothelin-converting-enzyme: structure, function and potential role in endosomal ligand processing	38
1.6.1 Background	38
1.6.2 Structure	39
1.6.3 Functions and potential roles of ECE-1 in endosomal ligand processing	41
1.7 GPCR-Activated ERK signalling pathways	45

1.7.1 G-protein-dependent pathway	48
1.7.1.1 $G\alpha_s$ stimulation of ERK1/2	48
1.7.1.2 $G\alpha_i$ stimulation of ERK1/2.....	50
1.7.1.3 $G\beta\gamma_i$ stimulation of ERK1/2	52
1.7.1.4 $G\alpha_q$ stimulation of ERK1/2.....	52
1.7.1.5 $G\alpha_{12/13}$ inhibition of ERK.....	53
1.7.1.6 Receptor tyrosine kinases in G-protein-mediated activation of ERK1/2	55
1.7.2 G-protein-independent, β -arrestin-dependent pathways of ERK activation.....	58
1.8 Aims and objectives.....	60
Chapter 2	61
Materials & Methods	61
2.1 Materials	61
2.1.1 Materials (cell culture, and peptides)	61
2.1.2 Concentrations of inhibitors, chemicals and antibodies used	63
2.1.3 Buffer used to study NmU-mediated signalling.....	64
2.2 Methods	65
2.2.1 Cell culture	65
2.2.2 Preparing frozen cell stocks	65
2.2.3 Recovery of frozen cells	66
2.2.4 Ca^{2+} signalling measurement using a NOVOstar plate-reader producing concentration response curve.....	66
2.2.5 Data Analysis	67
2.2.6 NMU re-sensitization protocol.....	68
2.3 Western blotting	69
2.3.1 Cell stimulation and sample preparation.....	69
2.3.2 Preparation of SDS-polyacrylamide gel and electrophoresis of proteins	69
2.3.3 Transfer of proteins using the semi-dry electrophoresis technique.....	70
2.3.4 Immunoblotting	70
2.4 Live/Dead viability/cytotoxicity kit for mammalian cells (Fluorescence Microscopy Protocol)	71
2.5 Protein digestion, analysis by mass spectrometry and data processing.....	72
2.6 β-arrestins and ECE-1 knockdown and transfection.....	73
2.7 Immunostaining	74
2.7.1 Sample preparation.....	74

2.7.2 ERK activation and distribution using immunocytochemistry approach, detection and analysis.....	75
2.8 Confocal imaging and binding of Cy3B-pNmU-8 to NMU2-eGFP and visualisation of receptor internalization.....	75
2.9 PathHunter express β-Arrestin Human and Ortholog GPCR kits:	76
2.9.1 Technology principle:	76
2.9.2 Thawing and plating frozen cells.....	78
2.9.3 Agonist compound preparation and addition.....	78
2.9.4 Preparation of 12-point concentration response curve	78
2.9.5 Substrate preparation and addition.....	78
2.10 hNmU-25 degradation by ECE-1 using recombinant human ECE-1.....	79
2.11 Bioassay approach	79
Chapter 3	80
NMU regulation: desensitisation, internalisation and re-sensitisation	80
3.1 Introduction	80
3.2 Results.....	83
3.2.1 NMU receptor-mediated Ca^{2+} : a comparison of natural ligands	83
3.2.2 NMU receptor desensitization, internalization & re-sensitization	88
3.2.3 Do protein phosphatase or protein kinase C activities play a role in re-sensitization of NMU2?	101
3.2.4 Effects of the ECE-1 inhibitor, SM-19712, on the recovery of NMU2-mediated Ca^{2+} signalling	104
3.2.5 Further characterization of effects of the ECE-1 inhibitor, SM-19712, on NMU2 re-sensitization	109
3.2.6 Is hNmU-25 degraded extracellularly by ECE-1?.....	116
3.2.7 Endothelin-converting enzyme-1 degrades neuromedin U.....	118
3.3 Discussion	131
Chapter 4	146
NMU2-regulated ERK activation	146
4.1 Background	146
4.1.1 Activation of ERK by NMU2.....	146
4.1.2 The role of endosomal acidification and ECE-1 activity in the regulation of NMU2-mediated ERK activity	146
4.1.3 The potential role of β -arrestins in NMU2 re-sensitization	148
4.2 Results.....	150

4.2.1 NMU2-mediated activation of ERK	150
4.2.2 pERK perhaps depends on ongoing activation of NMU2 in the presence of NmS but not NmU	154
4.2.3 Inhibition of endosomal acidification enhances ERK activity following hNmU-25, hNmS-33 and pNmU-8	156
4.2.4 Inhibition of ECE-1 activity enhances ERK activity following hNmU-25 but neither hNmS-33 nor pNmU-8.....	159
4.2.5 The role of arrestin in NMU receptor-mediated ERK responses	165
4.2.6 The role of β -arrestin-1 and -2 in re-sensitization of NMU2-mediated signalling.....	173
4.2.7 Arrestin recruitment by activated NMU receptors	180
4.3 Discussion	182
Chapter 5	189
Further investigation of signalling responsible for NMU2-mediated ERK activation	189
5.1 Background	189
5.1.1 Introduction	189
5.1.2 The detection of ERK activation and distribution	191
5.1.3 The role of β -arrestins-1 and -2 in ERK activation	192
5.2 Results.....	193
5.2.1 Investigating the role of PKC in ERK activation	193
5.2.2 The role of $G_{\alpha i}$ in the activation of ERK	196
5.2.3 Does transactivation of RTKs play a role in NMU2-mediated ERK activation?.....	200
5.2.4 Activation of ERK is dependent on $G_{\alpha q}$ subunit	203
5.2.5 Sub-cellular localization of pERK following agonist activation of NMU2 using different ligands	211
5.3 Discussion	222
Chapter 6	229
Neuromedin U analogues	229
6.1 Introduction.....	229
6.2 Results.....	232
6.2.1 Concentration-response curves for analogues-mediated Ca^{2+} elevation in	232
HEK-NMU1 and HEK-NMU2	232
6.2.2 Effect of endosomal acidification and ECE-1 on NMU2 re-sensitization following treatment with the analogues NM1 or NM2	242
6.2.3 Assessment of the potential antagonist activity of NmU analogues	248

6.2.4 Arrestin recruitment to NMU receptors activated by NmU analogues.....	250
6.3 Discussion	252
Future directions and considerations	261

1.1 Neuropeptides and neurotransmitters

Different chemical substances regulating different physiological processes such as locomotion, metabolism, homeostasis, reproduction and growth in multicellular organisms mainly perform signal transmission between neurons in the nervous system. These substances include neuropeptides and various types of neurotransmitters. Neuropeptides are produced by enzymatic cleavage of a precursor protein in order to make fragments that are active peptides specific for one or more GPCRs.

Neuropeptides are the largest and most diverse class of signalling molecules in the brain. They can act as neurotransmitters, as modulators of ongoing neurotransmission by other transmitters, as autocrine or paracrine regulators in a close cellular environment, and as hormones on long range. Many attempts have been made in order to define the neurotransmitters. Based on different concepts including that peptide hormones are chemical signals in the endocrine system, neurosecretion of peptides is a general principle in the nervous system; and the nervous system is responsive to peptide signals, neuropeptides can be defined as they are small proteinaceous substances produced and released by neurons through the regulated secretory route and acting on neural substrates (Klavdieva, 1996).

Neuropeptides production occurs within the ribosomes in the neuronal cell body. Gene transcription in the nucleus leads ultimately to the synthesis of a precursor protein, a pre-propeptide, in the rough endoplasmic reticulum (RER). The pre-propeptide is then transported to the Golgi apparatus where it is further modified and packaged into large dense-core vesicles (100-200 nm in diameter). The mature peptide in vesicles is then transported along the microtubules by motor proteins towards the pre-synaptic terminal and vesicles are stored in preparation for release. If an action potential reaches the pre-synaptic terminal, voltage gated calcium channels are opened resulting in an influx of

$[Ca^{2+}]_i$. The rise of cytosolic Ca^{2+} triggers fusion between the vesicle membrane and the plasma membrane of the pre-synaptic neuron and causes release of neuropeptide. The neuropeptide then binds to a receptor on the post-synaptic neuron and causes a postsynaptic effect that can be either an excitatory or inhibitory, but more common a modulatory effect in the CNS (Nassel, 2002). On the other hand, neurotransmitters are synthesized and packaged into small synaptic vesicles (50 nm in diameter) within the pre-synaptic terminal. One or more biosynthetic enzymes are required for production of the mature neurotransmitter. Moreover, removal of a neurotransmitter from the synaptic cleft (to remove a signal) is accomplished by uptake into the pre-synaptic terminal or into glial cells via vesicular transporters whereas neuropeptides are removed from the synaptic cleft by enzymatic degradation or diffusion (Nassel, 2002). Neurotransmitters are released from synaptic vesicles in synapses into the synaptic cleft, where they are received by receptors on other synapses.

Neuropeptides can function as neuromodulators when released at a short distance, synaptically or non-synaptically, or they can also act as neurohormones when released at a longer distance into the blood stream (O'Shea *et al.*, 1985; Nassel, 2009).

Neuropeptides play a role in signalling and were discovered in the 1970s by the fact that most hypothalamic signalling molecules were identified as small peptides (Hökfelt *et al.*, 2003). With rare exceptions, all neuropeptide receptors belong to the large family of G protein-coupled receptors (GPCRs). Indeed, they are ligands for about 20% of the GPCRs (Rashid *et al.*, 2004). Neuropeptides have the ability to modulate different activities in the central nervous system such as pain, addiction and depression. In the gastrointestinal tract (GIT), they can regulate absorption, motility, and smooth muscle tone (Hökfelt *et al.*, 2003; Rashid *et al.*, 2004).

In contrast to other smaller signalling molecules such as neurotransmitters, neuropeptides are released, expressed and used by neurons in order to communicate with each other by acting on the cell surface receptors. Moreover, neuropeptides can be present together with one or two neurotransmitters. This can help in synaptic communication as the neurotransmitters affect the excitability of neurons by depolarising or hyperpolarising them (Hökfelt *et al.*, 2003). In addition, neuropeptides are larger than neurotransmitters. They have 3-100 amino acid residues. This allows

them to contain more chemical information and possess several sites for receptor interaction (Hökfelt *et al.*, 2003; Rashid *et al.*, 2004). Therefore, neuropeptides have the ability to bind to receptors with high affinity (pM to nM affinities compared to neurotransmitters that have μ M affinities). Furthermore, neuropeptides are usually broken down by peptidases whereas removing small molecule neurotransmitter action is by reuptake mechanisms with exception of acetylcholine (Ach) that is broken down by acetylcholinesterase (Hökfelt *et al.*, 2003).

1.2 Neuromedins

1.2.1 Introduction

Neuromedin U (NmU) and neuromedin S (NmS) are members of the neuropeptide family known as the neuromedins. NmU was isolated from porcine cord in the early 1980s due to its ability to contract smooth muscle of rat uterus or guinea pig ileum (the suffix U represents the ability to contract uterus smooth muscle) (Kangawa *et al.*, 1983; Minamino *et al.*, 1983; Minamino *et al.*, 1984b; Minamino *et al.*, 1984a; Minamino *et al.*, 1985b; Mori *et al.*, 2005a). However, NmS was isolated in 2005 from rat brain extract and the suffix S given due to its high expression in the suprachiasmatic nucleus (SCN) (Mori *et al.*, 2005). Two GPCRs have been discovered for NmU and NmS termed NMU1 and NMU2 (Alexander *et al.*, 2008; Sharman *et al.*, 2011).

Moreover, there are two porcine versions of NmU showing equipotent contractile effects on strips of rat uterine smooth muscle. They were identified as pNmU-25 and pNmU-8, twenty five and eight amino acid peptides respectively. The number following the peptide relates to the number of amino acids. The generation of the biologically active, pNmU-8, has been suggested by the presence of a dibasic pairing Arg¹⁶ and Arg¹⁷ serving as a proteolytic cleavage site before the last eight C-terminal amino acids (Minamino *et al.*, 1985).

In both rat and man (Lo *et al.*, 1992) (Austin *et al.*, 1995), NmU is synthesized and located within the C-terminus of a 174 amino acid precursor protein. There is 74% homology between rNmU-23 and hNmU-25 and four out of five proteolytic sites in the rat are present in the human version (Brighton *et al.*, 2004a). This therefore

demonstrates evolutionary conservation of the precursor between hNmU-25 and rNmU-23.

NmS has been isolated from different species including human (hNmS-33), rat (rNmS-36) and mouse (mNmS-36) (Mori *et al.*, 2005). It has also been isolated from the dermal venoms of *Eurasian bombinid* toads (tNmS-17 and tNmS-33) (Chen *et al.*, 2006). NmS peptide was clearly detected in the rat brain. On the other hand, it was very difficult to detect it in the spleen and testis compared to NmU. In rat brain, NmS peptide was found in a number of areas including the hypothalamus, midbrain, and pons–medulla oblongata, whereas abundant expression of NmS mRNA was detected only in the hypothalamus. These differences in the distributions of mRNA and peptide indicate that nerve fibers originating from hypothalamic NmS neurons project into the midbrain, pons, or medulla oblongata. Furthermore, abundant expression of type 2 receptor mRNA was detected not only in the hypothalamus, but also in the midbrain and pons–medulla oblongata. These results suggest unknown physiological roles of NmS within this region (Mori *et al.*, 2012).

1.2.2 Structure and functions

NmU has been isolated from different species including rat (rNmU-23) (Domin *et al.*, 1986; Conlon *et al.*, 1988; Minamino *et al.*, 1988), guinea pig (gpNmU-9) (Murphy *et al.*, 1990; O'Harte *et al.*, 1991; Domin *et al.*, 1992), Japanese quail (jqNmU-25) (Shousha *et al.*, 2005), human (hNmU-25) (Austin *et al.*, 1995) and goldfish (gfNmU-21, gfNmU-25 and gfNmU-38) (Maruyama *et al.*, 2008).

Both NmU and NmS are located in separate genes and different chromosomes. NmU in man, for example, is located on chromosome 4q12 whereas NmS is located on chromosome 2q11.2. The amino acid sequence analysis and structure of both NmU and NmS has indicated three important points. These are the conservation of the amino acid sequence particularly at the C-terminus; an amidated C-terminus and variation of N-terminal length. Moreover, the different isoforms of NmU and NmS isolated from mammalian and non-mammalian species reveal a significant level of conservation and

homology (**Figure 1.1**). The C-terminal heptapeptide (FLFRPRN-NH₂) of NmU and NmS is conserved across all mammalian species, playing a fundamental role in their biological activities. The C-terminal five amino acids (FRPRN-NH₂) are conserved across all species with the exception of isoforms isolated from goldfish (Maruyama *et al.*, 2008) (**Figure 1.1**).

In addition, NmS isoforms of all species have the same C-terminal undecapeptide (Chen *et al.*, 2006). It has been suggested, in some mammalian forms such as pNmU-25 (Minamino *et al.*, 1985) and dNmU-25 (O'Harte *et al.*, 1991), that the presence of a dibasic pairing (Arg¹⁶ and Arg¹⁷) plays fundamental role in allowing proteolytic cleavage site. This, therefore, allows the generation of the biologically active octapeptide, NmU-8. In chicken, however, Arg¹⁷ is substituted by Gly, and a shorter nonapeptide NmU-9 has been detected. Therefore, Arg¹⁶ and Gly¹⁷ site has been suggested to be a cleavage site (O'Harte *et al.*, 1991) . On the other hand, Arg¹⁶ and Gly¹⁷ are present in NmU of other species such as hNmU-25 as well but there is no evidence for a shorter form (**Figure 1.1**).

The replacement, for example, of a single amino acid of NmU-8 by either Gly or the inactive *D*-moiety leads to reduction in contractile activity on chicken crop smooth muscle. Also, substitution of any of the last C-terminal seven amino acids of NmU-8 by Ala reduced the potency for Ca²⁺ mobilisation in cells expressing NMU2 (Funes *et al.*, 2002). Moreover, it has been suggested that variations in the neuromedin U amino acid sequence are associated with some diseases including the obesity (Hainerova *et al.*, 2006). For instance, it has been demonstrated that an Ala19Glu variant of NmU was associated with an increased prevalence of the combined phenotypes of overweight and obesity in middle-aged white people, and a rare mutation, Arg165Trp, co-segregated with childhood obesity.

Moreover, amide group incorporation at the C-terminus is present in about 50% of peptides with therapeutic use and this is a key in ligand-receptor interaction and in the protection of the peptide against the proteolytic activity of carboxypeptidases (Rink *et al.*, 2010). The C-terminal asparagine is important for NmU. It has been shown that pNmU-8 lacking this loses its hypertensive effect and contractile activity in both rat

uterus (Minamino *et al.*, 1985) and chicken crop smooth muscle (Kawai *et al.*, 2006). For example, in contrast to NmU-8, a non-amidated version did not stimulate Ca^{2+} responses in cells expressing human NMU1 (Hedrick *et al.*, 2000). In addition, in cells expressing mouse NMUs, non-amidated NmU-8, failed to evoke Ca^{2+} , whereas NmU-8-NH₂ elevated $[\text{Ca}^{2+}]_i$ at either NMU1 or NMU2 with similar potency (Funes *et al.*, 2002). Most of the differences in amino acid sequence of NmU and NmS between different species are present at the *N*-terminus. Despite this, there is some conservation, within *N*-terminal residues. In NmU-25, for instance, Gln⁸ is conserved and Asp⁴-Glu⁵ is present as well with the exception of goldfish NmU-25, while chicken NmU-25 does not have Pro¹⁰ (**Figure 1.1**). Because of these differences, it has been suggested that these residues are key in the potency and duration of action. pNmU-25 stimulates a longer hypertensive impact than pNmU-8 in rat and the contractile effect was three times more potent than pNmU-8 on rat uterus (Minamino *et al.*, 1985).

1.2.3 NmU and NmS distribution

NmU distribution has been studied in mammals including rat and man (Domin *et al.*, 1989; Austin *et al.*, 1995; Fujii *et al.*, 2000; Szekeres *et al.*, 2000) where it is found largely within brain and gut tissues. Thus, it is often termed a gut-brain peptide (Austin *et al.*, 1995; Szekeres *et al.*, 2000). On the other hand, NmS exists mainly in the (CNS), particularly in the (SCN) of the hypothalamus, the site of the master circadian pacemaker in mammals (Mori *et al.*, 2005).

NmS mRNA is highly expressed in the central nervous system, spleen and testis. In rat brain, NmS expression is restricted to the core of the SCN. The highest level of expression is detected in the hypothalamus (Mori *et al.*, 2005). Moreover, there is also low-level expression of NmS mRNA in other hypothalamic nuclei including the arcuate nucleus (ARC), paraventricular nucleus (PVN), and supraoptic nucleus (Mori *et al.*, 2005).

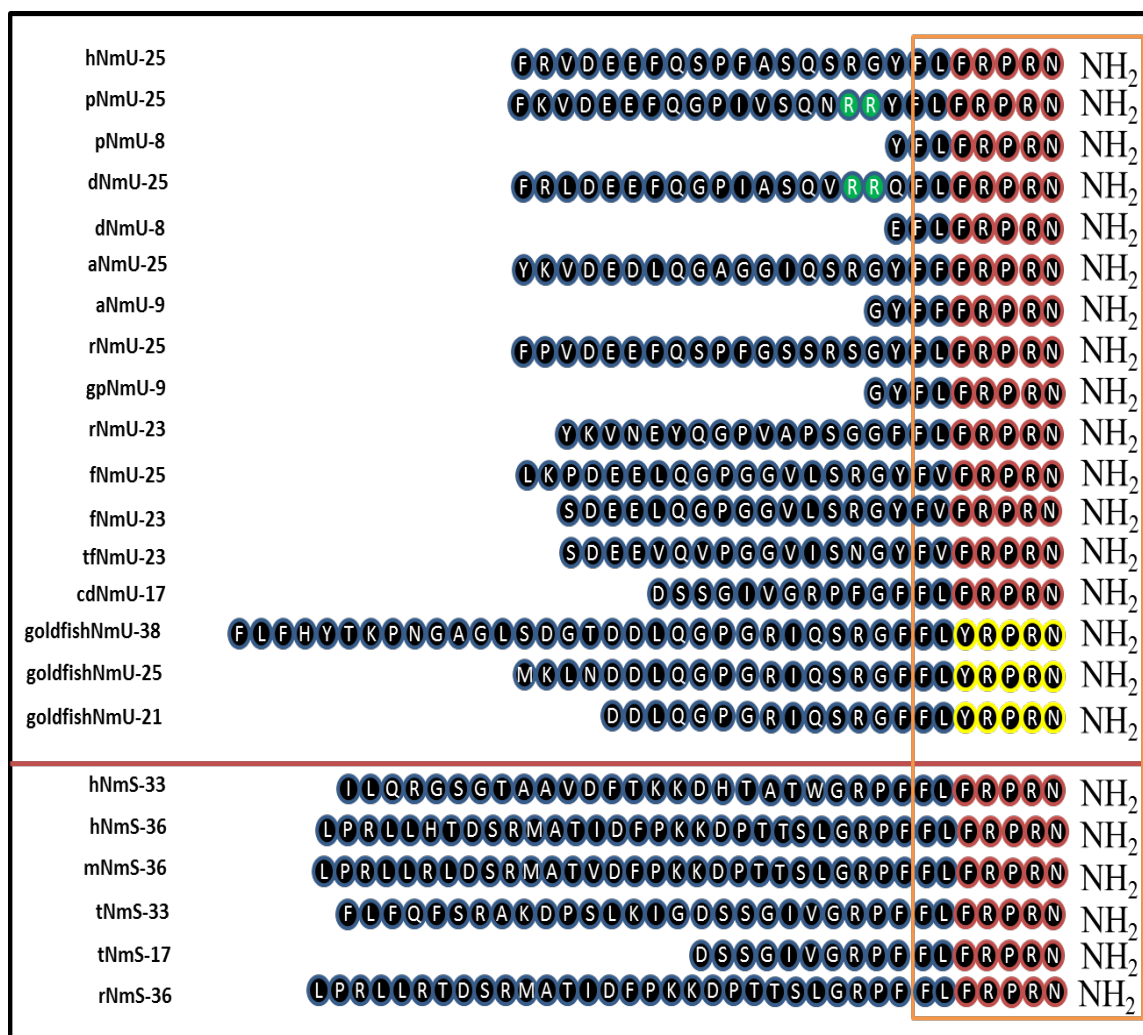


Figure 1.1 Amino acid sequences of the neuromedins, NmU and NmS, from different species

NmU and NmS isolated from different species are shown in upper and lower boxes, respectively. A conserved C-terminus pentapeptide (red circles) is present in all species except in gfNmU (yellow circles) (Maruyama *et al.*, 2008). All species have an amide group at the C-terminal asparagine (N-NH₂) (Domin *et al.*, 1989). The conserved C-terminal heptapeptide is indicated in the orange box. A cleavage site (Arg¹⁶-Arg¹⁷) is present in some species (green circles). NmU-8 is identical to the C terminus of NmU-25. Thus, it is the most highly conserved region of the entire peptide (Zeng *et al.*, 2006). Abbreviations; h, human; p, porcine; d, dog; a, avian; r, rabbit; gp, guinea pig; f, frog; cd, Chinese toad; m, mouse; t, toad; tf, tree frog.

1.2.4 Physiological roles of neuromedin U and S

Since the discovery of NmU and NmS, many studies have been conducted in order to understand the pathophysiology of both peptides. It has been shown that they are involved in different physiological and pathological activities in both the central and peripheral nervous systems. NmU can, for instance, stimulate the secretion of the somatostatin hormone from δ -cell of rat pancreatic islets (Kaczmarek *et al.*, 2009). It has also been indicated that NmU has the ability to inhibit bone formation and remodelling (Sato *et al.*, 2007).

It has also been indicated that NmU plays a role in specific types of cancer. Since treatment of leukemic cancer cell-line (K562) expressing dominant negative c-Myb may promote leukemogenesis. Real-time PCR analysis of NmU mRNA and c-Myb in primary acute myeloid leukaemia (AML), normal hematopoietic cells, and acute lymphatic leukaemia (ALL) revealed that c-Myb was present in both AML and ALL, while NmU was present only in AML (Shetzline *et al.*, 2004).

An increase in the blood pressure can be achieved in response to administration of NmU in rats in addition to an increase in heart rate whereas an increase in plasma noradrenaline was only demonstrated at higher doses (Minamino *et al.*, 1985; Chu *et al.*, 2002). As it has been mentioned early, the first function identified for NmU was the ability of porcine NmU to contract rat uterine smooth muscle (Minamino *et al.*, 1985). In addition to its ability to contract this type of smooth muscle, it contracts many other types of smooth muscles (Westfall *et al.*, 2002; Jones *et al.*, 2006; Prendergast *et al.*, 2006; Dass *et al.*, 2007; Mitchell *et al.*, 2009) and indeed human ileum, rat and mouse stomach can be directly contracted by NmU (Dass *et al.*, 2007).

Neuromedin U is a highly conserved neuropeptide regulating food intake and body weight. Mice lacking NmU are hyperphagic and obese and this makes NmU receptor a novel target for treating obesity (Howard *et al.*, 2000; Hanada *et al.*, 2004; Benzon *et al.*, 2014). NmU injection in rat brain regions including ARC and PVN decreases food intake, body weight and causes a transient increase in body temperature and locomotor

activity (Howard *et al.*, 2000a). A role for NmU in regulating food intake is consistent with the expression of NMU and its ligands in brain including ARC and PVN (Howard *et al.*, 2000; Kojima *et al.*, 2000). Moreover, it has been recently reported that long-term central administration of NmU reduces food intake, adiposity and body weight and the NMU2 is crucial for such physiological activities in female but not male mice (Egecioglu *et al.*, 2009). Indeed, the PVN and ARC are well known to be crucial for NmU-mediated central energy homeostasis. It has been shown that microinjection of NmU in these areas in the rat led to satiety and increased locomotor activity and temperature (Wren *et al.*, 2002; Novak *et al.*, 2006).

In addition, in contrast to corticotrophin-releasing hormone knockout mice CRH KO, intracerebroventricular (ICV) administration of NmU suppressed dark-phase food intake and fasting-induced feeding in wild-type mice and this suggest that NmU could play a role in feeding behaviour via CRH (Hanada *et al.*, 2003). In addition, ICV administration of NmU reduced feeding, suggesting that NmU enhances energy expenditure by increasing locomotor activity, body temperature and heat production (Nakazato *et al.*, 2000). On the other hand, it has been reported that NMU2 knockout mice have increased the body weight when fed a high-fat diet. The same study confirmed an anti-obesity role of the central NmU signalling system in diet-induced obesity (DIO) that could be mediated via NMU2 in female but not in male mice (Egecioglu *et al.*, 2009). Perhaps surprisingly NMU2 knockdown had no effect on food intake and body weight when rats were fed with a standard chow. In contrast, when they were fed with only high-fat diet, they gained more body weight. The data in this study suggest that NMU2 signalling in the PVN influences the intake of obesogenic food such as high-fat diet by selectively regulating preference for increased dietary fat. Also, NMU2 expression in the PVN minimises weight gain in an obesogenic circumstances, since NMU2 normally inhibits weight gain even when exposed to obesogenic food leading to weight gain increased, when NMU2 was knocked down (Benzon *et al.*, 2014).

It has been suggested that in order for NmU to exert its effects on feeding and satiety, a neuronal network with other appetite-regulating peptides could be involved. For instance, it has been indicated that the satiety hormone leptin regulates NmU action by

blocking the satiety effect of leptin when ICV injection with anti-NmU IgG prior to intraperitoneal administration of leptin was performed (Campfield *et al.*, 1995). In light of that, leptin is likely to exert its effects on food intake via NmU pathway (Jethwa *et al.*, 2005; Jethwa *et al.*, 2006). Also, the interaction between leptin, a protein hormone secreted from adipocytes acting at the hypothalamus mediating its anorectic effect (reducing appetite), and NmU has been observed in which expression of NmU mRNA is decreased within the hypothalamic of the leptin-deficient strain of mice and also in the ventromedial hypothalamus (nucleus of the hypothalamus) of fasted rats (Howard *et al.*, 2000). Furthermore, it has been shown that NmU is stimulated by leptin from hypothalamic explants (Wren *et al.*, 2002a). Moreover, it has been indicated that NmU expression is lesser within nucleus tractus solitarius (NTS) getting information connecting to gut nutrients delivering this to different locations in the brain that regulate food intake, including brain stem and forebrain (Rinaman *et al.*, 1998). Therefore, based on such outcomes, it is suggested that NmU free is mediated by leptin and the composite of NmU is inhibited in the lack of leptin. In contrast, it has been reported that that anti-NmU IgG had no effect on blocking leptin-mediated on satiety (Nakahara *et al.*, 2010).

It has been reported that NmU and NmS peptides produce central effect on energy homeostasis using NMU2 rather than NMU1. Therefore, a preferential central distribution of NMU2 mRNA in the CNS in particular the hypothalamic regions including the PVN in rat and mouse has been suggested (Howard *et al.*, 2000; Guan *et al.*, 2001; Jethwa *et al.*, 2006). It has also been suggested that NMU1 could be involved in food intake and body weight inhibition following peripheral administration of NmU.

A recent study highlights the crucial role of both NmU and NmS acting centrally on NMU2 in the regulation of body weight. Chronic centrally applied NmU or NmS can decrease body weight and food intake and NmU also increased body temperature over two weeks (Peier *et al.*, 2009). These data suggest that NmU produced its effects when administered centrally via NMU2 and through NMU1 when administered peripherally. Excess weight and diabetes are conditions associated with a high morbidity and mortality and an understanding of the regulation of the body weight is crucial for the identification and exploitation of potential therapeutic targets.

NmU and its receptors are also highly expressed in the SCN of the hypothalamus which is the biological clock control centre (Nakahara *et al.*, 2004). NmS is more highly expressed than NmU in the SCN, suggesting a crucial role of this neuropeptide in regulating the circadian system (Mori *et al.*, 2005). Despite a potentially key role of NmS in this, both NmU and NmS are regulated by the light-dark cycle with highest expression during the light phase (Moriyama *et al.*, 2005).

The functions of NmS in the brain have been validated by ICV administration of the peptide to rats. This has been associated with a phase-shift in circadian rhythm (Mori *et al.*, 2005), suppression of food intake (Ida *et al.*, 2005), reduced urine volume (Sakamoto *et al.*, 2007), increased milk secretion (Sakamoto *et al.*, 2008), and elevated plasma levels of luteinizing hormone (Vigo *et al.*, 2007). Although ICV-administered NmU induced the same responses, the activity of NmS was greater than that of NmU (Nakahara *et al.*, 2004; Ida *et al.*, 2005; Mori *et al.*, 2005; Sakamoto *et al.*, 2007; Sakamoto *et al.*, 2008). Also, it has been shown that cardiovascular function is regulated by NmS through the sympathetic nervous system in mice as ICV injection increased heart rate (Sakamoto *et al.*, 2011). In addition to reducing feeding behaviour, NmS also influences gut motility by reducing gastric emptying. It also disrupts the motor activity in the antrum and duodenum of conscious food-deprived mice (Atsuchi *et al.*, 2010). Several mechanisms have been suggested to account for the way in which the central administration of NmU controls feeding behaviour and energy expenditure. A previous study indicated that central infusion of oxytocin by activating brain stem projecting oxytocin-containing neuron is involved in the NmU-mediated inhibition of feeding (Olson *et al.*, 1991). Furthermore, it has been reported that activation of vasopressin or arginine-vasopressin containing neurons in the PVN by NmU inhibited water intake (Howard *et al.*, 2000). This suggests that this effect is mediated by arginine-vasopressin consistent with the ability of centrally administered NmU to stimulate release of this hormone from hypothalamic explants (Niimi *et al.*, 2001; Wren *et al.*, 2002).

1.3 Discovery and characterisation of receptors for NmU

1.3.1 Background

Two types GPCRs for NmU and NmS have been identified: NMU1 and NMU2 (Alexander *et al.*, 2008; Sharman *et al.*, 2011). Prior to de-orphanisation, these receptors were known as FM-3 and FM-4 respectively. FM-3 was cloned from mouse T-cell cDNA and human cDNA libraries according to its homology to the growth hormone secretagogue receptor (the ghrelin receptor) and the neurotensin-1 (NT1 receptor), which have 33% and 29% homology respectively to NMU1 (Tan *et al.*, 1998). FM-3 protein sequences from human and mouse are 73% homologous. FM-4, also previously known as TGR-1, was also cloned from both human and rat and was identified as a receptor for NmU and thus called NMU2 (Hosoya *et al.*, 2000; Howard *et al.*, 2000; Raddatz *et al.*, 2000). Human and rat NMU1 and NMU2 share 73% and 75% homology respectively (Howard *et al.*, 2000). NmU analogues have high affinity and stimulate NmU-mediated signalling at sub-nanomolar concentrations (Kojima *et al.*, 2000; Raddatz *et al.*, 2000; Szekeres *et al.*, 2000).

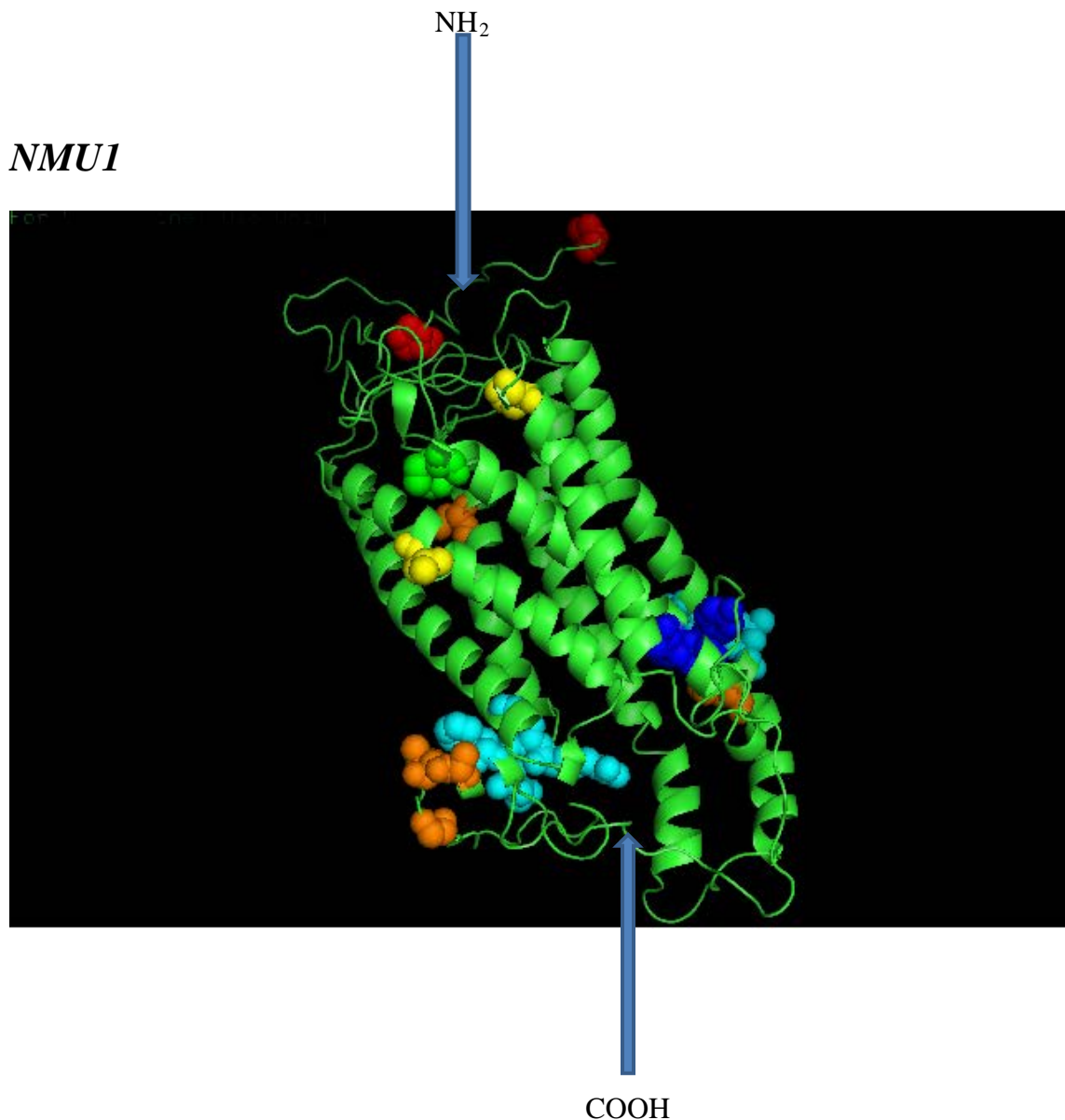
1.3.2 Structural characteristics of NMUs

Both NMU receptors are typical Family A GPCRs. The GPCRs have no sequence homology but the primary structure is known by a common structural motif of 7TM-spanning regions (Bockaert *et al.*, 1999). NMUs have seven putative transmembrane domains. The NMU2 C-terminus contains 88 amino acids whereas NMU1 C-terminus consists of 70 amino acids. The D/ERY (Asp, Arg, Tyr, Glu) motif is a highly conserved that plays a role in ligand binding (Rhee *et al.*, 2000; Rovati *et al.*, 2007), G-protein coupling (Scheer *et al.*, 2000) and the preservation of inactive receptors (Wilbanks *et al.*, 2002). NMUs have ERY motif at the boundary of TM 3 and the second intracellular loop.

The importance of Arg of the D/ERY motif in the formation of the receptor-G protein complex has been recently confirmed by the crystal structure of opsin in its G-protein-interacting conformation (Scheerer *et al.*, 2008; Rovati *et al.*, 2014). Furthermore, it has been suggested that Arg of the DRY motif is important for stabilizing the inactive and the active conformation through interaction with key residues in TM-III, -VI. However, the Arg micro-switch is not important for the actual G-protein activation. In addition, the mutation of Arg had no effect on $G\alpha_s$ signalling and internalisation, and only β -arrestin-2 mobilization was reduced (Valentin-Hansen *et al.*, 2012). NMU1 has either a shorter version, 403 amino acids (Tan *et al.*, 1998) or a longer version of 426 amino acids (Raddatz *et al.*, 2000) and a predicted molecular mass of 47450 Da. Similar to NMU1, NMU2 has two versions; either 412 amino acids (Hosoya *et al.*, 2000; Howard *et al.*, 2000a) or 415 amino acids (Raddatz *et al.*, 2000). The receptors show 45-50 % amino acid homology. Transmembrane domains of both receptor, NMU1 and NMU2, are highly conserved whereas the N- and C-terminals indicate little homology. The third intracellular loop of NMU2 is shorter than that in NMU1 (**Figure 1.2**). NMUs have phosphorylation sites within their intracellular domains potentially for PKA and PKC and casein kinases I and II. In contrast, GRKs phosphorylation sites have not been identified (Brighton *et al.*, 2004a) due to lack of information concerning consensus sequences. NMU2 contains a certain sequence (-YQSF) binding to the clathrin-coated

pit (CCP) playing a role in CCP-mediated GPCR ligand-dependent internalisation (Marchese *et al.*, 2008).

Disulphide bridges are likely between the conserved cysteine residues that are the same positions of other Family A GPCRs (Strader *et al.*, 1994; Perlman *et al.*, 1995). This disulphide bridge may be critical for ligand binding, protein folding and the stability of receptor conformation (Savarese *et al.*, 1992) (**Figure 1.2**). Serine-, threonine- and tyrosine-linked phosphorylation and asparagine (*N*)-linked glycosylation sites are also present. Unfortunately, due to the lack of information regarding consensus sequences, (Pitcher *et al.*, 1998), potential phosphorylation sites of GRKs have not been identified.



NMU2

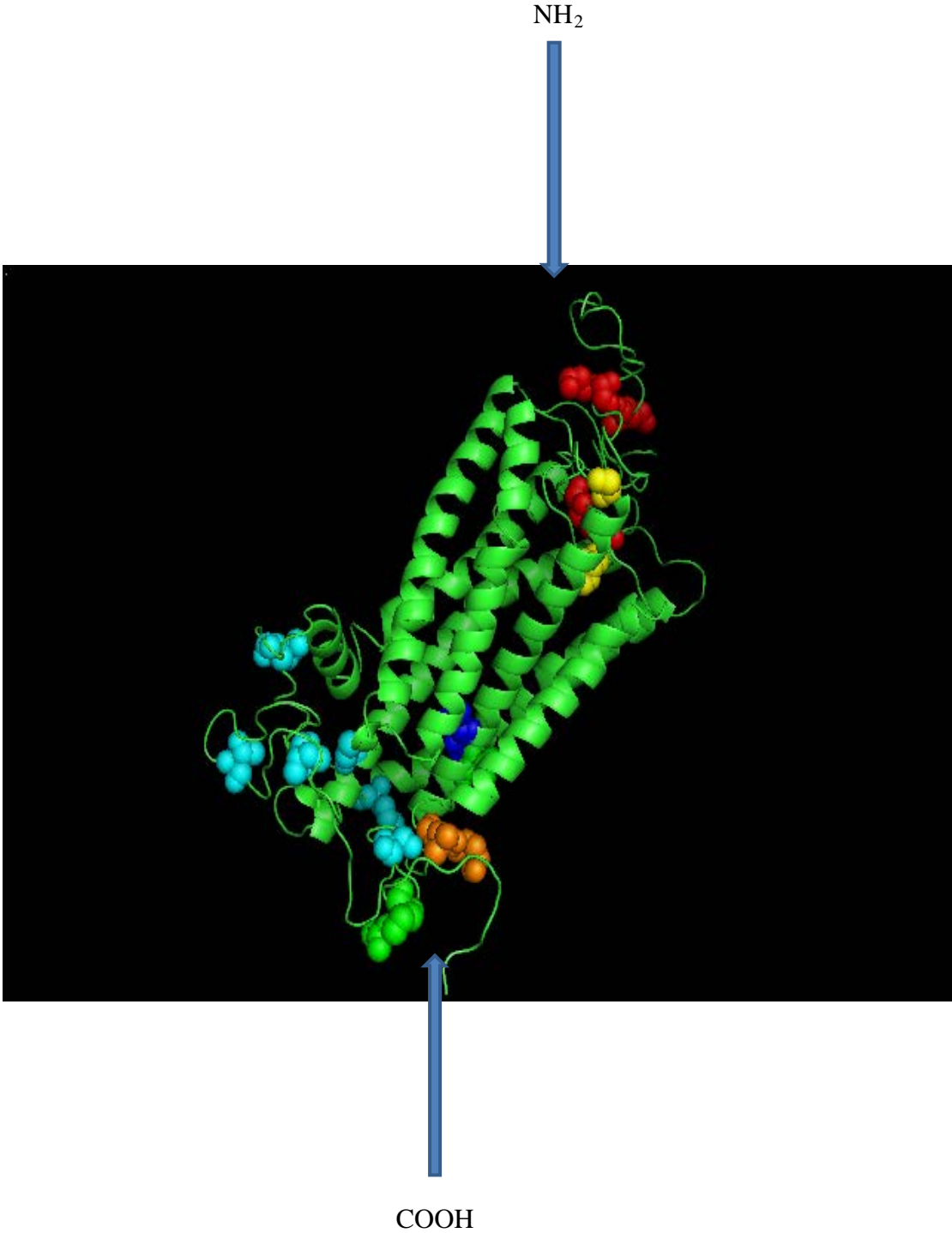


Figure 1.2 The structure of NMU1 and NMU2

The above structures were modified using the PyMol Molecular Graphics System. Sequences were acquired with NCBI accession numbers for both receptors NMU1 and NMU2 (AF272362 and AF272363, respectively). Prediction of the structures was carried out using the TASSER (Iterative Threading ASSEmblY Refinement approach). It is a hierarchical approach to protein structure prediction that consists of template identification by threading (a method of protein modeling which is used to model those proteins), followed by tertiary structure assembly via the rearrangement of continuous template fragments guided by an optimized C (alpha) and side-chain-based potential driven by threading-based, predicted tertiary restraints (Zhang *et al.*, 2004; Zhang *et al.*, 2006). The cysteine residues for disulphide bound formation are shown (s-s) (yellow Spheres) between the first and second extracellular loops. Identification of *N*-linked glycosylation sites are indicated (red Spheres). The sites most likely to be phosphorylated are shown (serine residues cyan Spheres, tyrosine residues orange Spheres, threonine residues green Spheres). The positions of the ERY motif at the transmembrane are illustrated (blue Spheres). Adapted from <http://cssb.biology.gatech.edu>.

1.3.3 The distribution of NMUs

It has been suggested that NMU1 in human is expressed predominantly in the periphery, especially the gastrointestinal tract, whereas NMU2 expression is predominantly in the CNS. In the human, mRNA for NMU1 exists in high levels in peripheral tissues including lung, spleen, ileum, jejunum, and the duodenum and at lower levels in femur, caecum, colon, and rectum (Fujii *et al.*, 2000; Gartlon *et al.*, 2004; Hsu *et al.*, 2007). Low amounts of NMU1 are also present in thyroid, thymus, trachea, kidney, stomach, adipose tissue and uterus but is not detectable in the adrenal gland or testis (Fujii *et al.*, 2000; Hsu *et al.*, 2007). NMU1 mRNA and protein have also been shown in isolated rat pancreatic islets (Kaczmarek *et al.*, 2006). In Man, many studies using Northern blot and dot blot analyses have indicated high levels of NMU1 mRNA in the periphery including bone marrow, adrenal cortex, jejunum, duodenum, small intestine, adipose tissue and testis. In addition, lower levels are present in prostate, kidney, lung, stomach, spleen, trachea, heart, and placenta (Hedrick *et al.*, 2000; Raddatz *et al.*, 2000; Szekeres *et al.*, 2000; Gartlon *et al.*, 2004).

NMU1 mRNA exist but at low levels in rat CNS but can be detected in striatum, thalamus, spinal cord, cortex, cerebellum, small-medium diameter of dorsal root ganglia and amygdale. In the mouse, NMU1 mRNA is present in small neurons of the dorsal root ganglia and in hippocampal neurons (Fujii *et al.*, 2000; Funes *et al.*, 2002; Gartlon *et al.*, 2004; Zhang *et al.*, 2010; Wang *et al.*, 2011).

NMU2 is present in high levels peripherally and has been identified often at both the mRNA and protein level. For instance, in the rat high levels are found in the uterus and ovary but at low levels in salivary gland, adipose tissue, stomach, large intestine, small intestine, bladder, testis and thymus (Fujii *et al.*, 2000; Hosoya *et al.*, 2000; Gartlon *et al.*, 2004). In contrast to NMU1, NMU2 mRNA or protein is absent from the adrenal gland (Fujii *et al.*, 2000; Hsu *et al.*, 2007; Rucinski *et al.*, 2007; Trejter *et al.*, 2008; Ziolkowska *et al.*, 2008). Also, species-dependent distribution has been suggested and this can be clearly seen as NMU2 is absent in human and dog uterus but present at high

levels in rat uterus (Raddatz *et al.*, 2000; Shan *et al.*, 2000). This may result from the impact of oestrogen that enhances NMU2 expression in rat (Nandha *et al.*, 1999). NMU2 mRNA has also been found in high levels in the pig including lung, heart, ovary, spleen, uterus, kidney, liver and colon with low levels in duodenum and thyroid gland (Yang *et al.*, 2012). NMU2 is detected in the ovary, gut, kidney and testis in goldfish peripheral tissues (Maruyama *et al.*, 2011).

NMU2 is also centrally distributed and this is consistent with the NMU ligands, NmU and NmS, indicating important functions of the ligands. NMU2 is present in high levels in rat hypothalamus particularly in the wall of the third ventricle with moderate levels in the par ventricular nucleus (PVN) (Howard *et al.*, 2000a; Guan *et al.*, 2001). Low levels of NMU2 mRNA have also been observed in different tissues including spinal cord, striatum, hippocampus and medulla oblongata (Fujii *et al.*, 2000; Hosoya *et al.*, 2000; Gartlon *et al.*, 2004). NMU2 is present in low levels in the cerebellum, thalamus and cortex (Fujii *et al.*, 2000; Hosoya *et al.*, 2000; Gartlon *et al.*, 2004). On the other hand, in mouse, the hypothalamus, medulla, pons and spinal cord, have the highest amounts of the receptors (Funes *et al.*, 2002). Furthermore, brain and pituitary in goldfish have NMU2 (Maruyama *et al.*, 2011). In addition, it has been recently demonstrated that NMU2 mRNA exists in spinal cord, medulla oblongata, hypothalamus, pons and pituitary in pig (Yang *et al.*, 2012). In human, it has been shown that NMU2 mRNA is expressed predominantly to specific regions within the brain including substantia nigra (Howard *et al.*, 2000), medulla oblongata, pontine reticular formation (Raddatz *et al.*, 2000), spinal cord and thalamus. It has also been observed in the hippocampus, hypothalamus, and cerebral cortex (Raddatz *et al.*, 2000). In addition, human NMU2 has been peripherally observed. For example, it has been found with high levels in testes whereas it was found with low levels in gastrointestinal tract, genitourinary tract, liver, pancreas, adrenal gland, thyroid gland, lung, trachea, spleen, thymus, and thyroid (Raddatz *et al.*, 2000; Shan *et al.*, 2000). In contrast, human NMU2 has not been peripherally observed with some researches either in liver, heart, skeletal muscle, intestines, pancreas, placenta, and kidneys (Howard *et al.*, 2000) or bladder (Westfall *et al.*, 2002).

As it has been early mentioned that two high affinity NmU and NmS receptors, NMU1 and NMU2, have been identified and NMU1 is predominantly expressed in the periphery, whereas NMU2 is primarily expressed in the brain and because the obesity is regulated centrally, and based on that, this study has focused on using NMU2 rather than NMU1. On the other hand, when required, the comparison between the receptors has been conducted. Therefore, human embryonic kidney cells (HEK293), either wild-type (HEK293-WT), or stably expressing either NMU1 or NMU2 (HEK-NMU1 and HEK-NMU2, respectively) were provided by GlaxoSmithKline (Harlow, UK). Moreover, HEK-NMU1-eGFP and HEK-NMU2-eGFP stable cell-lines were generated in our lab by a previous PhD student (Alhosaini, 2011). These cells were used in this project. On the other hand, the natural expression of NMUs and/or the ability of NmU to evoke NMU-mediated $[Ca^{2+}]_i$ mobilization in a range of cells endogenously expressing NMU, including K562 cells, mouse Th2 cells (Johnson *et al.*, 2004), primary mast cells (Moriyama *et al.*, 2005), pancreatic β -cells (Kaczmarek *et al.*, 2006), human pancreatic cancer cell-lines (Ketterer *et al.*, 2009) and eosinophils (Moriyama *et al.*, 2006) have been investigated. Unfortunately, no responses were detected in most of these studies. The reason for the lack of responses to NmU is unclear. One possibility could be the lack of receptors on the cell membrane.

1.4 G protein-coupled receptors (GPCRs)

NmU and NmS mediate their function via either NMU1 or NMU2 receptors belonging to Family A of the GPCRs superfamily. Therefore, it is important to understand how these receptors are activated and regulated depending on previous studies of other members of GPCRs.

GPCRs are polypeptides of 300-1200 amino acids, sharing seven transmembrane α -helices (7TM) and possessing an extracellular *N*-terminus and cytoplasmic *C*-terminus constituting the largest family of plasma membrane receptors. These receptors play a role in many diseases and are considered as potential therapeutic targets for around 40% of drugs (Millar *et al.*, 2010). Many functions are regulated by these receptors including electrical activity, metabolism, secretion and response to neurotransmitters and hormones (Stevens *et al.*, 2013). These functions are achieved by activating heterotrimeric G protein. In contrast, G protein signalling can also be activated by some receptors that do not have 7TM helices (Patel, 2004).

The seven transmembrane-domain GPCR superfamily is grouped based on sequence similarities and the length of the extracellular *N* terminus into three main sub-families, A, B and C. These sub-families have approximately 25% amino acid homology between them. Family A is the largest family with a short extracellular *N* terminal and many receptors belong to this sub-family including opsin receptors and adrenoceptors and they are known as rhodopsin-like receptors. Family B receptors are smaller than family A and include peptide hormones such as secretin and glucagon and therefore they are called secretin/glucagon receptors with an intermediate extracellular *N* terminal length that is ligand-binding domain. Family C is the smallest family with a long extracellular *N* terminal containing “venus flytrap” module that is the ligand binding site (Brauner-Osborne *et al.*, 2007). They contain Ca^{2+} -sensing receptors and gamma-aminobutyric acid type B (GABA_B) receptors. Both physiological and structural features have been used to classify GPCRs. However, more recently, an alternative classification system called GRAFS has been proposed. Thus, a large scale phylogenetic analyses of the majority of the GPCRs in the human genome has been performed providing the GRAFS system identifying five families named glutamate (G), rhodopsin (R), adhesion (A), frizzled/taste2 (F), and secretin (S) (Fredriksson *et al.*, 2003).

1.4.1 Activation and termination of signalling by G proteins

G protein-coupled receptors signal through a variety of mechanisms that impact many functions. G protein-dependent and G protein-independent pathways each have the capacity to initiate numerous intracellular signalling cascades to mediate these effects (**Figure 1.3**).

GPCRs are so named due to their interaction with G proteins. G proteins are heterotrimeric guanine nucleotide-binding proteins. They belong to the GTPase superfamily acting as transducers of the signal generated by the ligand-receptor complex and therefore signalling pathways can be either activated or inhibited. G proteins have three polypeptides grouped into two functional units; α -subunit and $\beta\gamma$ subunit. Both subunits are localized at the inner surface of the plasma membrane. Guanine nucleotide (GDP) is bound to the binding site of α -subunit that has GTPase activity facilitating GTP hydrolysis and G protein inhibition in α -subunit (Cabrera-Vera *et al.*, 2003). At the resting state, the G protein binds as a heterotrimeric complex with GDP bound to the α -subunit. Ligand binding leads to a conformational change of the receptor causing GDP to disassociate from the α subunit. This is replaced by GTP. The receptor-ligand complex behaves as a guanine nucleotide exchange factor (GEF) for the G protein resulting in disassociation of α -GTP from the $\beta\gamma$ complex. GDP-for-GTP exchange results in releasing α -GTP from the $\beta\gamma$ dimer leading to interaction of $G\alpha$ and /or $G\beta\gamma$ subunits with effectors. Once the GTP is hydrolysed to GDP by $G\alpha$ subunit GTPase activity, $G\alpha$ -GDP quickly rebinds to the $G\beta\gamma$ complex in order to recreate the inactive form of G protein heterotrimer. It is worthy to mention that GTPase activity is regulated by GTPase-activating proteins (GAPs) that in this instance are often members of the regulator G protein signalling (RGS) protein family (Pierce *et al.*, 2002) (**Figure 1.4**).

There are more than 20 subtypes of $G\alpha$ subunits with four main classes; $G\alpha_s$, $G\alpha_{12/13}$, $G\alpha_{i/o}$ and $G\alpha_{q/11}$. GPCRs can bind either promiscuously or selectively to specific $G\alpha$ members. $G\alpha_s$ activates adenylyl cyclase (AC) and this in turn promotes the synthesis of the second messenger adenosine cyclic-3',5'-monophosphate (cAMP) from ATP.

Protein kinase (PKA) is activated by cAMP and as a result of this activation, many cellular functions can be regulated by phosphorylation. In addition, $G\beta\gamma$ can activate cAMP production by increasing AC activity using some but not all isoenzymes. On the other hand, $G_{ai/o}$ inhibits AC activity and thus cAMP generation is inhibited. Moreover, many ion channels such as inwardly rectifying K^+ channels can be regulated by $G_{ai/o}$ (**Figure 1.5**).

$G_{\alpha q/11}$ plays a role in stimulating phosphoinositide turnover through activation phospholipase $C\beta$ ($PLC\beta$) and this enzyme hydrolyses phosphatidylinositol-4,5-bisphosphate (PIP_2) to both diacylglycerol (DAG) that activates protein kinase C (PKC), and IP_3 that induces Ca^{2+} release into the cytoplasm by stimulating IP_3 receptors on the endoplasmic reticulum (Dawson, 1997; Berridge *et al.*, 2000; Cordeaux *et al.*, 2002). The effectors of the $G_{\alpha 12/13}$ pathway are three RhoGEFs (p115-RhoGEF, PDZ-RhoGEF, and LARG), which, when bound to $G_{\alpha 12/13}$ activate the cytosolic small GTPase, Rho. Once bound to GTP, Rho can then go on to activate various proteins responsible for cytoskeleton regulation such as Rho-kinase (ROCK).

The majority of GPCRs that couple to $G_{\alpha 12/13}$ also couple to other sub-classes, often $G_{\alpha q/11}$. This results in facilitating GTP-for-GDP exchange on RhoGEF, which can regulate functions such as cell migration and proliferation (Chen *et al.*, 2005). Once the $G\beta\gamma$ is dissociated from the activated G proteins complex, in addition to ion channels, a huge number of effectors such as AC and PLC can be also modulated (Jacoby *et al.*, 2006). An example of $G\beta\gamma$ signalling is its effect of activating or inhibiting (AC) leading to the intracellular increase or decrease of the (cAMP) (Tang *et al.*, 1991). Despite that a study did not detect an effect of NmU on AC activity in HEK293 cells transiently expressing NMU1 (Szekeres *et al.*, 2000), it has recently been suggested that NMU1-mediated signalling occurs via $G_{\alpha q/11}$ while NMU2 signalling prefers downstream of $G_{\alpha i/o}$ (Hsu *et al.*, 2007). Coupling of NMUs has also been investigated with both recombinant (Brighton *et al.*, 2004b) and endogenous (rat colonic smooth muscle cells) NMU-expressing cells (Brighton *et al.*, 2008).

It has also been demonstrated that extracellular signal-regulated kinase (ERK) are activated following G protein-dependent and β -arrestin-dependent pathways (DeFea *et al.*, 2000; Marinissen *et al.*, 2001).

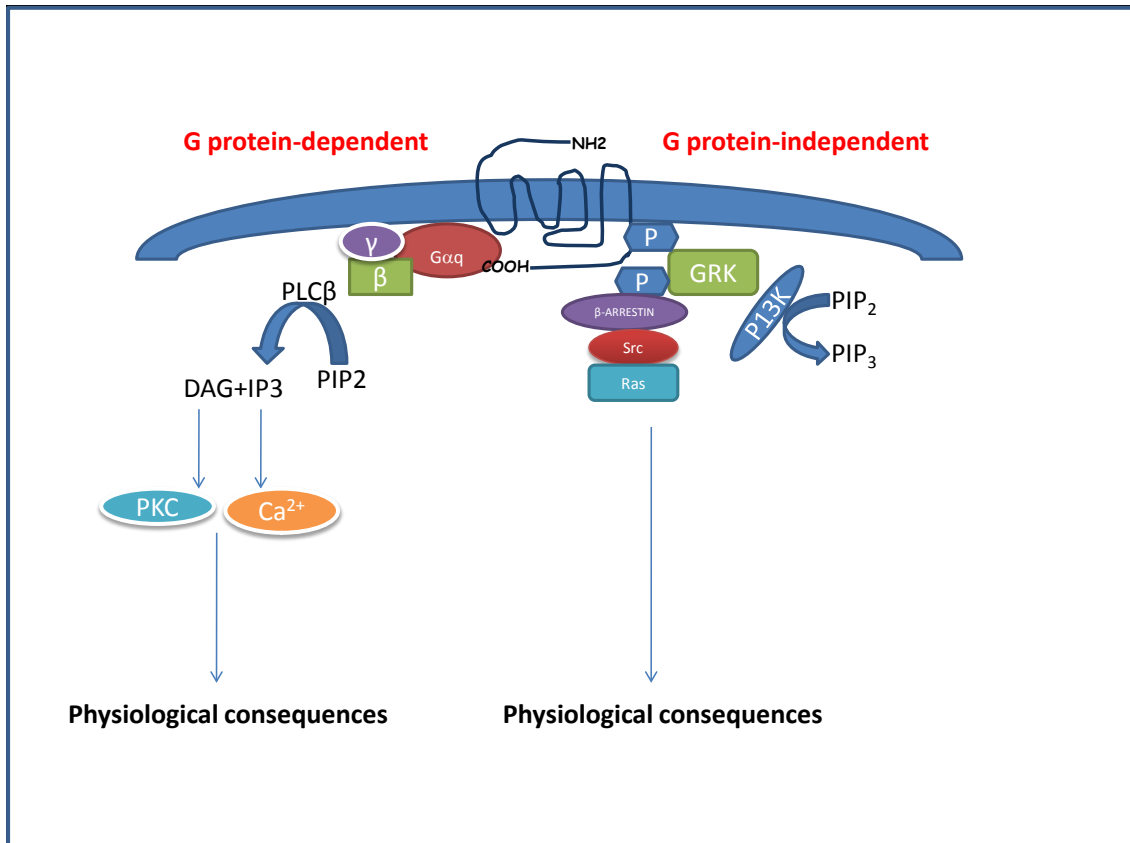


Figure 1.3 G-protein-dependent and G-protein-independent signalling pathways

Once the ligand binds to the receptor, the receptor activates a G α -subunit and the effector; in this example, PLC β is activated leading to downstream G-protein-dependent signalling. Following receptor phosphorylation and arrestin recruitment, alternatively, G-protein-independent signalling pathways are initiated including for example, ERK.

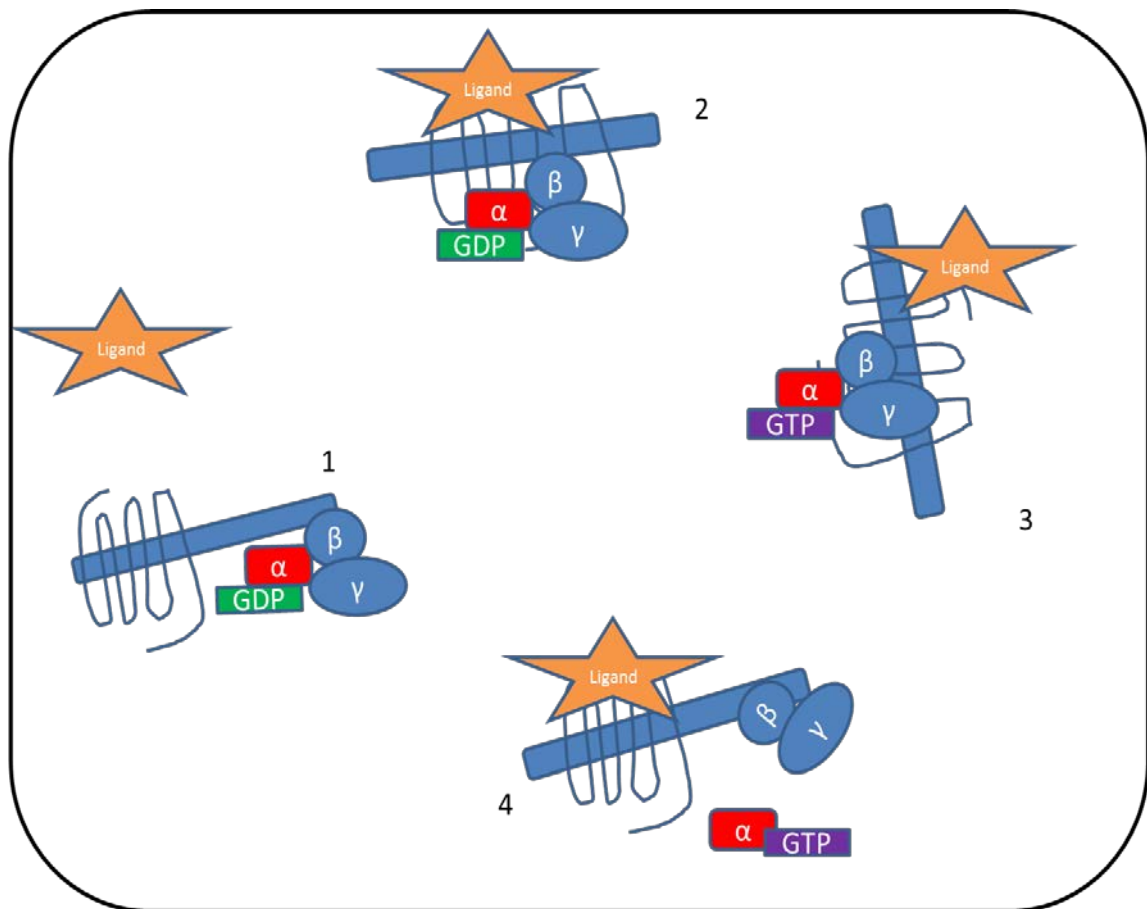


Figure 1.4 Activation cycle of a G-protein by a G-protein-coupled receptor receiving a ligand

GPCR in the resting state (1). When the ligand binds to the receptor, association of the membrane-heterotrimeric G protein with the intracellular domain of the receptor is promoted (2). Because of ligand binding, the GDP associated with the $G\alpha$ subunit is exchanged for GTP (3). The $G\alpha$ -GTP subunit dissociates from the $\beta\gamma$ subunits and therefore the separated subunits are able to modulate effector enzymes (4). Finally, GTP hydrolysis to GDP allows re-association of α and $\beta\gamma$ subunits.

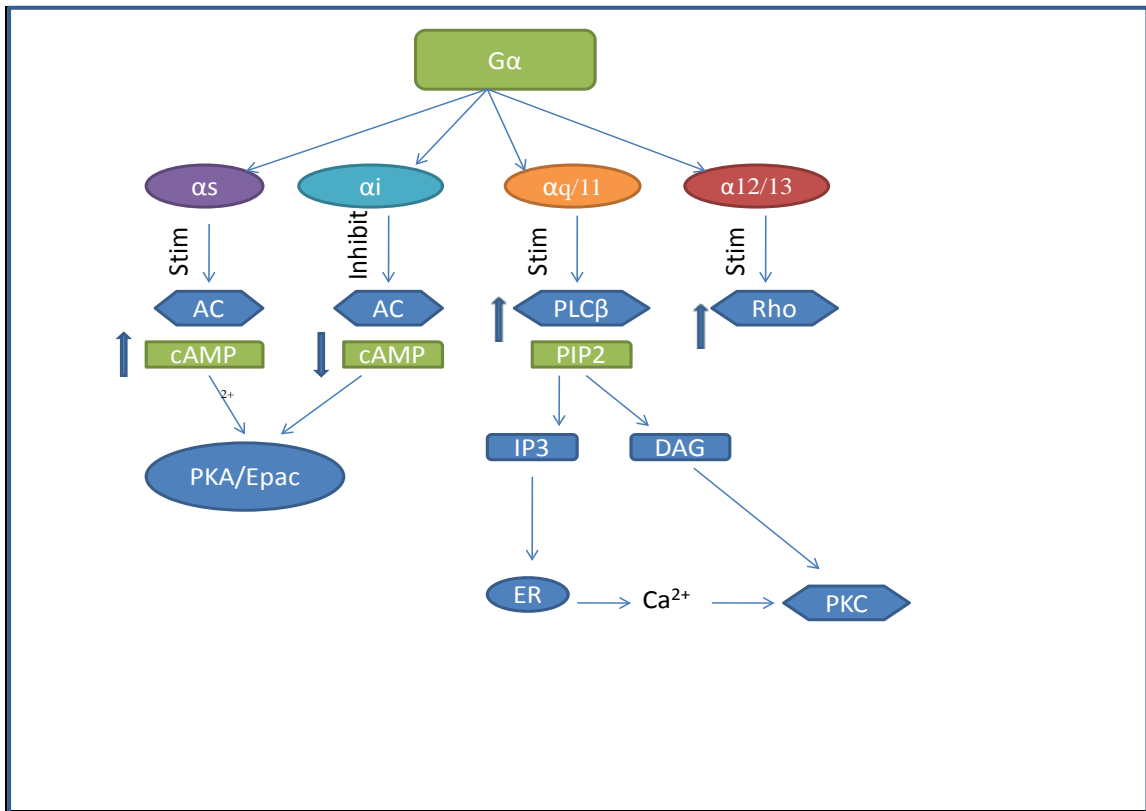


Figure 1.5 G α -mediated signalling pathways resulted by different G α subunits

Pathways regulated by different G α subunits. G α_s and G $\alpha_{i/o}$ activate and inhibit AC respectively. G $\alpha_{12/13}$ activates monomeric G-protein such as Rho. G $\alpha_{q/11}$ activates PLC hydrolysing PIP₂ to increase [Ca²⁺]_i and activate PKC. Abbreviations: AC; adenylyl cyclase. PKC; protein kinase C. PKA; protein kinase A. Epac; exchange protein directly activated by cAMP. ER; endoplasmic reticulum.

1.4.2 Phosphorylation and desensitization of GPCR

In order for a GPCR to transduce an extracellular signal, it must both traffic correctly to and be retained at the cellular surface to allow for receptor/ligand interaction. The well-characterised pathway for GPCR endocytosis occurs through clathrin-coated pits (CCPs) that contain clathrin and adapter protein-2 (AP-2) complexes. Once the ligand binds to the receptor, G proteins are activated allowing the regulation of cellular activity. However, such processes tightly regulate the sensitivity and responsiveness of cells to such activation as desensitisation in the face of repeated or persistent agonist stimulation to ensure the reduction of prolonged effects that may be detrimental effects to cell function and viability. Desensitisation can essentially be sub-divided into two types. Homologous desensitisation is where only active receptors (agonist-bound) are regulated, whereas heterologous desensitisation is where inactive receptors (i.e. those not bound by agonist) are regulated by the activity of other receptors that couple to the same or different signalling pathways (Lohse *et al.*, 1990). The general mechanisms for such desensitisation processes involves phosphorylation of serine/threonine residues within the third intracellular (i3) loop and C-terminal tail of the receptor by a range of protein kinases although it is notable that desensitisation can occur at other points in the signalling pathways (Pierce *et al.*, 2002). The kinase(s) responsible for this phosphorylation are either PKC or PKA for heterologous desensitisation or G protein coupled receptor kinases (GRKs) for homologous desensitisation) (Pierce *et al.*, 2002). Desensitisation can be either rapid within seconds to minutes or slow within hours to days and involve loss of receptor signalling function, removal or receptors from the plasma membrane into the sub-cellular compartments (internalisation) or loss of total receptor number (down-regulation).

NMU1 and NMU2 contain putative (serine/threonine) phosphorylation sites for PKA and PKC in their intracellular terminus (Brighton *et al.*, 2004a) (**Figure 1.2**). The consensus sequences for GRK phosphorylation have not been defined and it is therefore not possible to say with any certainty if the NMU receptors contain GRK phosphorylation sites (Brighton *et al.*, 2004a).

Receptor phosphorylation by GRKs results in β -arrestin recruitment and therefore removing of receptor-G protein coupling and G protein dependent signalling (Pierce *et al.*, 2002; Moore *et al.*, 2007; Marchese *et al.*, 2008).

1.4.3 Internalization and trafficking of GPCR

In addition to fulfilment an intracellular signalling role, GPCRs internalisation plays a role in receptor desensitisation, recycling and down-regulation (Moore *et al.*, 2007). As a result of GRK-mediated receptor phosphorylation and β -arrestin binding, the receptor complex is internalised using clathrin-coated pits (CCP) that is supported by GRK and β -arrestin in the presence of the adaptor protein-2 (AP-2) that facilitates translocation of the receptor- β -arrestin complex into CCP. In addition, the presence of GTPase proteins such as dynamin, which participates in the pinching of CCP from the cell surface, is crucial for processing of clathrin-dependent endocytosis that allows the complex to be moved to the early endosome. There are then two possibilities; the receptor either is degraded in lysosomes or dephosphorylated and recycled back to the cell surface (re-sensitisation) (Pierce *et al.*, 2002; Moore *et al.*, 2007) (**Figure 1.7**). The presence of (Tyr-X-X- ϕ where x is any amino acid, and ϕ is a bulky hydrophobic residue) at the C-terminus in the receptor is important in binding to the subunit of the AP-2. This regulates CCP-dependent GPCR internalisation and trafficking. Internalisation of NMUs has been confirmed by fluorescently-tagged pNmU-8 (Cy3B-pNmU-8) that can be inhibited by concanavalin suggesting the role of CCP-mediated internalisation (Brighton, 2005). Moreover, NMU2 has a tyrosine motif (YQSF) in its C-terminal indicating that this receptor is susceptible to AP-2-/clathrin-dependent internalisation (Marchese *et al.*, 2008). The Rab family of small GTPases is crucial in determining the fate of a GPCR. In addition, it has recently been indicated that sorting nexin 1 (SNX1) plays a role in endosomal to lysosomal GPCR sorting (Zhong *et al.*, 2002). Overexpression of a SNX1 carboxyl terminal-deletion mutant was able to impede endosome to lysosome sorting of PAR1 and thus markedly inhibit PAR1 degradation (Wang *et al.*, 2002). Whether SNX1 or other SNX proteins can mediate the endosomal to lysosomal sorting of GPCRs other than PAR1 remains to be determined. Moreover, receptor ubiquitination (an enzymatic, protein post-translational modification process) is integral in receptor degradation by means of lysosomes (Seachrist *et al.*, 2003; Drake *et al.*, 2006). Ubiquitin-dependent lysosomal degradation is applicable to GPCRs including vasopressin receptor (V_2R) (Martin *et al.*, 2003) and the protease-activated receptor2 (PAR2) (Jacob *et al.*, 2005).

1.4.4 The role of β -arrestins in the termination and transduction of GPCRs signals

Activation of GPCRs on the cell surface by ligand binding promotes functional signalling via G protein-dependent and independent pathways (Pierce *et al.*, 2002) (**Figure 1.5**). In addition, ligand binding to GPCRs induces phosphorylation of intracellular domains within receptors, the binding of β -arrestins and internalisation of the ligand-receptor- β -arrestin complex into intracellular compartments leading to signal termination, signal propagation and receptor re-sensitisation (Moore *et al.*, 2007; Marchese *et al.*, 2008) (**Figure 1.8**). Classical agonists bind the receptor and stabilise conformations that couple to and activate heterotrimeric G proteins and this results in canonical second-messenger signalling. Moreover, these activated receptors are substrates for G-protein-coupled receptor kinase (GRKs). After phosphorylation by GRKs, receptors bind β -arrestins sterically interdicting further G-protein signalling. This results in G-protein signal cessation, leading to receptor desensitisation. In addition, β -arrestins scaffold receptors to membrane-trafficking machinery and therefore cause receptor internalisation from the cell surface and sequestration from G proteins.

It has been recently shown that GPCRs exhibit different patterns of agonist-induced β -arrestin interaction, which allows the receptors to be grouped into two distinct classes. Class A receptors include the β_2 and α_{1B} adrenoceptor, μ opioid, endothelin A and dopamine D_{1A} receptors. These receptors bind to β -arrestin-2 with higher affinity than β -arrestin-1 and their interaction with β -arrestins is transient. β -arrestins are recruited to the receptor at the plasma membrane and translocate with it to clathrin-coated pits; however, the receptor- β -arrestin complex dissociates upon internalization of the receptor, such that, as the receptor proceeds into an endosomal pool, the β -arrestin recycles to the plasma membrane (Zhang *et al.*, 1999). Class B receptors, represented by the angiotensin AT_{1A} , neurotensin 1, vasopressin 2, thyrotropin-releasing hormone and neurokinin NK-1 receptors, bind to β -arrestin-1 and β -arrestin-2 with equal affinity. These receptors form stable complexes with β -arrestins, such that the receptor- β -arrestins complex internalizes as a unit that is targeted to endosomes (Zhang *et al.*,

1999; Oakley *et al.*, 2000b). By analogy with the known crystal structure of visual arrestin, β -arrestins are thought to be composed of two major structural domains, *N* and *C*, each comprising a seven-stranded β sandwich (**Figure 1.6**). Based upon mutagenesis studies performed using both β -arrestins and visual arrestins, the β -arrestins are comprised of two major functional domains, an *N*-terminal (A) domain responsible for recognition of activated GPCRs and a *C*-terminal (B) domain responsible for secondary receptor recognition. The A and B domains are separated by a phosphate sensor domain (P) (**Figure 1.6**). The functionally identified A and B domains correspond approximately to the *N* and *C* domains identified crystallographically. N (R1)- and C (R2)-terminal regulatory domains reside at either end of the protein (Luttrell *et al.*, 2002). The R2 domain contains the primary site of β -arrestin-1 phosphorylation, S412, as well as the LIEF (amino acid residues **LIEF**) binding motif for clathrin and the RXR binding motif for β_2 -adaplin (AP2). The recognition domain for inositol phospholipids (IP₆) resides within the B domain. One or more PXXP motifs located within the A domain of β -arrestin-1 mediates binding to the c-Src-SH3 domain. The MAP kinase, JNK3, and possibly other MAP kinases (MAPKs), interact with β -arrestin-2 via a consensus MAP kinase recognition sequence, RRSLHL, located within the B domain. Less precisely defined interactions, such as those between β -arrestin-1 (1-185) and Ask1 and Src-SH1 domains, β -arrestin-1 and NSF, and β -arrestin-2 and Mdm2, are also shown (**Figure 1.6**). Regions of the protein involved in receptor or membrane recognition are shown in blue; those involved in controlling β -arrestin interaction with the endocytic machinery are shown in red, while proposed interactions between β -arrestin and signalling proteins are shown in green (Luttrell, 2002). The signalling pathway (as a result of activation) needs to be interdicted; otherwise cell death or uncontrolled proliferation could occur. Therefore, in addition to its role in terminating receptor activation, the degradation of molecules produced by an activated receptor is facilitated by β -arrestin. For example, different enzymes including diacylglycerol kinase (DGK) and phosphodiesterase (PDE4) (as a result of mAChR and β -adrenoceptor activation, respectively) are recruited by β -arrestin resulting in DAG and cAMP degradation into phosphatidic acid (PA) and AMP, respectively (Perry *et al.*, 2002; Nelson *et al.*, 2007).

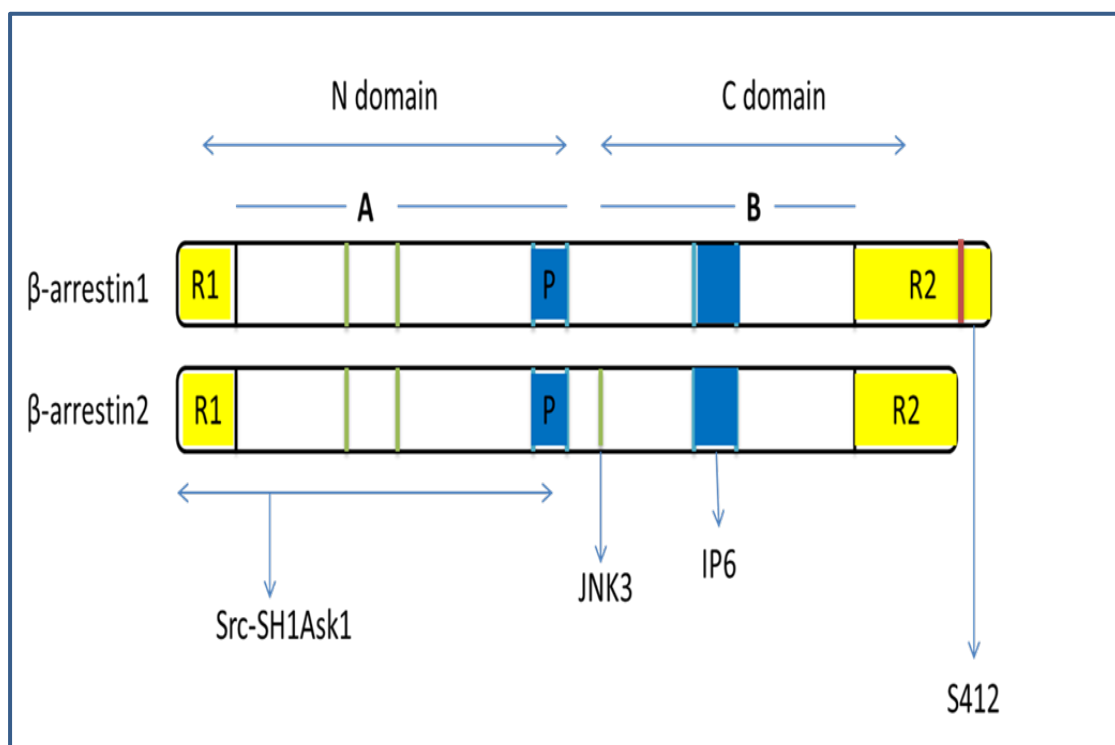


Figure 1.6 putative domain architecture of the β -arrestins (Luttrell *et al.*, 2002)

The β -arrestins are comprised of two major functional domains, an *N*-terminal domain responsible for recognition of activated GPCRs and a *C*-terminal domain responsible for secondary receptor recognition. The *N* and *C* domains are separated by a phosphate sensor domain (P). The functionally identified *N* and *C* domains correspond approximately to the *N* and *C* domains identified crystallographically. R1- and R2-terminal regulatory domains reside at either end of the protein. The R2 domain contains the primary site of β -arrestin-1 phosphorylation, S412, as well as the LIEF binding motif for clathrin and the RXR binding motif for β_2 -adapatin (AP2). The recognition domain for inositol phospholipids (IP₆) resides within the B domain. The MAP kinase, JNK3, and possibly other MAP kinases (MAPKs), interact with β -arrestin-2 via a consensus MAP kinase recognition sequence, RRS_LH_L, located within the B domain. Regions of the protein involved in receptor or membrane recognition are shown in blue; those involved in controlling β -arrestin interaction with the endocytic machinery are shown in red, while proposed interactions between β -arrestins and signalling proteins are shown in green.

1.4.5 GPCRs dephosphorylation

Dephosphorylation is a critical mechanism of GPCR re-sensitisation. After stimulation, the phosphorylated β_2 AR, for instance, appears in an endosomal vesicle fraction enriched with protein phosphatase type 2A (PP2A) activity (Pitcher *et al.*, 1995). It has been suggested that receptor internalisation is required for receptor dephosphorylation within the intracellular compartments, leading to receptor recycling and re-sensitisation. The β_2 AR, for instance, is phosphorylated in response to agonist stimulation and dephosphorylated after 20 min recovery in agonist-free media (Anborgh *et al.*, 2000).

PP2A is a cytosolic enzyme that is a member of a diverse family of phospho-serine and phospho-threonine specific enzymes expressed in eukaryotic cells (Zolnierowicz, 2000). Dephosphorylation of the β_2 AR could occur in acidified vesicles because the association of the receptor with PP2A could be prevented by the neutralization with ammonium chloride (Krueger *et al.*, 1997). A β -arrestin 2 β AR2-PP2A complex, in addition, is a signalling intermediate of the dopamine D2 receptor (Beaulieu *et al.*, 2005). Endocytic vesicles that are formed by invagination and pinching of clathrin-coated pits become uncoated in the cytoplasm and fuse with specialized membrane organelles known as endosomes, from which receptors and their ligands are sorted to various intracellular destinations. The pH of endocytic organelles and lysosomes is acidic, and acidification and its regulation constitute an important part of endosome maturation. Early endosomes have a pH in the 6.8–6.1 range, whereas the late endosomes in the 6.0–4.8 range and in lysosomes the pH can drop to values around 4.5 (Maxfield *et al.*, 1987). The low pH not only provides a better environment for hydrolytic reactions, but it is also essential for membrane trafficking, for the sorting and routing of cargo, for the inactivation of internalized ligands-receptor complexes (Huotari *et al.*, 2011).

Some phosphorylated receptors are rapidly dephosphorylated by protein phosphatase(s) at or near the plasma membrane directly following receptor activation. This suggests that these different mechanisms of receptor dephosphorylation could occur at different phosphorylation sites and this has been shown for the somatostatin receptor (Ghosh *et*

al., 2011). There also can be a mixture of dephosphorylation events. Thus, for example the NK₁R can be internalised, dephosphorylated, recycled and re-sensitised (Grady *et al.*, 1995), but some desensitised NK₁Rs remain at the cell surface where they are dephosphorylated by PP2A (Murphy *et al.*, 2011). Substance P (SP) induced association of β -arrestin 1 and PP2A with noninternalised NK₁R, since β -arrestin 1 knockdown prevented SP-induced association of cell-surface NK₁R with PP2A. This suggests that this interaction is mediated by β -arrestin. This rapid receptor dephosphorylation requires the scaffolding function of β -arrestin to recruit protein phosphatase(s) which in return prevent other forms of β -arrestin-dependent signalling.

Because nothing is known about the protein phosphatases responsible for NMU2 dephosphorylation and re-sensitisation, the mechanism of NMU2 re-sensitisation and the role of PP2A in this process were examined.

1.5 Ligand-receptor pseudo-irreversible binding and dual coupling of NMUs in recombinant systems

It has been indicated by previous studies in our laboratory that HEK293 cells stably express either NMU1 or NMU2 (HEK-NMU1 and HEK-NMU2, respectively) that increases in $[Ca^{2+}]_i$ observed on application of different NmU analogues did not return to basal levels even with extensive washing. In addition, no Ca^{2+} response was observed on re-application of NmU (Brighton *et al.*, 2004b; Alhosaini, 2011). Under these conditions, it was not clear whether a rapid complete of NMU1 and NMU2 desensitisation or a pseudo-irreversibility of NmU-binding occurred. Furthermore, this irreversible binding was proposed on the basis of inability to remove fluorescently-tagged pNmU-8 (Cy3B-pNmU-8) from the NMU receptors even with extended wash periods or even with displacing it by addition of 10-fold excess of unlabelled NmU (Brighton *et al.*, 2004b). This phenomenon (irreversible-binding) has been demonstrated by several GPCRs including substance P (SP), since repetitive application of SP in KNKR cells did not evoke repetitive $[Ca^{2+}]_i$ signalling via a neurokinin-1 receptor even with washing to remove ligands (Schmidlin *et al.*, 2001). Low pH solutions have been successfully used to remove high-affinity peptide ligands from their receptors at the cell-surface (Haigler *et al.*, 1980; Koenig *et al.*, 1997). Thus, this approach has been successfully exploited in our laboratory in order to remove receptor-bound Cy3B-pNmU-8. Washing with pH 7.4, 4, 3.5, 3 for 30 s failed to do so, while a rapid washing (15-25) at pH 2.0 was sufficient to completely displace Cy3B-pNmU-8 from the cell membrane. this can be achieved without affecting cell viability and their ability to respond to agonist re-application, since re-stimulation of the cells with pNmU-8-Cy3B (10 nM) restored fluorescence at the cell surface (Brighton *et al.*, 2004b; Alhosaini, 2011). In addition, Cy3B is considered to be relatively acid-insensitive (Amersham Bioscience, Fluorescence Screening Guide). The possibility that this irreversible binding result from a rapid and full NMUs desensitisation was observed by the fact that NK1 receptor required 3 h recovery to show full recovery of Ca^{2+} responses to SP (Schmidlin *et al.*, 2001).

In contrast to inhibition of forskolin-mediated cAMP generation (Hosoya *et al.*, 2000; Aiyar *et al.*, 2004; Brighton *et al.*, 2004b), activation of either NMU1 or NMU2 by

NmU or NmS resulted in an increase in $[Ca^{2+}]_i$ (Fujii *et al.*, 2000; Hedrick *et al.*, 2000; Hosoya *et al.*, 2000; Howard *et al.*, 2000; Raddatz *et al.*, 2000; Shan *et al.*, 2000; Aiyar *et al.*, 2004), PLC activity (Aiyar *et al.*, 2004; Brighton *et al.*, 2004b), arachidonic acid release (Fujii *et al.*, 2000; Aiyar *et al.*, 2004; Brighton *et al.*, 2004b) and $InsP_x$ generation (Raddatz *et al.*, 2000; Szekeres *et al.*, 2000; Aiyar *et al.*, 2004; Brighton *et al.*, 2004a). Inhibition of AC activity is abolished by PTX pre-treatment, while increases in $InsP_x$ and $[Ca^{2+}]_i$ are PTX-insensitive, indicating $G\alpha_{q/11}$ and $G\alpha_i$ coupling, respectively (Aiyar *et al.*, 2004; Brighton *et al.*, 2004b). This dual coupling to $G\alpha_q$ and $G\alpha_i$ has been confirmed for many recombinantly GPCRs including A_3 adenosine receptor (Palmer *et al.*, 1995) and M_1 and M_3 mACh receptors (Offermanns *et al.*, 1994). On the other hand, this dual coupling has also been reported for the endothelin (ET_A) receptor in adult rat cardiac myocytes (Hilal-Dandan *et al.*, 1992; Hilal-Dandan *et al.*, 1994) and NMU receptors in the cultured colonic myocytes (Brighton *et al.*, 2008) that are not recombinantly expressed.

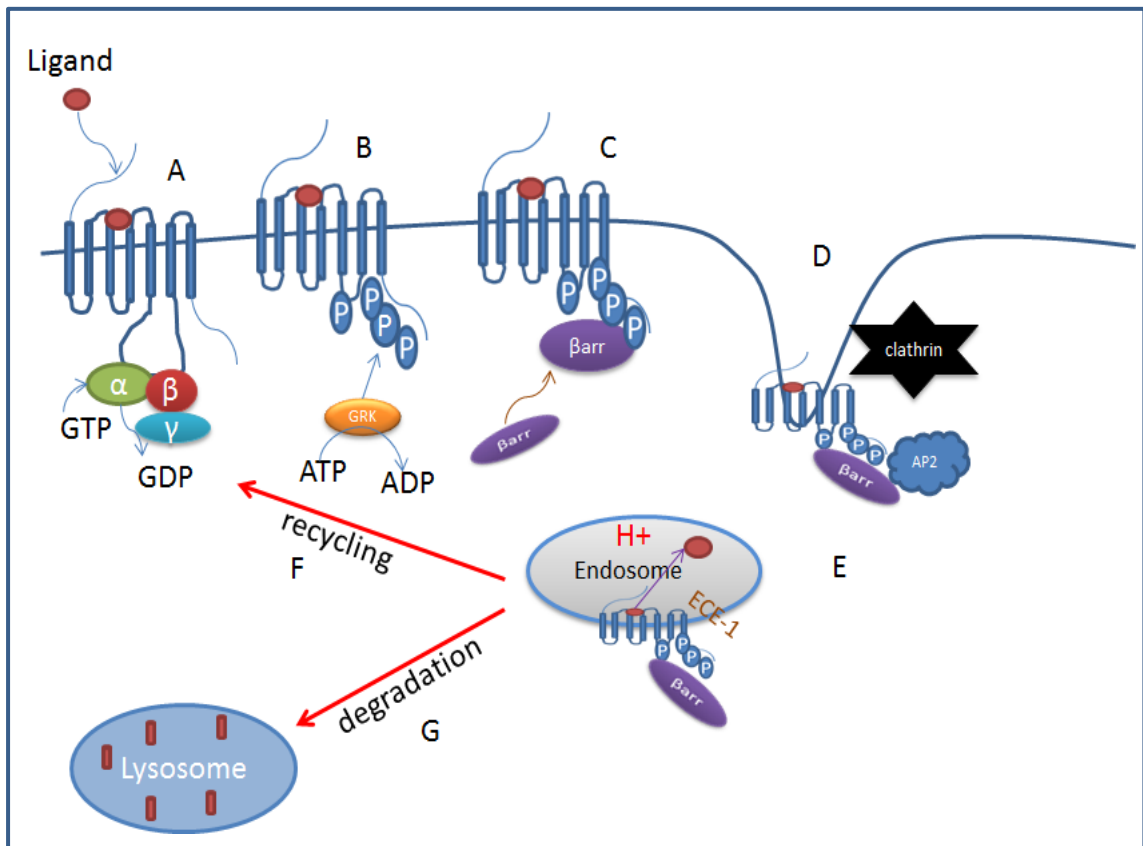


Figure 1.7 Major cellular events of GPCR signalling and trafficking

(A) Binding of agonist ligand to the GPCR initiates signalling by increasing guanine nucleotide exchange activity of the cognate heterotrimeric G protein, activating $G\alpha$ and releasing $G\beta\gamma$, each of which can transduce signals. (B) The majority of GPCRs are phosphorylated after agonist-induced activation, often by members of the GPCR kinase (GRK) family that selectively recognize agonist-occupied receptors. (C) Phosphorylated receptors are preferred substrates for association with arrestins. (D) Several arrestin isoforms also bind components of endocytic lattices (clathrin heavy chain, AP2 alpha subunit and PIP2), promoting agonist-dependent clustering of GPCRs in clathrin-coated pits. (E) GPCRs that engage the clathrin-dependent endocytic machinery internalize and are delivered to early endosomes, where it is thought that ligand dissociation and receptor dephosphorylation events occur as result of presence of low pH and ECE-1 activity, and where receptors engage distinct molecular sorting machineries that determine later trafficking fate. (G) Receptor sorting to lysosomes results in their proteolytic destruction and contributes to a long-term attenuation of cellular responsiveness (down-regulation) that is often observed after prolonged agonist

exposure. (F) Receptor sorting into a recycling pathway mediates non-destructive return of receptors to the plasma membrane. This is thought to support sustained cellular responsiveness, or promote functional recovery of cellular responsiveness from a desensitized state (re-sensitisation) after repeated agonist exposure (Irannejad *et al.*, 2014).

1.6 Endothelin-converting-enzyme: structure, function and potential role in endosomal ligand processing

1.6.1 Background

Two isozymes of ECE, ECE-1 and ECE-2, have been identified and make up a subfamily within this group of type II membrane-bound metalloproteases (Xu *et al.*, 1994; Noriaki *et al.*, 1995). Both enzymes have been shown to cleave big ET-1 to produce ET-1 with a similar overall profile of inhibitor sensitivity *in vitro* as well as in transfected cells. However, ECE-1 and ECE-2 exhibit the following striking differences; ECE-1 cleaves big endothelins in neutral pH, whereas ECE-2 functions in an acidic pH range. ECE-1 has a broader tissue distribution and is expressed at higher level than ECE-2. ECE-1 and ECE-2 have similar structures with a short *N*-terminal domain and a large *C*-terminal. In addition, they have a single transmembrane segment (Schweizer *et al.*, 1997).

Some studies (Padilla *et al.*, 2007; Roosterman *et al.*, 2007; Roosterman *et al.*, 2008; Pelayo *et al.*, 2011) have indicated that the receptor-ligand complex availability in the endosomes is controlled by the activity of the metalloendopeptidase endothelin-converting enzyme ECE-1 that determines stability of the peptide-receptor-arrestin complex and this in turn regulates receptor recycling and re-sensitisation. Therefore, the following section will focus on ECE-1.

Endothelin converting enzyme 1 is an enzyme which in humans is encoded by the ECE-1 gene. It is a membrane-bound metalloprotease that catalyses the conversion of inactive big endothelins into active endothelins (Schmidt *et al.*, 1994). Endothelin [ET] is a protein consisting of a family of three isopeptides, ET1, ET2 and ET3 (Yanagisawa *et al.*, 1988). ET1 is the most potent vasoconstrictor agent identified. It was isolated from the culture media of aortic endothelial cells. ET-1 is a 21-amino acid peptide. ETs are produced by cleavage of proproETs that are polypeptides of about 200 amino acids. The proproETs are then cleaved at a Trp-Val (Trp-Ile for big ET-3) site. The enzyme that is responsible of this process is endothelin-converting enzyme (ECE). It is a zinc metallopeptidase related to both neutral endopeptidase and the Kell blood group antigen.

1.6.2 Structure

ECE-1 is a type II integral membrane protein and shows homologies to both EC-24.11 and the erythrocytes blood group antigen Kell (King, 1994) in several tissues such as brain.

ECE-1 is present as a disulphide-linked dimer of subunits 120-130 kDa, whereas E-24.11 is not present. In addition, ECE-1 is not inhibited by E-24.11 inhibitors such as thiorphan (Turner *et al.*, 1996). Moreover, ECE belongs to a family of zinc metalloproteinase that also includes neutral endopeptidase-24.11 (NEP) and the erythrocyte cell-surface antigen, Kell. Like other family members, ECE is a type II integral membrane protein consisting of a short *N*-terminal cytoplasmic domain, a single transmembrane domain, and a large extracellular domain that includes the active catalytic site of the enzyme comprising the *C*-terminal end of the enzyme. The protein contains ten highly conserved cysteine residues and ten N-linked glycosylation sites that help to stabilize the protein (Xu *et al.*, 1994). It also contains a HEXXH (His591, Glu592, X, X, His595, where X represents any amino acid) zinc-binding motif in the extracellular catalytic domain that is characteristic of zincin proteinases (Jiang *et al.*, 1992; Bode *et al.*, 1993). Therefore, the fundamental proteolytic mechanism of ECE-1 is similar to that of E-24.11. The *N*-terminal cytoplasmic domain of bovine ECE is similar to the rat and human sequences (> 92%) (Shimada *et al.*, 1995). Thus, ECEs cloned are likely to be structurally similar and thought to be membrane-bound proteinase with a short cytoplasmic *N*-terminus, a single transmembrane domain, and a large extracellular *C*-terminus containing catalytic domain.

All forms of ECE cross species have homology in amino acid sequence in their putative extracellular domains (> 95%). This indicates that ECE-1 in different species has the similar functions. Regarding ECE-1, Arg102 is conserved in all isoforms cross species, whereas Arg747 is replaced by glutamyl residue playing a role in substrate binding. Moreover, Glu648 residue is present in ECE (Moual *et al.*, 1991).

There are four ECE-1 isoforms (a, b, c, and d) that are derived from a single gene through the use of alternative promoters. These four isoforms show clear differences in both tissue distribution and sub-cellular localization. ECE-1a has 758 residues whereas ECE-1b has 770 residues and ECE-1c has 754 residues and lastly ECE-1d possesses 767 residues. All ECE-1 isoforms share a common C-terminal catalytic domain but are differentially distributed as a result of the differences in their N-termini (Laurent *et al.*, 2003); (Schweizer *et al.*, 1997; Azarani *et al.*, 1998a; Brooks *et al.*, 2000; Hunter *et al.*, 2006) (**Figure 1.8**). Immunofluorescence studies have revealed that in endothelial cells, ECE-1b and ECE-1d are mainly in endosomal membranes (Laurent *et al.*, 2003) (Schweizer *et al.*, 1997; Azarani *et al.*, 1998) whereas ECE-1a and ECE-1c are mainly present at the plasma membrane but with a minor localization in endosomes (Schweizer *et al.*, 1997; Laurent *et al.*, 2003).

Northern blot analysis indicates abundant expression of ECE-1 in different tissues, including lung, pancreas, placenta, adrenal gland, ovary and testis. ECE is present in cells of the male and female reproductive tracts. ECE-1 has been seen in a number of cancers (Ahmed *et al.*, 2000). It is correlated with tumour progression in prostate cancer (PC) and lung cancer (Ahmed *et al.*, 2000; Dawson *et al.*, 2006). ECE-1 has neutral pH optimum for hydrolysing big-endothelin Trp-21-Val-22 bond (Davenport *et al.*, 2006). Moreover, neurogenic inflammation is regulated by the release of neuropeptides. In order to inhibit the neurogenic inflammation, neuropeptide receptor inhibitors could be used. A recent study has indicated that substance P neurokinin-1 receptor is mediated by ECE-1 (Keeble, 2009). Therefore, it could be possible to inhibit ECE-1 in order to stop the re-sensitization process.

1.6.3 Functions and potential roles of ECE-1 in endosomal ligand processing

As it has been mentioned early, the ECE-1 isoforms are widely sub-cellular distribution, suggesting a diversity of physiological functions. Cleavage of big ET to ET has been suggested to be by cell-surface ECE-1. The ET is produced in the endoplasmic reticulum (ER). Approximately 200-residue preproendothelins are first cleaved by a furin-like processing protease(s) into biologically inactive intermediates called big ETs (Blais *et al.*, 2002). Big ET is then converted into a 21 amino acid biologically active peptide, called ET by cleaving the Trp²¹-Val²² bond by membrane ECE-1. Furthermore, it has been shown that despite ECE-1 has lower affinity for bradykinin than Angiotensin converting enzyme (ACE) and neprilysin (NEP), ECE-1 inactivates and hydrolyses vasodilator peptide bradykinin in the extracellular (Hoang *et al.*, 1997) suggesting that membrane ECE-1 plays a role in the metabolism of some circulating peptides resulting in initiating or terminating cellular functions.

Based on that, the possible roles of ECE-1 in endosomes have been suggested. In contrast to peptides including neuropeptide Y and angiotensin II (ATII) that are poorly cleaved under acidic conditions, it has been observed that some neuropeptides including substance P (SP), angiotensin I (ATI), bradykinin (BK), neurotensin and calcitonin gene-related peptide (CGRP) can be cleaved by ECE-1 with an acidic pH optimum (Fahnoe *et al.*, 2000b; Padilla *et al.*, 2007; Roosterman *et al.*, 2007). It has been shown that CGRP was not degraded at pH 7.4 up to 360 min, but completely degraded within 240 min at pH 5.5 when the 250 μ M of CGRP was incubated with 415 nM of recombinant human ECE-1 (rhECE-1), suggesting the pH-dependence of ECE-1 function (Padilla *et al.*, 2007). The same experiment indicated that CGRP was degraded by rhECE-1 in a concentration-dependent manner and that the degradation was inhibited by ECE-1 inhibitor, SM-19712. Moreover, rhECE-1 degraded BK at both pH 7.4 and 5.5 and the degradation was inhibited by ECE-1 inhibitor. It has also been demonstrated that there was no detectable degradation of ATII up to 480 Min at pH 7.4 and 5.5, but it was degraded at pH 5.5. Thus, the function of ECE-1 is likely to be peptide- and pH-dependent. Intracellular degradation was investigated using ¹²⁵I-His⁸CGRP in which HEK293 expressing recombinant receptor for CGRP was incubated with ¹²⁵I-His⁸CGRP, a heterodimer of the calcitonin receptor-like receptor (CLR) and receptor

activity-modifying protein 1 (RAMP1), for 10 min to allow internalisation followed by acid wash and further incubation. It has been demonstrated by HPLC using fractions of cells lysates that endocytosed CGRP was degraded. Also, this degradation was inhibited by ECE-1 and endosomal acidification inhibitors, SM-19712 and bafilomycin A₁ (an inhibitor of vacuolar-type H⁺-ATPase), respectively (Padilla *et al.*, 2007). Thus, because ECE-1 is present in endosomes, it was suggested that CGRP degradation by ECE-1 is likely to occur in endosomes (Padilla *et al.*, 2007). The same study has also indicated that ECE-1 or endosomal acidification inhibition prolonged the interaction between CLR and β -arrestins implying that the recycling and re-sensitisation of the CLR are regulated by ECE-1 (Padilla *et al.*, 2007).

It has been shown that endocytosed receptors can continue to signal by β -arrestin-dependent manner (G protein-independent manner) (Lefkowitz *et al.*, 2005). Dissociation of the ligand-receptor-arrestin complex may be facilitated by the degradation of endocytosed peptides in endosomes. Endosomal ECE-1 degrades SP and inhibition or knockdown of ECE-1 induced a prolonged interaction between β -arrestins and the NK₁R in endosomes (Roosterman *et al.*, 2007). ERK activation may be influenced by this because sustained ERK activation is enhanced by inhibiting either ECE-1 or endosomal acidification using SM-19712 or bafilomycin A₁ (Cottrell *et al.*, 2009). ERK activation in the cytosol and nucleus was promoted by SM-19712. However, a weak and transient interaction with β -arrestins in response to SP resulted from a C-terminally truncated NK₁R and ERK activation was not regulated by ECE-1 suggesting that SP-induced β -arrestins-mediated ERK activation is regulated by endosomal ECE-1 (Cottrell *et al.*, 2009). A variety of functions including anti-apoptotic and proliferative were regulated by SP-induced ERK activation. In contrast, cell death in the nervous system can also be mediated by ERK (Lu *et al.*, 2006) and the transcription factor and nuclear receptor, Nurr77 are phosphorylated by SP resulting in cell death via β -arrestin-dependent ERK activation (Castro-Obregon *et al.*, 2004).

Some peptides were degraded by ECE either in the extracellular fluid or endosomes thereby regulating signalling from the cell membrane or endocytosed receptors. Most of the ECE-1 inhibitors that have been developed are not selective. For instance, phosphoramidon, the first ECE-1 inhibitor, inhibited the pathophysiological effects of

big ET-1 (Matsumura *et al.*, 1990; Vemulapalli *et al.*, 1993), the secretion of ET-1 from cultured endothelial cells (Ikegawa *et al.*, 1990; Sawamura *et al.*, 1990). In contrast, this inhibitor has higher affinity for NEP and a low affinity for angiotensin-converting enzyme (ACE) (Kukkola *et al.*, 1995). Another selective inhibitor is FR901533 but it did not inhibit endogenous ET-1 production (Xu *et al.*, 1994). Cytotoxic inhibitors are PD 069185 and PD 159790 and inhibit the production of both ET-1 and big ET-1 (Ahn *et al.*, 1998). A current inhibitor, SM19712, 4-chloro-*N*-[[[4-cyano-3-methyl-1-phenyl-1*H*-pyrazol-5-yl) amino] carbonyl] benzenesulfonamide monosodium salt, was found through the screening of the Sumitomo Pharmaceutical Library (Patent No. EP 885890). SM-19712 did not inhibit NEP, and nine other metalloprotease enzymes at up to 100 μ M. Radio ligand binding to receptors including AT1R, AT2R, ETA, ETB, EGFR and eight other receptors was not influenced by SM-19712. Furthermore, the endogenous production of ET-1 in endothelin cells was inhibited by SM19712 (Umekawa *et al.*, 2000). Thus, it has been reported that SM-19712 is a potent and selective endothelin converting enzyme ECE-1 inhibitor, both in vivo and vitro (Umekawa *et al.*, 2000).

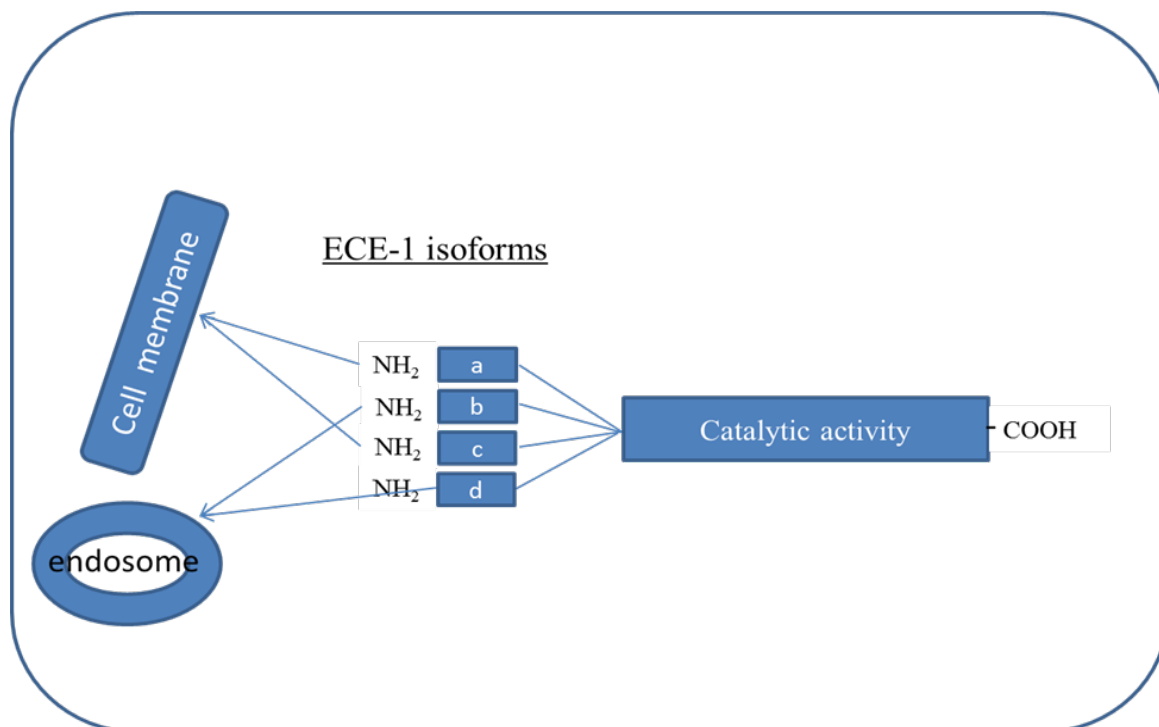


Figure 1.8 ECE-1 isoforms and their distribution.

The figure reveals the ECE-1 isoforms and indicates the different *N*-termini of each isoform. They share a common catalytic domain and differ only in their amino terminus, which determines their subcellular distribution: ECE-1a and ECE-1c are predominantly localized at the plasma membrane, whereas ECE-1b and ECE-1d are mostly found in endosomes. They are differentially tissue distributed.

1.7 GPCR-Activated ERK signalling pathways

The MAPK/ERK pathway consists of a chain of proteins in an intracellular signalling pathway that communicates a signal from a receptor on the surface of the cell, ultimately to the DNA in the nucleus of the cell. Currently, GPCRs are considered to utilize two primary types of transducers: G-proteins and β -arrestins.

It has been shown in recent years that multiple signal transduction pathways are engaged upon GPCR activation. One of the major cellular effectors activated by GPCRs is ERK. Both G-protein and β -arrestin mediated signalling pathways can lead to ERK activation (Ahn *et al.*, 2004; Goldsmith *et al.*, 2007) (**Figure 1.9**). Importantly, the subcellular destination of activated ERK1/2 is dependent on the activation pathway. For example, G-protein-dependent ERK activation results in the translocation of active ERK to the nucleus. In contrast, ERK activated via an arrestin-dependent mechanism remains largely in the cytoplasm. Un-phosphorylated ERK is found mainly in the cytoplasm associating with anchoring proteins, such as MEK1 and vinculin. Un-phosphorylated ERK is anchored in the cytoplasm forming a core signalling complex consisting of Raf, MEK, and ERK. When the receptor is activated, ERK1/2 are phosphorylated and released from the Raf/MEK/ERK signalling complex. The dissociated, phosphorylated ERK1/2 then binds to other cellular proteins carrying them to new destinations. The subcellular distribution of activated ERK is regulated by interactions with different proteins promoting ERK cytoplasmic and nuclear retention (Volmat *et al.*, 2001). It has been demonstrated that cytoplasmic confinement of ERK prior to its activation and nuclear transportation is under control of MEK1 (Fukuda *et al.*, 1997). Casein kinase 2 further phosphorylates ERK1/2 already phosphorylated via the G-protein-dependent pathway and they have the ability to bind to a nuclear anchor protein for nuclear translocation where different transcription factors can be activated and phosphorylated (Chuderland *et al.*, 2008; Plotnikov *et al.*, 2011).

The subcellular destinations of activated ERK1/2 can be selectively determined by specific ligands of the same GPCRs. For example, ERK can be activated by the μ -opioid receptor (MOR) agonists, morphine and etorphine resulting in morphine-induced ERK activation *via* a G-protein-dependent pathway and etorphine-induced ERK activation *via* a β -arrestin-dependent pathway (Belcheva *et al.*, 2005). The nuclear

translocation of pERK was not induced by morphine and the amount of pERK1/2 in the nucleus was similar to the basal level. Morphine-activated ERK1/2 remained in the cytoplasm in contrast to etorphine-activated ERK where pERK was found in nuclear fractions (Zheng *et al.*, 2008).

A wide variety of cellular processes including proliferation, differentiation, migration, survival, growth, growth arrest and apoptosis can be regulated by the ERK cascade.

The ERK pathway is activated by many stimuli including cytokines, growth factors, and GPCR ligands (Wei *et al.*, 2003; Ahn *et al.*, 2004; Leroy *et al.*, 2007). ERK activation by GPCRs can be mediated by the activation of Ras, Rap, PKC, tyrosine kinases (e.g., c-Src), transactivation of receptor tyrosine kinases, or *via* β -arrestins. It has also been indicated that ERK activation could be mediated by both pathways, G-protein and β -arrestins, for particular receptors and these pathways are independent of each other (DeWire *et al.*, 2007). For example, the ERK activation could be induced by the biased AT1R agonist SII that is incapable of activating G-protein signalling. Also, agonist and antagonist can activate ERK1/2. For instance, ERK1/2 can be activated by isoproterenol, the β 2-adrenergic agonist, by both pathways, whereas ERK1/2 can be completely activated by antagonist ICI118551 via the β -arrestin-dependent pathway (Azzi *et al.*, 2003). In addition, the time-course of both pathways is different. For example, ERK can be activated in two phases by parathyroid hormone (PTH) through its receptor PTH1R. The early rapid activation phase peaked at 5 min and a later sustained activation phase peaked at 30 to 60 min after stimulation (Gesty-Palmer *et al.*, 2006). The early phase of ERK activation was significantly diminished when the cells were treated with the PKA inhibitor, H89, or the PKC inhibitor, GF109203X, although these had little effect on the later phase of ERK activation. This suggests that the early phase of ERK activation is through a G-protein-dependent pathway, while the later phase ERK activation is through a G-protein-independent pathway. Indeed, knocking down both β -arrestin-1 and/or -2 altered the time-course of PTH-stimulated ERK activation. The rapid and transient ERK activation was observed at 5 min and then returned to basal levels suggesting that the late phase of ERK activation was dependent on a β -arrestin-dependent pathway.

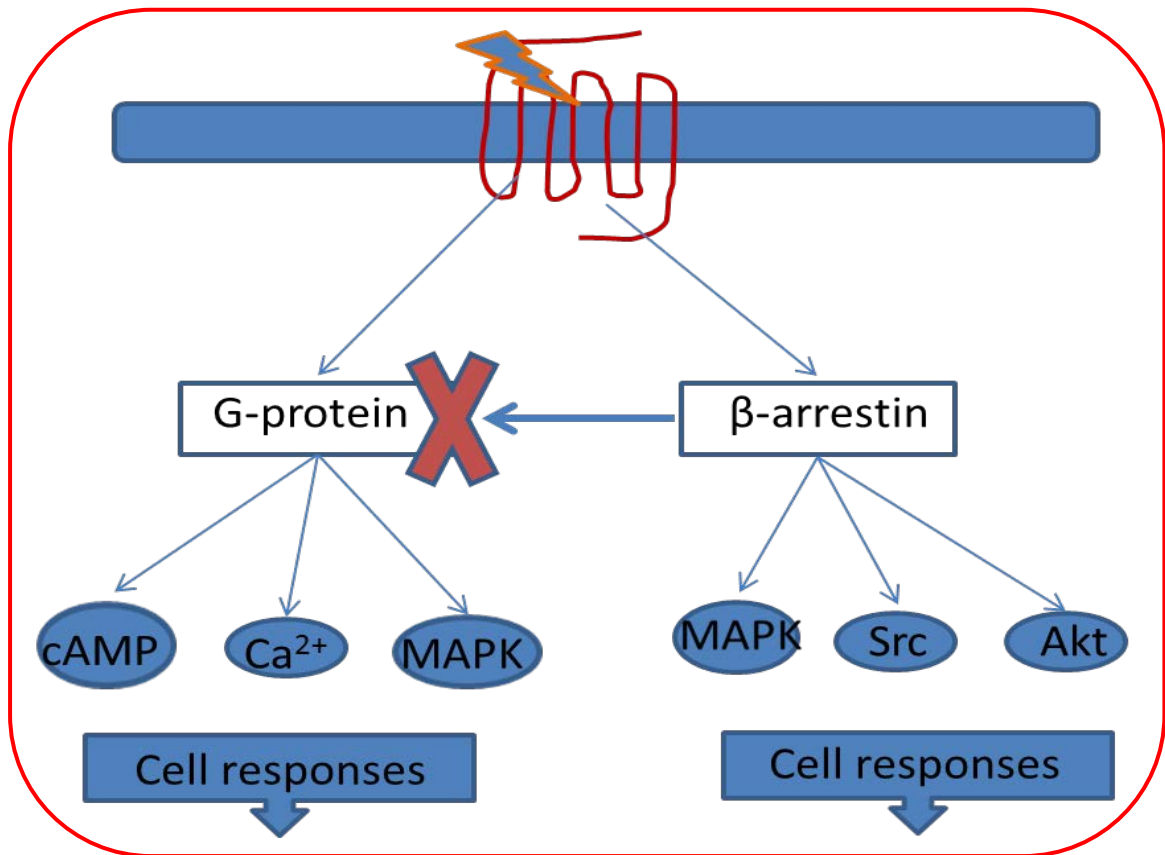


Figure 1.9 G-protein-dependent and G-protein-independent ERK1/2 activation pathways. Heterotrimeric G-proteins stimulate second-messenger systems such as IP₃ and (cAMP), as well as signal cascades such as (MAPKs). β-arrestins bind to GPCRs phosphorylated by GRKs, and thus terminate G-protein signalling and initiate a distinct set of signals, such as activation of MAPK, Src and Akt.

1.7.1 G-protein-dependent pathway

The activation of ERK cascades through G-protein α subunits including $G\alpha_s$, $G\alpha_i$, and $G\alpha_q$ along with G-protein $\beta\gamma$ subunit signalling to Ras has been demonstrated (Hawes *et al.*, 1995; van Biesen *et al.*, 1996; Jordan *et al.*, 1999; Saini *et al.*, 2007). PKC and PKA have been considered to be crucial components in G-protein-dependent signalling pathways. G-protein-dependent activation of ERK1/2 can be inhibited when the cells being treated with PKA and PKC inhibitors, H89 and GF109203X, respectively (Mochizuki *et al.*, 1999; Gesty-Palmer *et al.*, 2006).

1.7.1.1 $G\alpha_s$ stimulation of ERK1/2

Signals are transduced by $G\alpha_s$ from $G\alpha_s$ -coupled GPCRs to AC converting ATP to cAMP and subsequently to cAMP-mediated activation of PKA (Gilman, 1987). Consequently, cAMP as well as cAMP-activated PKA have been shown to play a major role in $G\alpha_s$ -mediated stimulation (Cook *et al.*, 1993; Wan *et al.*, 1998; Dumaz *et al.*, 2005; Houslay, 2006; Pearson *et al.*, 2006). The first observation that $G\alpha_s$ is involved in the regulation of ERK1/2 signalling module was from studies focused on defining the oncogenic pathways. It was shown that the stimulation of $G\alpha_s$ and subsequent generation of cAMP results in the activation of exchange protein directly activated by cAMP (EPAC) stimulating GDP–GTP exchange on Rap-1 (Laroche-Joubert *et al.*, 2002) and activation of guanine nucleotide exchange factor (GEF) specific for Rap-1 (Bos, 2006). The GTP-bound Rap-1, thus stimulated, activates B-Raf which subsequently activates ERK1/2. Another study also indicated that $G\alpha_s$ stimulation of ERK1/2 via Rap-1 involves a Rap-1 GEF other than EPAC in many cell types (Stork *et al.*, 2002). ERK1/2 can also be stimulated by $G\alpha_s$ via a pathway involving cAMP–PKA–Src-mediated activation of Rap-1-GEF known as Crk SH3 domain-binding guanine nucleotide-releasing factor (C3G). C3G stimulation of Rap-1 and Rap-1- is also able to mediate activation of B-Raf-MEK–ERK (Weissman *et al.*, 2004; Obara *et al.*, 2005; Wang *et al.*, 2006). It has also been demonstrated in different cell lines including COS-7, HEK293 (Norum *et al.*, 2003), thyrocytes (Tsygankova *et al.*, 2000), and melanoma cell lines (Amsen *et al.*, 2006) that $G\alpha_s$ -cAMP-mediated activation of Ras is involved in the stimulation of ERK1/2. In contrast, it has also been

demonstrated that the ERK pathways can be inhibited by the $G\alpha_s$ -mediated cAMP-PKA signalling pathway (Cook *et al.*, 1993; Wu *et al.*, 1993). PKA-mediated phosphorylation or Rap-1-mediated sequestration of a specific isoform of Raf (C-Raf) are thought to be involved in $G\alpha_s$ -mediated inhibition (Dhillon *et al.*, 2002) (**Figure 1.10**).

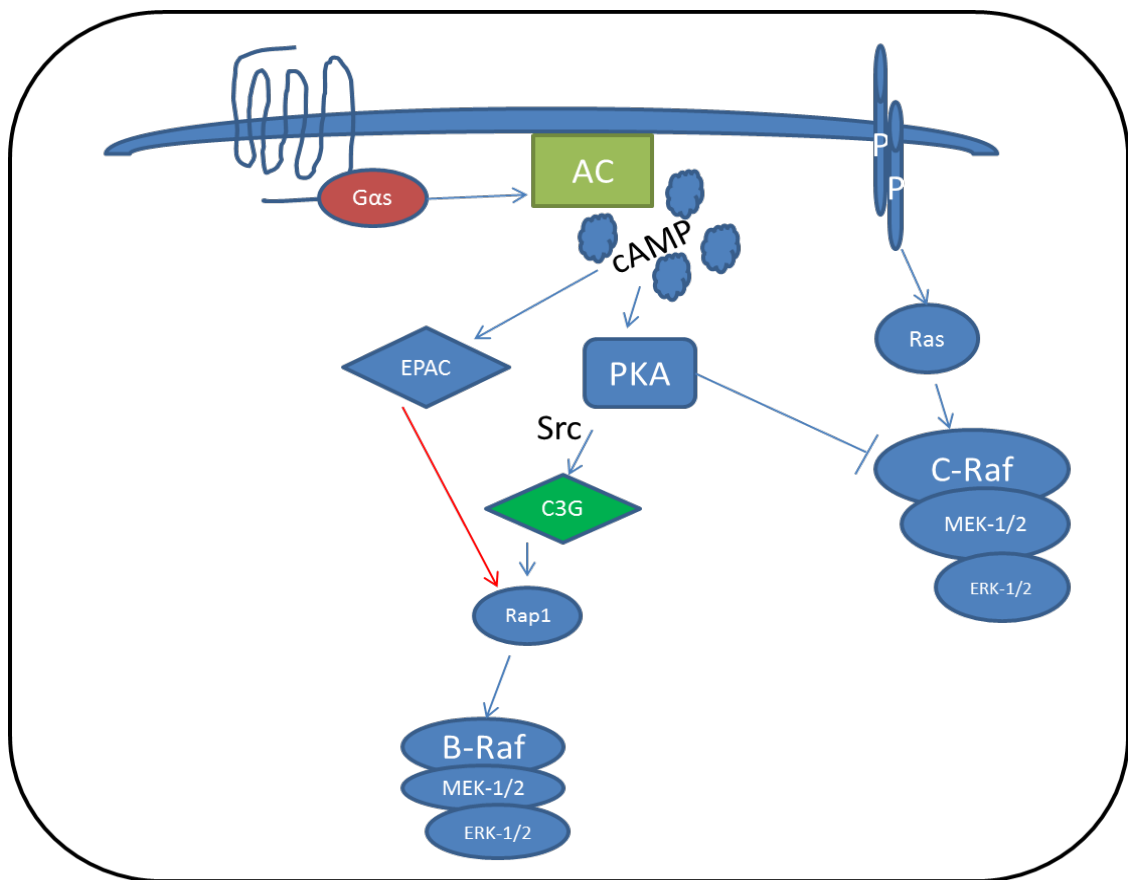


Figure 1.10 ERK1/2 regulation by $G\alpha_s$. The B-Raf-mediated activation of ERK1/2 is stimulated by $G\alpha_s$ via Rap-1 or Ras, and C-Raf-mediated activation of ERK1/2 is inhibited by phosphorylation of C-Raf by means of PKA. (adapted from (Goldsmith *et al.*, 2007)).

1.7.1.2 $G\alpha_i$ stimulation of ERK1/2

The $G\alpha_i$ family of G proteins includes the α -subunits $G\alpha_{i1}$, $G\alpha_{i2}$, $G\alpha_{i3}$, $G\alpha_z$, $G\alpha_{oA}$ and G_{oB} . A role for $G\alpha_i$ in the regulation of the ERK has been suggested by studies focused on defining the molecular basis for mitogenic activity of the activated mutants of $G\alpha_{i2}$ as the *gip2* oncogene in a tumor of the ovary (Lyons *et al.*, 1990). It has been suggested that two inhibitory pathways; effect on AC and effect on Rap-1 via Rap-1-GAP protein are involved in $G\alpha_i$ -dependent activation of ERK. The signal transduction role of $G\alpha_i$ is to couple specific receptors to the inhibition of AC (Johnson *et al.*, 1989; Tang *et al.*, 1992), since expression of the activated mutant of $G\alpha_i$ (*gip2*), resulted in a decrease in the accumulation of cAMP in cultured cells and subsequent decrease in PKA activity leading to a relief of the inhibitory effect of PKA on C-Raf, and the stimulation of Ras–C-Raf signalling to ERK (Radhika *et al.*, 2001). This was supported by the observation that activation of C-Raf was increased by the expression of $G\alpha_{i2}$ (Pace *et al.*, 1995). In contrast, the ERK pathway can be activated by $G\alpha_i$ via an alternate Ras-dependent mechanism (Pace *et al.*, 1995; Mochizuki *et al.*, 2000). It has been demonstrated that the expression of $G\alpha_{i2}$ and subsequent activation by A1 adenosine receptors results in the stimulation of ERK activity, since the expression of a PTX-resistant mutant of $G\alpha_{i2}$ in cells treated with PTX was used to control the effect of A1-adenosine receptors specifically coupled to the transfected PTX-resistant $G\alpha_{i2}$ (Pace *et al.*, 1995) (**Figure 1.11**). Cyclic AMP is synthesized from ATP by AC located on the inner side of the plasma membrane and anchored at various locations in the interior of the cell (Rahman *et al.*, 2013). AC is activated by a range of signalling molecules through the activation of AC stimulatory G ($G\alpha_s$)-protein-coupled receptors. However, AC is inhibited by agonists of AC inhibitory G ($G\alpha_i$)-protein-coupled receptors

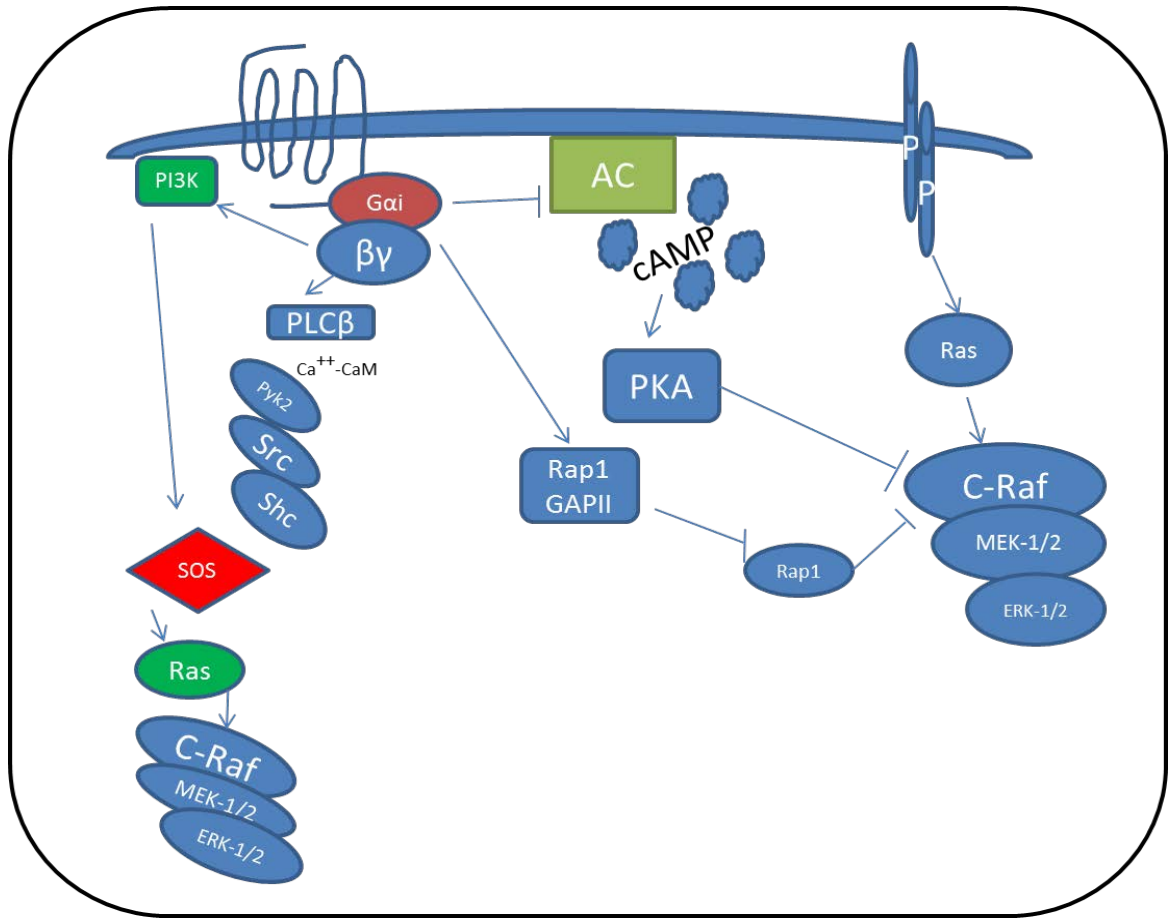


Figure 1.11 ERK1/2 regulation by Gα_i. Since the Gα_i-mediated decrease in cAMP levels and PKA activity relieves the inhibitory effect of PKA on C-Raf, this results in the stimulation of Ras-C-Raf signalling leading to ERK1/2 activation. ERK1/2 can also be activated by Gα_i through the disassociated βγ-subunits. PLCβ and PI3K can also be involved in βγ-mediated activation of ERK, both of which can be activated by βγ-subunits (adapted from (Goldsmith *et al.*, 2007)).

1.7.1.3 G $\beta\gamma$ i stimulation of ERK1/2

ERK can be stimulated by G α_i via mechanisms involving the dissociated $\beta\gamma$ subunits (Koch *et al.*, 1994). Such activation of ERK, has been demonstrated for a number of G α_i -coupled receptors including M $_2$ -muscarinic, α_2 -adrenergic, D $_2$ dopamine, A1 adenosine and lysophosphatidic acid receptors (LPARs) (Crespo *et al.*, 1994; Koch *et al.*, 1994). It has been demonstrated by transfection studies using COS-7 or HEK293 that PLC β is stimulated by $\beta\gamma$ released from G α_i -heterotrimers leading to (IP $_3$)-mediated increase in [Ca $^{2+}$] $_i$ and Ca $^{2+}$ -calmodulin-mediated activation of Pyk2 kinase. Pyk2 activates Src, which in turn stimulates the Shc adaptor protein, resulting in the activation of Ras via the Ras-GEF, mSOS (Hawes *et al.*, 1996; DellaRocca *et al.*, 1997) (**Figure 1.12**). It has also been demonstrated that $\beta\gamma$ -subunit transports signals through a Src- and Shc-independent mechanism involving the phosphorylation of dynamin II and its association with Grb2 (Kranenburg *et al.*, 1997). Since dynamin can connect Ras-GEF SOS to Ras, $\beta\gamma$ -mediated activation of Ras could be facilitated by dynamin in this case (Wunderlich *et al.*, 1999). As dynamin plays a role in vesicular endocytosis (Praefcke *et al.*, 2004) that is required for H-Ras-mediated activation of ERK1/2 (Roy *et al.*, 2002), it has been suggested that a critical role in $\beta\gamma$ -mediated activation of ERK1/2 could be played by dynamin II-mediated endocytosis.

1.7.1.4 G α_q stimulation of ERK1/2

Two mechanisms could be involved in ERK1/2 activation by G α_q , including PLC-DAG-PKC and PLC-IP $_3$ -Ca $^{2+}$. ERK1/2 can be stimulated either via G α_q -activated PKC by direct phosphorylation and activation of C-Raf (Ueda *et al.*, 1996; Schonwasser *et al.*, 1998), or through Ca $^{2+}$ -calmodulin-mediated activation of Pyk2 resulting in the activation of Ras and then ERK (Dikic *et al.*, 1996; DellaRocca *et al.*, 1997). This is likely to be cell type dependent. For example, ERK1/2 can be stimulated by G α_q via PKC-C-Raf in COS-7 and CHO cells expressing M $_1$ -muscarinic receptors (Luttrell *et al.*, 1995), and this is in contrast to G α_q -coupled bradykinin receptors that can activate ERK1/2 via Ca $^{2+}$ -calmodulin pathway involving Pyk2, Src and Ras (Dikic *et al.*, 1996). Moreover, the PKC- and Ca $^{2+}$ -mediated pathways are involved in ERK1/2 activation in HEK293 expressing α_1 -adrenergic receptor (DellaRocca *et al.*, 1997). A novel

mechanism has been observed for activating ERK1/2 via a $G\alpha_q$ involving DAG and Ca^{2+} -dependent Rap-1-GEF (Guo *et al.*, 2001). In this case, the release of DAG and Ca^{2+} results in activation of a Ca^{2+} - and diacylglycerol-regulated guanine nucleotide exchange factor (CalDAG-GEFI) that stimulates Rap-1 and this in turn can stimulate B-Raf and subsequently ERK1/2 (Guo *et al.*, 2001). As the $\beta\gamma$ -subunits dissociate from $G\alpha_q$ -coupled receptors and stimulate PLC β , it is likely that ERK1/2 can, therefore, be activated by $\beta\gamma$ -subunit. On the other hand, the $G\alpha_q$ -coupled receptor prefers using DAG/PKC- or IP_3/Ca^{2+} in order to activate ERK1/2 (Blaukat *et al.*, 2000). Also, it should be noted that ERK1/2 is activated by the $\beta\gamma$ -disassociated from $G\alpha_q$ via transactivation of RTK as in $G\alpha_q$ -coupled oxytocin receptors (Zhong *et al.*, 2003) (**Figure 1.12**). PKC isotypes are central signalling molecules coupling the $G\alpha_{q/11}$ family of G proteins to ERKs. Direct activation of PKC by tumor promoters such as PDBu leads to potent ERK activation (Burgering *et al.*, 1995). PKC is involved in the activation of ERK signalling because it is the major cellular effector for the tumor promoters. The involvement of PKC in $G\alpha_q$ -coupled GPCR activation of ERK is a little unclear. Fully PKC-dependent (Hawes *et al.*, 1995), PKC-independent (Crespo *et al.*, 1994b; Berts *et al.*, 1999), and partially PKC-dependent signalling to ERK via $G\alpha_q$ -coupled receptors (Crespo *et al.*, 1994a) has been reported.

1.7.1.5 $G\alpha_{12/13}$ inhibition of ERK

In some cells, ERK1/2 can be weakly stimulated in a Ras-dependent manner, whereas in some cells, ERK1/2 activation is attenuated by these cells at the levels of MEKs. Thus, the activation of ERK1/2 via $G\alpha_{12}$ and $G\alpha_{13}$ is attenuated in a cell-type-dependent manner (Voyno-Yasenetskaya *et al.*, 1996). For instance, Ras-mediated weaker stimulation of ERK1/2 is required for $G\alpha_{12}$ -induced G1-S phase cell cycle progression of NIH3T3 cells (Mitsui *et al.*, 1997). Although it remains to be demonstrated, it is possible that $G\alpha_{12/13}$ -mediated activation of protein phosphatase 5 (PP5) is involved in the attenuation of ERK1/2 by dephosphorylating Raf-1 at Ser-338 (von Kriegsheim *et al.*, 2006).

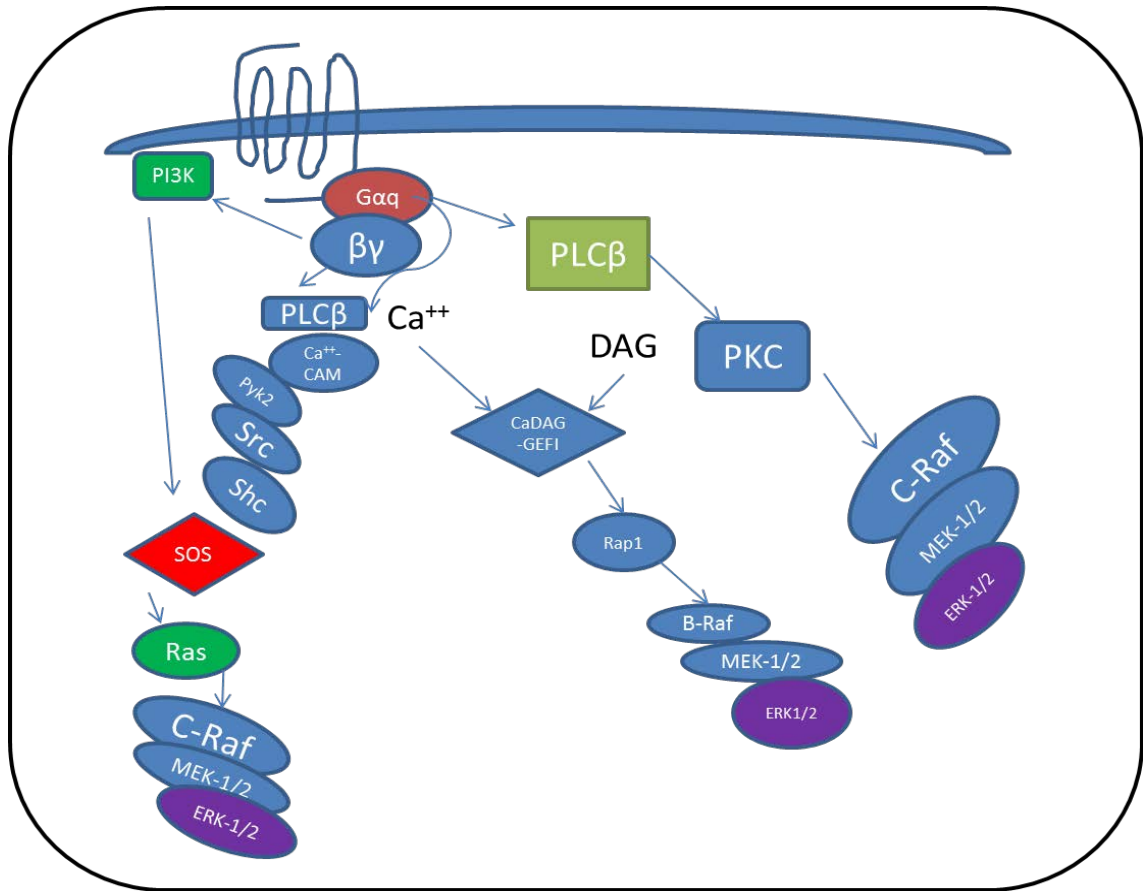


Figure 1.12 ERK1/2 regulation by $G\alpha_q$. ERK1/2 can be stimulated by $G\alpha_q$ via PKC and Ca^{2+} -dependent pathways. Similar pathway can also be stimulated by $\beta\gamma$ -subunits through their ability to stimulate PI3K and/or PLC β (adapted from (Goldsmith *et al.*, 2007).

1.7.1.6 Receptor tyrosine kinases in G-protein-mediated activation of ERK1/2

It has been demonstrated that ERK1/2 can be regulated by GPCRs through the transactivation of (RTKs). EGFR/ErbB (an event referred to as transactivation) has been demonstrated to be activated by several (GPCRs) including thrombin, Ang II, endothelin-1 (ET-1), carbachol, and (LPA) (Gschwind *et al.*, 2001). Several critical downstream signals and functions appear to be mediated by the EGFR transactivation by GPCRs, such as ERK activation (Eguchi *et al.*, 2003). This was observed in Rat1a cells stimulated with GPCR agonists including thrombin and endothelin resulting in the phosphorylation of (EGFR) and Her2 as well as ERK2 (Daub *et al.*, 1996). Treatment of these cells with the EGFR inhibitor tyrphostin (AG1478) indicated a role for EGFR in the activation ERK1/2 by GPCRs (Daub *et al.*, 1996). In addition, GPCR-mediated activation of ERK1/2 in different cell types that is dependent on EGFR transactivation has further been identified (Daub *et al.*, 1996; Eguchi *et al.*, 1998). EGFR is transactivated by $G\alpha_i$ and $G\alpha_q$ through a mechanism involving “*ectodomain shedding*” (an initial step for the activation of specific receptors) and generation of EGF-like growth factors that can activate the EGFR (Prenzel *et al.*, 1999). GPCRs transactivate EGFR by intracellular and extracellular mechanisms involving increases in Ca^{2+} (Zwick *et al.*, 1997; Soltoff, 1998; Iwasaki *et al.*, 1999), and activation of PKC, Src, and Pyk2 (Gschwind *et al.*, 2001). This results in the activation of matrix metalloprotease (MMP) proteins and/or a family of a disintegrin and metalloprotease (ADAM) through protein-protein interactions and phosphorylation (Higashiyama *et al.*, 2005; Ohtsu *et al.*, 2006). The ectodomain of membrane-bound EGFR ligands including heparin-binding EGF-like growth factor (HB-EGF) is cleaved by the activated transmembrane ADAMs, in particular, ADAM-10, -12, -15 and -17, leading to generation of EGF ligands that stimulate the EGFR (Schafer *et al.*, 2004; Higashiyama *et al.*, 2005; Ohtsu *et al.*, 2006). Also, β -arrestin may be involved in signalling by RTKs to ERK by G-proteins. For instance, G-protein-dependent and G-protein-independent pathways are involved in ERK activation by RTK ligands (Conway *et al.*, 1999). $G\alpha_i$ - and β -arrestins-mediated endocytosis is involved in the G-protein-dependent pathway. In contrast, a G-protein-independent pathway involves the recruitment of adaptor protein, activation of p42/p44,

and PDGF-activated platelet-derived growth factor receptors (PDGFR) by autophosphorylation on tyrosine residues. In the former pathway, β -arrestin and dynamin facilitate internalization of $G\alpha_i$ -activated GPCRs together with $G\alpha_i$ -activated cSrc, PDGFR, ERK1/2 and Grb2. It has been suggested that ERK activation in endosomes is promoted by the activation of Raf-1 by Src (Waters *et al.*, 2005).

An example of (RTKs) that undergo auto-phosphorylation is the EGFR. EGFR was the first discovered example of RTKs. Receptor-linked tyrosine kinases such as the (EGFR) are activated by extracellular ligands. Binding of epidermal growth factor (EGF) to the EGFR activates the tyrosine kinase activity of the cytoplasmic domain of the receptor (**Figure 1.13**). The EGFR becomes phosphorylated on tyrosine residues. Docking proteins such as growth factor receptor-bound protein 2 (GRB2) contain an SH2 domain that binds to the phosphor tyrosine residues of the activated receptor. GRB2 binds to the guanine nucleotide exchange factor Son of Sevenless (SOS) by way of the two SH3 domains of GRB2. When the GRB2-SOS complex docks to the phosphorylated EGFR, SOS becomes activated. Activated SOS then promotes the removal of GDP from a member of the Ras subfamily (most notably H-Ras or K-Ras). Ras then binds GTP and becomes active. Activated Ras activates the protein kinase activity of RAF kinase. RAF kinase phosphorylates and activates MEK (MEK1 and MEK2). MEK phosphorylates and activates a (MAPK) (**Figure 1.13**).

In addition to the EGFR, other cell surface receptors can activate this pathway via GRB2 including Trk A/B, fibroblast growth factor receptor (FGFR) and platelet-derived growth factor receptors (PDGFR).

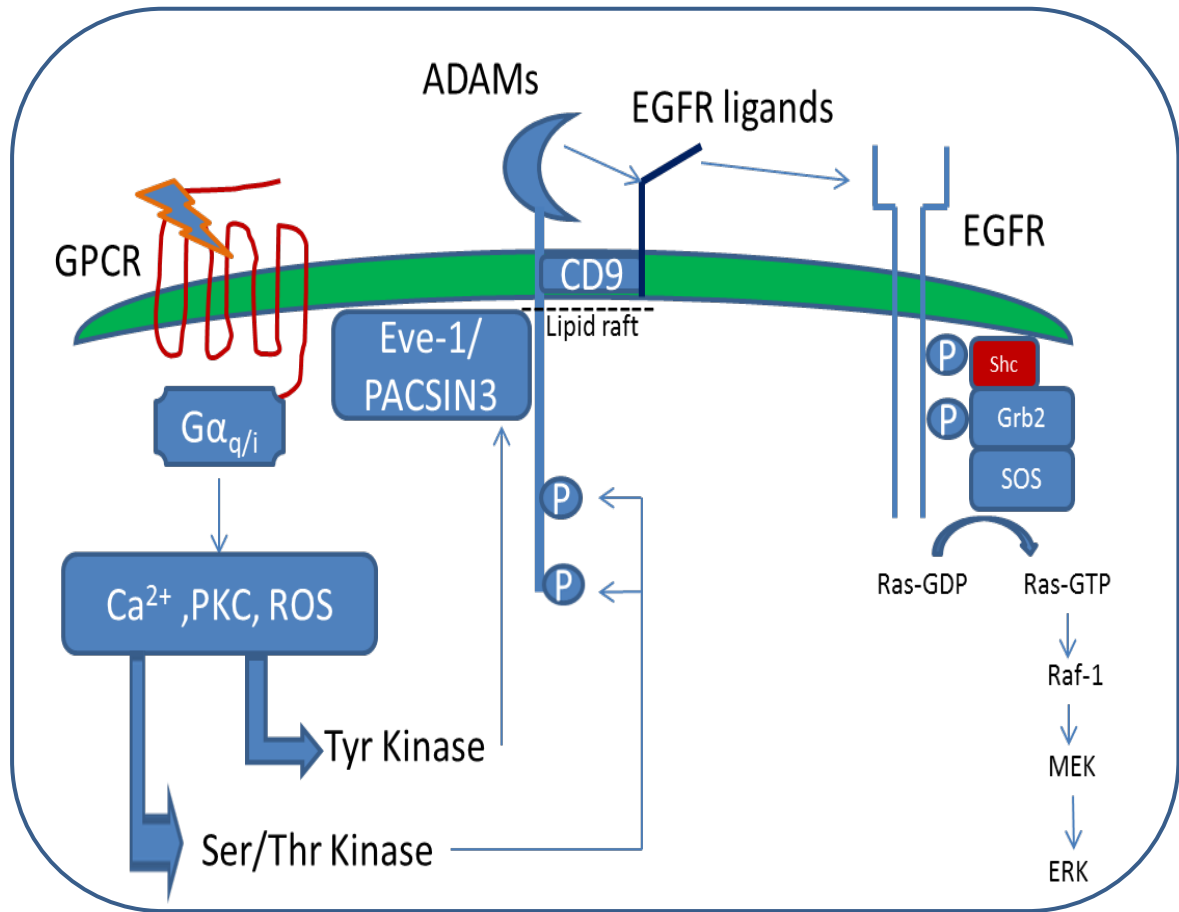


Figure 1.13 Proposed signalling mechanism leading to ADAM-dependent transactivation by GPCRs

GPCR-dependent signal transduction, ADAM kinases and interacting protein together with specific membrane localization such as in lipid rafts might be involved in ADAM activation by GPCRs leading to EGFR ligand shedding and subsequent EGFR transactivation. (EGF) binds to (EGFR) in the cell membrane, starting the cascade of signals. Further, phosphorylation (P) activates (MAPK), also known as (ERK). The signal then enters the cell nucleus and thus causes transcription of DNA leading to alterations in protein production. PACSIN3 associates with ADAM12 through its SH3 domain and is required for HB-EGF shedding induced by PMA and in part by ANG II in HT1080 cells. Eve-1 can be associated with ADAM9, 10, 15, and 17 through its SH3 domain and is required for HB-EGF shedding induced by PMA or ANG II. Abbreviations; Protein kinase C and casein kinase substrate in neurons protein 3 (PACSIN3), Reactive oxygen species (ROS) (adapted from (Ohtsu *et al.*, 2006)).

1.7.2 G-protein-independent, β -arrestin-dependent pathways of ERK activation

In addition to their classic roles in desensitisation and internalisation, β -arrestins can also act as signalling scaffolds for many pathways, including (MAPKs). The MAPKs are a family of serine/threonine kinases including ERK1/2, p38 kinases, and the c-Jun N-terminal kinases (JNK1, JNK2, JNK3). ERK1/2 activation exemplifies the prototypical MAPK signalling module: ERK1/2, a MAPK, is phosphorylated by MEK, a MAPK kinase (MAPKK). MEKs are phosphorylated by a variety of Raf isoforms, (that are therefore, MAPKKKs). A MAPKKK activates a MAPK, which in turn activates a MAPK. It has been demonstrated that β -arrestin-1 can recruit c-Src to the β_2 -AR resulting in ERK activation (Luttrell *et al.*, 1999a; DeFea *et al.*, 2000). Moreover, it has been shown that agonist stimulation leads to the formation of a complex containing the activated receptor, β -arrestin1, Raf-1 and phosphorylated ERK (DeFea *et al.*, 2000).

β -arrestins can directly bind to Src family kinase recruiting them to an agonist-occupied GPCR. The complex of the receptor with endogenous β -arrestin and Src kinases has been observed in (CCPs) in HEK293 cells following stimulation of β_2 -ARs (Luttrell *et al.*, 1999a). Src has also been observed to be recruited to the NK₁R by β -arrestins in KNRK cells (DeFea *et al.*, 2000). The interaction between Src homology (SH) 3 domain of the kinase and proline-rich PXXP motifs in the β -arrestin-1 N domain contributes in the binding of Src to β -arrestin-1. The N terminal catalytic (SH1) domain of Src and additional epitopes in the N terminal of β -arrestin-1 are also involved in the binding of Src to β -arrestin-1 (Miller *et al.*, 2000). This binding does not prevent β -arrestin binding to the receptor (Luttrell *et al.*, 1999a; DeFea *et al.*, 2000). The recruitment of Src to β -arrestin is involved in many GPCR-mediated events including ERK1/2 activation (Luttrell *et al.*, 1999b; DeFea *et al.*, 2000) (**Figure 1.14**). Src kinase activity is required for ERK to be activated via a Ras-dependent pathway (Luttrell *et al.*, 1996), since inhibiting Src binding to (CCPs) blocks β_2 -AR-mediated activation of ERK1/2 in HEK293 cells highlighting the importance of the interaction between β -arrestin-1 and Src (Luttrell *et al.*, 1999b).

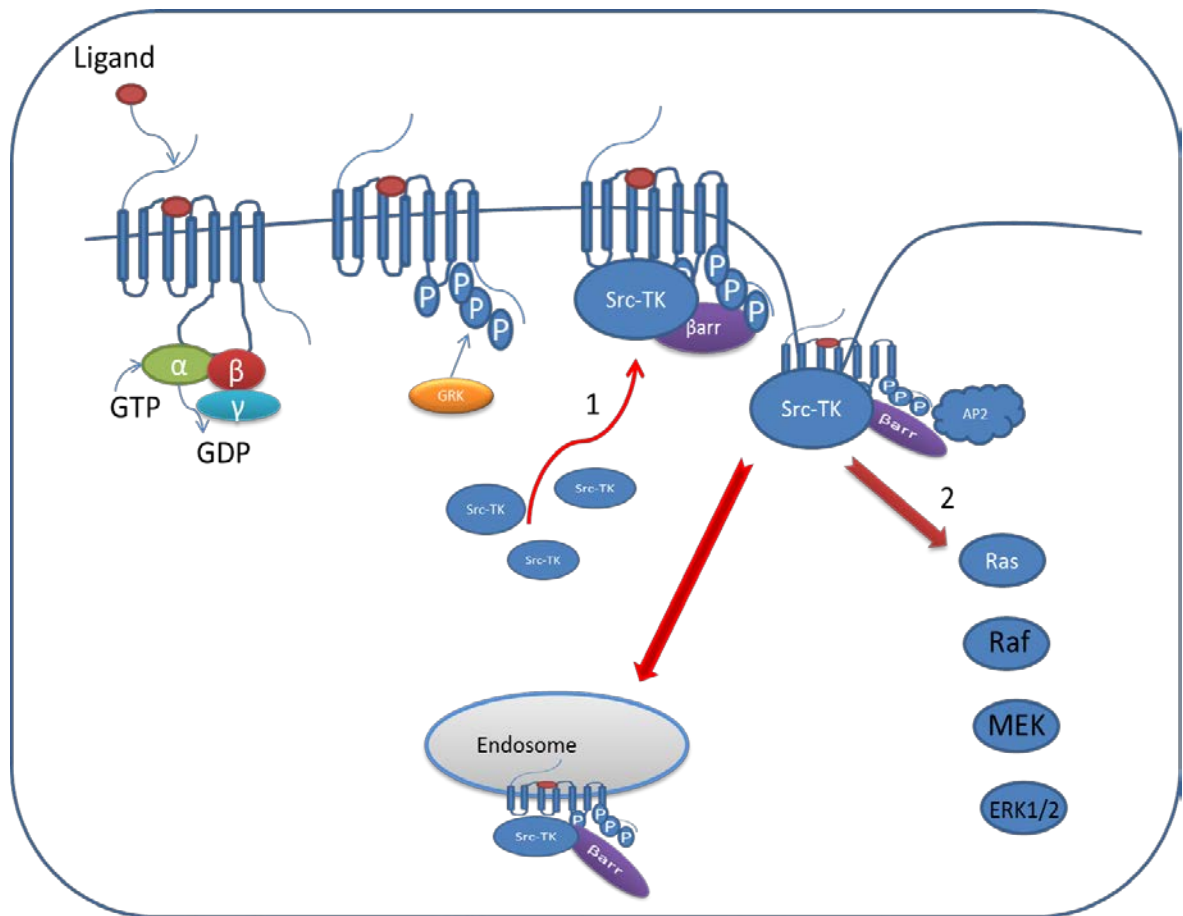


Figure 1.14 Proposed role of β -arrestins-dependent recruitment of Src kinases in GPCR-dependent, G-protein-independent ERK activation

The binding of β -arrestins to agonist-occupied GPCRs coincides with the recruitment of Src family tyrosine kinases, including c-Src to the receptor- β -arrestin complex (1). Several events have been reported to follow β -arrestin-dependent Src recruitment including Ras-dependent activation of ERK1/2 (2). Abbreviations; c-Src, proto-oncogene. TK, tyrosine kinase. GRK, G protein-coupled receptor kinase. β arr, β -arrestin. P, phosphate. GTP, guanosine triphosphate. GDP, guanosine diphosphate.

1.8 Aims and objectives

Although previous studies in our laboratory have demonstrated signalling by NMU1 and NMU2, including the mechanisms of receptor desensitisation and re-sensitisation, much remains to be investigated including the fate of the peptide after internalisation and driven into endosome where it could be degraded. The possibility of neuropeptides degradation by rhECE-1 was examined. Furthermore, the principle aim of the work described in this thesis was to further study the signalling pathways regulated by HEK-NMU2, in particular NMU2-ERK-mediated activation including the role of $G\alpha_q$ in ERK-mediated activation. Also, the sub-cellular localization of pERK following agonist activation of NMU2 using hNmU-25 and hNmS-33 will be examined. Moreover, the role of PKC in NMU2 re-sensitisation and ERK activation will be investigated.

Further, the roles of β -arrestin-1 and -2 in both re-sensitization of Ca^{2+} signalling and ERK activation by NmU and NmS at NMU2 will be explored. Further, the possibility of NmU degradation extracellularly will be examined. Moreover, given that NmU analogues are considered as valuable alternative strategies for the treatment of obesity, NMU2 re-sensitisation and its regulation by endosomal acidification and ECE-1 activity will be studied using some analogues to allow comparison to NmU.

Chapter 2
Materials & Methods

2.1 Materials

2.1.1 Materials (cell culture, and peptides)

Human embryonic kidney cells (HEK 293) stably expressing NMU1 and NMU2 (HEK-NMU1 and HEK-NMU2, respectively) have been previously characterised in a variety of signalling assays (Brighton *et al.*, 2004b; Brighton, 2005; Alhosaini, 2011). Water used was double-distilled (ddH₂O) and obtained through an ELGA System (ELGA, Marlow, UK). All the general chemicals, reagents and consumables were supplied by either Fisher Scientific (Loughborough, U.K.) or Sigma-Aldrich (Gillingham, U.K.) unless mentioned specifically. Tissue culture plastic ware and the cover-slips were from Nunc (VWR International, Lutterworth, U.K.). All mammalian cell culture reagents including, minimum essential medium (MEM), Dulbecco's phosphate-buffered saline (D-PBS) without calcium and magnesium, fetal calf serum (FCS), streptomycin and penicillin (100x, composition of stock solution: penicillin, 10,000 unit/mL and streptomycin 10,000 µg/mL) were supplied by Invitrogen (Paisley, U.K.). Peptides including hNmU-25, hNmS-33 and pNmU-8 were purchased from Bachem (Weil am Rhein, Germany). NmU analogues were provided by Dr. Piotr Ruchala; Department of Psychiatry and Biobehavioral Sciences, University of California at Los Angeles, USA.

Acrylamide/bis-acrylamide stock solution (30%, w:v) was supplied by National Diagnostics (U.K.) Ltd (Hessle, U.K.). Polyvinylidene fluoride (PVDF) transfer membrane was purchased from Millipore (U.K.) Ltd (Watford, U.K.). ECL⁺ reagents were from Amersham Biosciences (GE Healthcare U.K. Ltd, Chalfont, U.K.).

Fluo-4-acetoxymethyl ester (fluo-4-AM) and Lipofectamine RNAmixi for siRNA transfection were purchased from Invitrogen (Paisley, U.K.). Pre-stained protein molecular size marker was from New England Biolabs (Hitchin, U.K.).

ON-TARGET plus SMART pool consisted of four distinct siRNA duplexes of siRNA targeted to knockdown of human ECE-1 mRNA and the Scrambled siRNA were from ThermoFisher Scientific (New Jersey, U.S.A.) and Invitrogen (Paisley, U.K.), respectively. Flexi tube siRNA ARRB1, ARRB2 and All-stars Neg. siRNA Alex Fluor 488 were obtained from QIAGEN (Crawley, U.K.).

2.1.2 Concentrations of inhibitors, chemicals and antibodies used

Inhibitor/compound	Concentration (final concentration)	Supplier
AG1478, EGFR inhibitor	1 μ M	Sigma
Carbamylchlorine chloride, carbachol	0.3-300 μ M	Sigma
Cychlohexamide	5 μ g/mL; 17.5 μ M	Sigma
DL-thiorphan	10 μ M	Sigma
Dynasore	80 μ M	Tocris
Fostriecin sodium salt	300 nM	Tocris
GF109203X	1 μ M	Tocris
Recombinant human ECE-1	0.1 μ g/mL	R&D system
Ionomycin	2 μ M	Sigma
Monensin,	50 μ M	Sigma
Okadic acid	10 nM	Sigma
Pertussis toxin	100 ng	Tocris
Phorbol 12, 13-dibutyrate	1 μ M	Sigma
Ro 31-8220 mesylate	5 μ M	Tocris
SM-19712 hydrate	10 μ M	Sigma
UBO-GIB	1 μ M to 100 nM	Provided by Dr. Andrew Tobin
Anti-rabbit IgG HRP-linked antibody	1:2000 (pERK), 1:4000 (arrestins)	Cell signalling
Beta-arrestin 1&2 (D24H9) Rabbit	1:2000	Cell signalling
P-p44/42 MAPK (T202/Y204)(197G2) rabbit mAb	1:1000	Cell signalling
Dithiothreitol	15.4 mg/mL	Sigma
S6 ribosomal Protein (5G10)rabbit	1:20000	Cell signalling
Rabbit IgG polyclonal anti-ECE-1, GTX113676	1:1000	GeneTex
Hoechst staining solution	1:10,000	Sigma
siRNA β -arrestins 1 and/or 2	0.8 μ L/100 μ L \approx (60 nM)	Qiagen

2.1.3 Buffer used to study NmU-mediated signalling

Unless otherwise stated for NmU-mediated signalling experiments Krebs-HEPES buffer was used (KHB, composition: NaCl, 118 mM; KCl, 4.7 mM; HEPES, 10 mM; glucose, 11.7 mM; MgSO₄, 1.2 mM; NaHCO₃, 4.2 mM; KH₂PO₄, 1.2 mM and; CaCl₂, 1.3 mM, pH 7.4). BSA (0.1% w/v) was added to KHB in all NmU signalling experiments and the solution referred to simply as (KHB).

2.2 Methods

2.2.1 Cell culture

Cells were visually examined for quality and absence of contamination. Growth media was removed from the flask and the cells were gently washed twice using 5 ml of Dulbecco's-PBS to remove remaining FCS. Trypsin-EDTA (0.05% w/v trypsin, 0.04% w/v EDTA) (3 ml) was then added for approximately 3 min at 37° C to detach the cells from the flask's surface. Growth media (7 ml) was added after the cells had detached. The cells suspension was centrifuged at 140 xg for 4 min. The supernatant was then removed and the pellet suspended in growth medium to the desired confluence of cells. Flasks were sub-cultured every 5-7 days.

HEK-NMU1 and HEK-NMU2 were cultured in MEM supplemented with Earle's salts, FBS (10% v/v), non-essential amino acids, penicillin and streptomycin (100 µg/mL streptomycin and 100 units/mL penicillin sulphate) and glutamine 2 mM. All of the above cells were cultured in 75cm² flasks, maintained in 95% humidified air: 5% CO₂ environment at 37 °C and passaged every 4-5 days.

96 and 24 well/plates for cell growth were coated with 0.1% (w:v) poly-D-lysine hydrobromide. Before plating the cells, the 96 and 24 well/plates were incubated with 50 or 200 µL, respectively of poly-D-lysine for at least 20 min at RT and then washed with 200 µL of PBS. After removing PBS, the plates were ready for use.

2.2.2 Preparing frozen cell stocks

The cells (during the log phase of growth; 60-80%) were harvested as above and washed once with fresh medium. Cells were then suspended in a fresh medium and cell number determined. The cells collected by centrifugation (140 xg, 4 min) and re-suspended in freezing medium containing 90% FCS and 10% DMSO (v/v). Aliquots (1 ml) were transferred to a sterile cryotube and cooled to 4°C for at least 30 minutes and then transferred to either -80 °C or a liquid nitrogen store.

2.2.3 Recovery of frozen cells

Cells were removed from frozen storage and thawed quickly in a 37°C water bath with gentle agitation. Cells were transferred into a universal 30 ml tube containing suitable fresh medium (10 ml). The tube was then centrifuged (140 xg, 4 min) and the supernatant discarded. The cell pellet was then re-suspended in 10 ml of media and harvested again in order to remove any remaining DMSO. Cells were then cultured as described above.

2.2.4 Ca²⁺ signalling measurement using a NOVOstar plate-reader producing concentration response curve

Increase in free intracellular Ca²⁺ is typically measured as an increase in fluorescence caused by the binding of Ca²⁺ to a calcium chelator (dye) becoming fluorescent when binding calcium (Heding *et al.*, 2002). A NOVOstar plate-reader (BMG LABTECH, Offenburg, Germany) was used to measure the changes in [Ca²⁺]_i. The standard protocol is that the cells were pre-incubated with loading buffer (KHB) containing BSA (0.1% w/v) and fluo-4-AM (2 µM) as the fluorescent Ca²⁺ indicator and pluronic acid F-127 (0.036%, w/v) to facilitate the solubility of fluo-4 in the buffer (Heding *et al.*, 2002; Coopman *et al.*, 2010). Once the binding of Ca²⁺ associated with fluorescence, the increase in the fluorescence is monitored using an excitation wavelength of 488 nm with detection > 500 nm. The raw data are presented for the families of curves in terms of fluorescence, however, all subsequent data are presented as the calibrated [Ca²⁺]_i.

Cells were seeded into 96-well/plates at 10,000 cells/well and cultured for 24 h. Cell counts were achieved using a haemocytometer (Neubauer improved; Sigma-Aldrich, Poole, UK). In order to count the cells, they were suspended in 10 mL growth medium and mixed gently. 1 µL of cell suspension was then added between the haemocytometer and the cover glass. Cells inside the large square were counted and the average of 3-4 counts multiplied by 10⁴ to give approximate cell number in 1 mL of cell suspension. Cells were washed once with 1 ml of (KHB).

100 μ L of cell suspension was plated in poly-D-lysine coated 96-well plates for 24 h (Poly-D-lysine (0.1 mg/mL) was prepared by adding 9 mL KHB to 1 mL of a stock solution. 50 μ L or 200 μ L, (for 96 and 24 well/plate, respectively) of poly-D-lysine was added to each well and left for at least 20 minutes either at room temperature or at 4° C. Growth medium was removed gently and the cells were washed once with KHB and the cells were loaded with fluo-4-AM for 45 min (The concentration of fluo-4-AM was 2 μ M and the loading buffer was KHB-BSA (0.1%), pluronic acid F-127 (0.036%, w/v) (Granados *et al.*, 1997) and fluo-4-AM at 37°C and 5% CO₂). The cells were then washed twice with KHB and 100 μ L of KHB was added at 37°C. The change in fluorescence upon addition of buffer or ligand (20 μ L at speed of 230 μ L/s from reagent plate to measurement plate containing 100 μ L/well) was measured using a NOVOstar plate-reader. NOVOstar was adjusted to the required settings. The ligand had been prepared to the desired concentrations. A similar volume used to stimulate cells in the NOVOstar plate-reader was manually used in desensitisation experiments.

The $[Ca^{2+}]_i = Kd * (F - F_{min}) / (F_{max} - F)$ was used in order to calculate the intracellular calcium, where Kd of fluo-4-AM was 350 nM (Yamasaki-Mann *et al.*, 2009) and the calibration of the fluo-4 signal was taken by adding ionomycin, to equilibrate the concentration of intracellular and extracellular Ca²⁺, to a final concentration of 2 μ M. F_{max} was taken by manually adding 150 μ l of KHB-BSA buffer with a high concentration of Ca²⁺ (4 mM). This was measured for at least 10 min and the F_{min} was then obtained by replacing the buffer with 150 μ l of Ca²⁺-free KHB-BSA buffer with 2 mM EGTA and this was measured for at least 10 min.

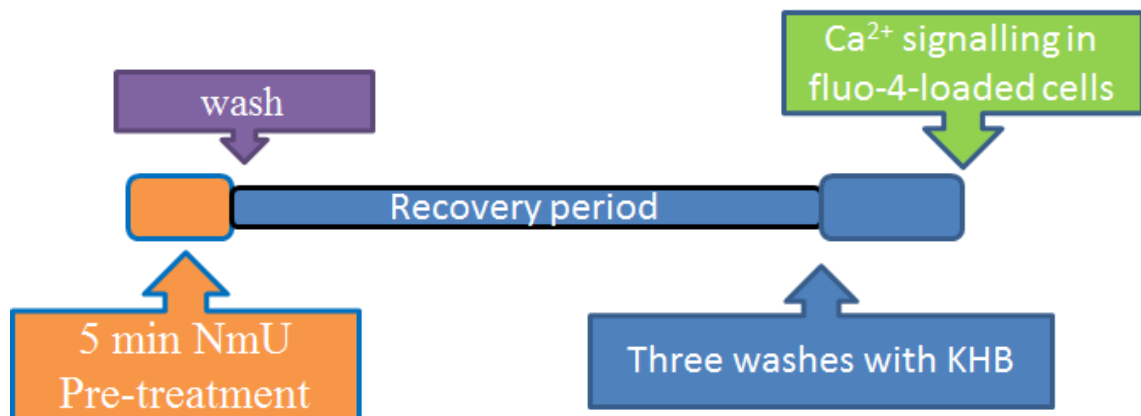
2.2.5 Data Analysis

Concentration-response curves were fitted using Prism (GraphPad Prism 6 Software Inc., San Diego, CA). All data shown are expressed as the mean of three experiments \pm S.E.M unless stated otherwise. For representative data, experiments were also performed to an n of three or more.

2.2.6 NMU re-sensitization protocol

The protocol used in this study was as follows: HEK-NMU cells were cultured for 24 h. Cells were then washed with KHB (unless otherwise stated) followed, by stimulation by ligand (30 nM, 5 min) (unless otherwise stated) and allowed to recover as required using normal media with no antibiotics (for the 6 h recovery period) or KHB (for periods less than 6 h recovery). The cells were then washed and loaded with fluo-4-AM in KHB for 45 min during the last 45 min of the recovery period. The inhibitors were added (30 min prior to stimulation) and present during the recovery time when required. The cells were washed with KHB and stimulated using a NOVOstar plate reader as shown below:

Protocol



2.3 Western blotting

2.3.1 Cell stimulation and sample preparation

Cell monolayers on poly-D-lysine coated 24-well plates were serum starved overnight. On the day of the experiments, growth medium was removed, and the cells were then washed twice with KHB (1 mL). To construct concentration-response curves for agonist-stimulated increases in extracellular signal-regulated kinase phosphorylation (pERK), cells were incubated with KHB (500 μ L) and challenged with KHB (100 μ L) alone or containing different concentrations of hNmU-25 (0.1-100 nM) for 5 min. For investigation of the time-course activation of pERK generation, cells were incubated with KHB (500 μ L). Cells were then challenged with KHB (100 μ L) or hNmU-25 (30 nM). Stimulation begun at the longest time-point first, allowing the reactions to be terminated at the same time. At the end of the reaction, cells were washed twice with ice-cold PBS and lysed by addition of ice-cold 2x sample buffer (Tris-HCL, 125 mM, SDS, 10% (w/v); glycerol, 20% v/v; bromophenol blue, 0.01% w/v; dithiothreitol, 250 mM (added on the day of the experiment, 200 μ L, pH 6.8). Following incubation on ice for 5 min, cell lysates were collected using a cell scraper and transferred to a new 1.5 mL microfuge tube. The supernatants were then centrifuged for 1 min at high speed at 4°C, then heated for 5 min at 100 °C, and then centrifuged in preparation for use.

2.3.2 Preparation of SDS-polyacrylamide gel and electrophoresis of proteins

A 10 % resolving gel (10 mL, composition: acrylamide, 30% v/v; Tris-HCL, 1.5 M, pH 8.8, sodium dodecyl sulphate (SDS), 10% w/v; ammonium persulfate (APS), 10% w/v; *N, N, N, N*,-tetramethylethylenediamine (TEMED), 0.06% v/v and water to 10 mL) was mixed gently and poured in-between two glass plates separated by two vertical 1.5 mm spacers of a Mini-BioRad electrophoresis system (Bio-Rad, Hemel Hempstead, UK). The top-layer of the gel was covered with water to ensure a flat edge. After 20 min, the gel was solidified and the top layer of water discarded carefully. A stacking gel (4 mL, composition: acrylamide, 30% v/v; Tris-HCL, 1 M, pH 6.8; SDS, 10% w/v; APS, 10% w/v; TEMED, 0.065 v/v and water to 4 mL) was poured onto the top of the resolving gel and a 10-well comb inserted to form loading wells. The gels were left to

solidify at RT for a further 20 min. The comb was then gently removed and washed by distilled water and then mounted into a Mini-BioRad gel electrophoresis tank. The gel tank and the upper loading tank were filled with running buffer (Tris-HCL, 25 mM, pH 8.6; glycine, 192 mM and SDS 0.1% *w/v*). 20 μ L of each sample was loaded into each well (or 5 μ L of samples in terms of β -arrestin experiments). The first well of each gel was loaded with a pre-stained protein ladder (2 μ L, Leon-Rot, Germany. Electrophoresis was performed using a POWER PAC 300 (Bio-Rad, Hemel Hempstead, UK) at 90 V for 100 min (until the bromophenol blue dye reached the bottom of the gel).

2.3.3 Transfer of proteins using the semi-dry electrophoresis technique

PVDF membrane and filter papers were cut to the size of the resolving gel. The membrane was then immersed in methanol (100%) for 10 s and then in H₂O for 2 min. Membrane and filter papers were then incubated for 10 min in transfer buffer (glycine, 40 mM; Tris, 48 mM; SDS, 0.0375% *w/v* and methanol, 20% *v/v*). The resolving gel was soaked in transfer buffer after removing the stacking gel. A blotting sandwich was made by placing three sheets of filter-paper cut to the size of the resolving gel on the negative plate followed by the PVDF membrane on top. The resolving gel was then placed on the top of the membrane and covered by a further three filter papers. The positive charged cover of the semi-dry transfer device was placed on the top of the sandwich. Using a POWER PAC 300 (Bio-Rad, Hemel Hempstead, UK), transfer was done at 15 V for 30 min.

2.3.4 Immunoblotting

Following transfer, the membrane was incubated in TBST (fat free milk, 5% *w/v*, 5 mL), composition : Tris-base, 50 mM, NaCl, 150 mM; Tween-20, 0.05% *v/v*, pH 7.5, at RT for 1 h with gentle rocking. The membrane was then washed three times using TBST 1 min each. The membrane was then incubated in a 50 mL Falcon tube overnight with TBST (BSA, 5%, 5 mL) containing either mouse monoclonal phosphor-p44/42 MAPK (ERK1/2) antibody (1:2000) or rabbit polyclonal p42 MAPK (ERK2) antibody (1:1000) with continuous rolling at 4 °C. the membrane was then washed three times 8 min each and followed by incubating the membrane in TBST (fat free milk, 5%, 5 mL) containing either goat anti mouse or rabbit IgG, HRP-linked secondary antibody

(1:3000) for 1 h at RT on shaking platform. The membrane was then washed three times 8 min each using TBST. Detection was carried out using UptiLight™ chemiluminescent reagent (1:1 v/v, 2 mL/membrane, 1 min) and exposure of membrane to X-ray film for 5-10 s, depending on the strength of the signal. Proteins of interest were detected by comparison of their size to the protein markers. The pERK signal was quantified as a relative to total ERK or ribosomal protein S6 (rpS6).

2.4 Live/Dead viability/cytotoxicity kit for mammalian cells (Fluorescence Microscopy Protocol)

The protocol used in this method is as suggested by manufacturer (Invitrogen). Briefly, the cells were cultured in 24 well/plates for 24 h as normal. On the day of the experiment, the cells were treated with the inhibitor for 30 min. The cells were then washed prior to the assay to remove serum esterase activity generally present in serum-supplemented growth media. 20 µL of the supplied 2 mM ethidium homodimer-1 (EthD-1) stock solution was added to 10 mL of sterile, tissue culture-grade D-PBS, vortexing to ensure thorough mixing. The reagents were then combined by transferring 5 µL of the supplied 4 mM calcein AM (component A) stock solution to the 10 mL EthD-1(component B) solution. 400 µL of the combined reagents was then added directly to the cells (after removal of the culture medium). The cells were then incubated for 30-45 minutes at room temperature. The polyanionic dye calcein is well retained within live cells, producing an intense uniform green fluorescence in live cells (excitation= ~495 nm, emission= ~515 nm). EthD-1 enters cells with damaged membranes and undergoes a 40-fold enhancement of fluorescence upon binding to nucleic acids, producing a bright red fluorescence in dead cells (excitation= ~495 nm, emission= ~635 nm). Finally, the labelled cells were viewed under the fluorescence microscope. The fluorescence intensity is related to the total number of cells present in the sample, which can be expressed in terms of percentages.

2.5 Protein digestion, analysis by mass spectrometry and data processing.

Products of rhECE-1 degradation of peptides were analyzed by LC-MS/MS using an RSLCnano HPLC system (Dionex, UK) and an LTQ-Orbitrap-Velos mass spectrometer (Thermo Scientific). Samples were loaded at high flow rate onto a reverse-phase trap column (0.3mm i.d. x 1mm), containing 5 μ m C18 300 Å Acclaim PepMap media (Dionex) maintained at a temperature of 37 °C. The loading buffer was 0.1% formic acid / 0.05% trifluoroacetic acid / 2% acetonitrile.

Peptides were eluted from the trap column at a flow rate of 0.3 μ l/min and through a reverse-phase PicoFrit capillary column (75 μ m i.d. x 400mm) containing Symmetry C18 100 Å media (Waters, UK) that was packed in-house using a high-pressure device (Proxeon Biosystems, Denmark). Peptides were eluted over a period of one hour using a gradient of 2%-45% acetonitrile and the output of the column was sprayed directly into the nanospray ion source of the LTQ-Orbitrap-Velos mass spectrometer.

To determine the identity of the degradation products, the LTQ-Orbitrap-Velos mass spectrometer was set to acquire a 1 microscan FTMS scan event at 60000 resolution over the m/z range 300-2000 Da in positive ion mode. The maximum injection time for MS was 500ms and the AGC target setting was $1e^6$. Accurate calibration of the FTMS scan was achieved using a background ion lock mass for C₆H₁₀O₁₄S₃ (401.922718 Da). Subsequently up to 10 data dependent HCD MS/MS were triggered from the FTMS scan. The isolation width was 2.0 Da, normalized collision energy 42.0. Dynamic exclusion was enabled. The maximum injection time for MS/MS was 250 ms and the AGC target setting was $5e^4$.

The raw data file obtained from each LC-MS/MS acquisition was processed using Proteome Discoverer (version 1.4.0.288, Thermo Scientific) and searched using Mascot (version 2.2.04, Matrix Science Ltd.) against a custom database containing the sequence of rhECE-1. The enzyme was selected as 'none', the peptide tolerance was set to 10 ppm and the MS/MS tolerance was set to 0.02 Da. Fixed modifications were set as carbamidomethyl (C) and variable modifications set as oxidation (M). A decoy database search was performed.

For quantification of the identified degradation products, mass spectrometry was performed as above but without triggering MS/MS. Extracted ion chromatograms were produced for each peptide and aligned using their m/z and retention time and the peak areas integrated for comparison.

2.6 β -arrestins and ECE-1 knockdown and transfection

HEK-NMU2 cells were maintained as described in the methods. Forty to 50% confluent cells in 24 well-plates, split 24 h before transfection, were transfected with siRNA using the Lipofectamine RNAiMAX reagent (Invitrogen, Life technologies, UK). The siRNA sequences targeting β -arrestin-1 and β -arrestin-2 are 5'-CTCGACGTTCTGCAAGGTCTA-3' and 5'-CTCGAACAAGATGACCAGGTA-3', respectively. 250 μ L of RNase-free water was added to 5 nmol scale as suggested by the company to obtain 20 μ M solution as stock. Briefly, 0.8 μ l of siRNA (Stock, 20 μ M) was added to 100 μ l of Opti-MEM media for each well and 1 μ l of the reagent was added to the solution and allowed to stand 10 min incubation at room temperature and mixed by gentle inversion. In the meanwhile, the normal media was replaced with Opti-MEM 500 μ l. After 10 min incubation at room temperature, the entire transfection mixture was added to cells in 24 well-plates containing 500 μ l of Opti-MEM. After cells were incubated for 4-5 h at 37°C in a humidified 5% CO₂ incubator, the mixture was replaced with 500 μ l of MEM containing 20% FBS and 2% penicillin/streptomycin and 2 mM glutamine. After 24 h incubation, the cells were starved, serum-free MEM including only the antibiotic and incubated for further 24 h. For ECE-1 knockdown; cells were plated into poly-D-lysine coated 24-well plates and left to attach for 5-6 h (50-60% confluence). The media was replaced with Opti-MEM (without serum; 500 μ L /well). The Lipofectamine RNAmixi reagent was diluted in Opti-MEM (3:50 v:v) and another equal volume of Opti-MEM containing an appropriate amount of siRNA (10 pmol/well) was prepared. The diluted siRNA was then added into the diluted reagent (1:1 v:v). After 20 min incubation at RT, the siRNA complex was added into each well (100 μ L for 24-well plates). After approximately 16 h incubation, the media was replaced to fresh complete medium. The cells were used for treatment after 48 h.

2.7 Immunostaining

2.7.1 Sample preparation

Cells were grown in 96-well black/clear plates (Becton Dickinson Labware, UK) (50-80% confluence) for 24 h. Cells were then starved (serum-free media for 24 h).

In the day of the experiment, cells were treated as required after removing the media and adding the KHB. To stop the reaction, the buffer was aspirated off, and the cells were fixed by adding 50 μ L of 4% PFA (paraformaldehyde) in PBS (phosphate buffer saline) and incubated for 5 min at RT. Cells were then washed X1 with PBS. Cells were then permeabilised by adding 50 μ L/well of methanol for 2 min and kept in freezer. The cells were then washed X2 with PBS. 50 μ L/well of 5% BSA in PBS was added and incubated at RT on a platform shaker for 2 h. 30 μ L/well of 1:400 dilution of anti-pERK mouse IgG polyclonal primary antibody (Santa Cruz) in PBS (2% BSA) was added and incubated overnight on a platform shaker at 4°C with shaking. Cells were then washed X3 with PBS. 30 μ L/well of 1:500 dilution of secondary Alexa 488 anti-mouse (Invitrogen) in PBS (2% BSA) was added and incubated and covered with foil for 90 min on a platform shaker at RT with shaking. The cells were then washed X2 with PBS. 50 μ L/well of 1:10000 dilution of Hoechst stain in PBS was added for 10 min at RT. Cells were then washed X1 PBS and kept in 100 μ L/well of PBS for scanning. The cells remained in 100 μ L PBS and plates were kept in the fridge with foil covered until scanned by an Olympus cell^R microscope with an Olympus LUCPLFLN 40 \times objective lens and an excitation wavelength of either 488 nm or 350 nm for Alexa fluor 488 and Hoechst respectively. Emitted light was collected above 510 nm for the fluorescent emission of Alexa fluor 488 or above 461 nm for Hoechst. 16 images/well (equal to a total area of 217 \times 165 μ m) were taken using a CCD camera. The images were exposed for 4 s/image or 1 s/image for the Alexa fluor 488 and Hoechst, respectively.

2.7.2 ERK activation and distribution using immunocytochemistry approach, detection and analysis

The area of nucleus was determined, using Olympus scan^R analysis software, by the intensity detection for the Hoechst signal and an area of 20 pixels around the nucleus was classified as cytoplasm. All of the signals were background-corrected by the intensity-conserving algorithm included in the software and only the signals reaching threshold were determined to minimize the inclusion of background signal. Abnormal signals, including multi-nucleated cells and any abnormal cell edge were excluded by the gates for the parameters of total intensity, area and circularity. For each cell, the background-corrected mean fluorescent intensity of the whole cell, the cytoplasm or the nucleus and the ratio of background-corrected mean fluorescent intensity of the cytoplasm to nucleus were generated and the mean data for the population of cells in each well were determined.

2.8 Confocal imaging and binding of Cy3B-pNmU-8 to NMU2-eGFP and visualisation of receptor internalization

HEK-NMU2-eGFP were grown on 25 mm coverslips for at least 25 h. Cells were then washed with KHB+BSA at 37 °C and mounted in a perfusion chamber containing KHB+BSA heated to 37 °C using a Peltier unit. The chamber volume was 500 µL. The addition of Cy3B-pNmU-8 (10 nM) was performed manually and images taken using an Olympus inverted microscope with a 60x oil immersion objective lens and an excitation wavelength of 568 nm using a Kr/Ar laser line. Emission was collected at approximately 570 nm using a red-green-blue (RGB) filter. Addition of ligand either hNmU-25 or hNmS-33 (30 nM) was performed manually directly to the bath containing the coverslip. Cells were imaged using a PerkinElmer UltraVIEW confocal imaging system (PerkinElmer LAS (UK) Ltd, Beaconsfield, UK) with a 40x oil-immersion objective lens and an excitation wavelength of 488 nm using Kr/Ar laser line. Emitted light was collected above 510 nm for the fluorescent emission of eGFP. Images were captured at 0 min and 5, 10, 20, 30, 40 and 60 min following ligand addition.

2.9 PathHunter express β -Arrestin Human and Ortholog GPCR kits:

2.9.1 Technology principle:

The association between receptors and β -arrestin has been extensively investigated using many techniques including fluorescence or bioluminescence resonance energy transfer (FRET/BRET) (Ouedraogo *et al.*, 2008), and bimolecular fluorescence complementation (BiFC) (Rose *et al.*, 2010). The latter was used in order to investigate the association between neuropeptide Y receptors (NPY) and β -arrestin-2 in which directly report underlying protein-protein interactions (Kilpatrick *et al.*, 2010). However, another method includes the restoration of β -galactosidase enzyme activity when association between receptor and β -arrestin occurs has been developed by DiscoverX (Carter *et al.*, 2005). This was a kit assay, gifted from the manufacturer, DiscoverX. The methods followed as the manufacturer's instructions. PathHunter β -arrestin products monitor GPCR activity by detecting the interaction of β -arrestins with the activated GPCR using β -galactosidase (β -gal) enzyme fragment complementation (EFC, **Figure 2.1**). In this protocol, the GPCR of interest (in our case NMU1) is fused in frame with small, 42 amino acid fragment of β -gal called ProLink and co-expressed in cells stably expressing a fusion protein of β -arrestins and the larger, *N*-terminal deletion mutant of β -gal (called enzyme acceptor or EA). Activation of the GPCR stimulates binding of β -arrestins to the ProLink-tagged GPCR and forces complementation of the two enzyme fragments, resulting in the formation of an active β -gal enzyme. This action leads to an increase in enzyme activity that can be measured using chemiluminescent PathHunter Detection Reagents. Because β -arrestin recruitment occurs independently of G-protein coupling, these assays provide a direct, universal platform for measuring receptor activation.

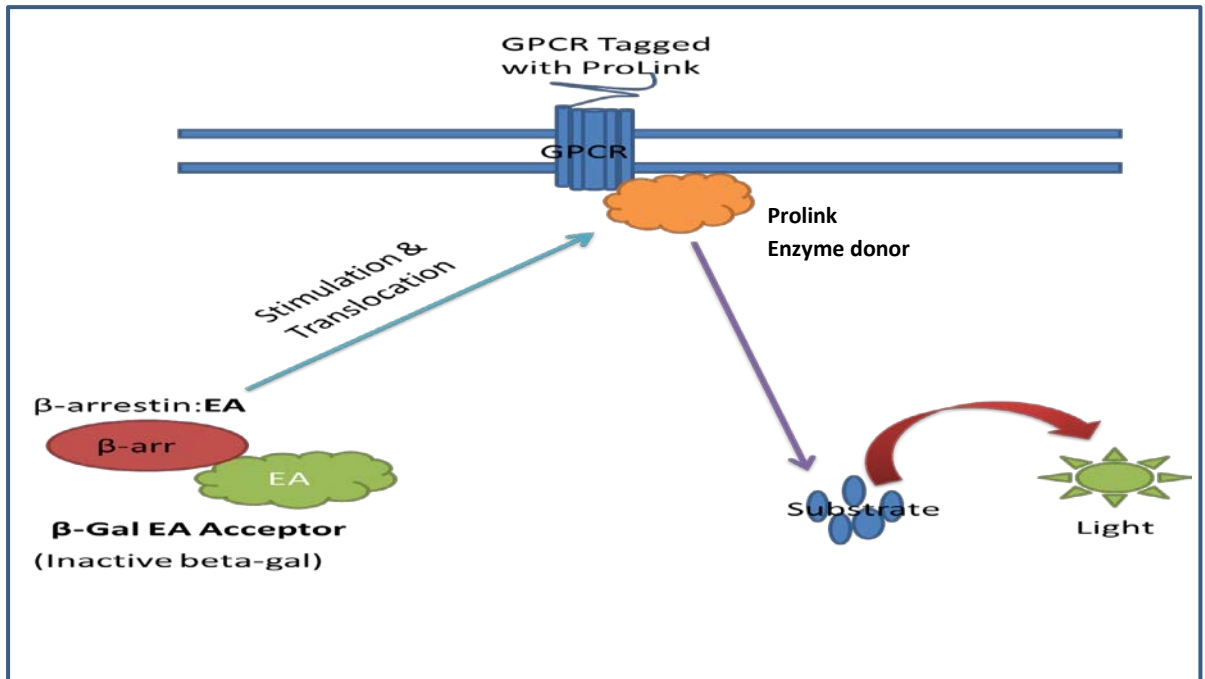


Figure 2.1 PathHunter β -arrestins recruitment assay principle

The G-protein coupled receptor (GPCR) is labelled with a mutationally altered peptide fragment of β -galactosidase (ProLink™ or enzyme donor). β -arrestins are labelled with a corresponding deletion mutant of β -galactosidase (enzyme acceptor). Recruitment of β -arrestins by the ligand-activated GPCR results in β -galactosidase complementation. The reconstituted holoenzyme catalyses the hydrolysis of a substrate, which yields a chemiluminescent signal that can be detected by a NOVOstar plate reader.

2.9.2 Thawing and plating frozen cells

Cell plating reagent was pre-warmed to 37°C. Cell vial (PathHunter eXpress cells) was removed from -80 °C and placed immediately on dry ice prior to thawing. The vial was then briefly placed (10s) in a 37°C water bath until the cell pellet was almost thawed. Pre-warmed cell plating reagent (0.5 mL) was added to the cell vial and the all re-suspended. The cells were then immediately transferred to 11.5 mL of pre-warmed cell plating reagent and poured into a disposable reagent reservoir. A 100 µL aliquate of cells was plated into each well of the 96-well tissue culture plate which was then incubated for 48 h at 37°C, 5% CO₂.

2.9.3 Agonist compound preparation and addition

The concentration of each dilution was prepared at 11X of the final screening concentration to allow 10 µL of compound addition to 100 µL of buffer in each well of cells)

2.9.4 Preparation of 12-point concentration response curve

A range of concentrations were prepared. After 48 h incubation, PathHunter eXpress cells were removed from the incubator and 10 µL from tubes 1-12 was transferred to each well from the high to the low concentration (12 → 1). The plate was then incubated for 90 minutes at 37°C.

2.9.5 Substrate preparation and addition

PathHunter detection reagents were prepared according to manufacturer's instructions by mixing **19 parts** Cell Assay Buffer, **5 parts** Substrate Reagent 1 and **1 part** Substrate Reagent 2. Detection reagent (55 µL) was then added to each well and incubated for 60 min. Samples were read using NOVOstar plate reader.

2.10 hNmU-25 degradation by ECE-1 using recombinant human ECE-1

In order to investigate whether ECE-1 degrades hNmU-25, the following experiment was conducted. Ligands (25 μ M) were incubated with 0.1 μ g rhECE-1 in 50 mM Mes/KOH (MES is the common name for the compound 2-(*N*-morpholino) ethanesulfonic acid) (pH 5.5) or 50 mM Tris-HCL (pH 7.4) for the required time at 37 °C. Reactions were stopped by centrifuging for 2 min using vivacon 500 concentrators that are disposable ultrafiltration devices optimally suited for protein separation, and for optimal performance with protein samples, they were equipped with the patented regenerated cellulose membrane hydrosart, and products were separated by high-performance liquid chromatography (HPLC) and identified using a 4000Q-Trap mass spectrometer. Mass spectrometry data were provided by the Protein Nucleic Acid Chemistry Laboratory (PNACL) facility at the University of Leicester, UK.

2.11 Bioassay approach

HEK-NMU2 or HEK-wt Cells were plated in either 24 or 96 well/plates for 24 h. In the day of the experiment, the HEK-NMU2 or HEK-wt cells in 24 well/plate were incubated with either inhibitor and challenged with hNmU-25, 10 nM and the ligand were left for 1, 2 and 3h. The solution containing the ligand from the wells were collected and used to stimulate the cells in 96 well/plate using the NOVOstar machine as described in (**Methods; 2.2.5**).

Chapter 3

NMU regulation: desensitisation, internalisation and re-sensitisation

3.1 Introduction

Both NmU and NmS can activate two family A GPCRs, NMU1 and NMU2 (Alexander *et al.*, 2008; Sharman *et al.*, 2011). The NMU1 and NMU2 isolated from human share 73 % and 75 % homology with those isolated from rat, respectively (Howard *et al.*, 2000). Also, NMU1 and NMU2 have 73-79% and 81% homology respectively to those isolated from the mouse (Tan *et al.*, 1998; Funes *et al.*, 2002). The receptors have 51% identity (Howard *et al.*, 2000a). The homology occurs within the transmembrane domains, whereas differences are located at the extracellular *N*-terminus and within the i3 loop (**Figure 1.2**). The *C*-terminus of NMU2 is longer than NMU1, whereas NMU2 has a shorter i3 region than NMU1. Both receptors are differently distributed. For instance, NMU2 is highly expressed in the central nervous system. In contrast, NMU1 is expressed mainly in peripheral tissues (**Section 1.3**).

Activation of either NMU receptor by NmU results in increases in $[Ca^{2+}]_i$ (Fujii *et al.*, 2000; Hedrick *et al.*, 2000; Howard *et al.*, 2000; Kojima *et al.*, 2000; Funes *et al.*, 2002; Aiyar *et al.*, 2004; Brighton *et al.*, 2004a; Johnson *et al.*, 2004; Brighton *et al.*, 2008), PLC activity (Aiyar *et al.*, 2004; Brighton *et al.*, 2004a), $InsP_x$ generation (Raddatz *et al.*, 2000; Szekeres *et al.*, 2000; Aiyar *et al.*, 2004; Brighton *et al.*, 2004a). In addition, an increase in arachidonic acid release (Fujii *et al.*, 2000; Hosoya *et al.*, 2000; Aiyar *et al.*, 2004; Brighton *et al.*, 2004a) and inhibition of forskolin-mediated cAMP generation (Hosoya *et al.*, 2000; Aiyar *et al.*, 2004; Brighton *et al.*, 2004a) have also been reported. Pre-treatment of NMU-expressing cells with pertussis toxin does not affect either phosphoinositide turnover or $[Ca^{2+}]_i$ responses to NmU, whereas the inhibition of the adenylyl cyclase activity is abolished, indicating respective likely dependency on $G_{\alpha_{q11}}$ and $G_{\alpha_{i/o}}$ coupling (Aiyar *et al.*, 2004; Brighton *et al.*, 2004a). In this chapter changes in $[Ca^{2+}]_i$ have been investigated by exposing the HEK293 cells expressing NMU1 and NMU2 to either NmU, NmS or pNmU-8 and in order to generate a pharmacological

ligand profile. Next, the desensitisation, internalisation and the recovery (re-sensitisation) of NMU2 is assessed.

In particular, using different conditions including using an internalisation inhibitor, using different times desensitisation and different times stimulation either with concentrations higher than the maximum concentration (30 nM) or lower than that in order to study the consequences from that on the receptors processing were examined in the current study (DeFea *et al.*, 2000; Pierce *et al.*, 2002).

For example, it has been suggested that high concentration (10 nM) could affect the re-sensitisation and the recovery for some receptors, including (Neurokinin 1 receptor) NK₁R (Roosterman *et al.*, 2004). Therefore, this possibility was assessed using different concentrations in this study.

In addition to the importance of GPCR phosphorylation by G protein- coupled receptor kinases (GKR), dephosphorylation is also a critical mechanism of some GPCR re-sensitisation including NK₁R (Murphy *et al.*, 2011). It has been reported that the phosphorylated β_2 AR appears in an endosomal vesicle enriched with protein phosphatase 2A (PP2A) (Pitcher *et al.*, 1995) and this enzyme is present in the cytosolic and it is a member of a diverse family of phospho-S- and T-specific enzymes. Therefore, the effect of this enzyme was investigated using different inhibitors that had been widely used in researches.

As the dephosphorylation is important for the receptor to be recycled and re-sensitised, the role of PP2A in re-sensitisation was explored using different types of protein phosphatase inhibitors.

For some GPCRs, re-sensitisation is reduced if endosomal acidification is inhibited, or ECE-1 activity is genetically or pharmacologically inhibited. In contrast, over-expression of ECE-1 has been shown to enhance the trafficking and re-sensitisation of some GPCRs (Padilla *et al.*, 2007; Roosterman *et al.*, 2007). It is interesting to note that HEK-293 cells are reported to express mRNA for ECE-1 (Padilla *et al.*, 2007; Roosterman *et al.*, 2007).

In order to understand whether hNmU-25 could be degraded extracellular and whether any related enzyme other than the ECE-1 could be involved in receptor processing, two

different approaches were used in this study including NEB inhibitor and bioassay as described in the Methods section (2.12). The CD10/neutral endopeptidase 24.11 ([NEB] EC 3.4.24.11, neprilysin) is a plasma membrane-bound zinc metalloprotease enzyme (Park *et al.*, 2003). It is a member of a gene family including the ECE-1. This enzyme regulates some biological activity of peptide substrates including endothelin-1 (ET-1) (Abassi *et al.*, 1992), atrial natriuretic factor (Gros *et al.*, 1989), bradykinin (Erdos *et al.*, 1989) and substance P (Skidgel *et al.*, 1984). The small peptides could be cleaved by this enzyme on the *N*-terminal side of hydrophobic amino acids (Ishimaru *et al.*, 1997). It has been reported that this enzyme could be inhibited by different agents including thiorphan (Schwartz *et al.*, 1990).

3.2 Results

3.2.1 NMU receptor-mediated Ca^{2+} : a comparison of natural ligands

Exposing either HEK-NMU1 or HEK-NMU2 to hNmU-25, hNmS-33 or pNmU-8 evoked concentration-dependent increases in fluorescence as an index of changes in $[\text{Ca}^{2+}]_i$ in populations of adherent fluo-4-loaded cells. High concentrations evoked greater and more rapid increases in $[\text{Ca}^{2+}]_i$. For instance, using a high concentration (30 nM) of any of the ligands led to a faster rate of increase in $[\text{Ca}^{2+}]_i$ (maximal change at 4 ± 0.6 s) e.g. hNmU-25, while using a lower concentration resulted in a slower rate of increase (for example at 3 nM maximal change at 12.33 ± 2.19 s) e.g. hNmU-25. The peak levels were attained after around (13 ± 0.58 s) at lower concentrations (**Figures 3.1, 3.2, 3.3**). The maximum increases in fluorescence were determined and used to generate concentration-response curves. Changes in fluorescence were also calibrated as described in **Methods** and increases in $[\text{Ca}^{2+}]_i$ determined (**Figure 3.1; B & C**). Following the initial peak, there was a slowly declining phase at all ligand concentrations used (0.1-100 nM). This decline lasted until the end of reading (50 s). From the concentration response curves, the pEC_{50} values for hNmU-25 and hNmS-33 in HEK-NMU1 were 8.53 ± 0.05 , 8.97 ± 0.12 , respectively, and in HEK-NMU2 8.62 ± 0.03 and 9.10 ± 0.07 , respectively (**Figures 3.1 & 3.2**). Furthermore, the pNmU-8 caused concentration-dependent increases in $[\text{Ca}^{2+}]_i$ in HEK-NMU1 and HEK-NMU2 with pEC_{50} values of 8.90 ± 0.12 and 8.88 ± 0.14 , respectively (**Figure 3.3; A & B**).

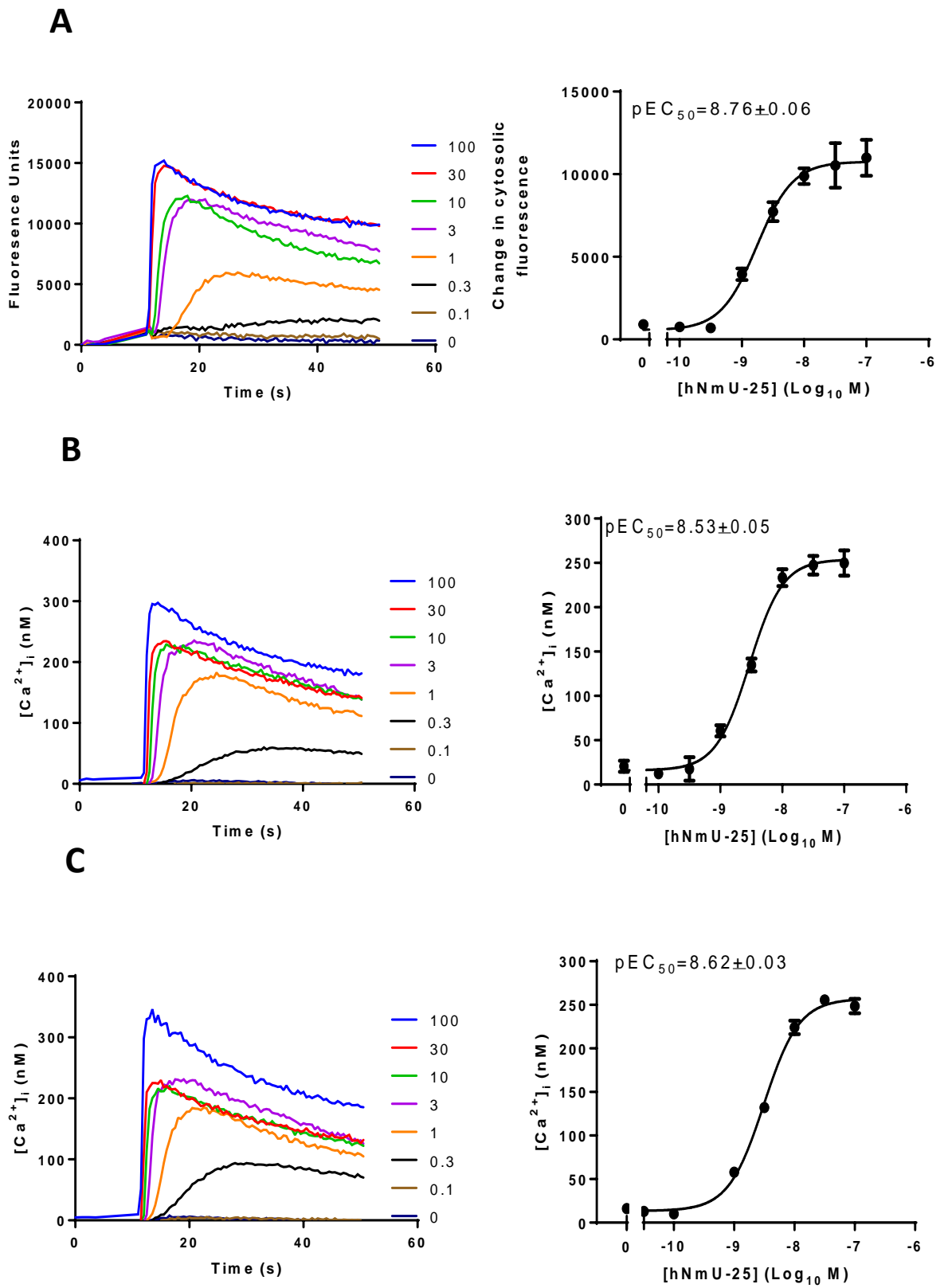


Figure 3.1 Concentration-responses curves for hNmU-25-mediated Ca²⁺ elevation in HEK-NMU1 and HEK-NMU2

HEK-NMU1 and HEK-NMU2 cells were plated in 96-well plates for 24 h. Cells were loaded with fluo-4 then challenged with different concentrations of hNmU-25 in HEK-NMU1 (**A**, uncalibrated) or HEK-NMU1 and HEK-NMU2 (**B & C**, calibrated, to show [Ca²⁺]_i changes). Changes in cytosolic fluorescence were then monitored as an index of [Ca²⁺]_i using a NOVOstar plate reader. Traces are representative of 3 experiments showing Ca²⁺ responses at different concentrations of hNmU-25. Data were calibrated as described in **Methods** and maximal changes used to construct concentration-responses curves. The pEC₅₀ values for hNmU-25 in HEK-NMU1 and HEK-NMU2 were either 8.76 ± 0.06, un-calibrated or 8.53 ± 0.05 and 8.62 ± 0.03, calibrated, respectively. Data are presented as means ± s.e.m.; n=3 or are representative of n=3 separate experiments.

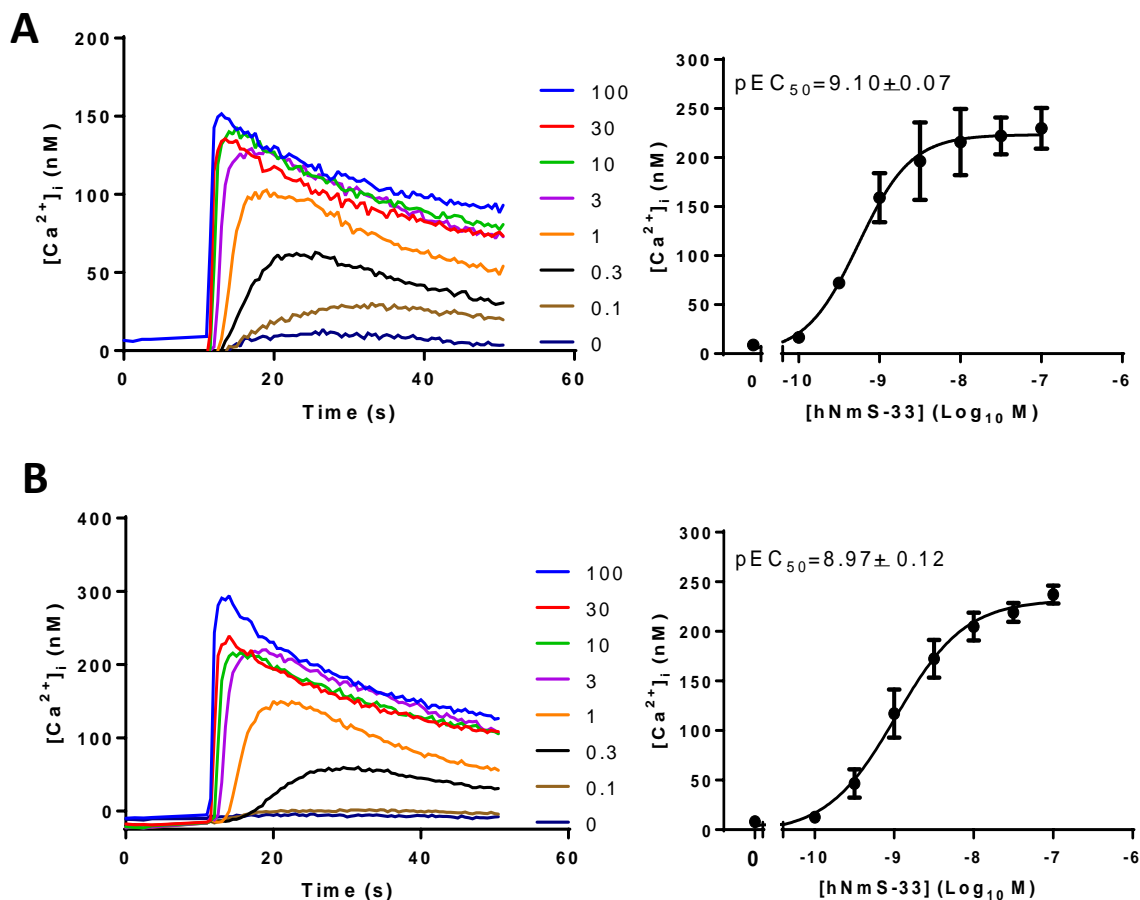


Figure 3.2 Concentration-response curves for hNmS-33-mediated Ca²⁺ elevation in HEK-NMU1 and HEK-NMU2

HEK-NMU1 and HEK-NMU2 cells were plated in 96-well plates for 24 h. Cells were loaded with fluo-4 then challenged with different concentrations of hNmS-33 in HEK-NMU1 (**A**) or HEK-NMU2 (**B**). Changes in cytosolic fluorescence were then monitored as an index of [Ca²⁺]_i using a NOVOstar plate reader. Traces are representative of 3 experiments showing Ca²⁺ responses at different concentrations of hNmS-33. Data were calibrated as described in Methods and maximal changes used to construct concentration-responses curves. The pEC₅₀ values for hNmS-33 in HEK-NMU1 and HEK-NMU2 were 9.10 ± 0.07 and 8.97 ± 0.12, respectively. Data are presented as means ± s.e.m.; n=3 or are representative of n=3 separate experiments.

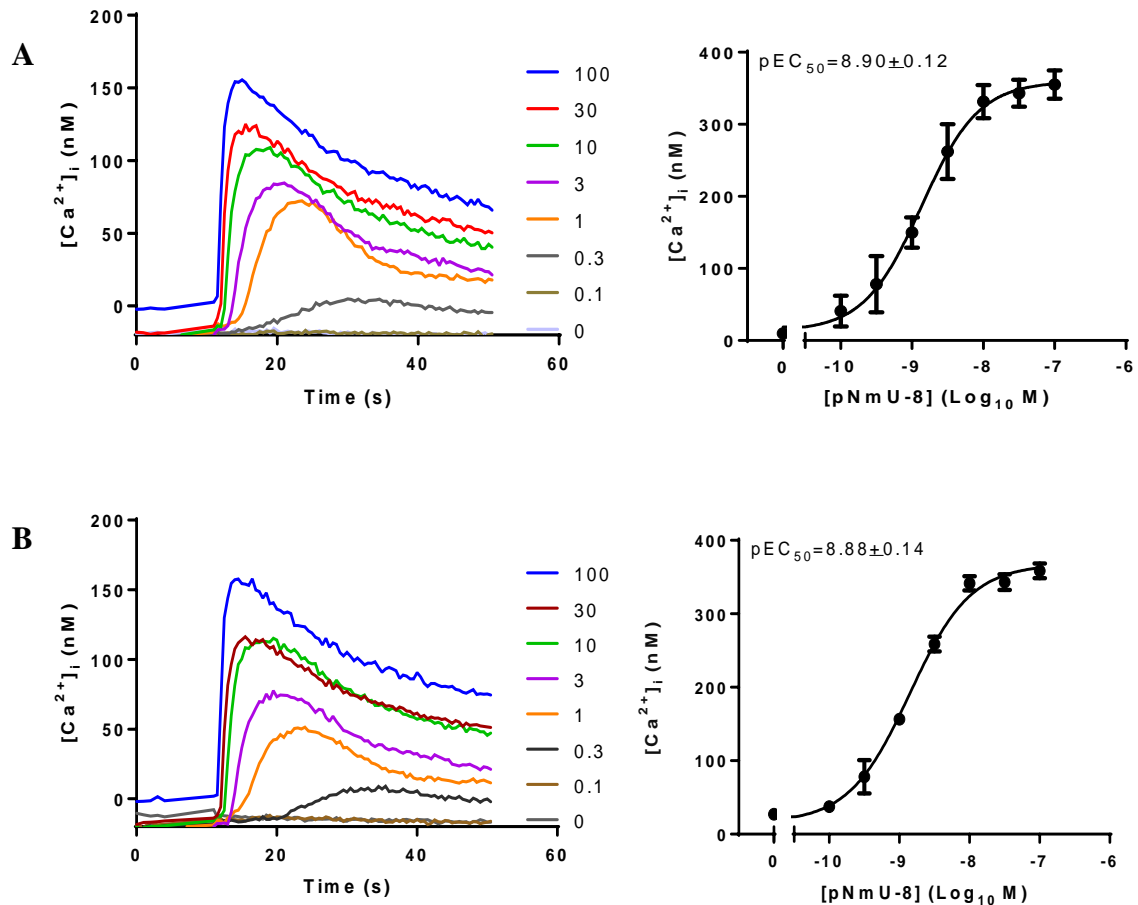


Figure 3.3 Concentration-response curves for pNmU-8-mediated Ca^{2+} elevation in HEK-NMU1 and HEK-NMU2

HEK-NMU1 and HEK-NMU2 cells were plated in 96-well plates for 24 h. Cells were loaded with fluo-4 then challenged with different concentrations of pNmU-8 in HEK-NMU1 (A) or HEK-NMU2 (B). Changes in cytosolic fluorescence were then monitored as an index of $[Ca^{2+}]_i$ using a NOVOstar plate reader. Traces show Ca^{2+} responses at different concentrations of pNmU-8. Data were calibrated as described in **Methods** and maximal changes used to construct concentration-responses curves. The pEC_{50} values for pNmU-8 in HEK-NMU1 and HEK-NMU2 were 8.90 ± 0.12 and 8.88 ± 0.14 , respectively. Data are shown as means \pm s.e.m.; $n=3$ or are representative of $n=3$ separate experiments.

3.2.2 NMU receptor desensitization, internalization & re-sensitization

This series of experiments will now primarily focus on NMU2 subtype. It has previously been demonstrated in our laboratory that following stimulation of HEK-NMU2 cells with hNmU-25 (30 nM, 5 min) and a short (5 min) washout/recovery period essentially no Ca^{2+} response is observed upon NmU re-addition (Brighton *et al.*, 2004b; Alhosaini, 2011). This did not show whether the receptor desensitized or not. In contrast, re-addition of the muscarinic acetylcholine receptor agonist, carbachol, following a similar pre-treatment protocol (carbachol (300 μM ; 5 min) addition followed by 5 min washout/recovery) resulted in a smaller, but still significant Ca^{2+} response (approx. 60 % attenuation of the initial Ca^{2+} response; (Alhosaini, 2011). However, when the cells were stimulated (30 nM hNmU-25 for 5 min) and then very briefly washed with acidified (pH 2) buffer, a Ca^{2+} response was observed upon re-challenge. These data suggest that the NMU2-ligand complex does not readily dissociate under normal physiological conditions (Brighton *et al.*, 2004b) and exposure to a low pH is necessary to dissociate the high-affinity neuropeptide-receptor complex (Haigler *et al.*, 1980; Koenig *et al.*, 1997). In the absence of a brief acid-wash, recovery of the Ca^{2+} response to hNmU-25 re-addition was observed only after a 2-3 h recovery period (Alhosaini, 2011). The kinetics of ligand association and dissociation from the receptor has been mapped using Cy3B-pNmU-8. Using this ligand it has been clearly shown that a pH 2.0 wash for 30 s is necessary to bring about a complete dissociation from the receptor (Alhosaini, 2011).

Because exposure to acidified buffer could have serious effects on the integrity of the cell and its ability to respond to agonists re-challenge, the effect of brief pH 2 exposure on Ca^{2+} responses was investigated. HEK-NMU2 cells were washed briefly (20 s) with KHB at either pH 2 or 7.4 (normal buffer) followed by washing and 5 min recovery in standard buffer (pH 7.4) and then stimulated using different concentrations of hNmU-25 (0.1-100 nM; **Figure 3.4**). The acid-wash did not significantly alter agonist potency (pEC_{50} (-log M) values for hNmU-25-mediated Ca^{2+} responses: 8.74 ± 0.08 and 8.58 ± 0.09 , respectively following acidified or standard buffer washes).

The Ca^{2+} response observed following an initial exposure to agonist and washout period was used as an index of NMU2 receptor desensitisation. HEK-NMU2 cells were incubated with hNmU-25 or hNmS-33 (each at 30 nM) for varying times (1-10 min) followed by a brief acid wash, a 5 min recovery period and subsequent re-challenge with a maximally effective concentration of the same ligand (**Figure 3.5**). Pre-incubation with hNmU-25 or hNmS-33 resulted in a time-dependent reduction in the Ca^{2+} response seen upon hNmU-25 or hNmS-33 re-challenge (**Figure 3.5 A, B**). Apparently, maximal decreases in the re-challenge Ca^{2+} response were observed for both ligands following either 5 or 10 min pre-incubation periods.

The ability of HEK-NMU2 cells to recover either hNmU-25- or hNmS-33-mediated Ca^{2+} responses was next assessed to determine the time-course over which re-sensitisation occurs. Cells were pre-incubated with a maximal concentration of either ligand to cause desensitisation (30 nM; 5 min) followed by three washes with KHB (pH 7.4). Cells were then allowed to recover for 1, 3, or 6 h and then re-challenged using the maximally effective concentration of ligand (**Figure 3.5, C**). The time-courses of recovery from desensitisation were found to depend on the ligand, with recovery occurring more slowly when hNmS-33 was studied. Whereas, essentially full recovery was achieved after 6 h when the cells were desensitised with hNmU-25, $\leq 50\%$ recovery was observed at this time following desensitisation of NMU2 by hNmS-33 (**Figure 3.5, C**).

Previous work has demonstrated internalisation of eGFP-tagged NMU2 receptor within 10 min of ligand addition (Brighton, 2005). Before using the HEK-NMU2-eGFP cell-line in my own work, I wished to confirm that C-terminal tagging of the receptor did not significantly alter signalling responses. hNmU-25 stimulated concentration-dependent Ca^{2+} responses in fluo-4-AM-loaded HEK-NMU2-eGFP cells. Although the maximal Ca^{2+} response to hNmU-25 was reduced (**Figure 3.6**), pEC_{50} values (8.64 ± 0.06 and 8.56 ± 0.08 , for NMU2 and NMU2-eGFP, respectively) were unaffected by eGFP-tagging (**Figure 3.6**).

The HEK-NMU2-eGFP cell-line was then used to assess whether receptor internalisation occurs following addition of either hNmU-25 or hNmS-33 (**Figures 3.7 and 3.8**). Real-time monitoring of NMU2-eGFP internalisation in HEK-NMU2 was

performed using microscopy and following challenge with hNmU-25 and hNmS-33 indicated gradual movement of NMU2-eGFP fluorescence from plasma membrane to the cytosol. The maximum internalisation in HEK-NMU2-eGFP was achieved after approximately 30-40 min, stimulated with either hNmU-25 or hNmS-33. In addition, to determine if the ligand and receptor internalise together, fluorescently tagged pNmU-8 (Cy3B-pNmU-8) was also used (**Figure 3.9**). Addition of Cy3B-pNmU-8 (10 nM) to HEK-NMU2-eGFP revealed that NMU2-eGFP are able to bind to its cognate ligand.

Having established that hNmU-25 and hNmS-33 cause the receptor to internalise, and a tagged analogue of pNmU-8 internalises with NMU2, I next examined the effect of the dynamin-dependent internalisation inhibitor, dynasore (Macia *et al.*, 2006), on the recovery of hNmU-25- and hNmS-33-mediated Ca^{2+} signalling. Pre-treatment of HEK-NMU2 cells with dynasore (80 μM) for 6 h did not significantly affect hNmU-25- and hNmS-33-mediated Ca^{2+} responses in agonist-naïve cells (**Figure 3.10 A, B**). Following an initial 5 min desensitising exposure to hNmU-25 or hNmS-33 (30 nM), washout and a recovery period of 6 h, re-challenging vehicle-treated cells with hNmU-25 (**Figure 3.10, A**) or hNmS-33 (**Figure 3.10, B**) evoked >90% and ~60% of the respective control Ca^{2+} responses. In the presence of dynasore a markedly reduced recovery was observed with respect to both agonists. These data suggest that recovery of NMU2-mediated response is dependent on dynamin-dependent internalisation, most likely of the NMU2-agonist complex.

To assess the role of endosomal acidification in the re-sensitisation of NMU2, two mechanistically-distinct inhibitors of endosomal acidification, monensin (50 μM ; a monovalent cation ionophore) and bafilomycin A1 (200 nM; a vacuolar H^{+} -ATPase inhibitor) were used. HEK-NMU2 cells were pre-treated with either inhibitor for 30 min and then stimulate with a agonist for 5 min and allowed to recover for either 3 or 6 h. both inhibitors significantly reduced the recovery of the NMU2-mediated Ca^{2+} response when the cells were stimulated using a maximally-effective concentration of hNmU-25 or hNmS-33 (**Figure 3.11**). it should be noted that while there was a trend for both monensin and bafilomycin to increase the naïve Ca^{2+} response to each ligand this possible effect did not achieve statistical significance in any individual dataset (**Figure 3.11**).

The requirement for de novo protein synthesis in the recovery of NMU2 from desensitisation was also investigated. Cycloheximide has been used by other groups in HEK293 cells to inhibit protein synthesis (Yu *et al.*, 1997). Indeed, previous work in our laboratory has demonstrated that a carefully titrated concentration of cycloheximide (17.5 μM) inhibits protein synthesis in these cells (Alhosaini, 2011). Cells were pre-treated with either KHB or inhibitor for 30 min then pre-exposed to buffer, hNmU-25 or hNmS-33 (30 nM, 5 min). Cycloheximide (17.5 μM) did not affect the respective recoveries of hNmU-25- or hNmS-33-mediated Ca^{2+} responses seen at 6 h (**Figure 3.12A, B**). Furthermore, the Ca^{2+} responses to either hNmU-25 or hNmS-33 seen in ligand-naïve cells incubated in the absence or presence of cycloheximide were not significantly different.

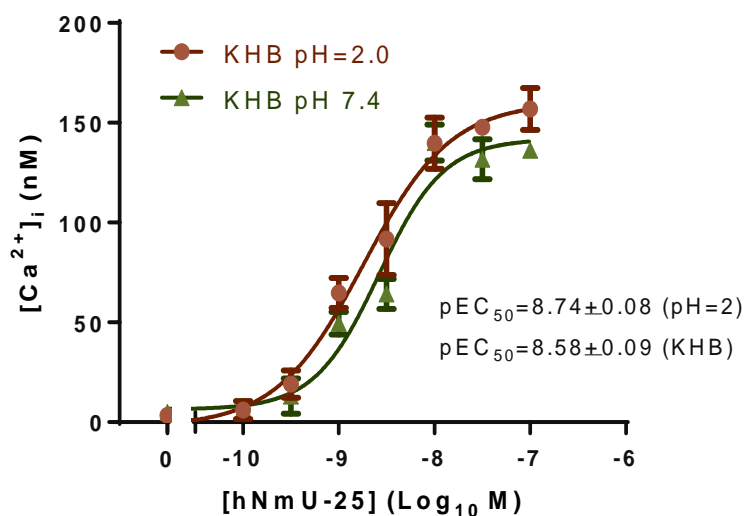


Figure 3.4 Effect of a brief acid wash (2.0) on hNmU-25-stimulated Ca^{2+} responses in HEK-NMU2

HEK-NMU2 cells were cultured in 96-well plates for 24 h. The cells were then loaded with fluo-4-AM for 45 min. Cells were exposed to a brief wash with either KHB pH (7.4) or KHB pH (2.0) for no longer than 25 s as followed by three washes with KHB pH (7.4) and allowed to recover for 5 min at 37 °C. Cells were then challenged with different concentrations of hNmU-25 (0.1-100 nM) and changes in fluorescence (as an index of $[\text{Ca}^{2+}]_i$) measured using a NOVOstar plate reader. The data were calibrated and the maximal changes were used to construct concentration-response curves. The pEC_{50} (-log M) values after washing with KHB (pH 7.4) or KHB (pH 2.0) were 8.58 ± 0.09 and 8.74 ± 0.08 , respectively. Data are presented as means \pm s.e.m.; n=3.

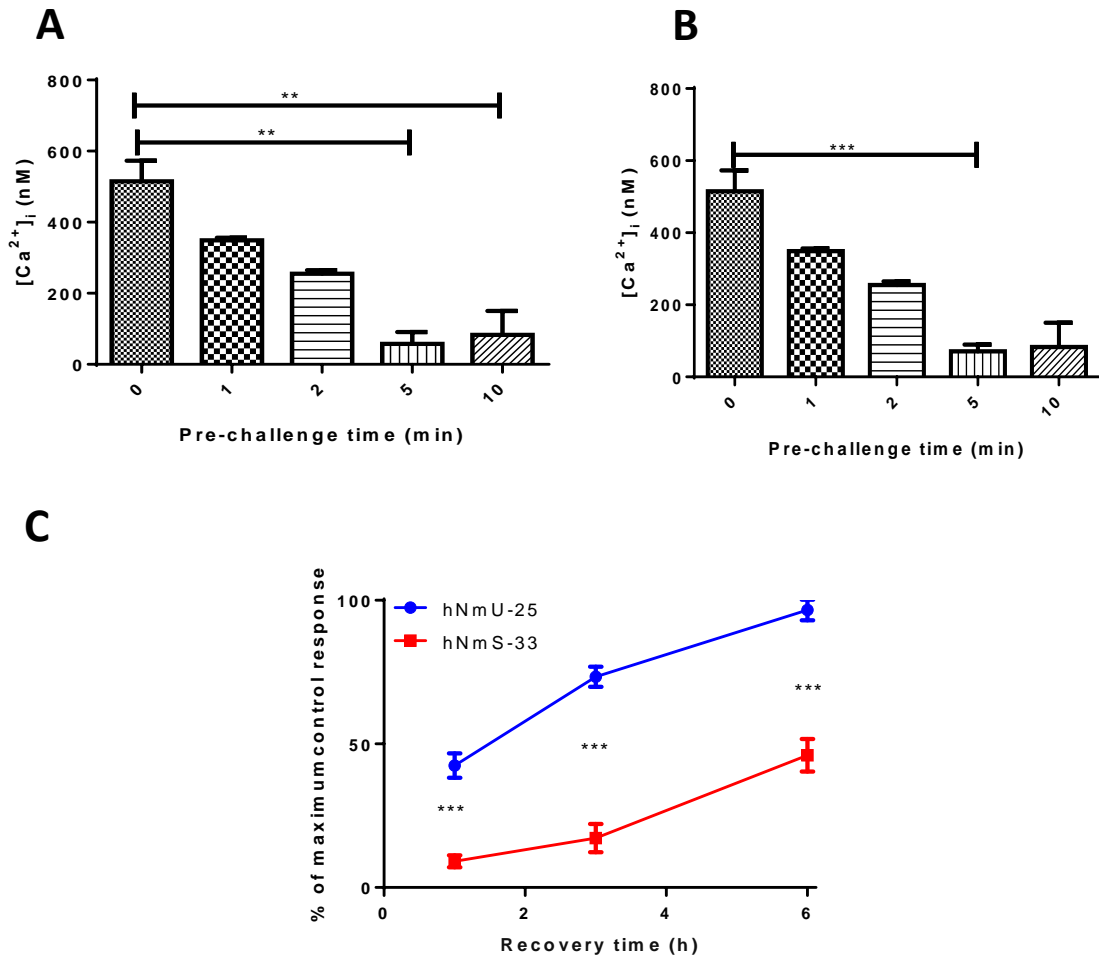


Figure 3.5 NMU2 desensitisation and re-sensitisation of Ca²⁺ signalling

For desensitisation, fluo-4-AM loaded cells were untreated or pre-treated with hNmU-25 (A) or hNmS-33 (B) (30 nM, 1-10 min), then washed using acidified buffer before a 5 min recovery period in normal KHB. For resensitisation, the cells were pre-treated with either hNmU-25 or hNmS-33 (30 nM, 5 min), and then washed using KHB and allowed to recover (C). During the last 45 min of the recovery period (1-6 h recovery) (resensitisation), cells were loaded with fluo-4-AM and then re-challenged with the same ligand. Changes in cytosolic fluorescence were recorded as an index of changes in [Ca²⁺]_i using a NOVOstar plate reader. In panel C, data are expressed as a percentage of the maximum response in HEK-NMU2 pre-challenged with KHB only. Data are presented as means \pm s.e.m.; n=3., ***P*<0.01, ****P*<0.001; by Bonferroni's multiple comparison test following one (panels A and B), or two-way (panel C) ANOVA. Significant differences between unchallenged cells and either 5 or 10 min recovery after stimulation were considered.

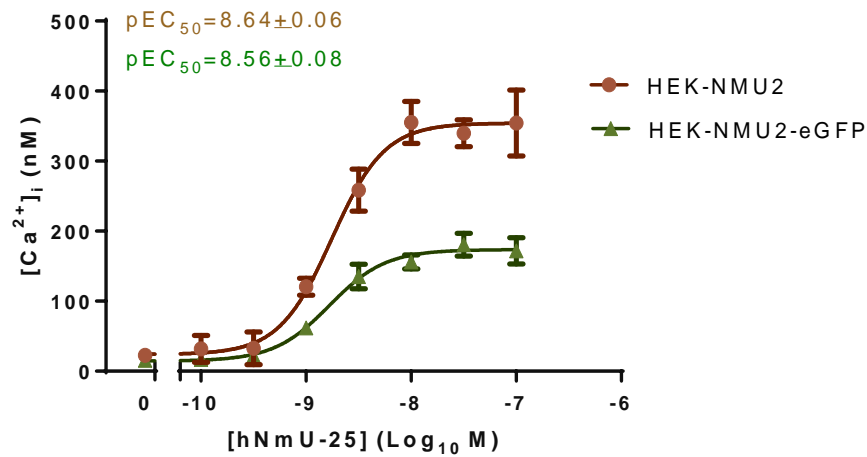


Figure 3.6 Concentration-response curves for hNmU25-mediated changes in $[Ca^{2+}]_i$ in HEK-NMU2 and HEK-NMU2-eGFP-expressing cells-lines

HEK-NMU2 and HEK-NMU2-eGFP cells were cultured in 96-well plates, for 24 h. The cells were then loaded with fluo-4-AM for 45 min at 37 °C. The cells were then challenged with different concentrations of hNmU-25 using a NOVOstar plate reader. Changes in fluorescence were monitored as an index of $[Ca^{2+}]_i$ and the data were calibrated as described in Methods. The maximal changes in fluorescence were used to construct concentration-response curves for both types of cells. The pEC_{50} values for hNmU-25 in HEK-NMU2 and HEK-NMU2-eGFP were 8.64 ± 0.06 and 8.56 ± 0.08 , respectively. Data are presented as means \pm s.e.m.; n=3.

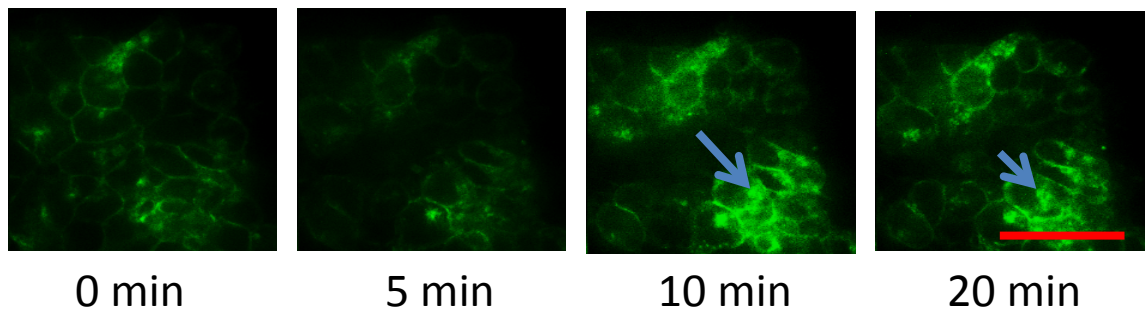


Figure 3.7 Confocal imaging of hNmU-25-mediated receptor internalisation in HEK-NMU2-eGFP

HEK-NMU2-eGFP cells were cultured on 25 mm glass coverslips for 24 h. Cells were then challenged with hNmU-25 (30 nM) and internalisation was visualised and captured using confocal microscopy at a laser excitation wavelength of 488 nm at the times shown. The location of HEK-NMU2-eGFP at the plasma membrane or in the cytosol is indicated by arrows. Images are representative of multiple images from 3 independent experiments. Scale bar is (10 μ m).

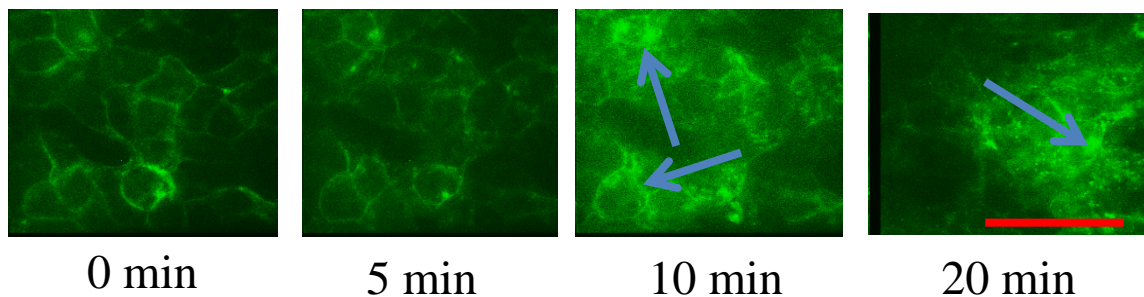
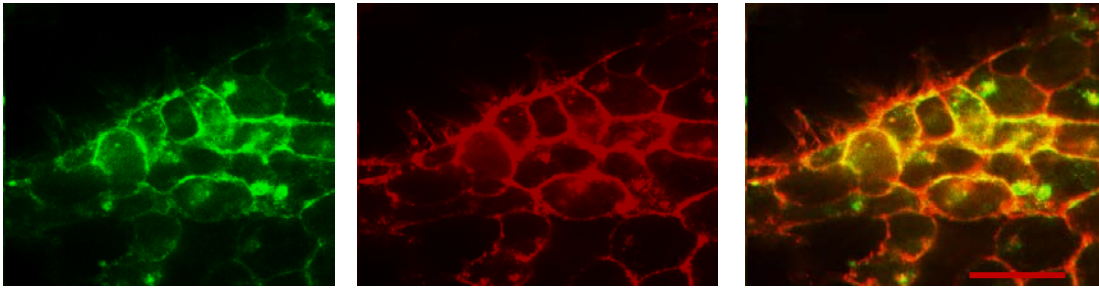


Figure 3.8 Confocal imaging of hNmS-33-mediated receptor internalisation in HEK-NMU2-eGFP

HEK-NMU2-eGFP cells were cultured on 25 mm glass coverslips for 24 h. Cells were then challenged with hNmS-33 (30 nM) and internalisation was visualised and captured using confocal microscopy at a laser excitation wavelength of 488 nm at the times shown. The location of HEK-NMU2-eGFP at the plasma membrane or in the cytosol is indicated by arrows. Images are representative of multiple images from 3 independent experiments. Scale bar is (10 μ m).

A



B

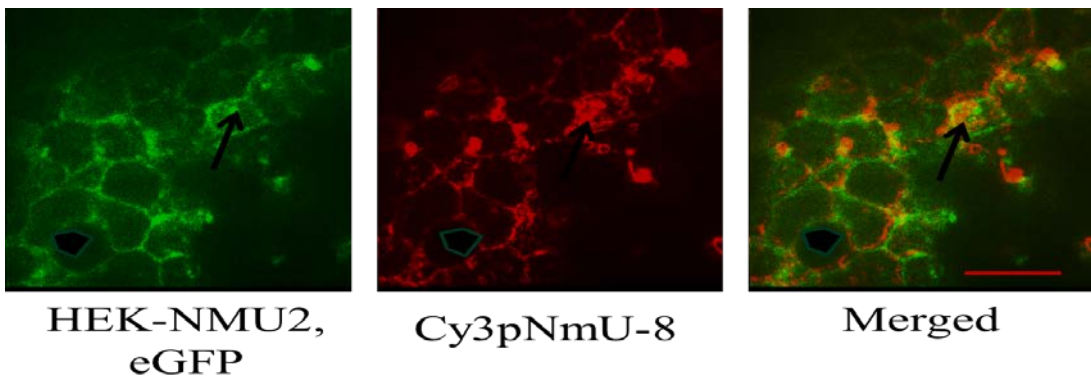


Figure 3.9 Bound fluorescently-tagged pNmU-8 (Cy3B-pNmU-8) is co-internalised with the NMU2 receptor in HEK-NMU2-eGFP

HEK-NMU2-eGFP cells were cultured on 25 mm glass coverslips for 24 h. Cells were exposed to Cy3B-pNmU-8 (10 nM) and then visualised following 5 (**A**) or 20 (**B**) min of the addition by confocal microscopy using laser excitation wavelengths of 488 and 568 nm for green fluorescent protein and Cy3B-pNmU-8, respectively. The presence of HEK-NMU2-eGFP or Cy3pNmU-8 at the plasma membrane or in the cytosol is indicated by arrowheads and arrows, respectively. Images are representative of multiple images from 3 independent experiments. Scale bar is 10 μ m indicated by a red line.

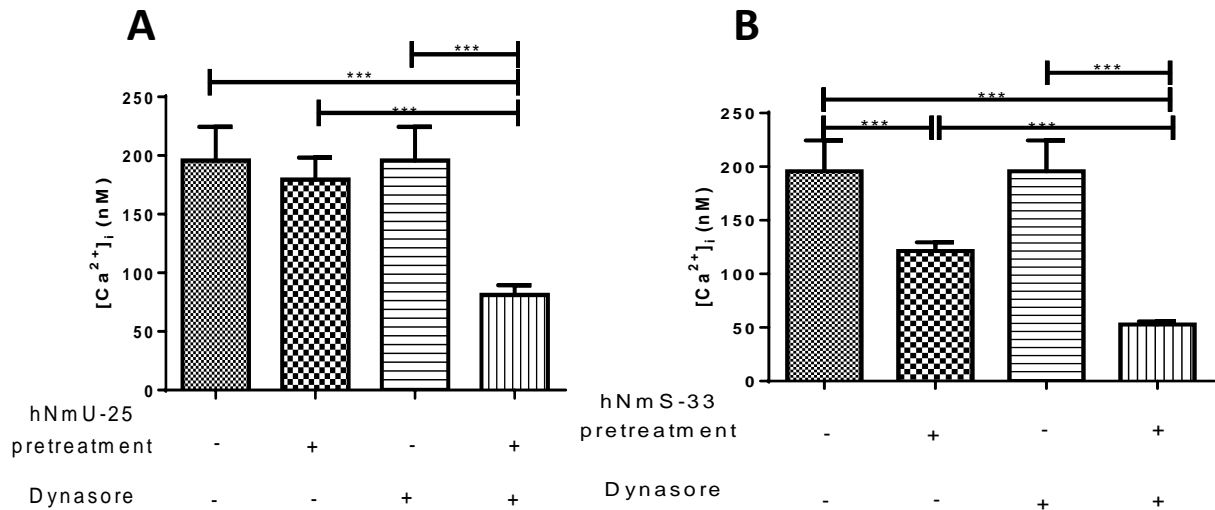


Figure 3.10 NMU2 re-sensitisation is reduced by inhibition of internalisation

HEK-NMU2 cells were pre-incubated \pm inhibitors of internalisation (dynasore, 80 μ M) for 30 min before challenge with buffer or ligands (hNmU-25 (**A**) or hNmS-33 (**B**)) (30 nM, 5 min). Cells were washed and allowed to recover for 6 h (\pm inhibitor), cells were then re-challenged with the same ligand and Ca^{2+} responses determined using a NOVOstar plate reader and changes in cytosolic fluorescence were recorded as an index of changes in $[\text{Ca}^{2+}]_i$. Data are mean \pm s.e.m, $n=3$., $***P<0.001$; by Bonferroni's multiple comparison following one-way ANOVA.

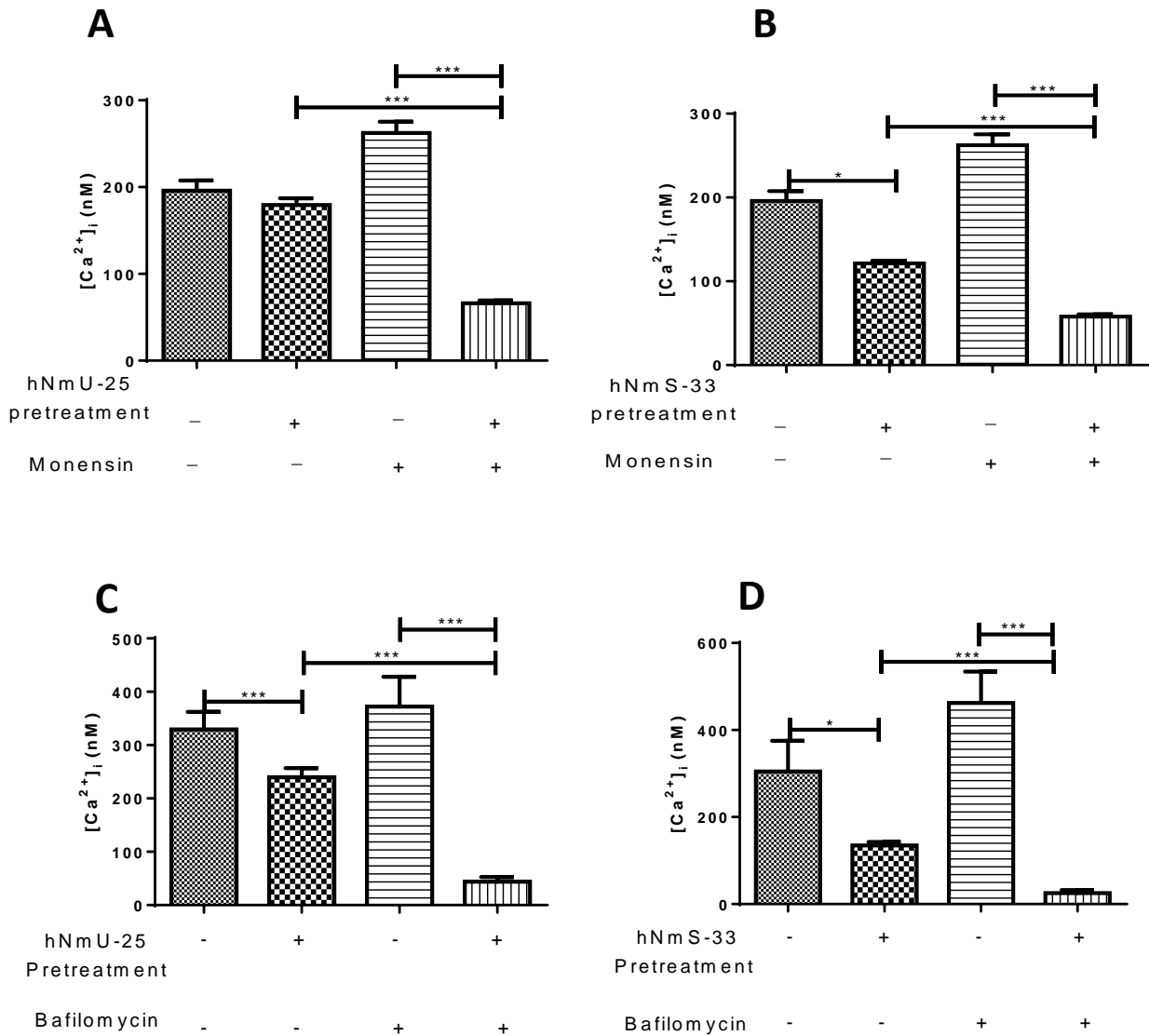


Figure 3.11 NMU2 re-sensitisation is markedly reduced by two different endosomal acidification inhibitors

HEK-NMU2 cells were pre-incubated \pm inhibitors of endosomal acidification, monensin (50 μ M; **A, B**) or bafilomycin (200 nM; **C, D**) for 30 min before challenge with buffer or ligands, hNmU-25 (**A, C**) or hNmS-33 (**B, D**) (each 30 nM, 5 min). Cells were washed and allowed to recover for either 3 (**C & D**) or 6 h (**A & B**) (\pm inhibitor) and then re-challenged with the same ligand. Ca²⁺ responses were determined using a NOVOstar plate reader and changes in cytosolic fluorescence were recorded as an index of changes in [Ca²⁺]_i. Data are presented as means \pm s.e.m.; n=3. Statistical analysis was performed using Bonferroni's multiple comparison following one-way ANOVA. * P <0.05, *** P <0.001.

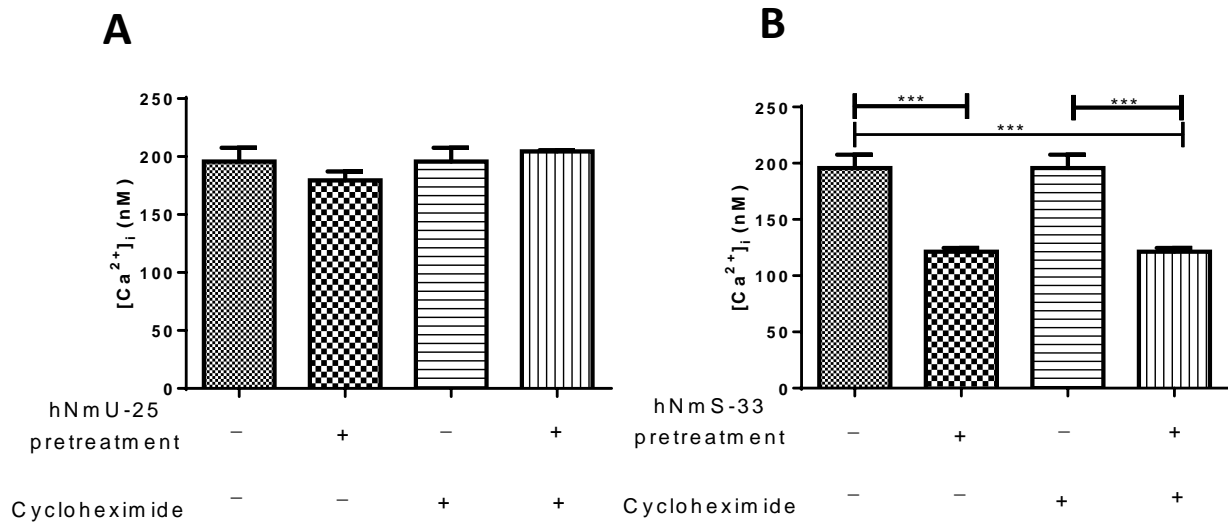


Figure 3.12 NMU2 re-sensitisation is unaffected by inhibition of protein synthesis

HEK-NMU2 cells were pre-incubated in the absence and presence of an inhibitor of protein synthesis (cycloheximide, 17.5 μ M) for 30 min before challenge with buffer or ligands (hNmU-25 (**A**) or hNmS-33 (**B**)) (30 nM, 5 min). Cells were washed and allowed to recover for 6 h (\pm inhibitor) before determination of Ca²⁺ responses to the same ligand (30 nM). Changes in cytosolic fluorescence were then monitored as an index of [Ca²⁺]_i using a NOVOstar plate reader. Data are presented as means \pm s.e.m.; n=3; ****P*<0.001; by Bonferroni's multiple comparison following one-way ANOVA.

3.2.3 Do protein phosphatase or protein kinase C activities play a role in re-sensitization of NMU2?

It has been suggested that after stimulation of the type 1 neurokinin receptor (NK₁R) by substance P, protein phosphatase type 2A (PP2A) associates with the receptor at the cell surface, where it brings about dephosphorylation and re-sensitisation (Murphy *et al.*, 2011b). Therefore, the impact of PP2A inhibition on re-sensitisation of NMU2 signalling was determined. Okadaic acid and fostriecin have been used previously to inhibit PP2A (Garcia *et al.*, 2002; Roosterman *et al.*, 2004; Beaulieu *et al.*, 2005; Murphy *et al.*, 2011a); okadaic acid, is a potent phosphatase inhibitor acting on both PP1 and PP2A (Cohen *et al.*, 1989; Walsh *et al.*, 1997; McCluskey *et al.*, 2001; Murphy *et al.*, 2011), and fostriecin is reported to exhibit selectivity towards PP2A (Lewy *et al.*, 2002). HEK-NMU2 cells were incubated with each PP2A inhibitor for 30 min and then stimulated with hNmU-25 or hNmS-33 (each at 30 nM for 5 min), washed and allowed to recover for 3 h. Neither of the inhibitors affected NMU2 re-sensitisation as assessed by challenge/re-challenge with either hNmU-25 or hNmS-33 after the 3 h recovery period (**Figures 3.13, A-D**).

PKC activity has been shown to affect the re-sensitisation of some receptors, including NK₁R (Toullec *et al.*, 1991). Therefore, the impact of PKC inhibition on the re-sensitisation of NMU2 has been assessed, in this case only with respect to hNmU-25 as the agonist (**Figure 3.14**). HEK-NMU2 cells were pre-incubated with the PKC inhibitor GF109203X (1 μ M), for 30 min and then stimulated with hNmU-25 (30 nM, 5 min) or vehicle, washed with KHB, and incubated in KHB for 3 h. The magnitude of the Ca²⁺ response to challenge/re-challenge with hNmU-25 (30 nM) was determined as an index of re-sensitisation. A complicating aspect for the interpretation of these data was that Ca²⁺ response of agonist naïve cells to challenge with hNmU-25 (30 nM) was greater in cells pre-treated with the PKC inhibitor (**Figure 3.14, B**), indicating that PKC-dependent phosphorylation attenuates the Ca²⁺ response to a single challenge with hNmU-25. Nevertheless, the extent of re-sensitisation in the presence of GF109203X (92%) was clearly greater than under control conditions (64% recovery at 3 h; **Figure 3.14, A**) suggesting that protein kinase C activity negatively impacts on NMU2 re-sensitisation.

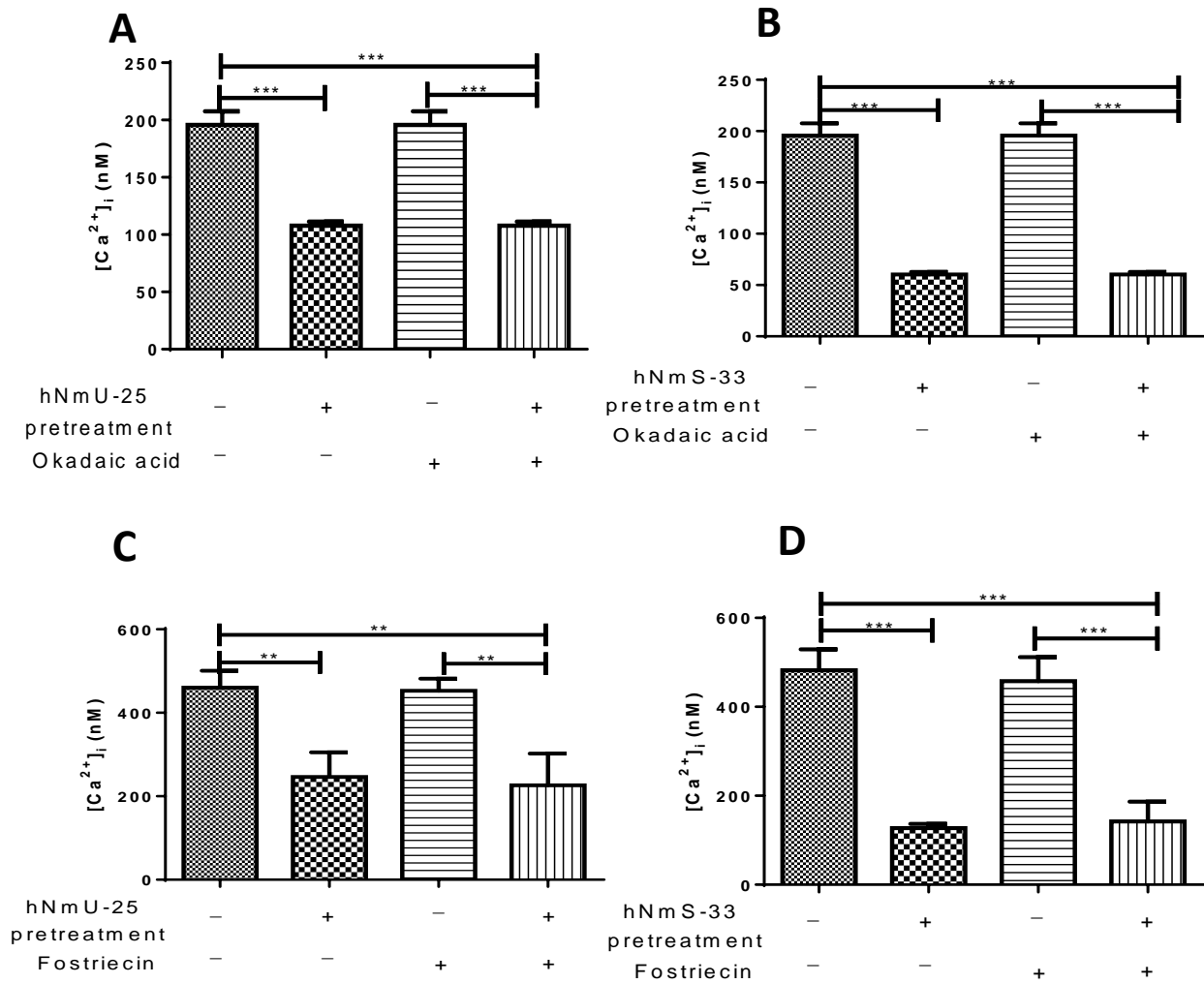


Figure 3.13 Effect of the PP2A inhibitors, okadaic acid and fostriecin on re-sensitisation of NMU2-mediated Ca^{2+} responses

HEK-NMU2 cells were cultured in 96-well plates for 24 h. Cells were pre-treated with either okadaic acid (**A, B**; 10 nM) or fostriecin (**C, D**; 300 nM) to inhibit PP2A or vehicle (buffer) for 30 min and then challenged with ligands (hNmU-25 (**A, C**) or hNmS-33 (**B, D**); each at 30 nM, 5 min) or buffer. Cells were then washed. When added, the inhibitor was present throughout all experimental steps. Cells were allowed to recover for 3 h following the initial agonist challenge and were then loaded with fluo-4-AM during the last 45 min of the recovery period and then re-challenged with ligands (30 nM) using a NOVOstar plate reader. Changes in cytosolic fluorescence were recorded as an index of change in $[\text{Ca}^{2+}]_i$. Data are presented as means \pm s.e.m., $n=3$. Data were analysed by Bonferroni's multiple comparison test following one-way ANOVA; $**P<0.01$, $***P<0.001$ were considered significant.

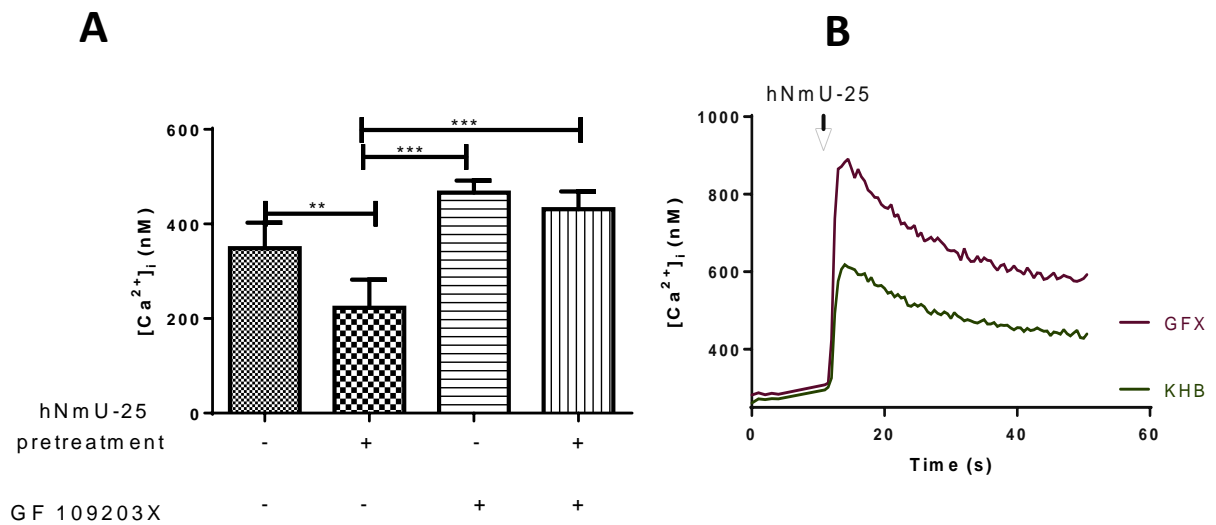


Figure 3.14 Role of PKC activity in NMU2 re-sensitisation

HEK-NMU2 cells were cultured in 96-well plates for 24 h. The cells were then pre-incubated with the PKC inhibitor GF 109203X (GFX; 1 μ M) or vehicle (KHB) for 30 min before stimulation with hNmU-25 (30 nM, 5 min) washing and a recovery period of 3 h. When added, the inhibitor was present throughout all experimental steps. During the last 45 min of the recovery period, cells were loaded with fluo-4-AM before challenge with ligand (30 nM) using a NOVOstar plate-reader and changes in cytosolic fluorescence were recorded as an index of change in [Ca²⁺]_i. GF 109203X (GFX) is auto fluorescent at 488 nM (its colour is orange). Data in panel A are representative of means \pm s.e.m., n=4. Panel B shows example Ca²⁺ traces for agonist-naïve cells incubated in the absence or presence of GFX and stimulated with hNmU-25 (30 nM). Data were analysed by Bonferroni's multiple comparison test following one-way ANOVA; ** P <0.01, *** P <0.001. Significant differences between unchallenged and recovery in the presence and absence of inhibitor were considered.

3.2.4 Effects of the ECE-1 inhibitor, SM-19712, on the recovery of NMU2-mediated Ca²⁺ signalling

In addition to endosomal acidification causing dissociation of the ligand-receptor complex, it has been suggested that ECE-1 activity may be required for the degradation of certain peptide ligands to allow receptor recycling and re-sensitization of signalling (Roosterman *et al.*, 2007b). The effect of ECE-1 activity on the recovery of hNmU-25- and hNmS-33-mediated Ca²⁺ signalling in HEK-NMU2 was therefore examined. Cells were pre-treated with either buffer or the ECE-1 inhibitor, SM-19712 (10 µM) (Umekawa *et al.*, 2000) for 30 min and challenged with buffer, hNmU-25 or hNmS-33 (30 nM, 5 min). The inhibitor concentration used here has been used previously (Murphy *et al.*, 2011). Cells were then washed with KHB and allowed to recover for either 3 or 6 h. SM-19712 inhibited recovery at all times studied following desensitisation with hNmU-25 (**Figure 3.15; A, B**) but not when cells had been desensitised with hNmS-33 (**Figure 3.15; C, D**).

The impact of knocking-down expression of ECE-1 using an anti-ECE-1 siRNA was also determined. Cells were transfected with either a scrambled siRNA (control) or anti-ECE-1 siRNA. ECE-1 expression was reduced (by 69 ± 3%) 48 h after transfection with ECE-1 siRNA, but not following transfection with scrambled siRNA (**Figure 3.16; A**). The reduced expression did not affect the Ca²⁺ response of naïve cells to 30 nM hNmU-25 or hNmS-33 (**Figure 3.16; A & B**). However, knockdown of ECE-1 reduced the response to agonist re-challenge after 6 h recovery in cells pre-stimulated with hNmU-25 (30 nM, 5 min) (**Figure 3.16; B**) but not hNmS-33 (**Figure 3.16; C**).

The potential role of other peptidases in receptor re-sensitisation was investigated using DL-thiorphan (10 µM), as a potent and specific inhibitor of membrane metallo-endopeptidase, neprilysin (NEP) (Tan *et al.*, 1992). This enzyme was selected, since it has been extensively studied and can be regarded as the prototypical neuropeptides degrading enzyme (Bohm *et al.*, 1997). Cells were pre-treated with or without the inhibitor for 30 min and then challenged with either hNmU-25 (**Figure 3.17; A**) or hNmS-33 (**Figure 3.17; B**) (each at 30 nM, 5 min) and following a wash, allowed to recover for 3 h. The cells were then re-challenged with the same ligand at the same

concentration and Ca^{2+} responses recorded using a NOVOstar plate reader. This inhibitor did not affect the Ca^{2+} response of naïve cells to 30 nM of hNmU-25 or hNmS-33 and did not affect the re-sensitisation (**Figure 3.17; A, B**).

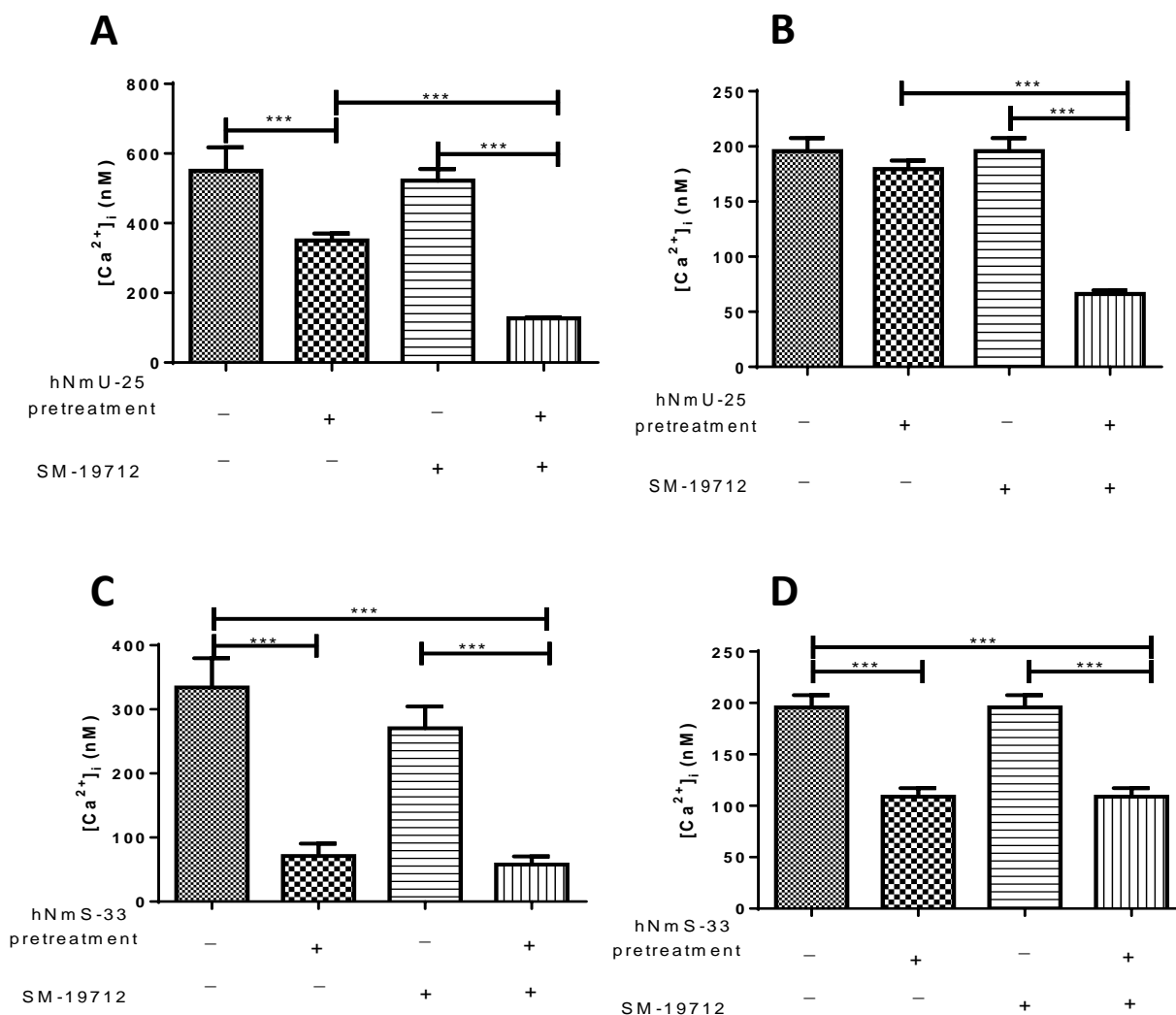


Figure 3.15 Inhibition of ECE-1 reduces receptor re-sensitisation following desensitisation with hNmU-25 but not hNmS-33

HEK-NMU2 cells were pre-incubated \pm the ECE-1 inhibitor, SM19712 (10 μ M), for 30 min and then challenged with buffer or the ligands hNmU-25 (A & B) or hNmS-33 (C & D) (30 nM, 5 min). Cells were washed and allowed to recover for 3 (A & C) or 6 h (B & D) (\pm inhibitor) before determination of Ca²⁺ responses to the same ligand (30 nM). Changes in cytosolic fluorescence were then monitored as an index of [Ca²⁺]_i using a NOVOstar plate-reader. Data are mean \pm s.e.m., n=4. Data were analysed by Bonferroni's multiple comparison test following one-way ANOVA; ****P*<0.001.

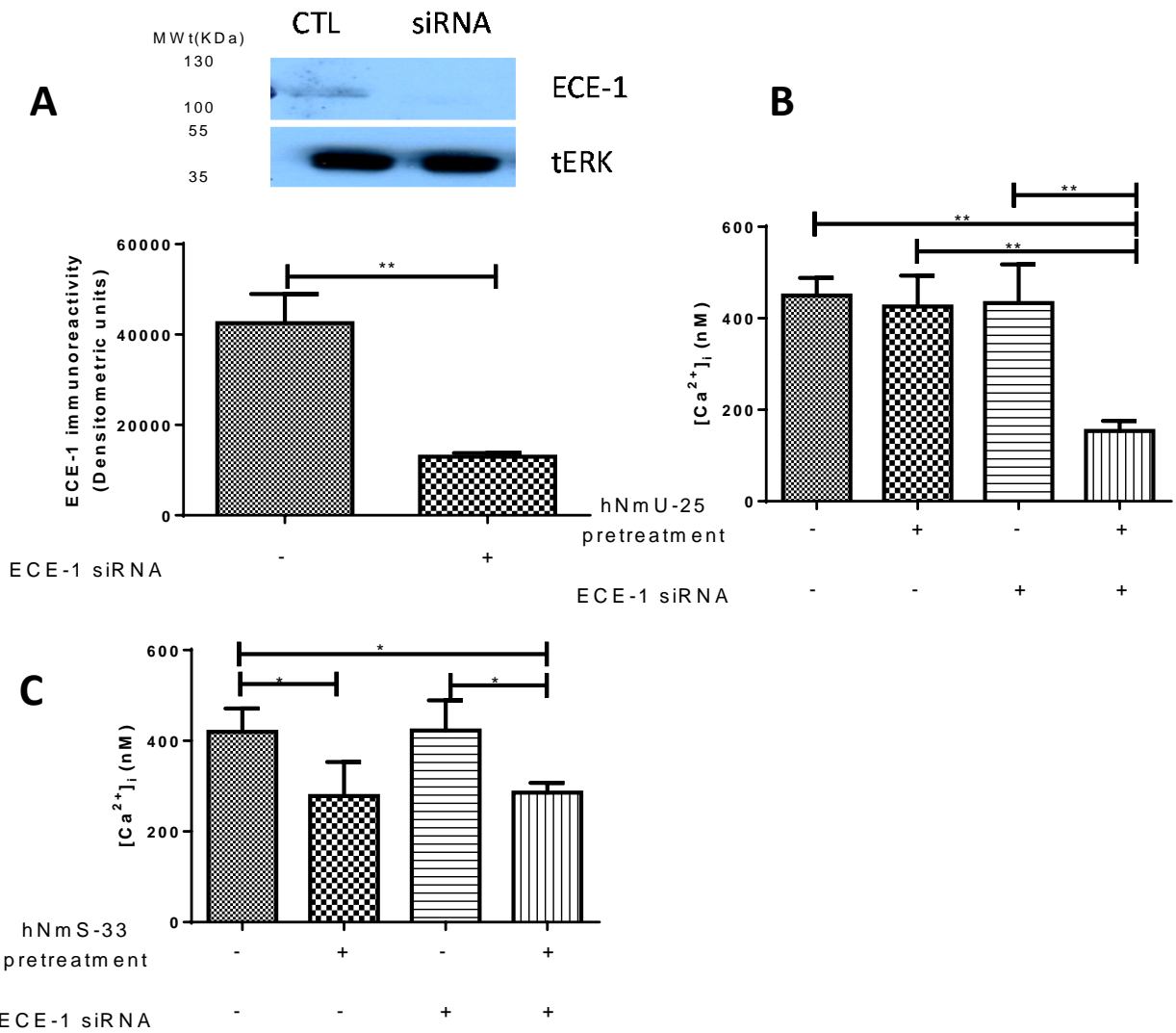


Figure 3.16 Knockdown of ECE-1 inhibits re-sensitisation of NMU2-mediated Ca²⁺ signalling

A. HEK-NMU2 cells were transfected with ECE-1 siRNA or scrambled as described in Methods. Scrambled siRNA was used as control (CTL). The expression of ECE-1 was determined by immunoblotting. Blotting of total ERK was used as a loading control (**A**). Transfected cells were pre-treated with either buffer (control), hNmU-25 (**B**) or hNmS-33 (**C**) (30 nM, 5 min) washed with KHB followed by 6 h recovery. Cells were then either challenged or re-challenged with the same concentration using a NOVOstar plate reader and changes in cytosolic fluorescence were recorded as an index of changes in [Ca²⁺]_i. The data were analysed by Student's paired *t* test (**A**) or Bonferroni's multiple comparison test following one-way ANOVA (**B**); **P*<0.05, ***P*<0.01. Data are representative or mean ± s.e.m., n=3.

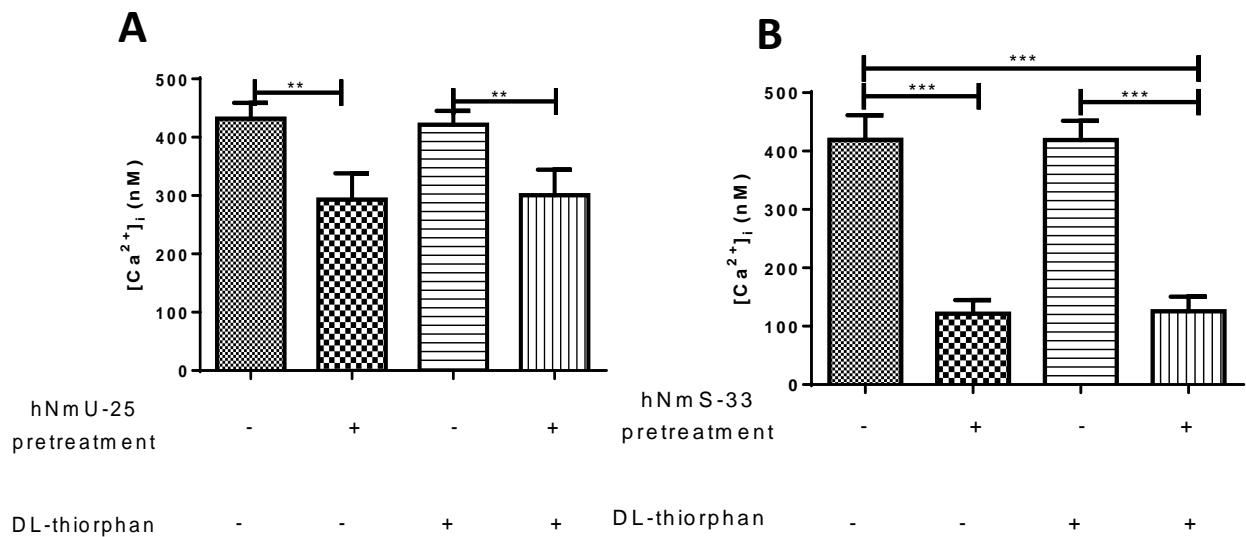


Figure 3.17 Effect of NEP inhibitor on re-sensitisation of NMU2-mediated Ca²⁺ signalling

HEK-NMU2 cells were cultured in 96-well plates for 24 h. Cells were then pre-treated with vehicle or DL-thiorphan (10 μ M) for 30 min and then challenged with buffer or ligand hNmU-25 (**A**) or hNmS-33 (**B**) (30 nM, 5 min) followed by three buffer washes. This was followed by a recovery period of 3 h. NEP inhibitor was present or absent throughout all experimental steps. During the last 45 min of the recovery period, cells were loaded with fluo-4-AM before challenge with ligand (30 nM) using a NOVOstar plate-reader. Changes in cytosolic fluorescence were recorded as an index of changes in [Ca²⁺]_i. Data are mean \pm s.e.m., n=3. Data were analysed by Bonferroni's multiple comparison test following one-way ANOVA; ** P <0.01, *** P <0.001.

3.2.5 Further characterization of effects of the ECE-1 inhibitor, SM-19712, on NMU2 re-sensitization

In order to assess the extent of the Ca^{2+} signal recovery following pre-treatment with different agonist concentrations, HEK-NMU2 cells were challenged with a range of concentrations of hNmU25 (30 nM, 300 nM and 1 μM ; 5 min) and then washed and allowed to recover for 6 h. The cells then were re-challenged with a maximally-effective hNmU-25 concentration (30 nM) and the Ca^{2+} responses recorded using the NOVOstar plate-reader. After 6 h it could be seen that recovery varied with concentration of the initial agonist pre-treatment. Whereas the Ca^{2+} response had recovered to 92% of the response observed in untreated HEK-NMU2 cells, this was reduced to 63 and 38% in cells pre-treated with 0.3 and 1 μM hNmU-25, respectively (**Figure 3.18; A**). At the highest agonist concentration tested (hNmU-25, 1 μM), the ECE-1 inhibitor significantly reduced NMU2 re-sensitisation (**Figure 3.18; B**).

The ability of ECE-1 to regulate re-sensitisation of cells following challenge with a concentration that was sub-maximal for the Ca^{2+} response was also investigated. HEK-NMU2 cells were pre-incubated with ECE-1 inhibitor for 30 min and the cells were then stimulated with hNmU-25 (3 nM, 5 min) and the cells then washed and allowed to recover for 1 h (**Figure 3.19**). Under these conditions, hNmU-25-induced Ca^{2+} signals were almost completely re-sensitised after 1 h recovery either in the presence or in absence of the ECE-1 inhibitor SM-19712 (**Figure 3.19**).

Having already established that Ca^{2+} response recovery was faster following 5 min pre-treatment with hNmU-25 compared to hNmS-33, we investigated the effect of reducing the agonist pre-treatment period on response recovery. Pre-treatment with hNmU-25 (30 nM, 1 min) resulted in a more rapid re-sensitisation with 68% recovery of the Ca^{2+} response to re-challenge after 1 h and almost full recovery after 3 h (**Figure 3.20; A**). the rate of recovery was significantly reduced in the presence of the ECE-1 inhibitor at both the 1 and 3 h time-points (**Figure 3.20; A & B**). In contrast, Ca^{2+} response recovery after pre-treatment with hNmS-33 (30 nM, 1 min) was unaffected by ECE-1 inhibition (**Figure 3.20; C**).

The effects of brief acid washing (to facilitate ligand-receptor dissociation) on the recovery of NMU2 from desensitisation were assessed in absence and presence of ECE-1 inhibitor. In this experiment, the cells were pre-incubated (\pm inhibitor) for 30 min and following challenge with hNmU-25 (30 nM, 5 min) cells were briefly washed with acidified buffer and allowed to recover for 6 h (**Figure 3.21**). In these experiments, an almost complete recovery of the Ca^{2+} response was observed irrespective of whether the brief acid wash applied. However, in the presence of SM-19712 recovery was markedly inhibited irrespective of whether the acid wash was applied (**Figure 3.21**). The duration of the agonist pre-treatment and the timing of ECE-1 inhibitor addition were also investigated. It has been demonstrated that ECE-1 is present both at the plasma membrane and in the endosomes (Roosterman *et al.*, 2007), and therefore it is likely that inhibition of ECE-1 at the cell surface could prevent extracellular peptide from breakdown, which might enhance desensitisation or prevent recovery. Thus, the inhibitor was added after pre-treatment and subsequent removal of NmU. Prolonging the pre-treatment period with hNmU-25 (30 nM, 5, 15 or 30 min) had a relatively modest effect on re-sensitisation with respect to the Ca^{2+} response, however, in all cases SM-19712 applied either before or subsequent to the agonist pre-treatment reduced the extent to which re-sensitisation occurred in the 6 h recovery period (**Figure 3.22**).

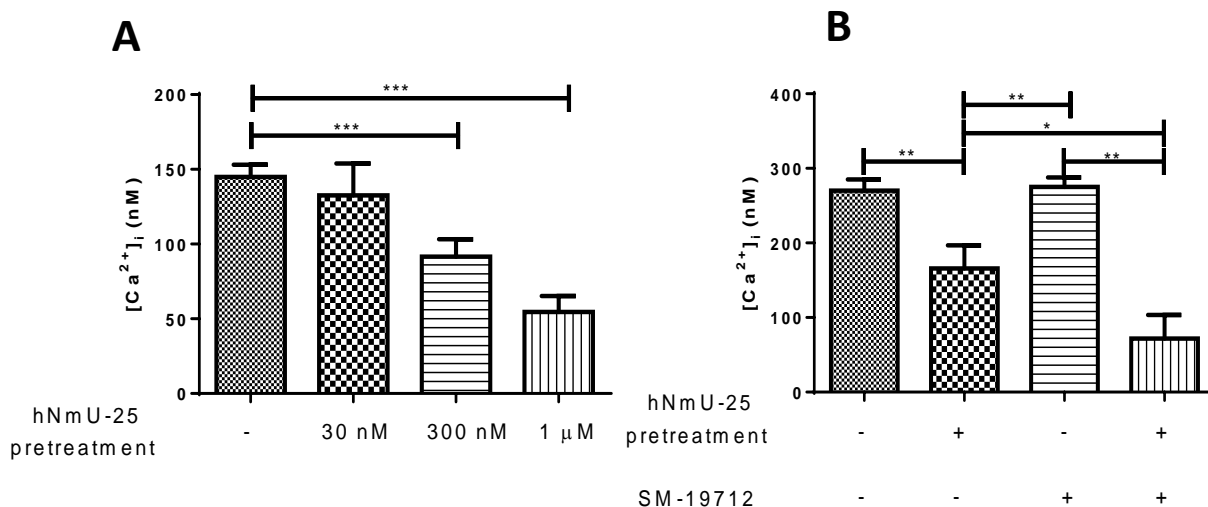


Figure 3.18 Effect of ECE-1 inhibition on the re-sensitisation of NMU2 following desensitisation with hNmU-25 using (1 μ M)

HEK-NMU2 cells were cultured in 96-well plates for 24 h. Cells were then challenged with different concentrations of hNmU-25 (30, 300 nM or 1 μ M, 5 min) followed by washing with buffer and a 6 h recovery (**A**). Alternatively, cells were pre-incubated with or without the ECE-1 inhibitor, SM-19712 for 30 min and then challenged with hNmU-25 (1 μ M, 5 min) followed by a buffer washing and a 6 h recovery (**B**). During the last 45 min of the recovery period, cells were loaded with fluo-4-AM before challenge with hNmU-25 (30 nM) using a NOVOstar plate reader and changes in cytosolic fluorescence were recorded as an index of change in [Ca²⁺]_i. Data are means \pm s.e.m, n=3; data were compared by Bonferroni's multiple comparison test following one-way ANOVA: * P <0.05, ** P <0.01, *** P <0.001.

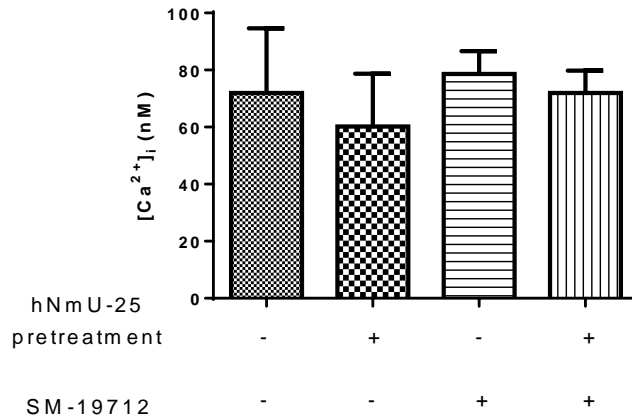


Figure 3.19 The effect of sub-maximal concentration of ligand on the recovery of NMU2-mediated Ca²⁺ signalling

HEK-NMU2 cells were cultured in 96-well plates for 24 h. Cells were pre-incubated with or without the ECE-1 inhibitor, SM19712 (10 μ M) for 30 min and then challenged with buffer or ligands hNmU-25, (3 nM, 5 min). Cells were washed and allowed to recover for 1 h in the presence and absence of the inhibitor. During the last 45 min of the recovery period, cells were loaded with fluo-4-AM before challenge with ligand using the same concentration using a NOVOstar plate-reader. Changes in cytosolic fluorescence were recorded as an index of changes in [Ca²⁺]_i. The data were analysed by Bonferroni's multiple comparison test following one-way ANOVA. Data are means \pm s.e.m.; n=3.

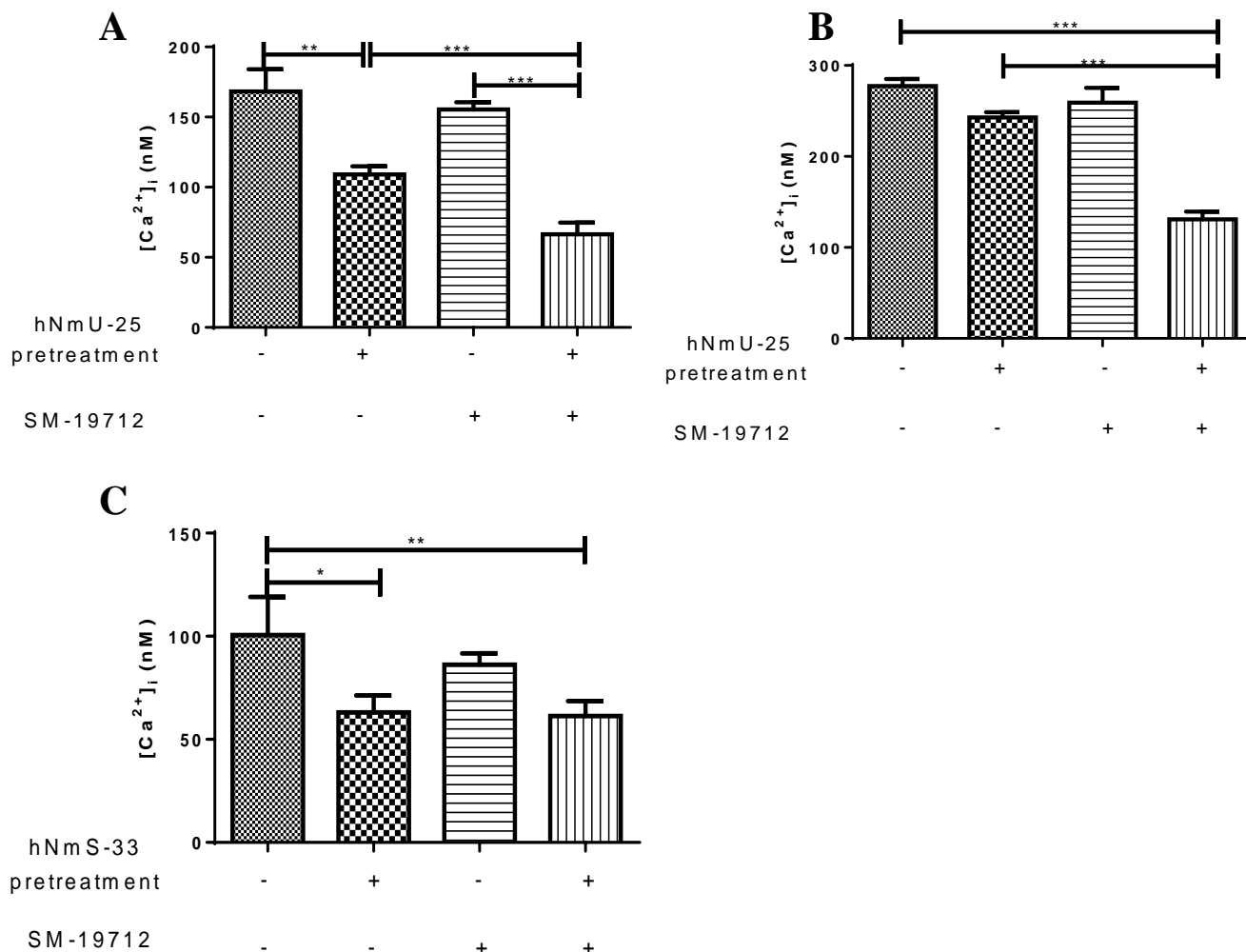


Figure 3.20 Effect of reducing the time of pre-treatment with NmU/NmS ligands on NMU re-sensitisation in the absence and presence of ECE-1 inhibitor

HEK-NMU2 cells were cultured in 96-well plates for 24 h. Cells were pre-incubated with or without the ECE-1 inhibitor, SM19712 (10 μ M) for 30 min and then challenged with buffer, hNmU-25 or hNmS-33 (in all cases 30 nM for 1 min). Cell monolayers were washed and allowed to recover for 1 h (**A**, **C**) or 3 h (**B**). During the last 45 min of the recovery period, cells were loaded with fluo-4-AM before challenge with ligand (30 nM) using a NOVOstar plate-reader and changes in cytosolic fluorescence were recorded as an index of change in $[Ca^{2+}]_i$. Data are mean \pm s.e.m.; n=3. Data were analysed by Bonferroni's multiple comparison test following one-way ANOVA; * $P < 0.05$ ** $P < 0.01$, *** $P < 0.001$.

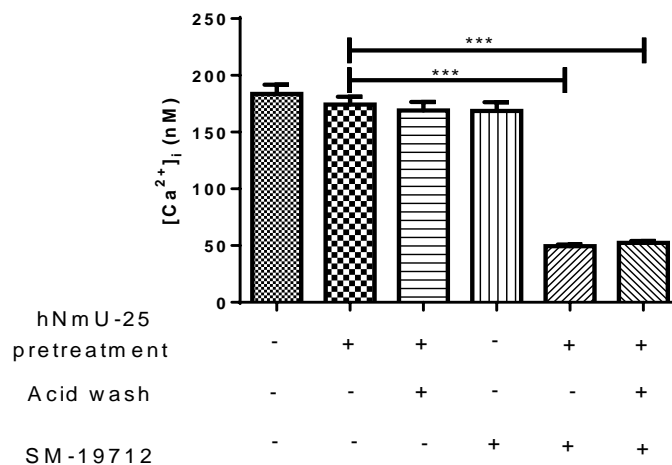


Figure 3.21 Effect of brief acid-washing and ECE-1 inhibition on NMU2 re-sensitisation

HEK-NMU2 cells were cultured in 96-well plates for 24 h. Cells were pre-incubated with or without the ECE-1 inhibitor, SM-19712 (10 μ M) for 30 min and then challenged with hNmU-25 (30 nM, 5 min) followed by a brief acid wash and by a 6 h recovery period. During the last 45 min of the recovery period, cells were loaded with fluo-4-AM before challenge with ligand (30 nM) using a NOVOstar plate-reader and changes in cytosolic fluorescence were recorded as an index of change in $[Ca^{2+}]_i$. Data are mean \pm s.e.m.; n=3. Data were analysed by Bonferroni's multiple comparison test one-way ANOVA; *** $P < 0.001$.

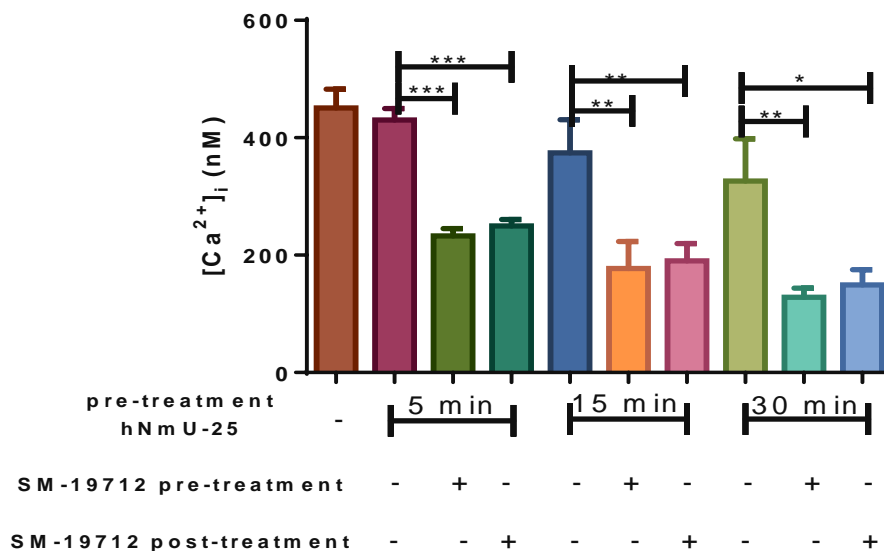


Figure 3.22 Effect of the duration of the desensitising challenge on the recovery of NMU2 in the presence of ECE-1 inhibitor added either before or after the challenge

HEK-NMU2 cells were cultured in 96-well plates for 24 h. Cells were pre-incubated with KHB or SM-19712 either before the stimulation (10 μ M, 30 min) or during the re-sensitisation period after agonist stimulation. Treatment was included in all subsequent experimental steps. The cells then either challenged with hNmU-25 for different times (30 nM, 5, 15 or 30 min) or unchallenged. The ligand was then removed by washing with KHB and allowed to recover for 6 h. During the last 45 min of the recovery period, cells were loaded with fluo-4-AM and then re-challenged with hNmU-25 (30 nM) using a NOVOstar plate-reader and changes in cytosolic fluorescence were recorded as an index of changes in $[Ca^{2+}]_i$. The data were then calibrated as described in Methods and are presented as means \pm s.e.m., n=4. Data were analysed by Bonferroni's multiple comparison test following two-way ANOVA; * $P<0.05$, ** $P<0.01$, *** $P<0.001$.

3.2.6 Is hNmU-25 degraded extracellularly by ECE-1?

Peptides are removed from the extracellular fluid principally by enzymatic degradation by cell surface enzymes, exemplified by neutral endopeptidases, such as ECE-1 (Grady *et al.*, 1997). In order to examine the possibility that the effects of ECE-1 inhibition were a consequence of reducing peptide degradation at the cell surface, different approaches were used.

The extracellular degradation of hNmU-25 was assessed using a bioassay. Agonist-naïve HEK-NMU2 cells were used to assess Ca^{2+} response stimulated by hNmU-25 that had first been incubated with either HEK-NMU2 cells or wild-type HEK293 cells (i.e. cell devoid of NmU-sensitive receptors) for different periods of time (1-3 h; at 37°C). To assess the effects of the ECE-1 inhibitor (SM-19712; 10 μM) and/or dynamin inhibitor, dynasore (80 μM) these agents were added to HEK-NMU2 cells (**Figures 3.23; A-C**) in 24 well plates for 30 min before addition of hNmU-25 (10 nM) for 1, 2 or 3 h. After the appropriate time-period incubation, medium was transferred on to monolayers of fluo-4-loaded HEK-NMU2 cells and Ca^{2+} responses assessed. Incubation with HEK-NMU2 cells for increasing period of time diminished the Ca^{2+} responses observed on transfer to fresh, fluo-4-loaded HEK-NMU2 cells (**Figure 3.23; A-C**) indicating that the medium hNmU-25 concentration is decreasing. In the presence of SM-19712 and/or dynasore there was a trend towards greater Ca^{2+} responses being maintained, suggesting that ECE-1 inhibition and or dynamin inhibition diminish the extent of hNmU-25 degradation. In the HEK-293 cell background there was again some evidence for SM-19712/dynasore protecting the agonist from degradation.

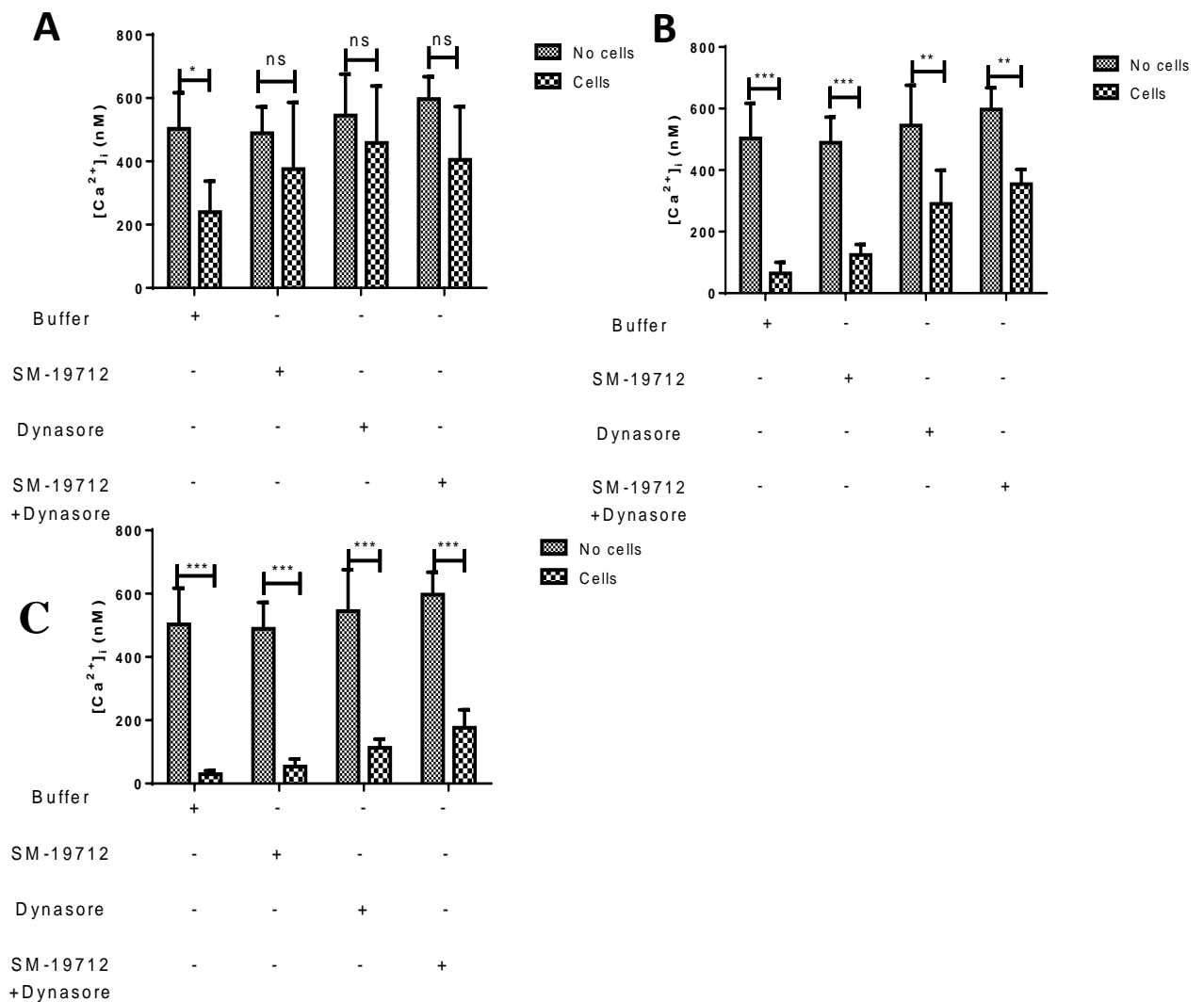


Figure 3.23 Assessment of hNmU-25 degradation using a bioassay

HKE-NMU2 or wild-type HEK293 cells were cultured in both 96 and 24-wells-plate for 24 h. Cells were pre-incubated with buffer or inhibitors: SM-19712 (10 μ M) and/or dynasore (80 μ M) for 30 min prior to stimulation. The cells, HEK-NMU2 (**A**, **B**, **C**) in 24 wells-plates were challenged with hNmU-25 (10 nM) for the indicated time (1 (**A**), 2 (**B**), or 3 (**C**) h). The cells in 96-wells plate were loaded with fluo-4-AM for 45 min. The extracellular medium taken from the 24-well plates was then used to stimulate the cells in 96-wells plate after the required pre-incubation times. Changes in cytosolic fluorescence were then monitored as an index of $[Ca^{2+}]_i$ using a NOVOstar plate-reader in order to estimate how much hNmU-25 remained. Data are means \pm s.e.m., n=3. Data were analysed by Bonferroni's multiple comparison test following two-way ANOVA; * P <0.05, ** P <0.01, *** P <0.001.

3.2.7 Endothelin-converting enzyme-1 degrades neuromedin U

Having established that ECE-1 plays a role in the re-sensitisation of NMU2 and peptide degradation, the degradation of peptide ligands by recombinant (rhECE-1) was studied *in vitro*. ECE-1 is a neprilysin-related metallo-peptidase present in both endosomes and at the plasma membrane. The ECE-1 could degrade neuropeptides either at the cell surface or within the acidic endosomal environment (Fahnoe *et al.*, 2000a). The rate at which rhECE-1 degrades selected peptides was therefore examined under both conditions. The experiments performed in this project were done according to the current publication (Roosterman *et al.*, 2007). Thus, the first experiment was done by diluting hNmU-25 (25 μ M) using pH 5.5 and pH 7.4 without incubation to ensure the peptide is present in the absence of rhECE-1. The reaction was stopped by centrifuging the mixture (peptide + rhECE-1) in vivacon 500 tubes to separate the peptide from the enzyme at 14.0 x g for 2 minutes and the peptide was then collected in microfuge tube and the products were separated by **HPLC** prior to analysis by LC-MS/MS using an LTQ-Orbitrap-Velos mass spectrometer (Thermo Scientific, UK) as described in Methods. Briefly, samples were loaded at high flow rate onto a reverse-phase trap column (0.3mm i.d. x 1mm), containing 5 μ m C18 300 Å Acclaim PepMap media (Dionex) maintained at 37 °C. The loading buffer was 0.1% formic acid / 0.05% trifluoro acetic acid / 2% acetonitrile as described in Method (**Methods 2.5**). Products were collected and analyzed by time-of-flight mass spectrometry. Mass spectrometry data were provided by the Protein and Nucleic Acid Chemistry Laboratory (PNAACL) at the University of Leicester, UK. The data revealed that the intact peptide was present in both conditions (**Figure 3.24**). In order to optimise the best conditions for the experiments, some approaches were used. Firstly, the time course incubation was investigated. hNmU-25 (25 μ M) was incubated using (Mes/KOH, pH 5.5) buffer in the presence and absence of rhECE-1 (0.1 μ g) for different time (0, 2, 5, and 30 min) at 37°C. The reaction was stopped by spinning at 14.0 x g using Vivacon 500 tube to separate the enzyme from the peptide (**Figure 3.25**). The peptide was fully degraded in the presence of pH 5.5 at all-time points. At time 0, the majority of the fragments were absent. In contrast, also, most of the fragments were not detectable in the absence of the enzyme.

Based on the above results and after we determined the suitable conditions, the main experiments were conducted. Briefly, three peptides were investigated: hNmU-25, hNmS-33 and pNmU-8. The experiments were done in parallel. Peptides (25 μ M) were added in the presence and absence of rhECE-1 (0.1 μ g) and incubated in 37°C, at either pH (5.5) or pH (7.4) for 2 min and then centrifuged 14.0 x g for 2 minutes to stop the reaction by separating the enzyme from the peptide using Vivacon 500 tube containing filter. The products were separated and analyzed as described. The final products of all ligands are shown (**Figures 3.26, 3.27, 3.28**). Some peptides were degraded in both pH 7.4 and 5.5. On the other hand, the fragments were more in pH 5.5 than pH 7.4. The bioactivity of NmU is mediated mainly through its C-terminal conserved region; F, L, F, R, P, R and N. Therefore, from the fragments at pH 5.5, it can be seen that some of them could be active. The active fragments produced from hNmU-25 include EEFQSPFASQSRGYFLFRPRN, FQSPFASQSRGYFLFRPRN, SPFASQSRGYFLFRPRN, PFASQSRGYFLFRPRN, FASQSRGYFLFRPRN, ASQSRGYFLFRPRN, SQSRGYFLFRPRN, SRGYFLFRPRN, YFLFRPRN, and FLFRPRN. In addition, the possible active fragments obtained from hNmS-33 include FTKKDHTATWGRPFLLFRPRN, WGRPFLLFRPRN, GRPFLLFRPRN, and FLFRPRN. Finally, only two fragments were identified from pNmU-8 including YFLFRPR, FLFRPRN. For clarification, these conserved regions were underlined.

In addition, based on the final products of peptide degradation, our second aim was to determine the expected cleavage sites for all ligands. The fragments were compared to the intact peptides and then the cleavages sites were identified (**Figure 3.29**) in both conditions at either pH 5.5, so we can compare the cleavages site between each other. It is clear from identifying these predicted cleavage sites that the last five amino acids including F, R, P R, and N and protected and conserved in both hNmU-25 and hNmS-33, but not pNmU-8 that L, F, R, P, and R were protected and conserved.

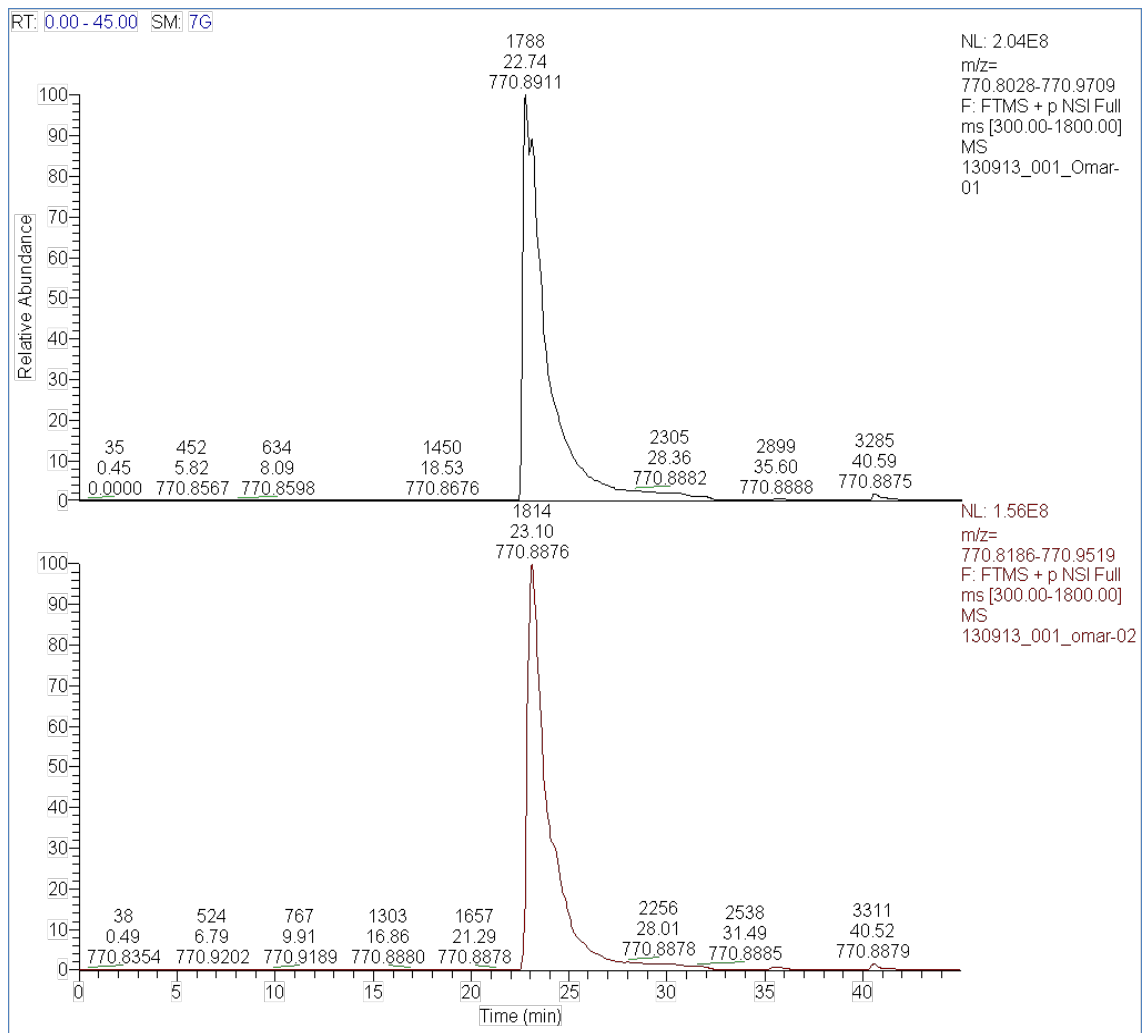
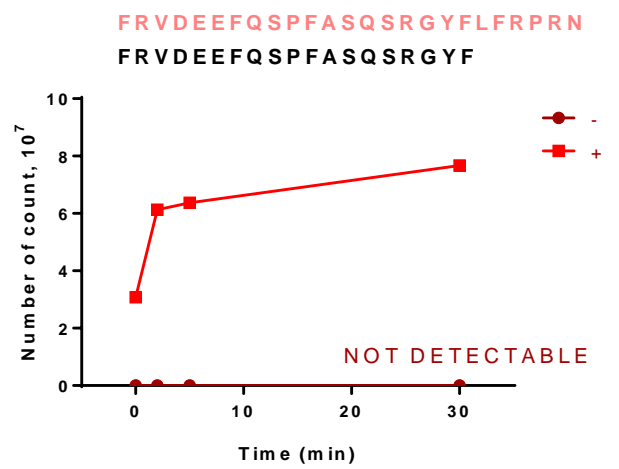
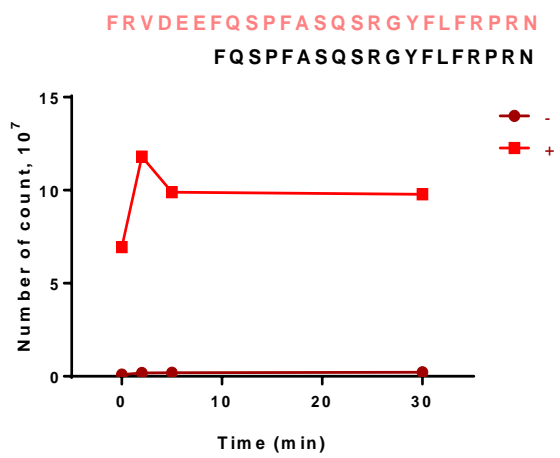
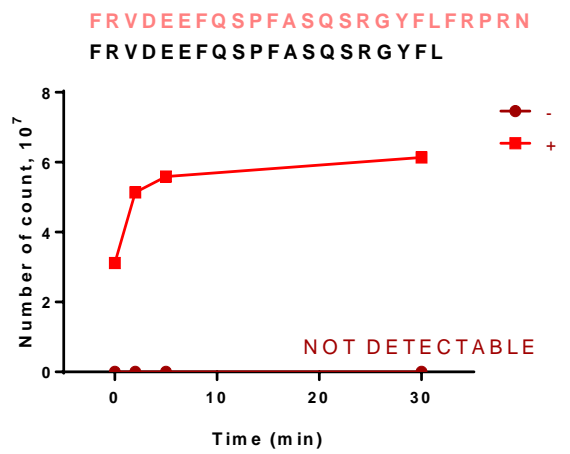
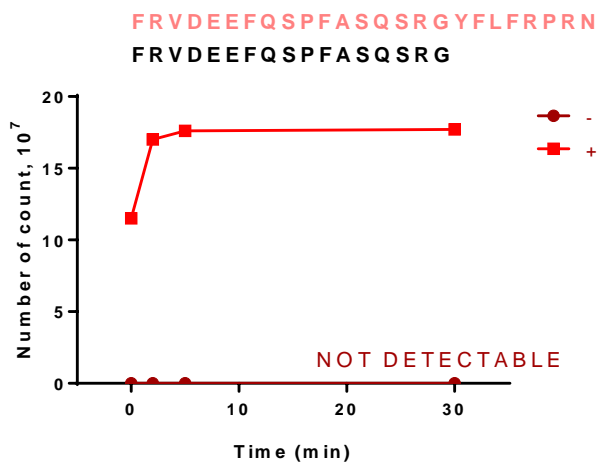
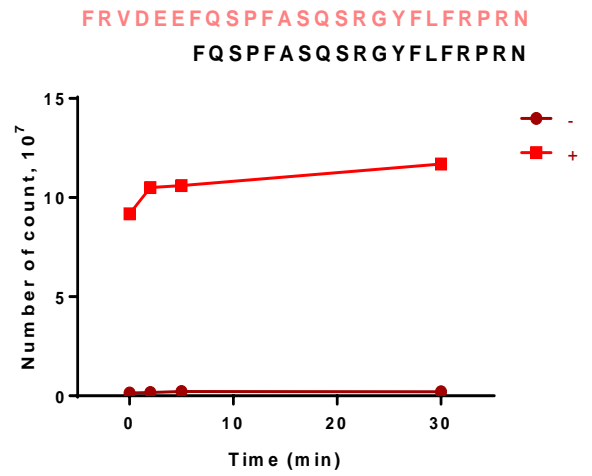
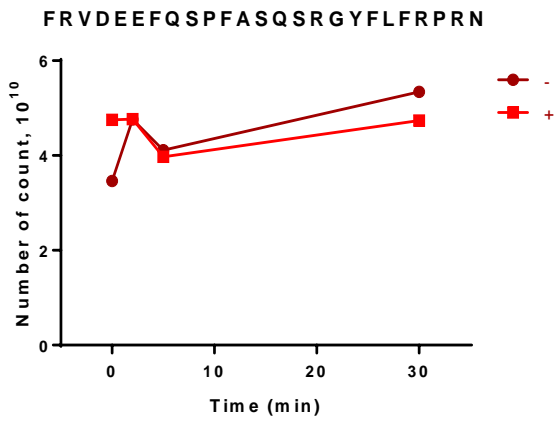
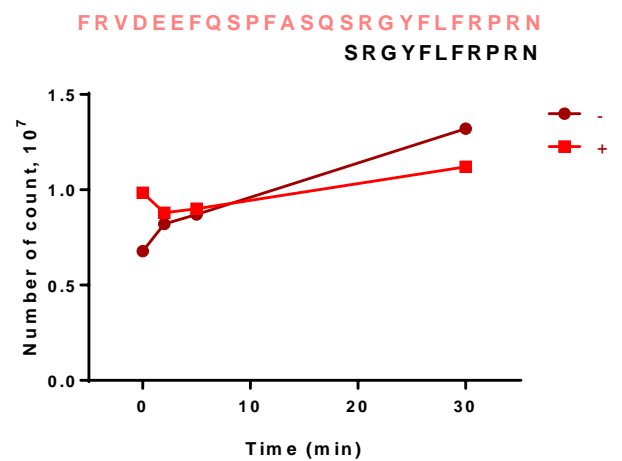
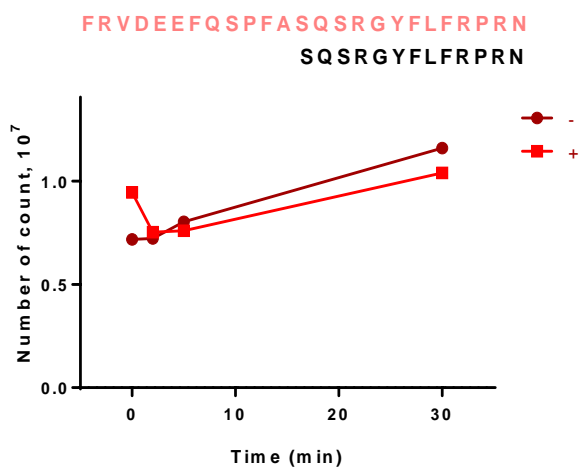
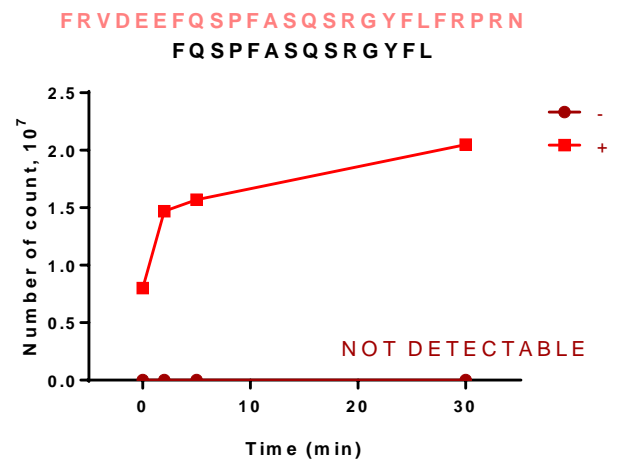
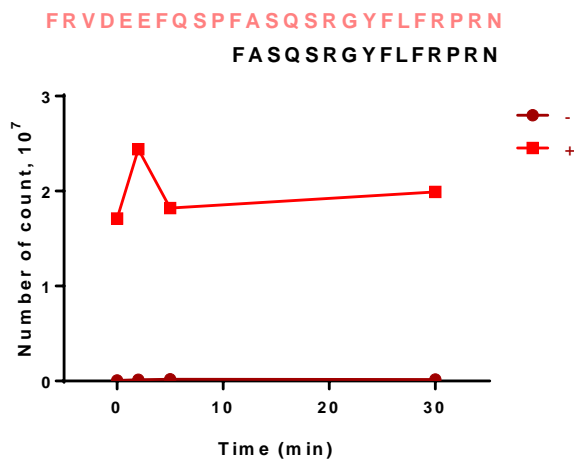
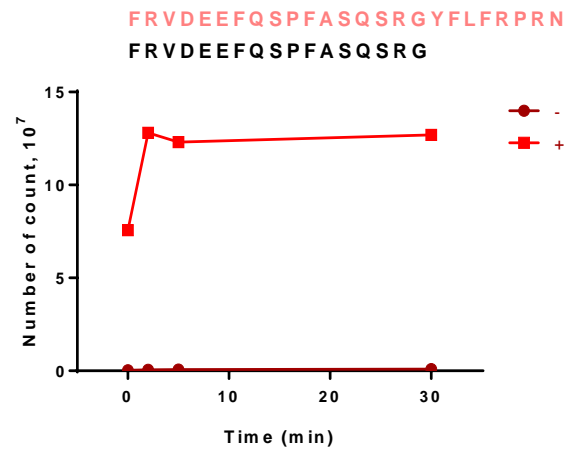
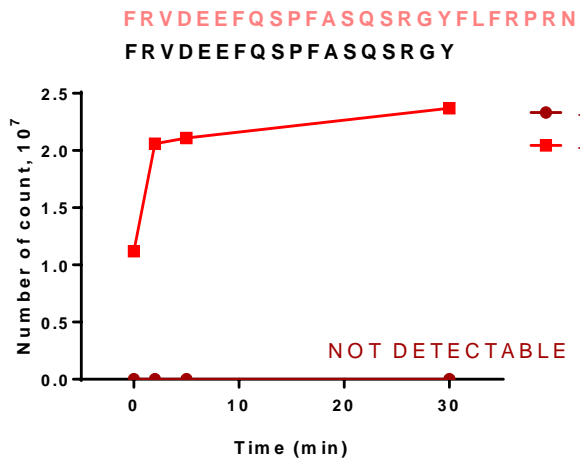
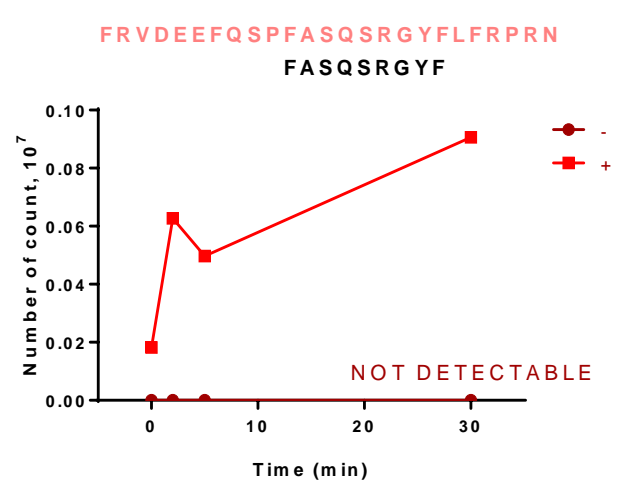
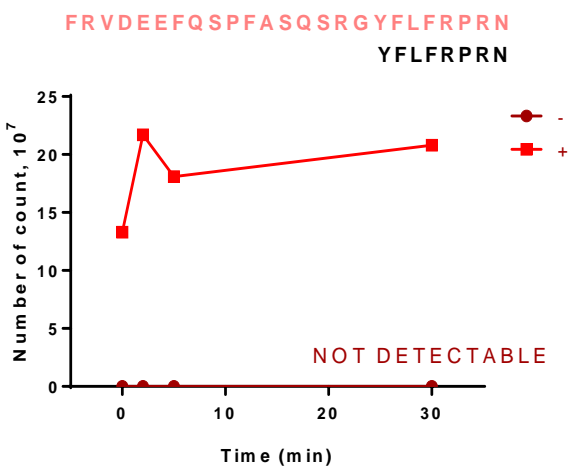
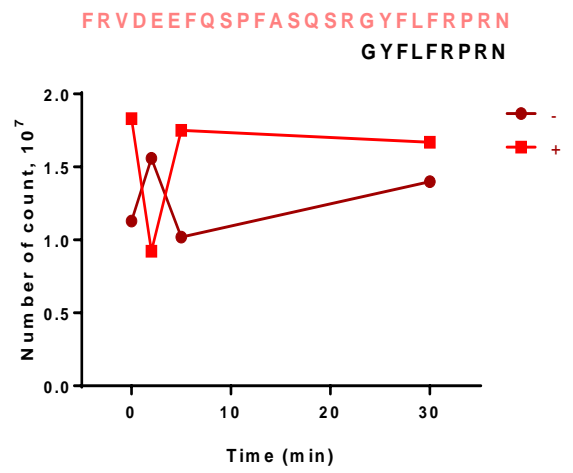
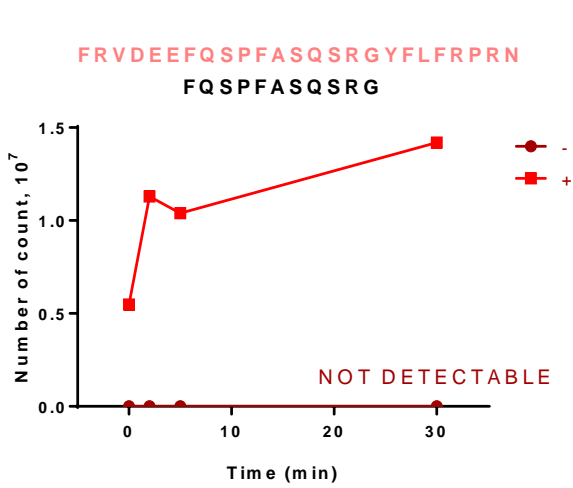
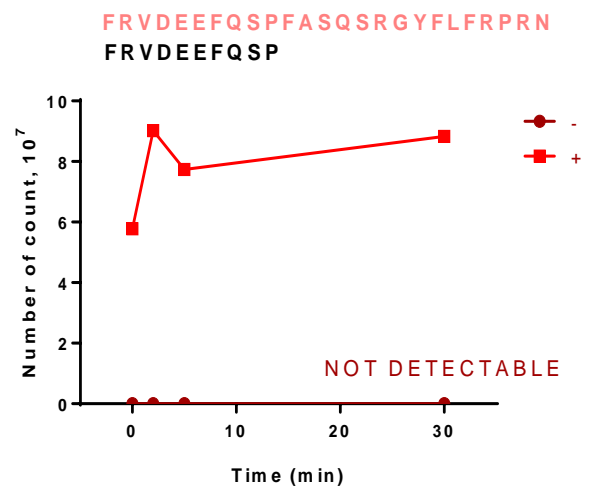
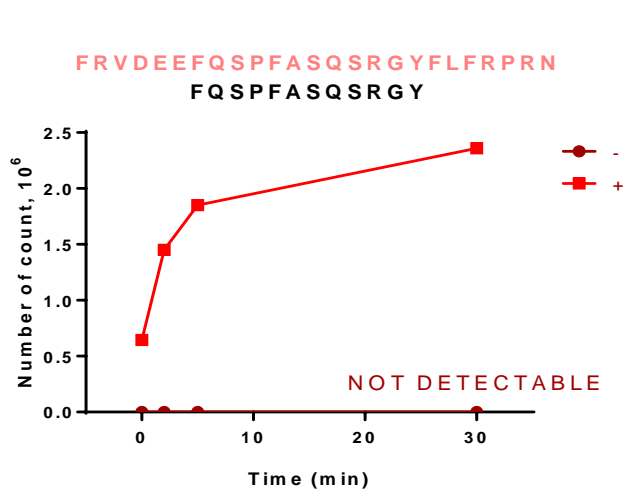


Figure 3.24 The effect of incubation on the peptides in the absence of rhECE-1

hNmU-25 (25 μ M) was added in the absence of rhECE-1 at either pH (5.5, MES/KOH) sample 1 or (7.4, Tris-HCL) sample 2, (Sample 1 = Upper Trace, Sample 2 = Lower Trace), without incubation and the reaction was stopped by spinning at 14.0 x g for 2 min using Vivacon 500 filter as described in Methods. Both samples showed the intact peptide very clearly.







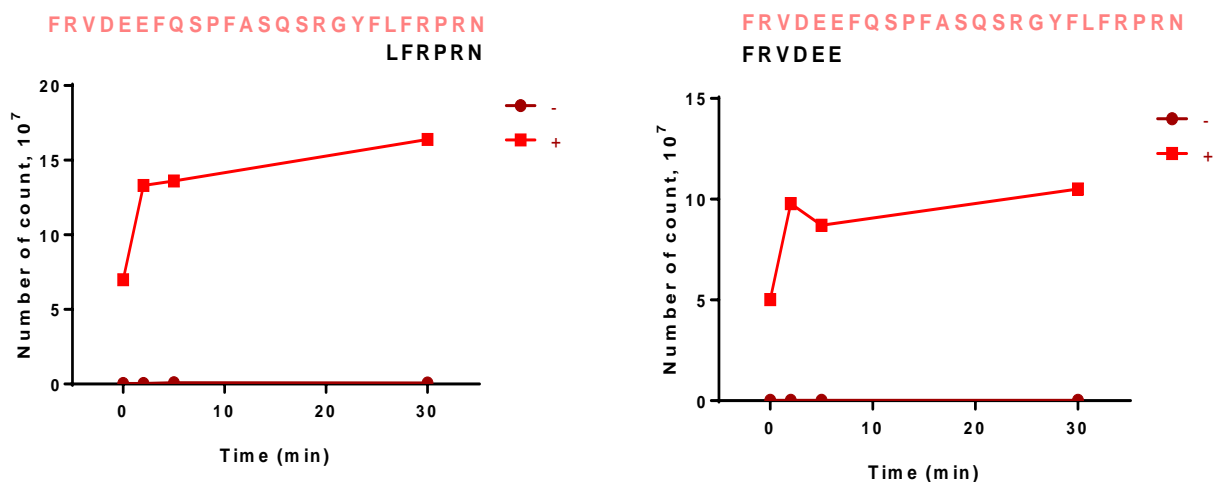


Figure 3.25 The *in vitro* assessment of hNmU-25 degradation by rhECE-1

Time course of degradation of hNmU-25 by rhECE-1. hNmU-25 (25 μ M) was added in the presence and absence of rhECE-1 (0.1 μ g) and incubated at 37°C, pH (5.5) for the time periods as shown. Fragments, as a result of degradation, are indicated in black with the parent sequence shown above in red. The y axis is considered to be a number of count (See Methods for more details). - represents in the absence of rhECE-1. + represents in the presence of rhECE-1.

	Peptide Sequence	XIC m/z	hNmU-25				hNmU-25			
			pH 5.5				pH 7.4			
			- Enzyme		+ Enzyme		- Enzyme		+ Enzyme	
			RT	Area	RT	Area	RT	Area	RT	Area
G1	FRVDEEFQSPFASQSRGYFLFRPRN	770.6395 (4+)	23.97	80603674729	23.96	49873490616	25.45	73584594478	25.15	78929109563
	FRVDEEFQSPFASQSRGYFL	1205.5784 (2+)	not detected		27.01	117330985	not detected		28.4	313856411
	FRVDEEFQSPFASQSRGYF	1149.0392 (2+)	not detected		25.39	228751499	27.19	7098809	26.59	86158877
	FRVDEEFQSPFASQSRGY	717.6714 (3+)	not detected		23.17	327813550	24.96	6386403	24.21	10061871
	FRVDEEFQSPFASQSR	965.4471 (2+)	not detected		19.48	40599391	24.01	1345739529	23.46	953114111
	FRVDEEFQSP	627.2876 (2+)	not detected		20.85	63240289	not detected		not detected	
	FRVDEEF	471.2163 (2+)	not detected		21.37	63240289	not detected		not detected	
	FRVDEE	397.6874 (2+)	not detected		15.33	579269075	not detected		16.1	1201245
G2	FRVDE	333.1639 (2+)	not detected		15.03	986994	not detected		not detected	
	EEFQSPFASQSRGYFLFRPRN	854.7499 (3+)	22.66	8917493	23.26	11426061	25.35	17840047	24.59	21070821
	FQSPFASQSRGYFLFRPRN	768.7224 (3+)	not detected		22.8	530190692	not detected		not detected	
	SPFASQSRGYFLFRPRN	677.0137 (3+)	23.97	220837502	23.98	120092554	25.71	203253987	24.94	222512646
	PFASQSRGYFLFRPRN	648.0045 (3+)	24.01	266836772	23.96	163161624	25.7	286940903	24.95	305445275
	FASQSRGYFLFRPRN	615.6532 (3+)	not detected		19.77	156088301	not detected		21.19	392875
	ASQSRGYFLFRPRN	566.6315 (3+)	not detected		19.77	14238890	20.91	4292002	19.85	2976313
	SQSRGYFLFRPRN	542.9528 (3+)	18.42	23598968	18.39	22923264	20.94	21163527	19.88	25078477
	SRGYFLFRPRN	471.2568 (3+)	18.46	18027611	18.58	13432805	21.14	50833883	20.01	13248078
	YFLFRPRN	556.3056 (2+)	not detected		19.72	2539114636	22.28	12312644	21.23	40048957
	FLFRPRN	474.7759 (2+)	16.56	12797961	17.08	77914023	19.46	15499445	18.56	12750093
	LFRPRN	401.2426 (2+)	not detected		11.51	2144109138	13.61	17417260	12.72	113362126
G3	FRPRN	344.7032 (2+)	not detected		11.52	226831941	13.59	1278537	12.73	11004873
	FQSPFASQSRGYF	761.3525 (2+)	not detected		23.88	56797102	not detected		not detected	
	FQSPFASQSRGY	687.8183 (2+)	not detected		20.8	10018409	not detected		not detected	
	FQSPFASQSRG	606.2875 (2+)	not detected		19.06	82216825	not detected		not detected	
	FASQSRGYF	531.7485 (2+)	not detected		18.84	5964825	not detected		not detected	
	FASQSRGY	458.2165 (2+)	not detected		13.06	1054693	not detected		not detected	

Figure 3.26 Peptide fragments identified following incubation with rhECE-1

hNmU-25 (25 μ M) was added in the presence or absence of rhECE-1 (0.1 μ g) and incubated in 37°C, at either pH 5.5, MES/KOH, or 7.4, Tris-HCL for 10 min and then centrifuged 14.0 xg for 2 min using Vivacon 500 filter as described in Methods to stop the reaction. Extracted ion chromatograms were produced for each peptide and aligned using their m/z and retention time (RT) and the peak areas (Area) integrated for comparison as described in Methods. The table shows the peptide sequence after degradation in the presence and absence of rhECE-1 at either pH 5.5 or pH 7.4. It also indicates whether the fragment was detected or not. Fragments were identified compared to the intact peptide and classified into three groups based on conserved terminals (G1, G2, and G3).G; group.

		hNmS-33				hNmS-33			
		pH 5.5				pH 7.4			
		- Enzyme		+ Enzyme		- Enzyme		+ Enzyme	
Peptide Sequence	XIC m/z	RT	Area	RT	Area	RT	Area	RT	Area
ILQRGSGTAAVDFTKKDHTATWGRPFFRPRN	758.8046 (5+)	22.41	3569204921	22.38	17906988490	22.71	21906483776	22.59	20838591168
ILQRGSGTAAVDFTKKDHTATWGRPF	477.5842 (6+)	not detected		19.4	1378138	not detected		20.1	1616979
ILQRGSGTAAVDFTKKDHTATWGRP	453.0736 (6+)	not detected		17.48	5968509	not detected		not detected	
ILQRGSGTAAVDFTKKDHTATWGR	654.8439 (4+)	17.15	3100376	17.05	3043557	17.85	8022724	17.57	5974159
ILQRGSGTAAVDFTKKDHTATWG	615.8183 (4+)	18.09	2822715	18.03	2810755	18.88	7842047	18.68	5626993
ILQRGSGTAAVDFTKKDHTAT	739.7237 (3+)	not detected		15.32	19100175	16.05	2038095	15.9	1953147
ILQRGSGTAAVDFTKKDHTA	706.0408 (3+)	not detected		15.14	3400379	16.07	1081391	15.9	869024
ILQRGSGTAAVDFTKKDHT	682.3621 (3+)	not detected		15.23	35458452	16.01	146483	15.84	171132
ILQRGSGTAAVDFTKKDH	648.6791 (3+)	not detected		15.06	8597800	15.91	706077	15.71	541427
ILQRGSGTAAVDFTKKD	602.9924 (3+)	15.86	1213403	15.83	6193851	16.54	2566253	16.4	2205888
ILQRGSGTAAVDFTKK	564.6503 (3+)	15.67	3302567	15.64	2985299	16.41	10440295	16.23	6563525
ILQRGSGTAAVDFTK	521.9517 (3+)	17.01	1537420	16.96	1324885	17.8	9791818	17.57	5947013
FTKKDHTATWGRPFFRPRN	874.4669 (3+)	not detected		20.05	6572160	21.34	2602203	21.04	2171271
WGRPFFRPRN	531.2941 (3+)	22.59	109863009	22.51	143935860	23.85	44323071	23.53	40872072
GRPFFRPRN	469.2677 (3+)	19.83	24840345	19.79	26272673	20.96	34283043	20.65	30503565
FFFRPRN	365.8769 (3+)	20.49	149280	20.5	29455142	21.75	259316	21.51	790844
FLFRPRN	474.7776 (2+)	16.8	2129886	16.74	8226707	17.88	9686353	17.5	6122399
LFRPRN	401.2448 (2+)	not detected		11.26	304237401	12.23	2796840	11.85	25104778
FFRPRN	344.7030 (2+)	not detected		11.25	23708175	12.22	289977	11.85	3026235

G1

G2

Figure 3.27 Peptide fragments identified following incubation with rhECE-1

hNmS-33 (25 μ M) was added in the presence or absence of rhECE-1 (0.1 μ g) and incubated in 37°C, at either pH 5.5, MES/KOH, or 7.4, Tris-HCL for 10 min and then centrifuged 14.0 xg for 2 min using Vivacon 500 filter as described in Methods to stop the reaction. Extracted ion chromatograms were produced for each peptide and aligned using their m/z and retention time (RT) and the peak areas (Area) integrated for comparison as described in Methods. The table shows the peptide sequence after degradation in the presence and absence of rhECE-1 at either pH 5.5 or pH 7.4. It also indicates whether the fragment was detected or not. Fragments were identified compared to the intact peptide and classified into two groups based on conserved terminals (G1 and G2).G; group.

		pNmU-8				pNmU-8			
		pH 5.5				pH 7.4			
		- Enzyme		+ Enzyme		- Enzyme		+ Enzyme	
Peptide Sequence	XIC m/z	RT	Area	RT	Area	RT	Area	RT	Area
<u>YFLFRPN</u>	556.3085	19.84	38358851779	19.58	24778945555	19.78	15279749476	19.91	27955633671
<u>YFLFRPR</u>	499.7787	20.72	78274163	20.78	101967353	21.23	223768432	21.02	629083080
<u>FLFRPN</u>	474.7779	19.81	5219651510	19.65	2995219714	19.76	2017695081	19.87	4108460072
<u>LFRRPN</u>	401.243	19.81	1959814624	19.65	1122237686	19.76	714239122	19.79	1394433028

Figure 3.28 Peptide fragments identified following incubation with rhECE-1

pNmU-8 (25 μ M) was added in the presence or absence of rhECE-1 (0.1 μ g) and incubated in 37°C, at either pH 5.5, MES/KOH, or 7.4, Tris-HCL for 10 min and then centrifuged 14.0 xg for 2 min using Vivacon 500 filter as described in Methods to stop the reaction. Extracted ion chromatograms were produced for each peptide and aligned using their m/z and retention time (RT) and the peak areas (Area) integrated for comparison as described in Methods. The table shows the peptide sequence after degradation in the presence and absence of rhECE-1 at either pH 5.5 or pH 7.4. It also indicates whether the fragment was detected or not. Fragments were identified according to the intact peptide.

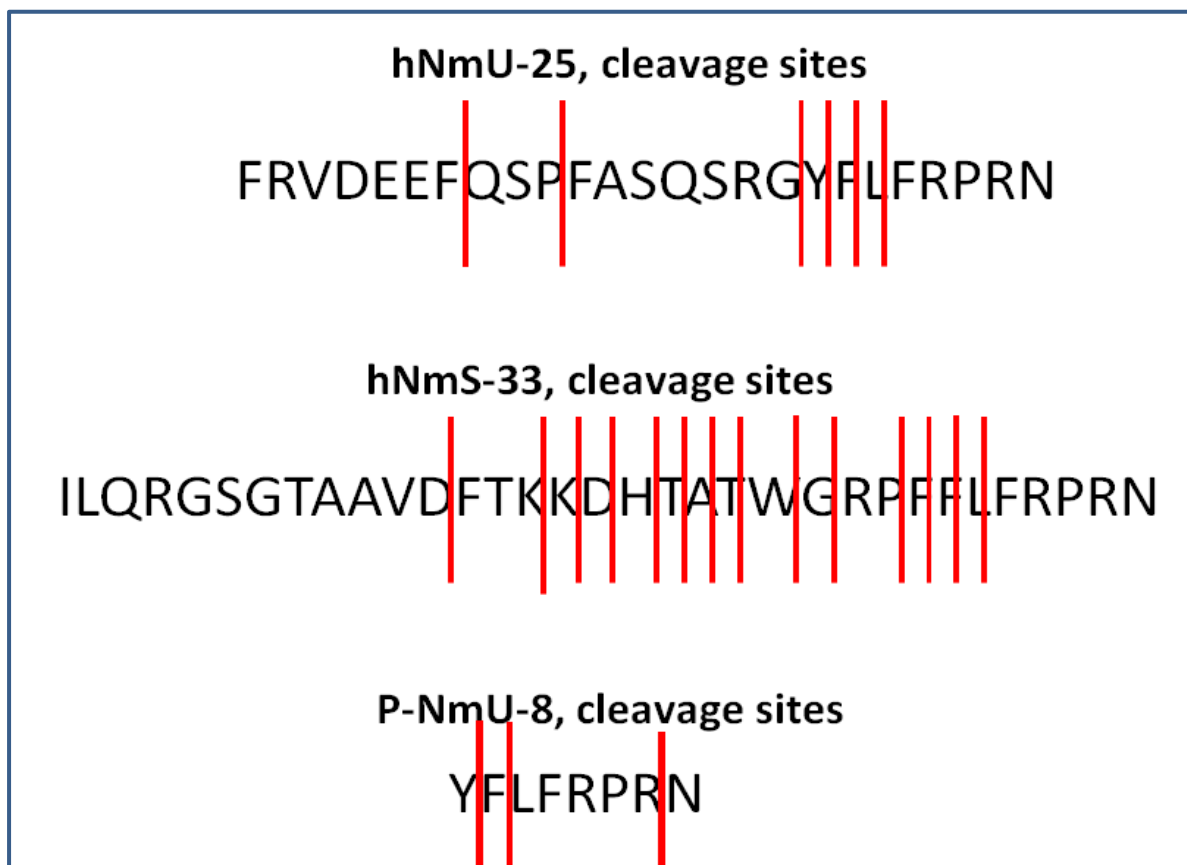


Figure 3.29 Potential cleavage sites for all peptides

This figure shows the possible cleavage sites for hNmU-25, hNmS-33, pNmU-8. It represents cleavage sites at pH 5.5 at incubation for 10 min as described in Methods. The fragments were compared to the intact peptide and then the cleavages sites were identified. The final products shown in previous figures are as a result of the activity of rhECE-1 at those sites indicated by red lines.

3.3 Discussion

Stimulation of HEK-NMU1 and HEK-NMU2 with either hNmU-25, hNmS-33 or pNmU-8 led to an increase in $[Ca^{2+}]_i$. There was a slowly decrease phase at all agonist concentrations studied, following the initial peak response.

An increase in $[Ca^{2+}]_i$ on both receptors (NMU1 and NMU2) by NmU and NmS has been investigated in both recombinant systems and in endogenous NMU-expressing cell-types (Shan *et al.*, 2000; Szekeres *et al.*, 2000; Aiyar *et al.*, 2004; Brighton *et al.*, 2004a; Johnson *et al.*, 2004; Mori *et al.*, 2005; Moriyama *et al.*, 2006). The peak Ca^{2+} response is likely to be caused by activation of PLC β and generation of IP₃ and this in turn leads to IP₃ receptor-dependent Ca^{2+} mobilization (Zhu *et al.*, 1998; Tong *et al.*, 1999). However, the plateau phase depends on Ca^{2+} influx across the cell membrane, since removal of Ca^{2+} from the extracellular environment prevents the plateau phase (Brighton *et al.*, 2004a). This was demonstrated previously by pre-treatment of the cells with thapsigargin (an irreversible inhibitor of the sarcoplasmic/endoplasmic reticulum Ca^{2+} -ATPase (SERCA), which abolished NmU-mediated increases in $[Ca^{2+}]_i$ (Cahalan, 2009). The mechanism that has been suggested and accepted for the entry of Ca^{2+} from the extracellular space in order to refill intracellular stores is termed store-operated Ca^{2+} entry (SOCE), or capacitative Ca^{2+} entry (CCE). Mammalian endoplasmic reticulum (ER) membranes have stromal interaction molecule (STIM1 and STIM2) that are found as a dimer. STIM contains an EF-hand motif serving as a Ca^{2+} sensor localized at the N-terminus of STIM in the lumen of the ER. When intracellular Ca^{2+} stores are full with Ca^{2+} (~400 μ M), Ca^{2+} binds to the STIM-EF-hand motif. Depletion of ER Ca^{2+} stores leads to dissociation of bound Ca^{2+} from the low affinity EF-hand motif and this in turn causes STIM to form oligomeric clusters, which then translocate to the ER-plasma membrane junction. Interaction of STIM clusters with plasma membrane Orai dimers results in formation of a Ca^{2+} release-activating Ca^{2+} (CRAC) channel and Ca^{2+} influx. Rebinding of Ca^{2+} to the STIM-EF-hand motif results in disassembly of STIM clusters and CRAC channel closure (Cahalan, 2009). STIM1 can also stimulate Ca^{2+} entry by means of channels such as transient receptor potential cation channels (TRPC) (Cahalan, 2009).

In terms of the desensitisation, exposure of receptors in intact cells or tissues to agonists often leads to a rapid loss of receptor responsiveness. This agonist-induced process is called desensitisation. It can be subdivided into a homologous desensitisation referring to phenomena that are agonist-specific; i.e. changes affect only the receptors of interest. In contrast, heterologous desensitisation is a process whereby activation of one receptor causes desensitisation of other types of receptor as well (Lohse *et al.*, 1990). The desensitisation can be explained by two different observations. It has been observed that after a agonist exposure, the receptors are internalised away from the cell surface into a membrane associated compartment (Hadjiivanova *et al.*, 1984). Also, it has been found that these receptors become functionally uncoupled from their effector system occurring faster than sequestration (Sibley *et al.*, 1985), likely caused by phosphorylation of the receptors (Benovic *et al.*, 1988). It has been indicated previously that NmU binds pseudo-irreversibly to either NMU1 or NMU2 in recombinant expression system (Brighton *et al.*, 2008; Alhosaini, 2011) and demonstrated that a brief acid wash (pH 2; 20 s) could be applied to dissociate receptor-bound NmU. Thus, this protocol was used to investigate the desensitisation without affecting cell viability. It was found that 5 min pre-exposure (without acid wash) to either hNmU-25 or hNmS-33 (30 nM) resulted in a significant desensitisation of Ca²⁺ signalling to application of the same ligand following 5 min recovery. This time (5 min) was therefore used to investigate the time-course of any subsequent re-sensitisation. In these experiments, cells were pre-exposed to ligands (30 nM, 5 min) followed by three washes with KHB, and a 1 to 6 h recovery period after which the cells were re-stimulated with maximally-effective concentration of ligands (30 nM). Pre-exposure to hNmU-25 (30 nM, 5 min) followed by 1 h to 6 h recovery resulted in gradually recovered over time and full re-sensitisation was evident after 6 h recovery. In order to assess the re-sensitisation profile of hNmS-33-mediated Ca²⁺ signalling in HEK-NMU2, the same protocol used with hNmU-25 was used. The recovery rate of hNmS-33-mediated Ca²⁺ responses was significantly slower than that of hNmU-25. Regulation of GPCR signalling is crucial in physiological systems in order to regulate cellular responses according to needs. The time required for receptors to fully recover (re-sensitise) differs among GPCRs and it can be between minutes to hours. A 90 % re-sensitisation was observed for hNmU-25-treated cells in contrast to only 65% recovery in hNmS-33-treated cells after 6 h recovery. These results are similar to that *in vivo*, as (ICV) injection of NmS resulted in a more prolonged

anorexigenic effect than rNmU-23 in rats (Ida *et al.*, 2006). In HEK-NMU2 stimulated by hNmS-33, SM-19712 had no effect on the recovery despite that the experiments were conducted in parallel. The reason for this lack of effect is not understood. Functionally, two classes of GPCRs, denoted class A and class B, can be defined, based on the stability of GPCR/ β -arrestin interaction. The slow rates of re-sensitisation and recycling are consistent with that of a class B GPCR that forms sustained, high affinity interactions with β -arrestin-1 and -2. Thus, the current study suggests that NMUs belong to a class B receptor, as they take a long time to be recycled. Also, it has been suggested that the stability of the receptor- β -arrestin complex could affect the period time of re-sensitisation. For instance, β -arrestin dissociates from some GPCRs, such as (β_2 AR) at or near the plasma membrane, therefore excluded from receptor-containing vesicles, resulting in rapid receptor de-phosphorylation and recycling. In contrast, some receptors including vasopressin V2 receptor (V2R), are more stable with β -arrestin and therefore are internalised into endosome where they prevent the association of receptor with phosphatase and therefore V2R is not dephosphorylated resulting in slow recycle back to the plasma membrane (Oakley *et al.*, 1999; Oakley *et al.*, 2001). This was because of the conserved motif in V2R, including serine and threonine residues, since the absence of this motif resulted in less stable complex, while the presence of this motif led to making stable complex.

It has been suggested that removing bound ligand by an acid wash increased the rate of NMU2 re-sensitisation (Alhosaini, 2011), suggesting that the presence of ligand affects NMU2 re-sensitisation, likely by influencing receptor recycling. An acid wash has been used in many studies in order to remove bound ligand (Widmann *et al.*, 1997; Li *et al.*, 2008). However, it is not clear that if the receptor on the cell membrane, after removing the ligand, is internalised. Data suggest that desensitised receptor remains phosphorylated even after the dissociation of ligand and in this case therefore the receptors still undergo internalisation after removing the ligand (Chang *et al.*, 2002). Thus, some receptors internalisation could have already occurred after pre-treatment (5 min), but the amount of internalised receptors without ligand bound compared to those with ligand bound is not obvious.

In order to study whether the recovery and the re-sensitization depend on the recycling of the receptors rather than anything else including for example protein synthesis, the confocal microscope was used. The functional characterization of HEK-NMU2-eGFP was investigated. Ca^{2+} responses to hNmU-25 in fluo-4-AM-loaded HEK-NMU2-eGFP showed concentration-dependent increases in $[\text{Ca}^{2+}]_i$ and this was followed by a slow reduction that was similar to that of responses in HEK-NMU2. In contrast, the maximal responses in NMU2-eGFP were reduced by 2-3 fold compared to HEK-NMU2. The EC_{50} values for hNmU-25 in HEK-NMU2 and HEK-NMU2-eGFP were 8.64 ± 0.06 and 8.56 ± 0.08 , respectively. The reduction in hNmU-25-mediated Ca^{2+} responses observed in fluo-4-AM loaded NMU-eGFP cell lines compared to the untagged NMU-expressing cell lines could be due to overlap of spectral range of eGFP and fluo-4-AM and it is not as a result of altering coupling efficiency. Indeed, several ideas have been suggested and it has been confirmed in our laboratory by a previous study that tagging NMUs with eGFP has no effect on NMU activation of the $G\alpha/q$ -PLC signalling pathway and the differences in the fluorescence of the $[\text{Ca}^{2+}]_i$ responses could be due to the interference between eGFP and the dye fluo-4-AM (Alhosaini, 2011).

Therefore, in order to study this issue, firstly, binding of fluorescently-tagged pNmU-8 (Cy3B-pNmU-8) to HEK-NMU2-eGFP was investigated. The results clearly show binding. In addition to that, the internalisation was studied for both ligand hNmU-25 and hNmS-33 using HEK-NMU2-eGFP. The internalisation occurred after 15 min from ligand addition for hNmU-25 and hNmS-33.

As many of GPCRs, once the ligand binds to the receptor, the complex is internalised inside the cells through the cell membrane following the desensitisation. Thus, this possibility was also investigated. It has been shown in our laboratory that different inhibitors of receptor internalisation including concanavalin A (250 $\mu\text{g}/\text{mL}$, 60 min), sucrose (0.45 M), monodansylcadaverine MDC (400 μM), and phenylarsine oxide PAO (5 μM) had an effect on the initial hNmU-25-mediated Ca^{2+} responses in naïve HEK-NMU2. Also, it has been confirmed that dynasore (80 μM), a selective inhibitor of dynamin GTPase (Macia *et al.*, 2006) in order to determine the role of dynamin in NmU-induced endocytosis of NMU in HEK cells, delays the recovery of NMU2-

mediated responses (Alhosaini, 2011) and this inhibitor, therefore, was used to study the effect of internalisation on the receptor re-sensitization. Our data revealed that this inhibitor reduced the re-sensitization of NMU2 exposed to either hNmU-25 or hNmS-33.

It has been shown that the decision between fast and slow recycling pathways may depend on the affinity of the GPCR for β -arrestin. In order to know the pathways followed by the ligand-receptor complex in the physiologically re-sensitisation process, time-courses of re-sensitisation were investigated.

It is thought that endosomal acidification could play a role in inducing conformational changes that induce ligand-receptor dissociation. Endosomal pH is regulated by the vacuolar H^+ -ATPase-pump (Huotari *et al.*, 2011). Endosomal acidification (pH 5.5) will change the charges and their distribution on amino acids leading to conformational changes of the peptide ligand and/or the receptor thereby promoting the separation of ligand-receptor complex providing accessibility for the degradation by ECE-1 located at endosomes, despite that the possibility of degradation of bound ligand cannot be ignored (Mellman *et al.*, 1986).

Both inhibitors monensin, that is a monovalent ionophore and bafilomycin A, that is a vacuolar H^+ -ATPase inhibitor have been used to study endosomal-mediated re-sensitisation of GPCRs. Both have similar effects but using different mechanisms. NMU2-re-sensitisation was markedly reduced by these two endosomal acidification inhibitors (**Figure 3.11; A-D**). It is clear that endosomal acidification disrupts endosomal function and this in turn may disrupt receptor-ligand dissociation (Bennett *et al.*, 2002; Padilla *et al.*, 2007; Mundell *et al.*, 2008). One possible mechanism explaining the inhibition of NMU2 re-sensitisation by endosomal inhibition is that acidification reduction could interfere with the rate of both hNmU-25 and hNmS-33-NMU2 dissociation since acidification is crucial in determining ligand receptor dissociation (Mellman *et al.*, 1986). Moreover, reduced acidification may lead to a reduction in NMU2 dephosphorylation (Krueger *et al.*, 1997). In addition, it is also possible that endosomal trafficking may be impaired by monensin (Mollenhauer *et al.*, 1990; Krueger *et al.*, 1997). In addition, it has been demonstrated the importance of a pH much lower than endosomal acidity in order to dissociate the ligand-receptor

complex (Alhosaini, 2011). Monensin, a Na^+ -selective ionophore, is believed to raise intracellular sodium $[\text{Na}^+]_i$ which in turn elevates intracellular calcium $[\text{Ca}^{2+}]_i$ (Mulkey *et al.*, 1992). This, thus, could explain the increase fluorescence in the naïve cells. Moreover, it has been suggested that the raise of cytoplasmic sodium concentration was responsible for the stimulation of active sodium-potassium transport occurring in bafilomycin A1-treated cells as judged by a 50% increase of ouabain sensitive potassium uptake (Hou *et al.*, 2000). Increased $[\text{Na}^+]_i$ stimulates the production of (IP_3) and the intracellular Ca^{2+} deposits is equipped with IP_3 -sensitive Ca^{2+} release channels. Therefore, Na^+ accumulation might elevate $[\text{Ca}^{2+}]_i$ through $\text{Na}^+/\text{Ca}^{2+}$ exchange gradient (Nassar-Gentina *et al.*, 1994).

It is not evident if NMU2 is re-sensitised via recycling or the need for protein synthesis is important. In order to investigate the effect of protein synthesis on the recovery of Ca^{2+} , cycloheximide (protein synthesis inhibitor used by other groups) was used (Yu *et al.*, 1997) by interfering with the translocation step in protein synthesis. This inhibitor has been used according to its ability to block protein synthesis including in HEK293 cells (Gray *et al.*, 2001; Lalo *et al.*, 2010). Cycloheximide had no significant effect on NMU2 re-sensitisation stimulated by hNmU-25 and hNmS-33 (**Figure 3.12**). The current results are consistent with previous study done in our laboratory indicating that NMU2 is likely to be internalised and re-sensitised/recycled (Alhosaini, 2011).

Dephosphorylation is an important mechanism of GPCR re-sensitisation. The phosphorylated $\beta_2\text{AR}$ appears in an endosomal fraction enriched with protein phosphatase type 2A (PP2A) activity. This is a cytosolic enzyme and a member of a diverse family of phospho-S- and phospho-T-specific enzymes expressed in eukaryotic cells (Zolnierowicz, 2000). The role of PP2A in the re-sensitisation was investigated using different types of PP2A inhibitors (okadaic acid and fostriecin) (**Figures; 3.13; A-D**). It was discovered that OA could cause inhibition of certain protein phosphatases (PP), particularly PP of type 1 (PP1) and 2A (PP2A) with a significantly higher affinity for PP2A (Bialojan *et al.*, 1988; Takai *et al.*, 1992). The reason why OA is an invaluable pharmacological tool in the study of cellular signalling, comes from the observation that PP inhibition leads to a dramatic increase of phosphorylation of a number of proteins resulting in important cell alterations (Cruz *et al.*, 2013). Previous

studies have demonstrated that PP2A can dephosphorylate endocytosed GPCRs including β_2 AR in order to promote their rapid re-sensitization (Yang *et al.*, 1988; Pitcher *et al.*, 1995; Krueger *et al.*, 1997), in contrast to the current study indicating that SP caused PP2A trafficking to the plasma membrane (Murphy *et al.*, 2011). In this study, it has been demonstrated that the interaction of NK₁R with PP2A is dependent on β -arrestin-1, since the interaction was inhibited by β -arrestin-1 depletion.

Our results indicated that neither inhibitor has an effect on the re-sensitisation. The possible explanation for this is that either these inhibitors are not potent for this enzyme or there is another mechanism involved in this dephosphorylation. Because we investigated the effect of okadaic acid (OA) on NMU2 re-sensitisation after 6 h recovery, it has been suggested that critical time period during which PP2A might be acting to dephosphorylate the receptor is crucial. For example, when the SB1 cells were treated with 5-HT and okadaic acid was added at different times, PP2A blocked 5-HT_{2A} recycling up to 60 minutes after addition of 5-HT. However, okadaic acid had no effect on recycling after addition of ligand at 90 minutes (Raote *et al.*, 2013). Thus, it is highly recommended to try such conditions. In addition, in the same experiment, it was suggested that PP2A is required for receptor recycling in the case of ligands that bring about PKC-dependent receptor internalisation (Raote *et al.*, 2013). Thus, PKC-dependent receptor internalisation needs to be investigated to see whether NMU internalisation requires the activity of PKC and then study this possibility. Therefore, the reason no effect of the inhibitor of PP2A could be this. This area needs more studies. Phosphorylation allows receptors to interact with cellular machinery enabling for trafficking, re-sensitization, and the formation of a scaffold involved in signalling. It is strongly believed that kinases involved in GPCR phosphorylation are GRKs (Benovic *et al.*, 1989; Lorenz *et al.*, 1991; Blaukat *et al.*, 2001). On the other hand, other kinases, such as protein kinase C (PKC), have been shown to play a significant role in this issue (Blaukat *et al.*, 2001; Pollok-Kopp *et al.*, 2003). A current study has shown that PKC phosphorylation attenuated Ca²⁺ responses to a single challenge with SP and inhibition of PKC inhibited re-sensitisation of SP-induced Ca²⁺ signalling, suggesting that re-sensitisation of the NK₁R is prompted by PKC phosphorylation (Murphy *et al.*, 2011). The author suggested that NK₁R is phosphorylated by PKC, and β -arrestins are recruited to non-internalised receptors by PKC phosphorylation sites (Murphy *et al.*,

2011). Therefore, this possibility was examined using GF 109203X, PKC inhibitor. Despite the inhibitor had an effect on naïve cells, it had no effect on the re-sensitisation. The effect of the inhibitor on naïve cells by increasing the signal could result from the interference from the colour of this inhibitor (orange) with the dye (fluo-4-AM) when measuring Ca^{2+} . Thus, in addition to GFX 109203X as a PKC inhibitor, many inhibitors are available such as sphingosine and it is recommended to use colourless inhibitor (Raote *et al.*, 2013). However, since the PKC consists of over 10 isozymes grouped into three subfamilies based on their second messenger requirements. Classical PKCs (α , β , γ) are activated by Ca^{2+} and DAG. Novel PKCs (δ , ϵ , η , θ) are activated by only DAG. Atypical PKCs (ξ , ι) are not activated by either. Different concentrations of GFX109203X can be exploited to discriminate among PKCs. For example, the classical and novel PKCs can be inhibited using 2 μM , whereas classical PKCs can be inhibited using 0.2 μM . Finally, at high concentration (25 μM), GFX109203X can be used to inhibit all PKCs (Carriba *et al.*, 2012).

The re-sensitisation of NMU2-mediated Ca^{2+} mobilisation was markedly reduced by inhibition of either endosomal acidification or ECE-1, suggesting that NMU2 re-sensitisation could be regulated by endosomal ECE-1 by regulating receptor recycling. The ECE-1 isoforms are present at the plasma membrane and within intracellular compartments such as endosomes (Azarani *et al.*, 1998; Valdenaire *et al.*, 1999; Muller *et al.*, 2003), suggesting two possible mechanisms explaining the inhibition of NMU2 re-sensitisation by the ECE-1 inhibitor. The NmU could be degraded by cell-surface ECE-1 resulting in reduction of ligand concentration in extracellular environment. This could lead to a greater desensitisation in the presence of the ECE-1 inhibitor in contrast to a reduction in re-sensitisation. In such circumstances, addition of SM-19712 after the initial stimulation and ligand removal would be predicted to have no effect. The results indicate that reduction in NMU2 re-sensitisation was equal to that observed when applying the SM-19712 either before or after pre-treatment, suggesting that NMU2 re-sensitisation could be regulated by intracellular ECE-dependent processing.

The ligand-receptor re-association could be prevented by ligand degradation by ECE-1 activity, resulting in conformational change of the receptor and preventing coupling of β -arrestin to allow NMU2 recycling back to the cell membrane.

The impact of knocking-down expression of ECE-1 using siRNA was also determined. HEK-NMU2 cells were transfected with either scrambled siRNA (control) or ECE-1 siRNA. ECE-1 expression was reduced after 48 h transfection with ECE-1 siRNA but not following transfection with scrambled siRNA. This reduced expression did not affect the Ca^{2+} response of naïve cells to 30 nM hNmU-25 or hNmS-33. However, knockdown of ECE-1 reduced the response to a re-challenge with hNmU-25 after 6 h recovery in cells pre-stimulated with hNmU-25 (30 nM, 5 min) but not hNmS-33.

Furthermore, experiments were designed to address the issue of whether there are other enzymes that could degrade the NmU and therefore, influence re-sensitisation as was observed with ECE-1. The potential role of other peptidases in receptor re-sensitisation was investigated using DL-thiorphan (10 μM), as a potent and specific inhibitor of membrane metallo-endopeptidase, neprilysin (NEP) (Tan *et al.*, 1992). This enzyme NEP is an integral plasma membrane ectopeptidase of the M13 family of zinc peptidases. It plays an important role in turning off peptide signalling events at the cell surface (Turner *et al.*, 2001). It is expressed at the cell surface and functions as an ectoenzyme (i.e. an enzyme that is secreted by a cell and functions outside of that cell) that catalyse peptide hydrolysis at the extracellular side of the membrane (Turner *et al.*, 2001). It has been indicated that SP is degraded by NEB and the signalling is attenuated and this happens only when it is expressed in the same cells as the NK_1R (Okamoto *et al.*, 1994). In contrast, this enzyme has no degradation effect on our ligand, hNmU-25 under our conditions. The reason is not clear. On the other hand, this could be because NEB is present on the cell membrane and the ligand-receptor complex is internalised and the enzyme does not have time to exert its function on the complex. Another possibility is that hNmU-25 is not substrate for this enzyme.

However, it should be taken into account that this observed protein synthesis-independent recovery is due to 5 min desensitisation and that desensitisation for longer than this period could redirect receptor to lysosomal degradation rather than endosomal recycling. As NMU2 belongs to GPCRs, it may include dynamin/CCP-endocytosis, translocation to endosomes either recycled to the cell-surface or degraded by lysosomes, GRK-phosphorylation and β -arrestin binding. The extent of desensitisation was different between 5, 15, and 30 min. Therefore, the mechanism of re-sensitization was

different. The plausible explanation of this is that prolonged exposure directs receptors such as β_2 -adrenoceptors to lysosomal degradation and down-regulation (Roosterman *et al.*, 2004; Cottrell *et al.*, 2006; Cottrell *et al.*, 2007). Our observation that the nature of agonist alters trafficking of NMU2 supports observation of other GPCRs. NK₁R rapid recycled and re-sensitised when it was briefly stimulated with low concentration of substance P (Roosterman *et al.*, 2004). On the other hand, sustained stimulation with high concentration of substance P caused degradation of this receptor (Cottrell *et al.*, 2006). In addition, the nature of ligand exposure affects trafficking of calcitonin receptor-like receptor (CLR) and receptor activity-modifying protein (RAMP1) (Cottrell *et al.*, 2007). When the cells were pre-exposed to 15 and 30 min and then allowed recover, it was noticed the slow recycling after 6 h recovery. This is supported by the fact that prolonged exposure to agonist can redirect the receptor to lysosomes for degradation (Cottrell *et al.*, 2007). In this case, it is important for the receptors to be available on the cell surface via protein synthesis at least under these conditions.

In further experiments, the effect of ligand concentration on receptor recycling and thus the re-sensitisation was examined. A number of different concentrations (30, 300 nM and 1 μ M) were used. Our results show that the recovery after 6 h was significantly different. This means that the concentration of hNmU-25 has a dramatic effect on the pathway of NMU2 trafficking. The plausible explanation for this is that high concentration (300 nM and 1 μ M) drives the receptors to lysosomes for degradation (Long pathway). On the other hand, exposure to a low concentration of hNmU-25 (30 nM) triggers a different pathway of NMU2 recycling. Here, the receptor could locate beneath the plasma membrane and thus rapidly returned to the plasma membrane. These results are consistent with previous study (Roosterman *et al.*, 2004). More studies are required to investigate this issue. Exposure to a low concentration (3 nM) of hNmU-25 triggers a different pathway of NMU2 recycling (**Figure 3.19**). It has been hypothesised that the extent of agonist-induced phosphorylation of the NK₁R determines association with β -arrestins and regulates the pathway and kinetics of NK₁R trafficking (Roosterman *et al.*, 2004). In contrast to 10 nM of SP that causes extensive phosphorylation, 1 nM induces minimal phosphorylation of the NK₁R (Vigna, 1999). The extent of phosphorylation could affect interaction with β -arrestin-1 and-2 and thereby controls the pathway of receptor trafficking. Therefore, stimulation with high

concentration (300 nM and 1 μ M) of hNmU-25, the NMU2 and β -arrestins are likely to remain colocalised for prolonged period in sorting endosomes, whereas stimulation with low concentration (3 nM) induces minimal phosphorylation of NMU2 that colocalises with β -arrestins transiently and re-sensitisation is rapid and depends on phosphatase activity. Also, it has been suggested that in cells stimulated with low concentration (1 nM) of SP, the recycled NK₁R did not re-internalize but remains at the cell surface. This was confirmed by the observation indicating the recovery of cell-surface binding sites was almost complete (Murphy *et al.*, 2011). Therefore, it seems that stimulation with 3 nM, the NMU2 re-sensitises rapidly in an ECE-1-independent manner and this is consistent with a previous study (Murphy *et al.*, 2011). However, more studies are required to confirm this hypothesis.

Having established that the recovery of hNmU-25 was faster than hNmS-33 at all times points when the cells were stimulated with ligand for 5 min, we investigated the effect of reducing desensitisation time on the recovery. Thus, the stimulation with (hNmU-25, 1 min) led to rapid re-sensitisation after recovery of 1 h and almost full recovery after 3 h and the recovery was dependent on ECE-1 activity. The effect of 1 min stimulation of hNmS-33 (30 nM, 1 min) and allowed to recover for 1 h therefore was studied. The recovery also was rapid and it was not affected by ECE-1 activity. This could be explained by the fact that the time required for full desensitisation as it has been confirmed previously is 5 min and when this time was reduced, some of the receptors could remain (un-internalised) on the cell surface ready for second wave of stimulation. In other words, this response after re-stimulation with 1 min could be resulting from un-internalised receptors. However, this possibility needs further study using for example binding assay to study the effect of different concentrations on receptors numbers.

Having shown above that intracellular ECE-1 may be relevant, measurements the amount of peptide left for periods of times outside the cells could answer whether peptide could be degraded extracellularly. Cellular responses to agonists of the GPCRs are rapidly removed and the signals are attenuated by mechanisms operating at different levels including the agonist, the receptor and the G proteins. Several mechanisms contribute to the removal of neurotransmitters from the extracellular fluid including

dilution in the extracellular fluid, uptake by high-affinity transporters such as glutamate/aspartate transporters and the major mechanism of removing acetylcholine, for example, from the extracellular fluid, extracellular degradation. Thus, a bioassay was also used to determine the possible extracellular degradation of NmU.

Our receptors are recombinant expressed in HEK-293 and the possibility of internalisation of bound receptor was expected. Dynasore was used to prevent receptor internalization and therefore internalization of any bound ligand and this would enable assessment of left peptide. The hNmU-25 (10 nM) was then added to the wells stimulated for the required time (1, 2, and 3 h). When HEK-NMU2 were present during the incubation with hNmU-25 in the 24 well plates, addition of the aqueous phase to HEK-NMU2 in 96-well plates resulted in Ca^{2+} response that decreased with an increasing period of exposure of the hNmU-25 to the cells in the 24 well plate. Thus, it seems that the loss of response was dependent on the presence of NMU2. When no cells were present in the initial incubation, addition of the aqueous phase to HEK-NMU2 in 96-well plates resulted in a sustained Ca^{2+} response with increasing duration of incubation. The Ca^{2+} responses in HEK-NMU2 in the presence of inhibitors were higher than that with only KHB with an increasing period of exposure of the hNmU-25 to the cells in the 24 well plates. However, the Ca^{2+} responses were sustained in the presence of the inhibitors. These data are consistent with the previous data in this thesis using the NEB inhibitor in that the hNmU-25 is intracellularly processed. The reduction over the incubation time could be due to more bound ligand is internalised rather than left on the cell membrane. The high amount left in the presence of dynasore compared to SM-19712 could support this idea.

In order to identify the concentration of peptide left after the exposure periods above, the data were then interpolated using GraphPad Prism in order to get the maximum concentration that is around 3 nM.

Our data reveals that ECE-1 has the ability to modulate hNmU-25-NMU2 and hNmS-33-NMU2 in a different manner despite that both ligands are trafficked in a dynamin-dependent manner. The reason for this different effect could be the specificity of ECE-1. Our results indicated that ECE-1 could degrade hNmU-25, hNmS-33 and pNmU-8.

The degradation experiments were performed using rhECE-1 (*in vitro*) as described in Methods. The experiments used two different conditions either pH 7.4 or 5.5 to mimic the cytoplasm and endosome environment, respectively. The ECE-1 degraded all ligands despite that SM-19712 had only effect on the NMU2 re-sensitisation depending on the using Ca^{2+} as an indicator. The reason for that is not clear. However, the specificity of the enzyme is one issue. In addition, it should bear in mind that both Ca^{2+} assay and rhECE-1 assay are different. The calcium assay is (*in vivo*) and depends on the sensitivity of Ca^{2+} to dye whereas the rhECE-1 is (*in vitro*) and depends on peptide itself whether it is substrate or not. Another possibility is the SM-19712 inhibits the complex dissociation but it does not show any details about the degradation. Therefore, both assays are completely different. (Figure 5.23) shows the time course of rhECE-1 mediated degradation of hNmU-25 in an acidic and neutral environment. At pH 5.5, rhECE-1 rapidly degraded hNmU-25. After 5 min incubation, the hNmU-25 was fully degraded producing new fragments. Interestingly, prolonged incubation with rhECE-1 did not result in increasing the amount of the fragments.

In addition, it has been noticed that ECE-1 degraded all ligands at both pH 5.5 and 7.4 but the fragments observed in pH 5.5 were more than those in pH 7.4. This is likely to be because of presence of cleavage sites in all ligands. On the other hand, the results from identifying the cleavage sites indicated that the last five amino acids F, R, P, R, N in both hNmU-25 and hNmS-33, but not pNmU-8 are protected from cleaving and conserved. In terms of pNmU-8, L, F, R, P, R, and N were identified as a protected region.

The amide structure at the C-terminal of pNmU-8 (X-Asn-NH₂, X=H-Tyr- Phe-Leu-Phe-Arg-Pro-Arg) was reported to have an important role on its biological activity (Minamino *et al.*, 1985). In addition, it has been indicated that the deamidation at the C-terminal of NmU peptides brought about a great loss in the biological and immunochemical binding activities (Kawai *et al.*, 2006). Clear roles for F¹ L² F³ R⁴ P⁵ R⁶ N⁷-amide have been demonstrated by structure-activity relationship studies (SAR) (Minamino *et al.*, 1985; Brighton *et al.*, 2004a). In addition, R⁶ and N⁷-amide are necessary for binding and activation respectively of the avian peripheral receptor and substitution of F³ → Y results in improved bioactivity. N-terminal modifications with

pyroglutamic acid, succinic acid and glutaric acid are optional and it can be used, showing improved amino peptidase resistance and increased agonistic activity in contractility assays (Sakura *et al.*, 1995).

The active fragments produced from hNmU-25 include EEFQSPFASQSRGYFLFRPRN, FQSPFASQSRGYFLFRPRN, SPFASQSRGYFLFRPRN, PFASQSRGYFLFRPRN, FASQSRGYFLFRPRN, ASQSRGYFLFRPRN, SQSRGYFLFRPRN, SRGYFLFRPRN, YFLFRPRN, and FLFRPRN. In addition, the possible active fragments obtained from hNmS-33 include FTKGDHTATWGRPFFLFRPRN, WGRPFFLFRPRN, GRPFFLFRPRN, FFLFRPRN. Finally, only 2 fragments were identified from pNmU-8 including YFLFRPR, FLFRPRN. For clarification, the amidated C-terminal heptapeptide structures were underlined. Since the last seven amino acids are conserved in both hNmU-25 and hNmS-33, two major biodegradation sites have been identified and were identical in both ligands. These are Phe¹-Leu² and Leu²-Phe³.

From these fragments, it can be seen that hNmU-25 could be grouped into three subgroups. Firstly, truncated fragments that N-terminal is conserved. Secondly, fragments that C-terminal is protected. Finally, fragments that do not have either N- or C-terminal. Interestingly, hNmS-33 fragments could be classified into only two groups; both of them have either N- or C-terminal. The factor that determines the difference in ECE-1 degradation between hNmU-25 and hNmS-33 is likely to be their N-terminal structure. A recent study has found that the structure of the N-terminal influenced thrombin degradation of hexapeptidic agonists (Takayama *et al.*, 2015).

Whether peptide cleavage by ECE-1 could generate fragments that still retain biological activity needs to be investigated. In related to this issue, a recent study indicated that the C-terminal in addition to N-terminal could affect activity of the peptide, since any change in either terminal failed or reduced the responses using C²⁺ assay (Micewicz *et al.*, 2015). For instance, the effects of N-terminal lipidation of the amidated cholecystokinin tetrapeptide, CCK4-NH₂, with a focus on enhancing membrane permeability have been investigated. It has been shown that both acetylation and/or caproylation of CCK4-NH₂ resulted in increased peptide stability, permeability and intestinal absorption (Fujita *et al.*, 1998).

Therefore, ECE-1 degrades some but not all vasoactive peptides. Also, the pH optimum favors degradation in acidified endosomes and prevents degradation at the cell surface. This is consistent with the previous study indicating that bradykinin (BK) is also degraded by ECE-1. On the other hand, there are conflicting reports about the pH optimum (Hoang *et al.*, 1997; Fahnoe *et al.*, 2000). For example, rhECE-1 degraded BK at pH 5.5 and 7.4, and SM-19712 prevented this degradation, but degradation was faster at pH 5.5. In the case of bradykinin, ECE-1 degrades it at endosomal pH but ECE-1 and endosomal acidification have no effect on bradykinin receptors (B₂R) re-sensitisation. This indicates that B₂R recycles without trafficking to ECE-1-containing endosomes.

Some studies in HEK293 cells that possess endogenous ECE-1 activity have indicated that ECE-1 plays a role in peptide degradation (Padilla *et al.*, 2007; Roosterman *et al.*, 2007). However, it has been shown that SM-19712 had no effect on re-sensitisation of Ca²⁺ responses to other peptides such as angiotensin II and the AT_{1A} receptor and bradykinin. This indicates that the function of ECE-1 in receptor recycling is not common among all GPCRs (Padilla *et al.*, 2007).

ECE-1 also degrades substrates such as substance P, somatostatin and CGRP at acidic pH (Padilla *et al.*, 2007; Roosterman *et al.*, 2007). The lack of degradation at pH 7.4 suggests that ECE-1 present at the plasma membrane is unlikely to degrade hNmU-25 in the extracellular fluid to regulate activation of NMUs. This is consistent with the ability of ECE-1 to degrade CGRP at pH 5.5 but not at pH 7.4. The inability of ECE-1 to degrade CGRP and SP in the extracellular fluid contrasts with NEP, which degrades SP at the cell surface to limit activation of the NK₁R (Okamoto *et al.*, 1994).

Chapter 4
NMU2-regulated ERK activation

4.1 Background

4.1.1 Activation of ERK by NMU2

It has recently become clear that multiple signal transduction pathways are employed upon GPCR activation. One of the major cellular effectors activated by GPCRs is extracellular signal-regulated kinase (ERK) (Eishingdrelo *et al.*, 2013). Both G-protein and β -arrestin mediated signalling pathways can lead to ERK activation. Many types of GPCR have been reported to activate ERK using a variety of signalling pathways (see **Introduction**). Both NMU receptors have been reported to activate ERK in a pertussis toxin-independent manner (Brighton *et al.*, 2004b) but the mechanisms and potential differences between ligands of these receptors are unclear. Here ERK signalling by NMU2 using both NmU and NmS has been explored.

4.1.2 The role of endosomal acidification and ECE-1 activity in the regulation of NMU2-mediated ERK activity

It has been hypothesised that the mechanisms that regulate GPCRs at the plasma membrane also have the ability to control receptor signalling and trafficking at the endosomal membrane. HEK 293 cells express all ECE-1 isoforms (Padilla *et al.*, 2007; Roosterman *et al.*, 2007) and it has been reported that ECE-1 at the endosomal membrane degrades neuropeptides including SP and somatostatin that are internalised with their cognate receptors. This requires endosomal acidification as the substrate specificity of ECE-1 is pH-dependent (Padilla *et al.*, 2007; Roosterman *et al.*, 2007; Roosterman *et al.*, 2008). Thus, by degrading neuropeptides, ECE-1 may regulate the stability and activity of ligand-receptor- β -arrestin-MAPK signalosomes (signalosomes are complexes involved in the regulation of signalling; MAPK/ERK) to control the

duration of ERK activation. In the previous chapter, it was shown that the re-sensitisation of NMU2 signalling was reduced by inhibition of either endosomal acidification or ECE-1 activity. The impact of endosomal acidification and ECE-1 activity on the activity of ERK (as determined by the levels of active phospho-ERK (pERK)) was assessed in this chapter.

4.1.3 The potential role of β -arrestins in NMU2 re-sensitization

The accepted model of GPCR re-sensitisation is that ligand binding promotes GRK-mediated phosphorylation of the cytoplasmic surface of the GPCR and subsequent β -arrestin translocation and binding to the receptor. β -arrestin binding, in turn, facilitates the subsequent recruitment of AP-2 and clathrin and GPCR inclusion in CCPs before endocytosis via CCVs. Following endocytosis, GPCRs may be either dephosphorylated and then recycled to the plasma membrane or sorted for lysosomal degradation (see **Introduction 5.1**). There is much evidence to support the hypothesis that many GPCRs are internalised and that this is crucial for re-sensitisation (Sibley *et al.*, 1986; Ferguson, 2001). Using inhibitors of endocytosis such as dynasore or concanavalin has demonstrated that sequestration is required for re-sensitisation of some receptors. Overexpression of β -arrestins, in COS-7 cells, for example, enhances the rate of β_2 -adrenoceptors re-sensitisation showing the importance of β -arrestins in this process (Zhang *et al.*, 1997). Moreover, phosphorylated β_2 -adrenoceptors appear in an endosomal vesicle fraction that is enriched in GPCR-specific protein phosphatase PP2A activity (Pitcher *et al.*, 1995). Dephosphorylation of the receptor occurs in either an acidified vesicle compartment where internalisation is required for re-sensitisation (Krueger *et al.*, 1997) or at the plasma membrane where internalisation is not required for re-sensitisation (Rozengurt, 2011). GPCRs have been grouped into two different classes based on the interaction between the receptor and β -arrestins (Oakley *et al.*, 2000). Class A receptors transiently bind to β -arrestin-2 with higher affinity than β -arrestin-1 and the β -arrestin is recruited to the receptor at the plasma membrane and translocated with it to (CCPs). However, the receptor- β -arrestin complex dissociates rapidly at the plasma membrane or directly after internalization of the receptor leading to fast re-sensitisation (Moore *et al.*, 2007). The β -arrestin then recycles to the plasma membrane (Zhang *et al.*, 1999).

Class B receptors bind equally with high affinity to β -arrestin-1 and β -arrestin-2 and stable complexes may be formed with β -arrestin allowing, the receptor- β -arrestin

complex to internalize as a unit that is targeted to endosomes and dissociates at low rate, delaying re-sensitisation (Moore *et al.*, 2007).

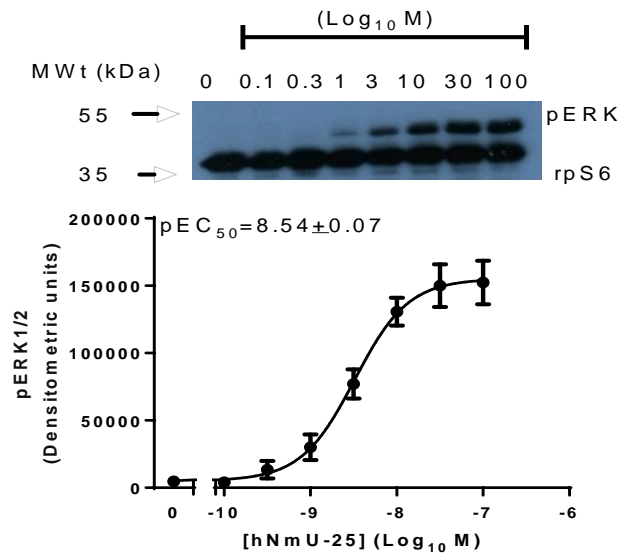
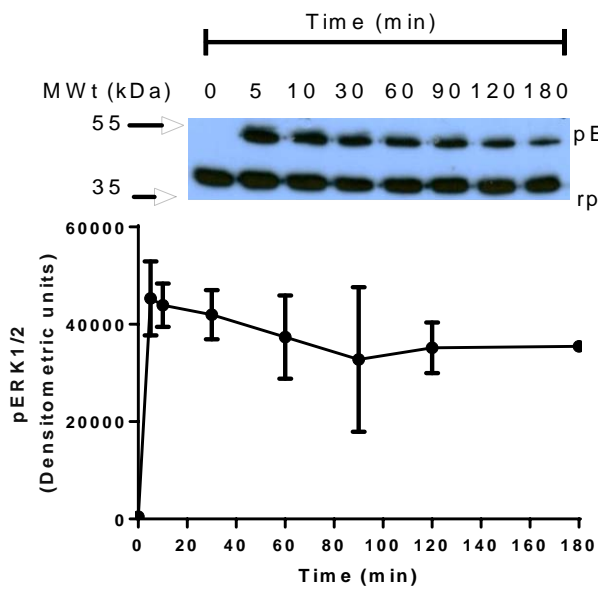
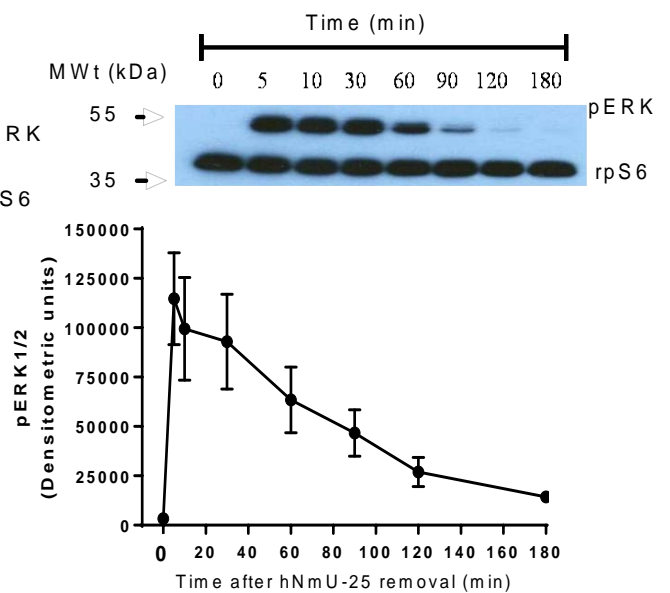
The aims of this chapter were to examine the effect of inhibiting the endosomal acidification on ERK activation following hNmU-25, hNmS-33 and pNmU-8. This was followed by studying the effect of ECE-1 activity. In addition to that, siRNA technique was used to reduce β -arrestin activity and then study the effect of that on ERK activation by knocking down either β -arrestin-1 or -2 or combination of both of them.

4.2 Results

4.2.1 NMU2-mediated activation of ERK

Concentration-response curves and the time-course of NMU2-mediated ERK activation in response to hNmU-25 and hNmS-33 were generated. For concentration response curves, HEK-NMU2 cells were plated for 24 h in 24-well plates and starved for a further 24 h. Cells were then stimulated with buffer or different concentrations of either hNmU-25 or hNmS-33 (0.1-100 nM). For the time-course, HEK-NMU2 cells were cultured for 24 h and starved for a further 24 h. Cells were then stimulated with maximum a concentration of either hNmU-25 or hNmS-33 without removing the ligand for up to 3 h. Alternatively, cells were stimulated with a maximum concentration of either hNmU-25 or hNmS-33 (30 nM for 5 min). Only after which time the ligand was washed off and the cells allowed to recover for the required time.

Stimulation of HEK-NMU2 with either hNmU-25 or hNmS-33 resulted in an increase of pERK (as an index of ERK activation) in a concentration-dependent manner with pEC₅₀ values of 8.54±0.07 and 8.83±0.08, respectively (**Figure 4.1; A & D**). The peak of ERK activation upon stimulation with a maximum concentration of either ligand (30 nM) was achieved within 5 min. When the ligand was not removed, ERK activation following a maximal concentration of either hNmU-25 or hNmS-33 was relatively sustained over the 3 h period of stimulation (**Figure 4.1; B & E**). In contrast, when the ligand was removed after a 5 min period of stimulation, ERK activity declined slowly following hNmU-25 and returned to the basal level after about 60 min (**Figure 4.1; C**). In contrast, ERK activation following a 5 min period of stimulation with hNmS-33 was relatively sustained over the 3 h recovery period (**Figure 4.1; F**).

A**B****C**

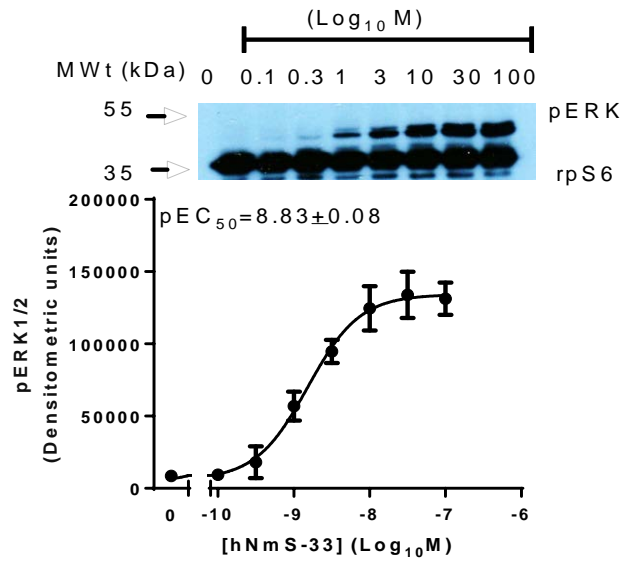
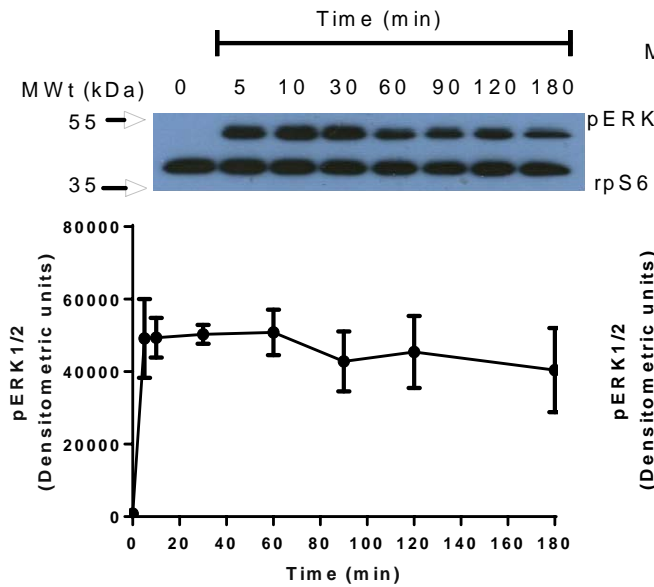
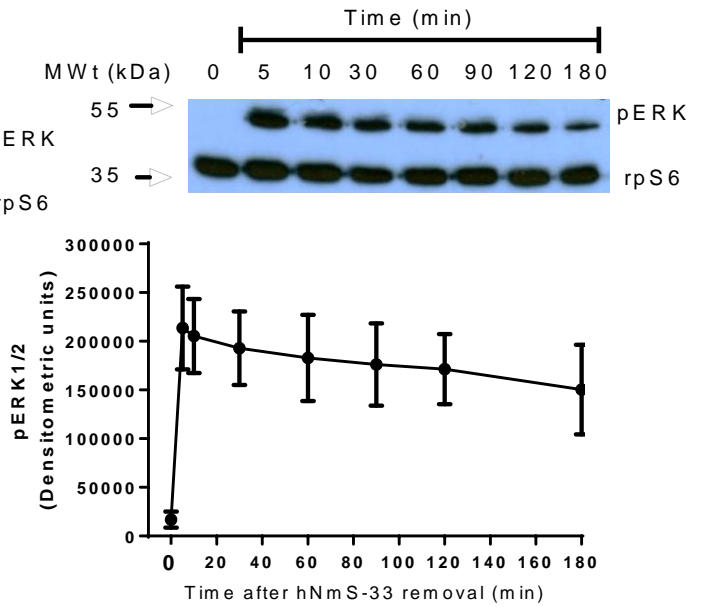
D**E****F**

Figure 4.1 Concentration-response curves and time-course of hNmU-25 and hNmS-33-mediated ERK activation by NMU2

HEK-NMU2 cells were cultured on 24-well plates for 24 h and serum-starved overnight. To construct concentration-response curves (**A & D**) for agonist-stimulated increases in pERK, cells were washed with KHB, and challenged with KHB alone or different concentrations of either hNmU-25 (**A**) or hNmS-33 (**D**) (0.1-100 nM, 5 min). In order to study the time-course of changes in pERK (**B, C, E and F**), cells were challenged with KHB alone or a maximum concentration (30 nM) of either ligand that was then left in place for the duration of the experiment (**B & E**). Alternatively, cells were challenged with KHB alone or a maximum concentration of either ligand (30 nM) for 5 min) and then washed twice with KHB. Incubation was then continued in the absence of ligand for the required time (5-180 min) (**C & F**). The pERK and rpS6 were determined by Western blotting and the signal density of each quantified using Image J software. Data are representative blots or means \pm s.e.m., n=3.

4.2.2 pERK perhaps depends on ongoing activation of NMU2 in the presence of NmS but not NmU

The previous results indicated that cells stimulated by hNmU-25 (30 nM) for 5 min) after which the ligand was removed, resulted in a reduction of pERK to basal levels after 3 h recovery (**Figure 4.1; C**). On the other hand, levels of pERK were relatively sustained at 3 h when the cells were stimulated with hNmS-33 in the same way (i.e. 30 nM for 5 min followed by ligand removal) (**Figure 4.1; F**). In order to investigate whether this reduction was a result of dissociation of ligand, receptor and β -arrestins, the following experiment was conducted. The HEK-NMU2 cells were challenged with either KHB or hNmU-25 and hNmS-33 (30 nM, 5 min). The cells were then allowed to recover for 3 h. The cells were then re-stimulated by either ligand for 5 min and allowed to recover for 5 min. Under these conditions, the pERK was peaked as it was with 5 min for hNmU-25 (**Figure 4.2; A**) and hNmS-33 (**Figure 4.2; B**).

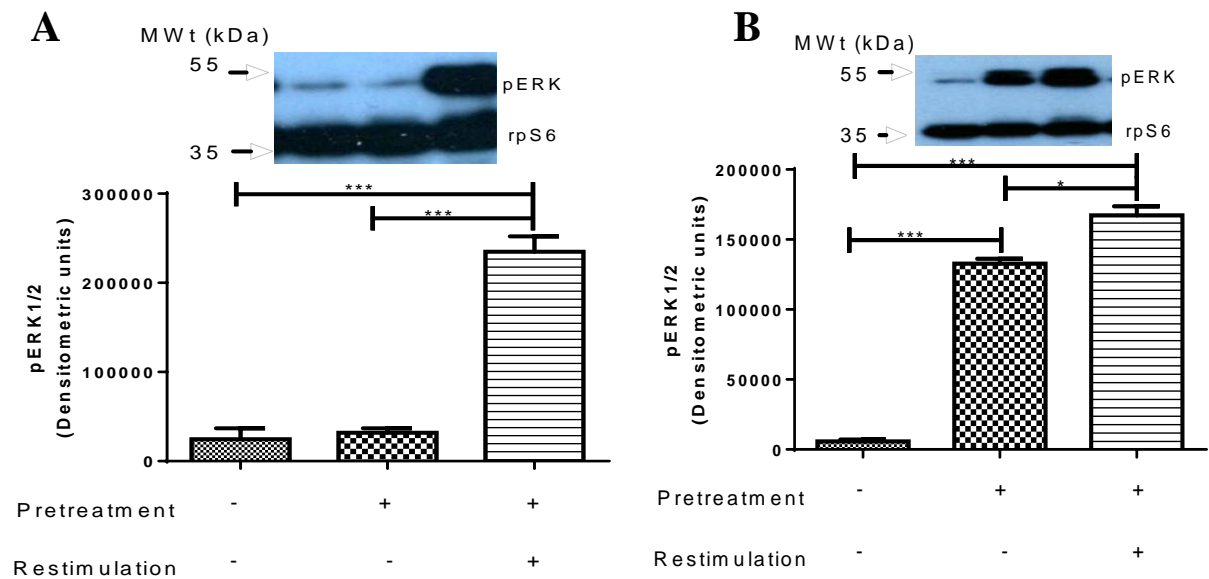
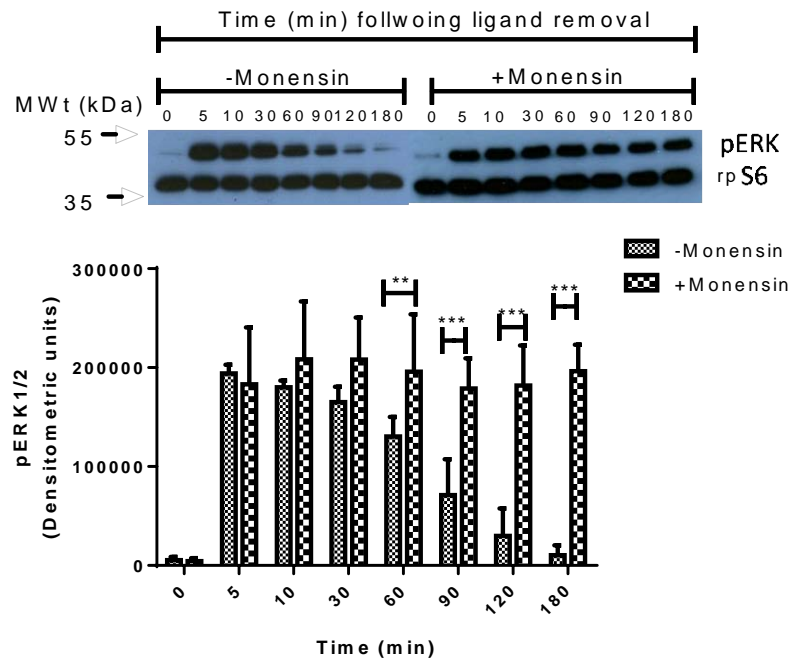
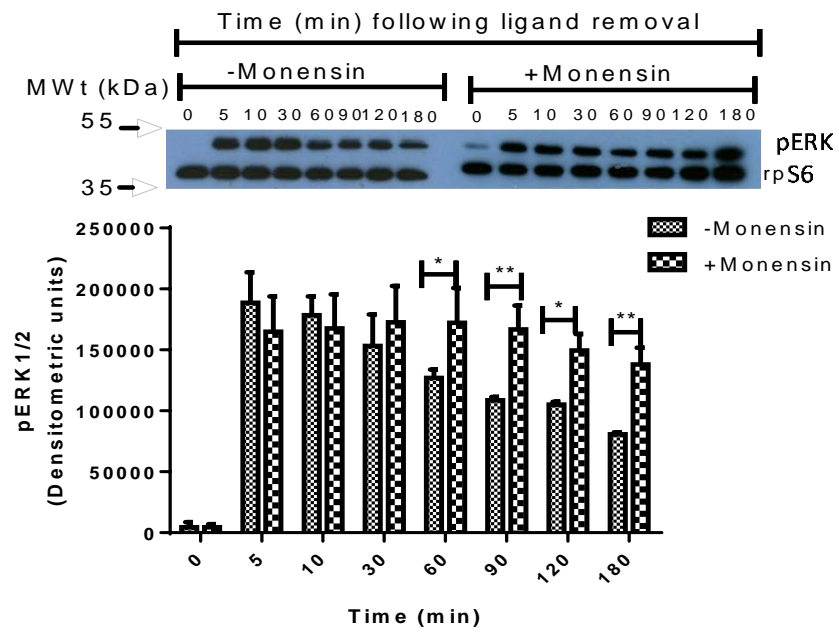


Figure 4.2 pERK perhaps depends on ongoing activation of NMU2 in the presence of NmS but not NmU

HEK-NMU2 cells were serum-starved overnight, washed and KHB was added prior to challenge with either hNmU-25 (**A**) or hNmS-33 (**B**) (30 nM, 5 min). Cells were then washed to remove free ligand and allowed to recover for 3 h. The cells were then restimulated with 30 nM of the appropriate ligand for 5 min before solubilisation and assessment of pERK by immunoblotting and densitometry. The pERK and rpS6 were determined by Western blotting and the signal density of each quantified using Image J software. Data are representative or means \pm s.e.m., $n=3$. Data were analysed by Bonferroni's multiple comparison test following one-way ANOVA; * $P<0.05$, *** $P<0.001$.

4.2.3 Inhibition of endosomal acidification enhances ERK activity following hNmU-25, hNmS-33 and pNmU-8

Endosomal acidification is thought to be a key driver in inducing conformational changes promoting ligand-receptor dissociation. It has been indicated that the complex of the ligand, receptor and β -arrestins are delivered into the endosomes where both the endosomal acidification and ECE-1 could play a role in both signalling and receptor processing, particularly by regulating the life-time of the ligand-receptor complex. Therefore, the endosomal acidification inhibitor, monensin, was used in the current study in order to investigate the importance of endosomal acidification on ERK activation. HEK-NMU2 cells were pre-treated with or without monensin (50 μ M) for 30 min and then stimulated with, hNmU-25, hNmS-33 or pNmU-8 (**Figure 4.3; A, B and C, respectively**) (30 nM, 5 min) followed by ligand removal and washing of the cell monolayer. In the absence of monensin, challenge with hNmU-25 or pNmU-8 produced responses that were maximal at 5 min but then decreased following ligand removal, returning to basal levels at 180 min (**Figure 4.3; A & C**). In contrast, challenge with hNmS-33 resulted in a peak at 5 min that was sustained throughout the experiment despite removal of ligand (**Figure 4.3; B**). Under these circumstances (i.e. ligand removal after a 5 min stimulation period), monensin, prolonged ERK activation following hNmU-25, hNmS-33 or pNmU-8 (**Figure 4.3; A, B and C, respectively**).

A**B**

C

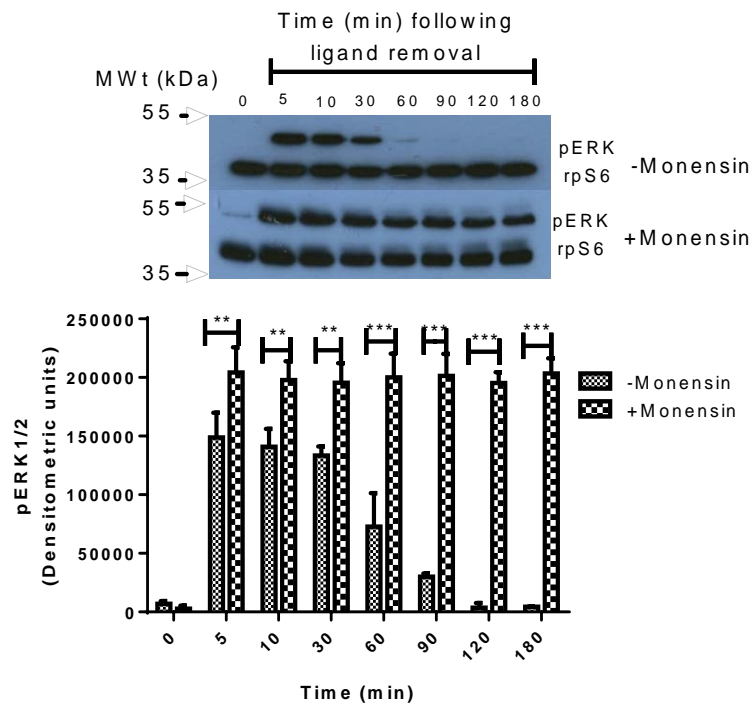


Figure 4.3 Time-course of NMU2-mediated ERK activation in the presence and absence of an inhibitor of endosomal acidification

Impact following ligand removal. HEK-NMU2 cells were serum-starved overnight, washed with KHB and then incubated with or without monensin (50 μ M) for 30 min prior to challenge with ligand (hNmU-25 (A), hNmS-33 (B) or pNmU-8 (C) (30 nM, 5 min). Cells were then washed to remove free ligand and left for the required time before solubilisation and assessment of pERK by immunoblotting and densitometry. The levels of pERK and rpS6 were determined by Western blotting and the signal density of each quantified using Image J software. Data are representative or mean \pm s.e.m., n=3. Data were analysed by Bonferroni's multiple comparison test following two-way ANOVA; * P <0.05, ** P <0.01, *** P <0.001. The stimulated cells were all greater than controls and only differences between \pm monensin were considered.

4.2.4 Inhibition of ECE-1 activity enhances ERK activity following hNmU-25 but neither hNmS-33 nor pNmU-8

Challenge of HEK-NMU2 with 30 nM hNmU-25 or hNmS-33 evoked a rapid activation of ERK as determined by immunoblotting of pERK1/2. The response was maximal at 5 min and then sustained in the continued presence of agonist for the duration of the experiment (3 h) for all ligands. HEK-NMU2 cells were pre-incubated with the ECE-1 inhibitor, SM-19712 for 30 min and then stimulated with hNmU-25 (30 nM), in the continued presence of hNmU-25, ERK activation remained elevated for the duration of the experiment (3 h) and this was unaffected by SM-19712 (**Figure 4.4; A & B**). In an alternative protocol, cells were stimulated for 5 min and free extracellular ligand was removed by washing with KHB. Under these conditions, when the cells were challenged with hNmU-25 (30 nM), the response was again maximal at 5 min but then decreased following ligand removal, returning to basal levels at 180 min (**Figure 4.5; A**). In contrast, using the same protocol but challenging the cells with hNmS-33 (30 nM) resulted in a peak at 5 min that was sustained throughout the experiment (**Figure 4.5; B**). Under these circumstances (i.e. Ligand removal), The ECE-1 inhibitor, SM19712, prolonged ERK activation following hNmU-25 (**Figure 4.5; A**) but did not affect the already sustained response to hNmS-33 (**Figure 4.5; B**).

Despite the shorter bioactive version of hNmU-25, pNmU-8, mimicking hNmU-25 in terms of potency and the time-course, ECE-1 activity did not modulate pERK levels following the ligand removal (**Figure 4.6**). Thus, cells were pre-incubated with either or without ECE-1 inhibitor; SM-19712, for 30 min and the cells were then stimulated with pNmU-8 (30 nM for 5 min) followed by ligand removal and cell washing. Under these conditions, when the cells were challenged with pNmU-8 (30 nM), the response was maximal at 5 min but then decreased following ligand removal, returning to basal levels at 180 min. However, SM-19712 did not affect ERK activation over the time-course of the experiment (**Figure 4.6**).

In order to investigate the effect of SM-19712 on pERK responses to a lower concentration of agonist as with Ca^{2+} signalling experiments (see **Chapter 3, Figure 3.16; A**), cells were stimulated using a sub-maximal concentration of either hNmU-25 or hNmS-33 (3 nM) (**Figure 4.7; A & B**). Stimulation with this sub-maximal concentration resulted in a lower activation of ERK than when the cells were stimulated with a maximum concentration (30 nM) (It is difficult to make the comparison as the blots are not on the same film) (**Figures 4.5; A & B**). When the cells were challenged with hNmU-25 (3 nM), the response was again maximal at 5 min but as with the maximal concentration, then decreased following ligand removal, returning to basal level at 90 min. In contrast, using the same protocol but challenging the cells with hNmS-33 (3 nM) resulted in a peak at 5 min that was sustained throughout the experiment (**Figure 4.7; B**). Under these conditions (i.e. ligand removal), the ECE-1 inhibitor, SM19712, prolonged ERK activation following hNmU-25 (**Figure 4.7; A**) but did not affect the already sustained response to hNmS-33 (**Figure 4.7; B**).

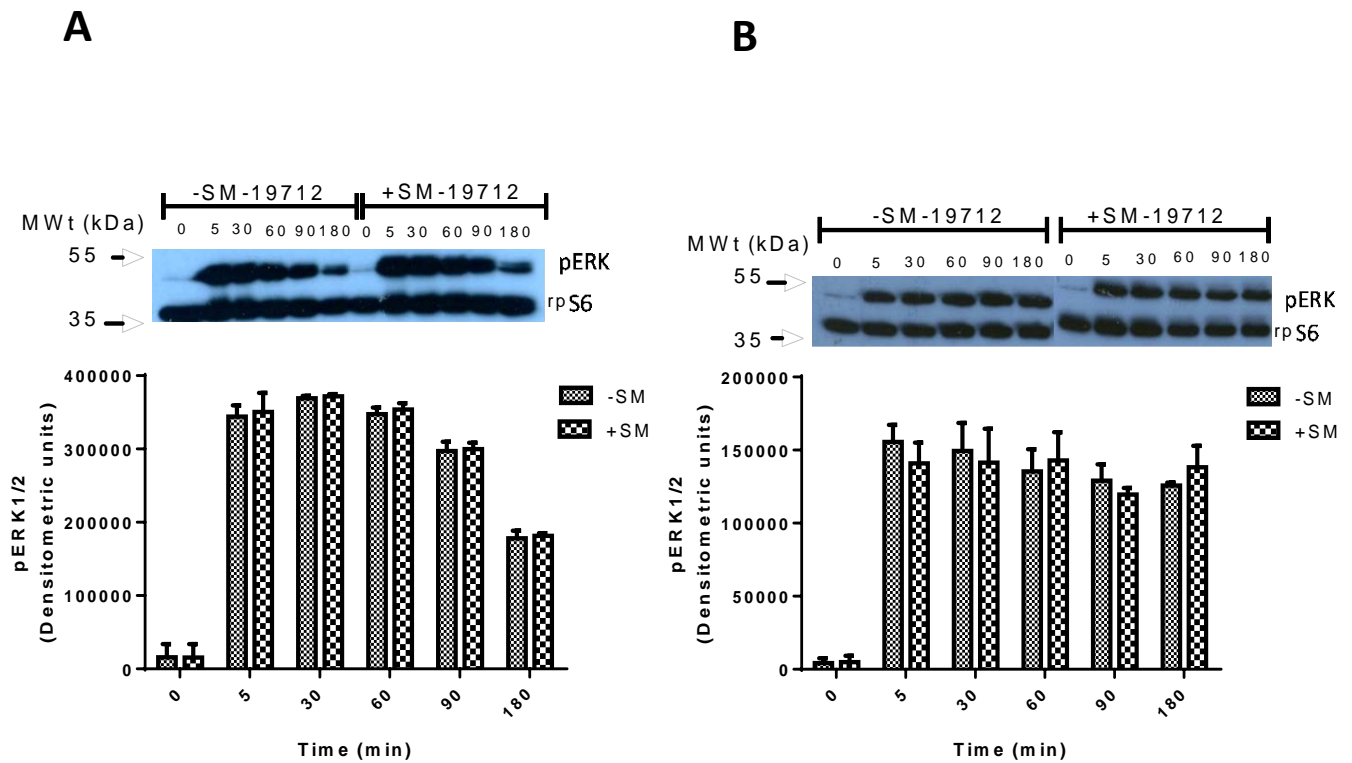


Figure 4.4 Time-course of NMU2-mediated ERK activation in the presence and absence of ECE-1 inhibitor: impact in the continued presence of ligand

HEK-NMU2 cells were serum-starved overnight, washed with KHB and then incubated with or without SM19712 (10 μ M) for 30 min prior to challenge with ligand (30 nM). Cells were left for the required time before solubilisation and assessment of pERK by immunoblotting and densitometry following stimulation with hNmU-25 (A) and hNmS-33 (B). The levels of pERK and rpS6 were determined by Western blotting and the signal density of each quantified using Image J software. Data are representative or mean \pm s.e.m., n=3; statistical comparisons were by Bonferroni's multiple comparison test following two-way ANOVA. The stimulated cells were all greater than controls ($P < 0.01$) and only differences between \pm SM-19712 were considered.

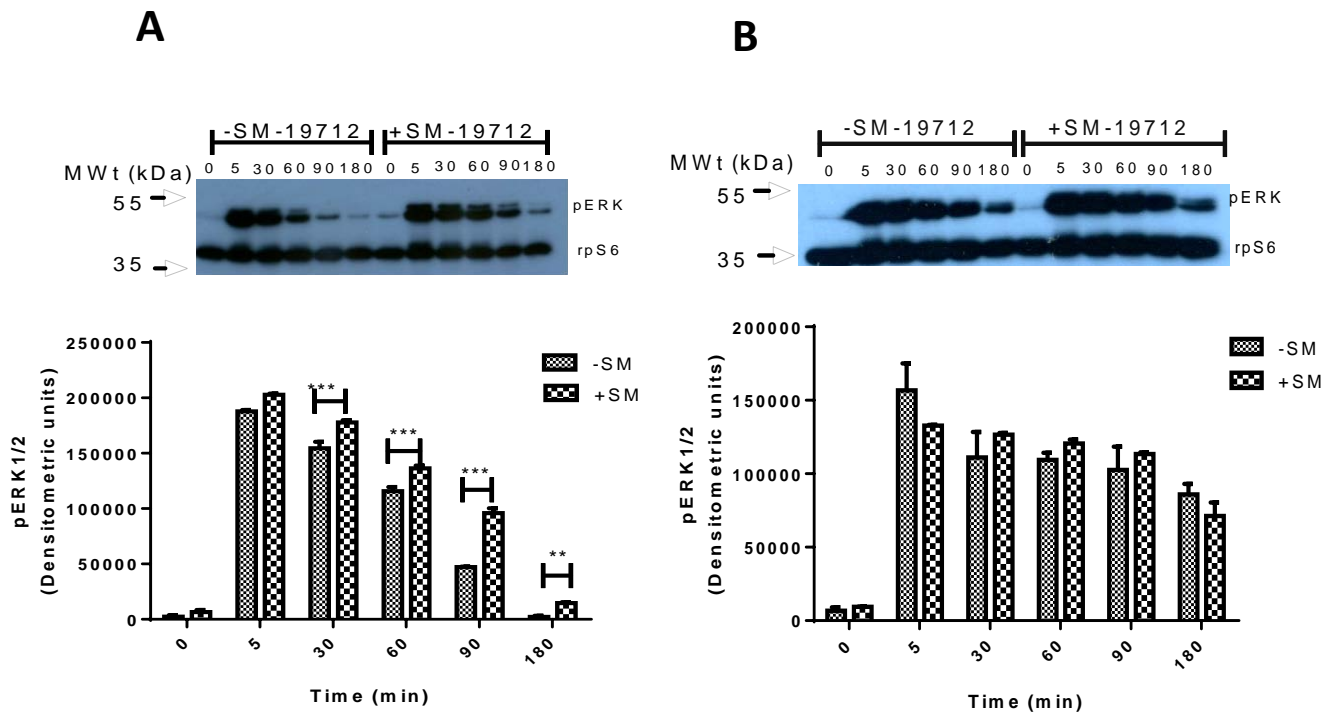


Figure 4.5 Time-course of NMU2-mediated ERK activation in the presence and absence of ECE-1 inhibitor: impact following ligand removal

HEK-NMU2 cells were serum-starved overnight, washed with KHB and then incubated with or without SM-19712 (10 μ M) for 30 min prior to challenge with ligand (hNmU-25 (A) or hNmS-33 (B), 30 nM) for 5 min. Cells were then washed to remove free ligand and left for the required time before solubilisation and assessment of pERK by immunoblotting and densitometry. The levels of pERK and (rpS6) were determined by Western blotting and the signal density of each were quantified using Image J software. Data are representative or mean \pm s.e.m., $n=3$, ** $P<0.01$, *** $P<0.001$; statistical comparisons by Bonferroni's multiple comparison test following two-way ANOVA. The stimulated cells were all greater than controls ($P<0.01$) and only differences between \pm SM-19712 were considered.

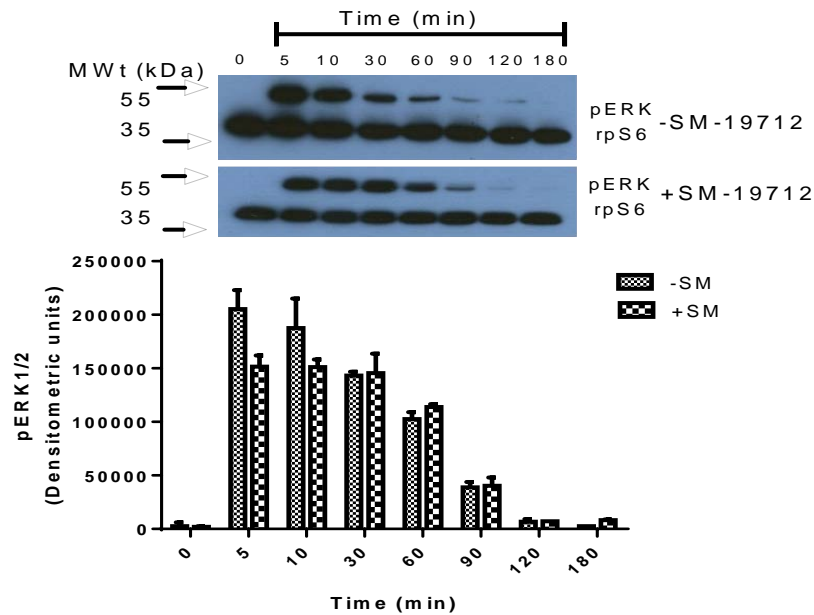


Figure 4.6 Time-course of NMU2-mediated ERK activation in the absence and presence of inhibitor of ECE-1 followed by stimulating with pNmU-8: Impact following ligand removal

HEK-NMU2 cells were serum-starved overnight, washed with KHB and then incubated with or without SM-19712 (10 μ M) for 30 min prior to challenge with ligand (pNmU-8, 30 nM) for 5 min. Cells were then washed to remove free ligand and left for the required time before solubilisation and assessment of pERK by immunoblotting and densitometry. The levels of pERK and (rpS6) were determined by Western blotting and the signal density of each were quantified using Image J software. Data are representative or mean \pm s.e.m., n=3. Data were analysed by Bonferroni's multiple comparison test following two-way ANOVA. The stimulated cells were all greater than controls and only differences between \pm SM-19712 were considered.

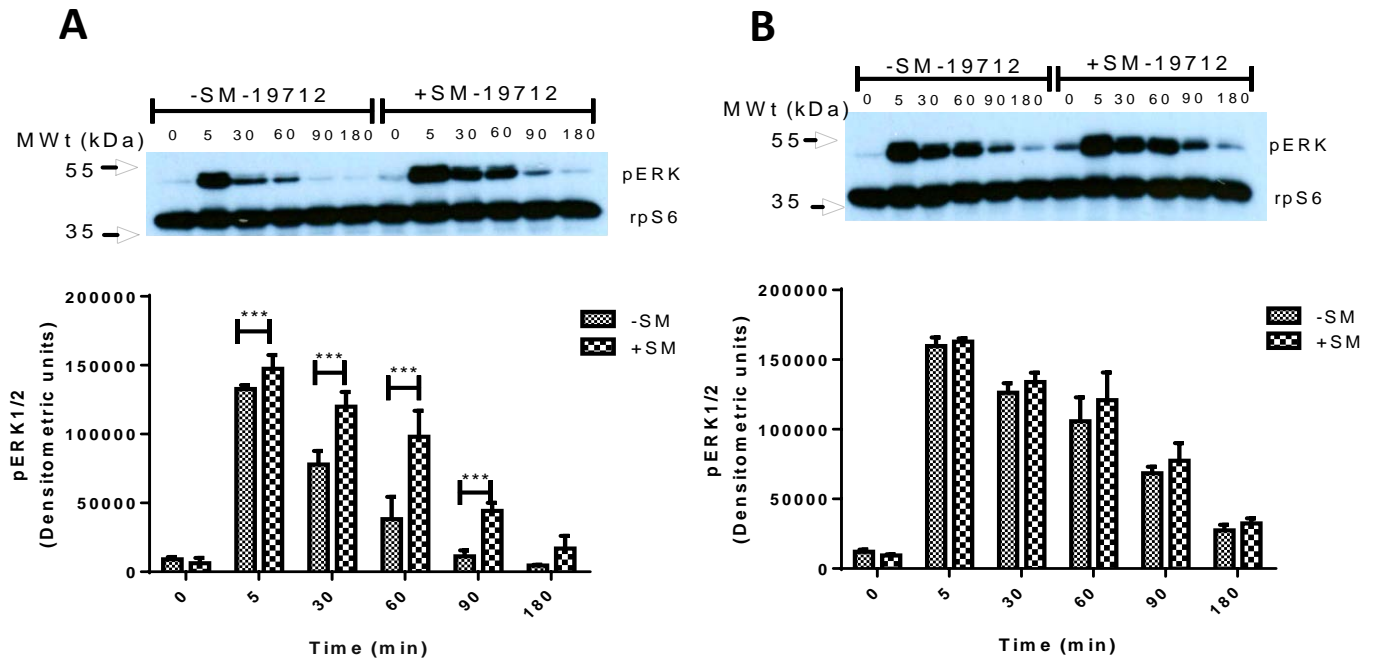


Figure 4.7 Time-course of NMU2-mediated ERK activation in the presence and absence of ECE-1 inhibitor using a sub-maximal concentration of ligand: Impact following ligand removal

HEK-NMU2 cells were serum-starved overnight, washed with KHB and then incubated with or without SM19712 (10 μ M) for 30 min prior to challenge with ligand (hNmU-25 (A) or hNmS-33 (B), 3 nM) for 5 min. Cells were then washed to remove free ligand and left for the required time before solubilisation and assessment of pERK by immunoblotting and densitometry. The levels of pERK and (rpS6) were determined by Western blotting and the signal density of each quantified using Image J software. Data are representative or mean \pm s.e.m., n=3. Data were analysed by Bonferroni's multiple comparison test following two-way ANOVA; *** P <0.001. The stimulated cells were all greater than controls (P <0.001) and only differences between \pm SM-19712 were considered.

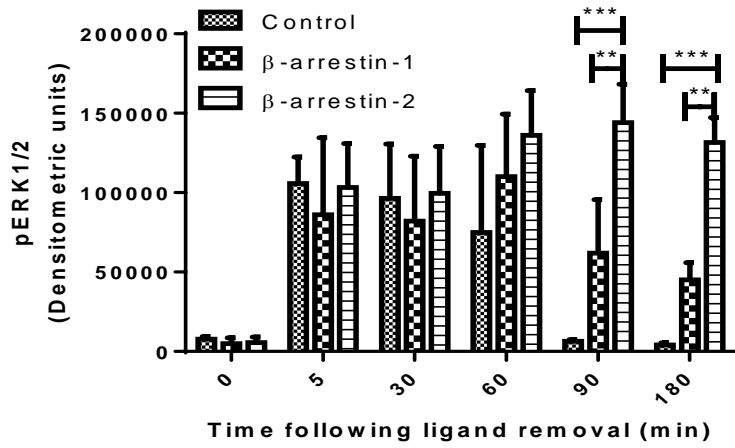
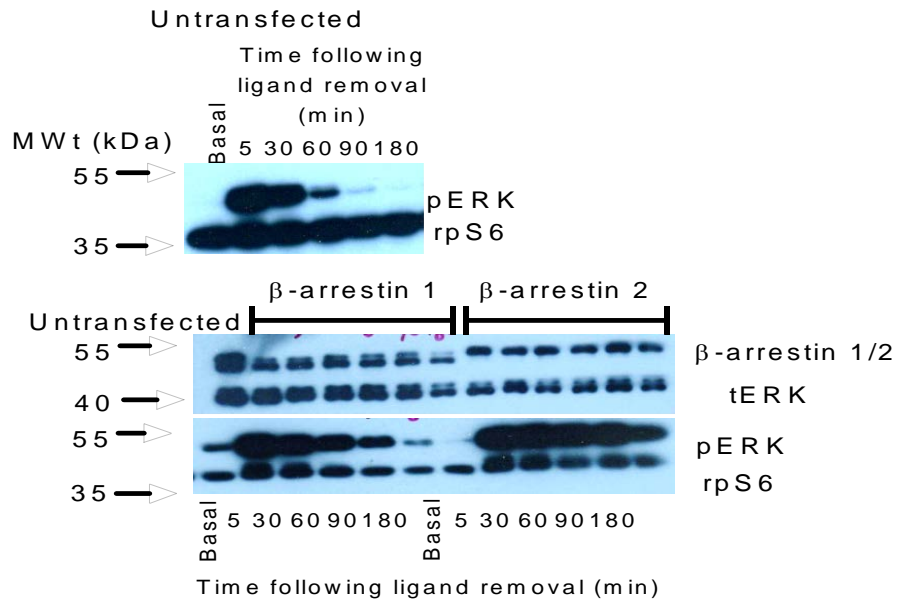
4.2.5 The role of arrestin in NMU receptor-mediated ERK responses

HEK-NMU1 or HEK-NMU2 cells were cultured and maintained as described in the methods before transfecting the cells. Transfection was carried out using Lipofectamine RNA iMAX (Invitrogen) reagent according to the manufacturer's instructions. The siRNA sequences targeting β -arrestin-1 and β -arrestin-2 were used. After 24 h, the cells were washed and incubated for an additional 24 h in serum-free growth medium. Silencing of β -arrestin-1 and β -arrestin-2 expressions was assessed by immunoblotting using anti- β -arrestins1/2 (1:2000; Cell Signalling, UK) (Ahn *et al.*, 2013).

As shown earlier, hNmU-25 and hNmS-33 evoked time- and concentration-dependent activation of ERK by NMU2 (**Figure 4.1; A-F**). Moreover, a short period of stimulation (5 min) with hNmU-25 or hNmS-33 maximally activated ERK at 5 min, which then declined to basal levels over the subsequent 3 h following hNmU-25 (**Figure 4.1; C**), but was sustained following hNmS-33 (**Figure 4.1; F**). Knockdown of β -arrestin-1 or -2 individually (**Figure 4.8; A**) or in combination (**Figure 4.8; B**) significantly enhanced and extended the duration of hNmU-25-mediated ERK activation (**Figure 4.8**). In contrast, individual knockdown of β -arrestin-1 or -2 had a much more limited impact on hNmS-33-mediated ERK activation (**Figure 4.9; A**). However, combined knockdown of both β -arrestin-1 and -2 (**Figure 4.9; B**) enhanced the levels of pERK at least at later time points, for example, at 90 and 180 min (**Figure 4.9; B**).

The same experimental conditions (i.e. 5 min stimulation followed by ligand removal) were used in order to examine the role of the arrestins in NMU1-mediated ERK activation. The pattern of ERK activation following challenge of NMU1 with either hNmU-25 or hNmS-33 (30 nM) was similar to that following activation of NMU2 (i.e. hNmU-25 and hNmS-33 evoked time- and concentration-dependent activation of ERK). By knocking down β -arrestin-1 or -2 individually (**Figures 4.10; A**) or in combination (**Figure 4.10; B**), hNmU-25-mediated ERK activation by NMU1 was significantly enhanced at later time points. In addition, knockdown of both β -arrestins1/2 enhanced the pERK at least at later time points; 90 and 180 min followed activation the cells with hNmS-33 (**Figure 4.11**).

A



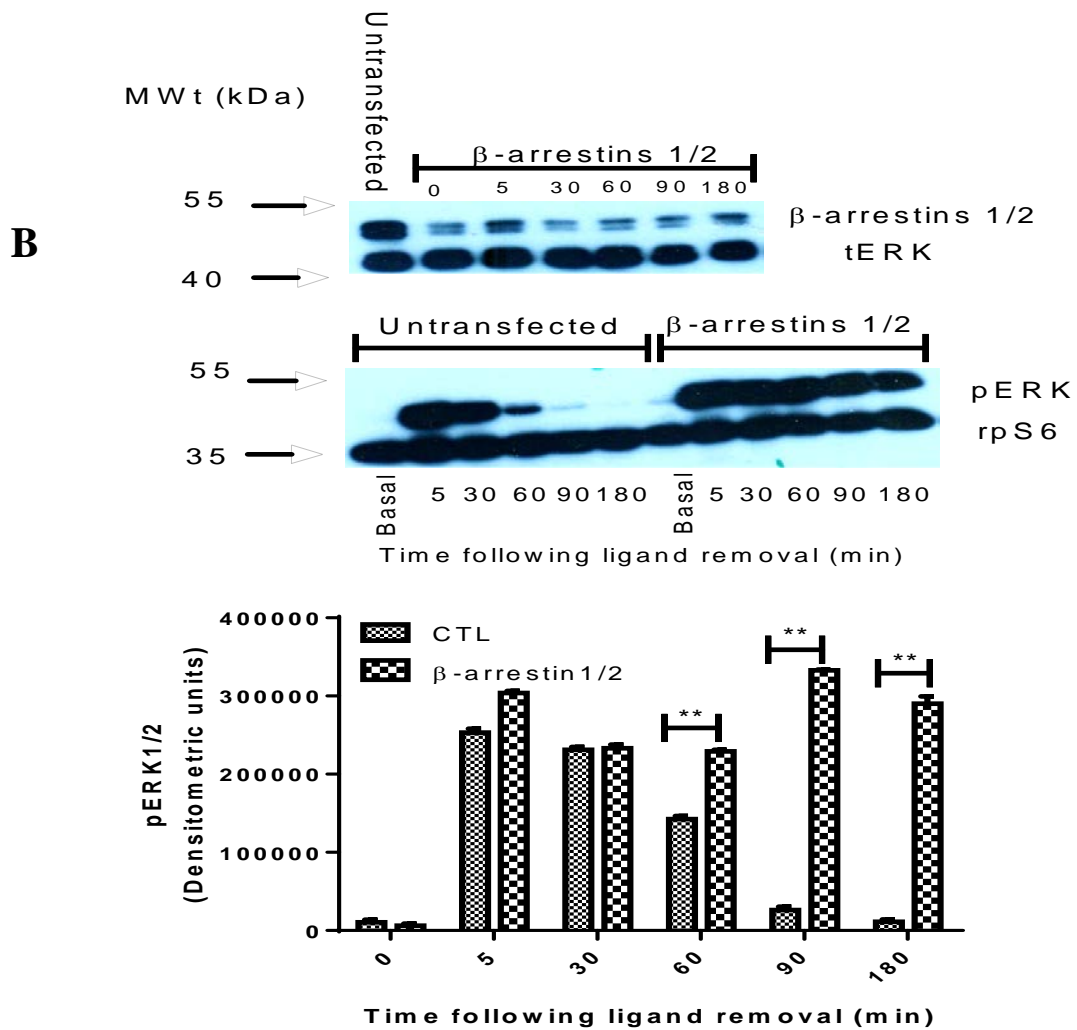
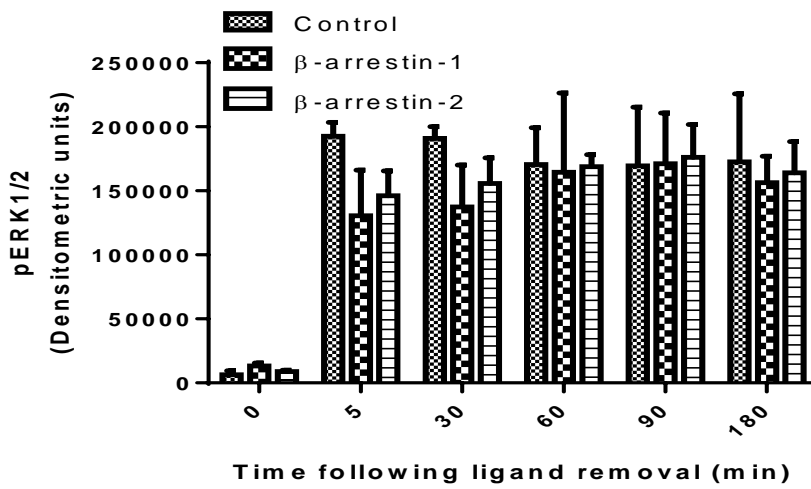
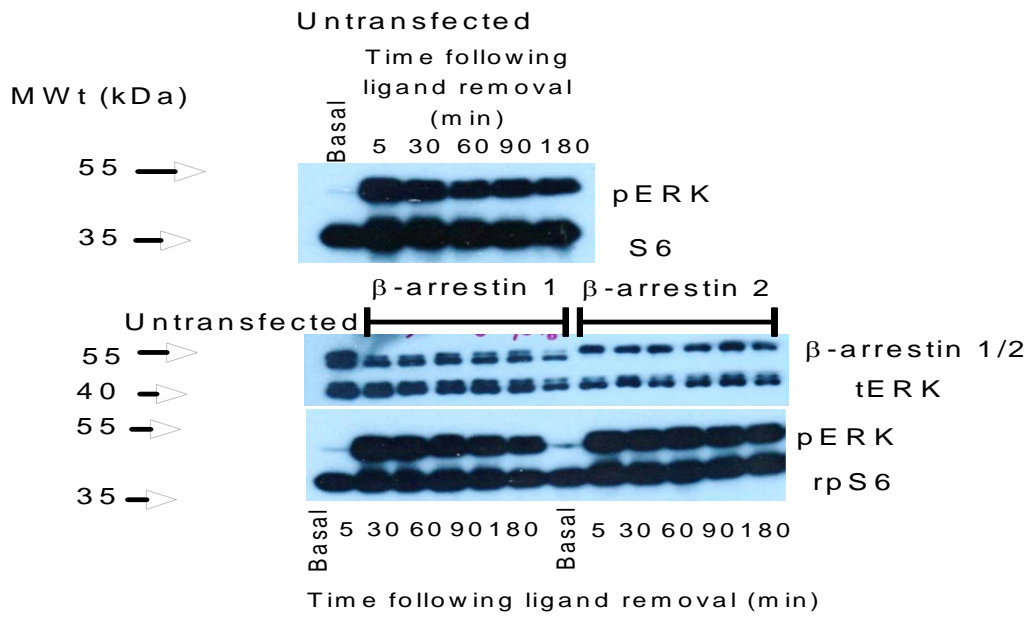


Figure 4.8 hNmU-25-mediated ERK activation following knockdown of β -arrestin-1 and/ or-2 in HEK-NMU2

HEK-NMU2 cells were either not transfected or transfected with siRNA against β -arrestin-1, or -2 (A) or 1 & 2 in combination (B) and incubated for 24 h and then serum-starved for a further 24 h. Following a 5 min challenge with 30 nM -hNmU-25, cells were washed and the levels of pERK measured over the subsequent 180 min. The pERK and (rpS6) or tERK was determined by Western blotting and the signal density of each quantified using Image J software. Data are representative of mean \pm s.e.m., $n=3$. Data were analysed by Bonferroni's multiple comparison test following two-way ANOVA; ** $P < 0.01$, *** $P < 0.001$. The stimulated cells were all greater than controls and only differences between transfected and un-transfected cells were considered at each time point. CTL; control.

A



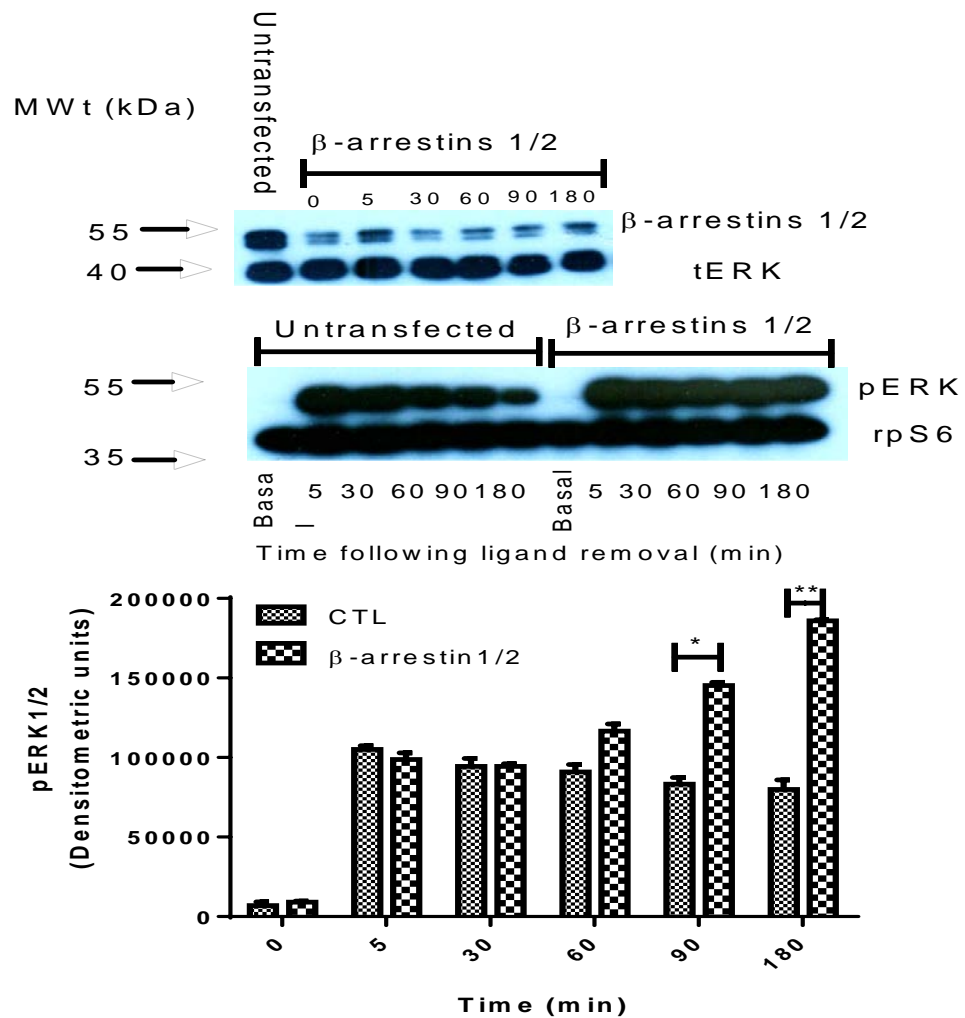
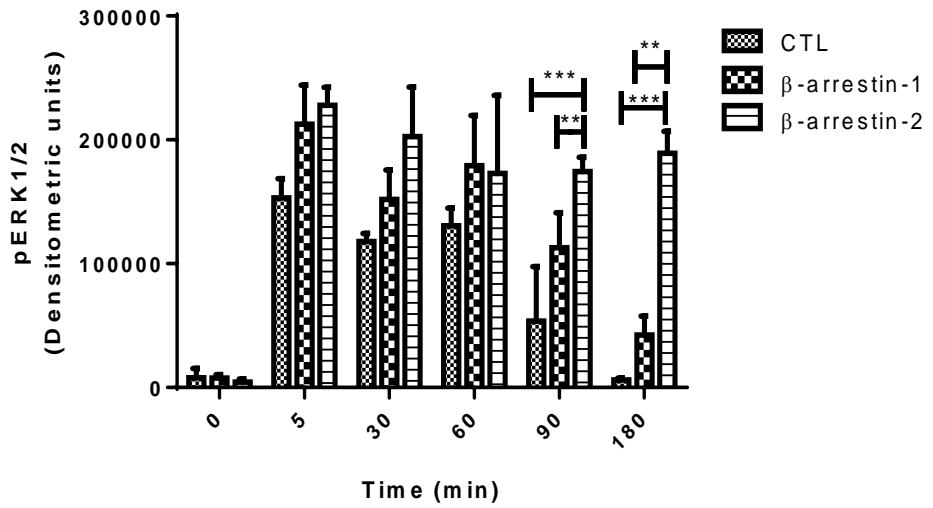
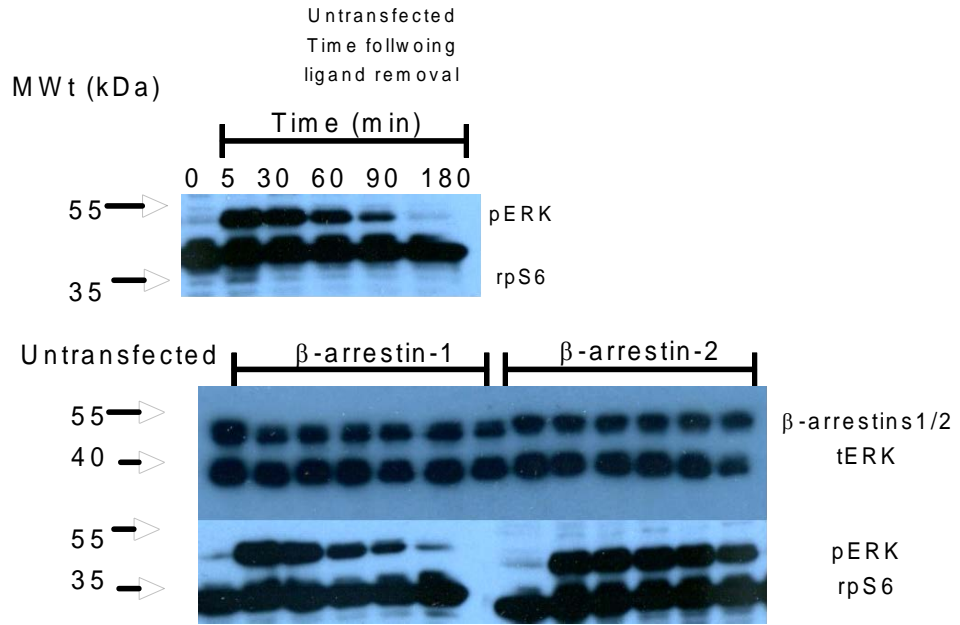
B

Figure 4.9 hNmS-33-mediated ERK activation following knockdown of β -arrestin-1 and/or -2 in HEK-NMU2

HEK-NMU2 cells were either not transfected or transfected with siRNA against β -arrestin-1, or -2 (A) or -1 & -2 in combination (B) and incubated for 24 h and then serum-starved for a further 24 h. Following a 5 min challenge with 30 nM hNmS-33, cells were washed and pERK measured over the subsequent 180 min. The levels of pERK, rpS6 and tERK was determined by Western blotting and the signal density of each quantified using Image J software. Data are representative or mean \pm s.e.m., n=3. Data were analysed by Bonferroni's multiple comparison test following two-way ANOVA; * $P < 0.05$, ** $P < 0.01$. The stimulated cells were all greater than controls and only differences between transfected and un-transfected cells were considered at each time point. CTL; control.

A



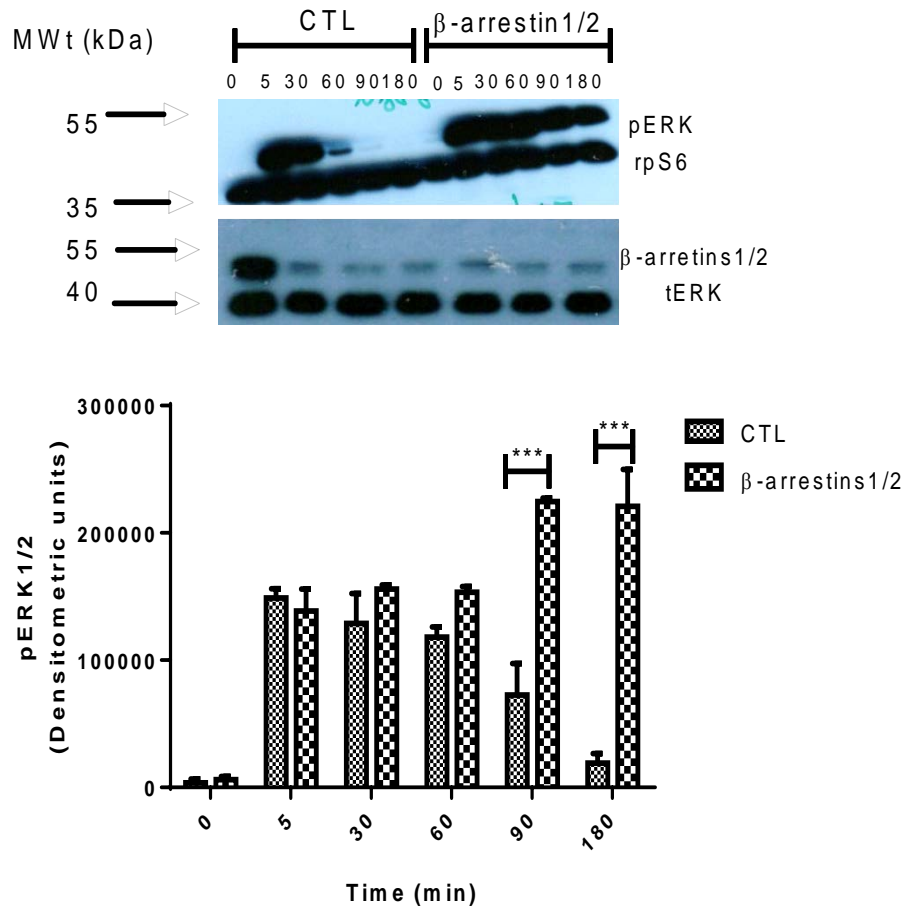
B

Figure 4.10 hNmU-25-mediated ERK activation following knockdown of β -arrestin-1 and or -2 in HEK-NMU1

HEK-NMU1 cells were either not transfected or transfected with siRNA against β -arrestin-1, or -2 (A) or -1 & -2 in combination (B) and incubated for 24 h and then serum-starved for a further 24 h. Following a 5 min challenge with 30 nM hNmU-25, cells were washed and levels of pERK measured over the subsequent 180 min. The pERK, rpS6 and tERK were determined by Western blotting and the signal density of each quantified using Image J software. Data are representative or mean \pm s.e.m., n=3. The data were analysed by Bonferroni's multiple comparison test following two-way ANOVA; ** P <0.01; *** P <0.001. The stimulated cells were all greater than controls and only differences between transfected and un-transfected cells were considered at each time point. CTL; control.

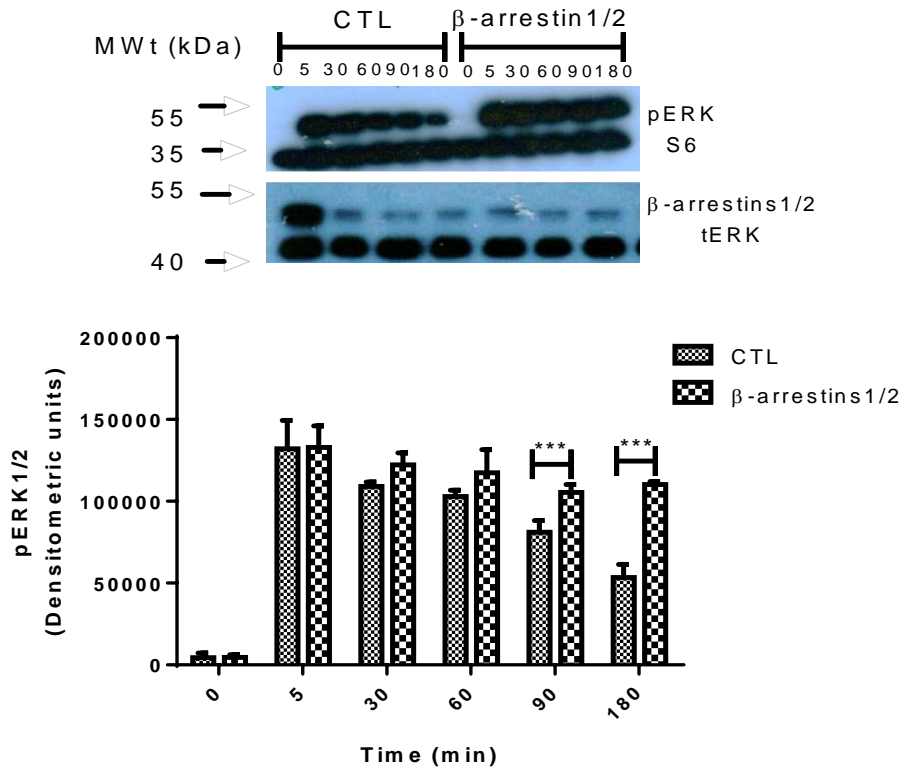


Figure 4.11 hNmS-33-mediated ERK activation following knockdown of β-arrestin-1 and -2 in HEK-NMU1

HEK-NMU1 cells were either not transfected or transfected with siRNA against β-arrestin-1 & -2 in combinations and incubated for 24 h and then serum-starved for a further 24 h. Following a 5 min challenge with 30 nM hNmS-33, cells were washed and levels of pERK measured over the subsequent 180 min. The pERK and (rpS6) were determined by Western blotting and the signal density of each quantified using Image J software. Data are representative or mean \pm s.e.m., n=3. Data were analysed by Bonferroni's multiple comparison test following two-way ANOVA; *** P <0.001. The stimulated cells were all greater than controls and only differences between transfected and un-transfected cells were considered at each time point. CTL; control.

4.2.6 The role of β -arrestin-1 and -2 in re-sensitization of NMU2-mediated signalling

It has been suggested that β -arrestins are involved in receptor re-sensitisation. For example, it has been reported that endocytosis via (CCVs) is fundamental for (β_2 AR) re-sensitization and the receptors proceed from CCVs to early endosomes, where they are dephosphorylated and re-sensitized by a mechanism that is proposed to involve a conformational change in the receptor brought about by acidification in the endosomal compartment. This putative conformational change is proposed to enhance dephosphorylation of GRK phosphorylation sites by a membrane-associated G protein-coupled receptor phosphatase (Zhang *et al.*, 1997). It is unclear whether this contributes to the dissociation of β -arrestin from the receptor. However, β -arrestin dissociation may be particularly important considering the evidence that arrestin binding to rhodopsin prevents dephosphorylation of the visual pigment.

Whether re-sensitization of NMU2-mediated Ca^{2+} signalling is dependent upon β -arrestin was investigated. Initially, the impact of β -arrestin knockdown on the $[\text{Ca}^{2+}]_i$ concentration-response curve was assessed. Because the combination of β -arrestins generally had a greater effect on NMU2-mediated pERK activation than knockdown of individual β -arrestins (**Figure 4.8 and 4.9**), knockdown of both arrestins was used in this particular experiment. HEK-NMU2 cells were either un-transfected or transfected with a combination of siRNA against β -arrestin-1 and -2 in 96 well/plates followed by 48 h incubation at 37 °C. The cells were then loaded with fluo-4-AM for 45 min and then stimulated with different concentrations of hNmU-25 (0.1-100 nM) (**Figure 4.12**). Knockdown of the arrestins had no effect on Ca^{2+} signalling with pEC₅₀ values of 8.56 \pm 0.11 and 8.65 \pm 0.08, in knockdown and control cells, respectively.

To assess re-sensitisation, HEK-NMU2 cells were transfected with siRNA against either β -arrestin-1, -2 or 1 & 2 in combination (**Figure 4.13; B**) and incubated for 48 h as described in Methods. Following either no challenge or desensitization by 5 min exposure to 30 nM of either hNmU-25 (**Figure 4.13; A**) or hNmS-33 (**Figure 4.14**), cells were washed and allowed to recover for 1, 3 or 6 h. Ca^{2+} responses to 30 nM of the appropriate ligand were then determined by stimulating the cells using a NOVOstar

plate-reader as described in Methods. Data presented earlier in this Thesis demonstrated that hNmU-25 and hNmS-33 evoked time- and equipotent concentration-dependent elevations of $[Ca^{2+}]_i$ by NMU2 (**Figure 3.1, Chapter 3**). Moreover, a relatively short exposure (5 min) to either hNmU-25 or hNmS-33 caused desensitization of subsequent NMU2-mediated Ca^{2+} signalling (**Figure 3.4; A & B, Chapter 3**). Furthermore, the earlier data demonstrated that the recovery of NMU2-mediated Ca^{2+} signalling was more rapid following pre-treatment with hNmU-25 compared to hNmS-33 and that this depended on the concentration and the exposure time of the desensitising stimulus (**Figure 3.4; C, chapter 3**). Here knockdown of a combination of both β -arrestins1/2 delayed the re-sensitisation of cells stimulated with hNmU-25 (30 nM, 5 min) at all recovery times (1, 3 and 6 h; (**Figure 4.13; A**)). When the cells were stimulated with hNmS-33 (30 nM, 5 min), the re-sensitisation was slower in cells in which the arrestins had been knocked down after 3 and 6 h recovery (**Figure 4.14**).

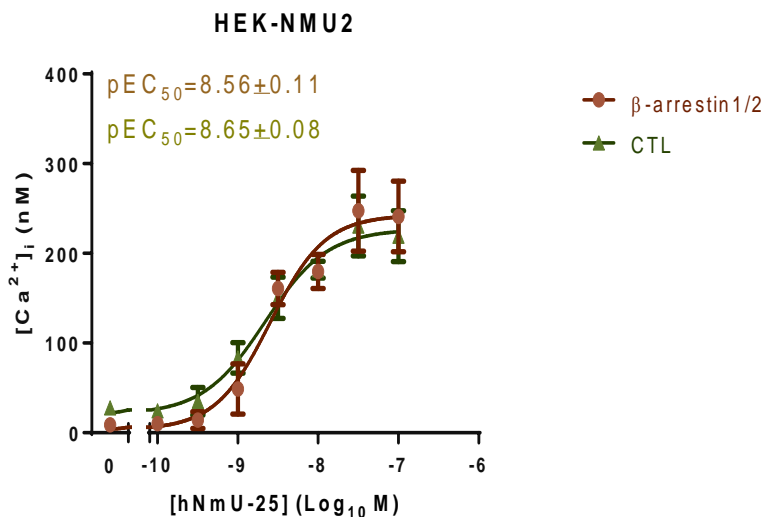
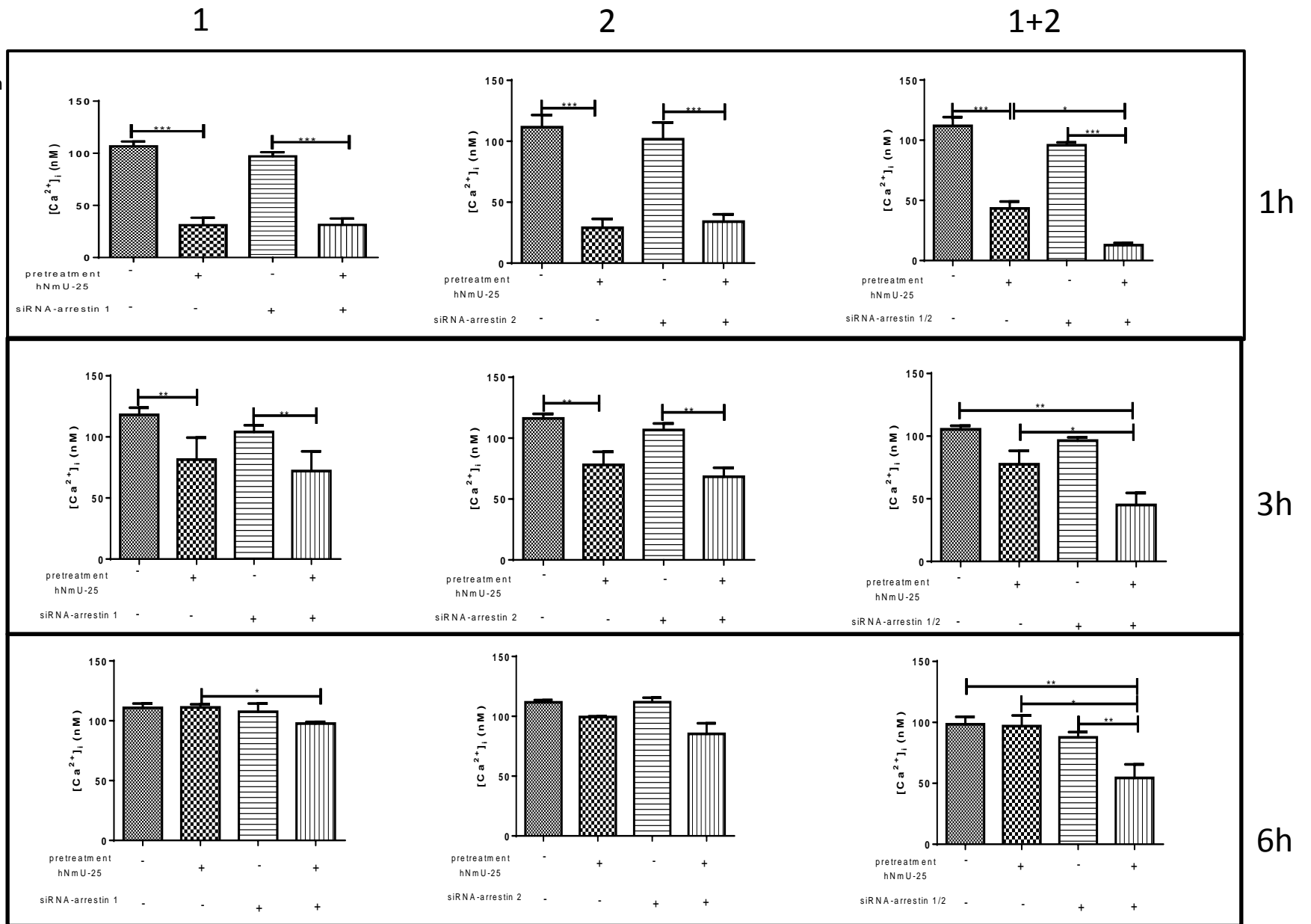


Figure 4.12 Effect of β -arrestin-1 and -2 knock down on hNmU-25-stimulated Ca^{2+} responses in HEK-NMU2

HEK-NMU2 cells were either un-transfected or transfected with siRNA against β -arrestin-1 and -2 and cultured in 96-well plates for 48 h. The cells were then loaded with fluo-4-AM for 45 min. Cells were then challenged with different concentrations of hNmU-25 (0.1-100 nM) using a NOVOstar plate reader. Changes in cytosolic fluorescence were monitored as an index of $[\text{Ca}^{2+}]_i$ and the data were calibrated and the maximal changes were used to construct concentration-response curves. The pEC_{50} values in either HEK-NMU2-un-transfected or HEK-NMU2-transfected cells exposed to hNmU-25 were 8.65 ± 0.08 and 8.56 ± 0.11 , respectively. Data are means \pm s.e.m.; n=3. CTL; control.

A
HEK-NMU2;
hNmU-25
 β -arrestin knockdown



B



Figure 4.13 β-arrestin-1 and-2 contribute to NMU2 re-sensitisation following desensitisation with hNmU-25

For resensitisation investigation, cells were transfected with siRNA against β-arrestin-1, -2 or -1 and -2 in combination and incubated for 24 h. The cells were then serum-starved for a further 24 h. Following either no challenge or desensitization by 5 min exposure to 30 nM of hNmU-25, cells were washed and allowed to recover for 1, 3 or 6 h (A). Ca^{2+} responses to 30 nM of hNmU-25 were then determined. Changes in cytosolic fluorescence were monitored as an index of $[Ca^{2+}]_i$ and the data were calibrated using cells in which arrestin was present or had been knocked-down as appropriate. The maximal changes in fluorescence were used to construct columns. In order to confirm knockdown occurrence, cells were transfected with siRNA against β-arrestin-1, -2 or -1 and -2 in combination and incubated for 24 h followed by Western blotting as described in Methods (B). Data are mean + s.e.m., n=3 (A), or representative (B). Data were analysed by Bonferroni's multiple comparison test following one-way ANOVA; * $P<0.05$, ** $P<0.01$, *** $P<0.001$.

HEK-NMU2;
hNmS-33
 β -arrestin knockdown

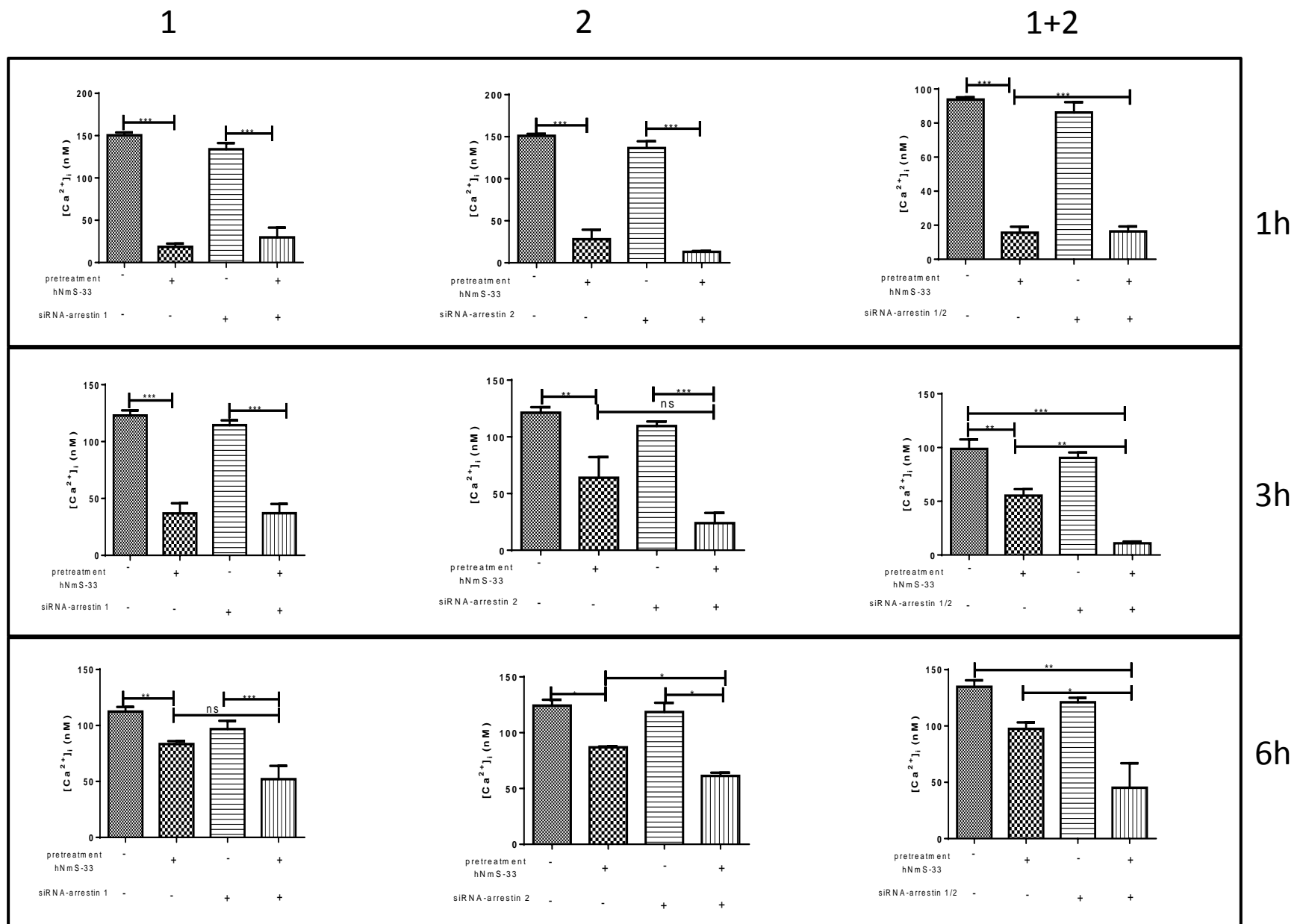


Figure 4.14 β -arrestin-1 and -2 contribute to NMU2 re-sensitisation following desensitisation with hNmS-33

Cells were transfected with siRNA against β -arrestin-1, -2 or -1 and -2 in combination and incubated for 24 h. The cells were then serum starved for further 24 h. Following either no challenge or desensitisation by 5 min exposure to 30 nM of hNmS-33, cells were washed and allowed to recover for 1, 3 or 6 h. Ca^{2+} responses to 30 nM of hNmS-33 were then determined. Changes in cytosolic fluorescence were monitored as an index of $[\text{Ca}^{2+}]_i$ and the data were calibrated using cells in which arrestin was present or had been knocked-down as appropriate. The maximal changes in fluorescence were used to construct columns. Data are means \pm s.e.m., n=3. Data were analysed by Bonferroni's multiple comparison test following one-way ANOVA; * P <0.05, ** P <0.01, *** P <0.001.

4.2.7 Arrestin recruitment by activated NMU receptors

A adapted β -galactosidase complementation assay, denoted to as PathHunter™ technology, has recently become present sanctioning GPCR- β -arrestin closeness to be read on conventional luminometers available in most laboratories (Olson *et al.*, 2007). The assay makes utilization of a unique low-affinity peptide derived from the amino terminus of *Escherichia coli* β -galactosidase, which is tied to the C-terminus of the GPCR of interest (enzyme donor), and a ω -effacement mutant of β -galactosidase, which is attached to β -arrestin (enzyme acceptor) (**Figure 2.1**). The use of the low-affinity peptide, mentioned to as ProLink™, guarantees that the enzyme fragment complementation (EFC) reaction is determined by the ligand-stimulated, reversible interaction of the GPCR with β -arrestin and not by β -galactosidase complementation in the nonappearance of receptor activation (Wehrman *et al.*, 2005). The rebuilt holoenzyme catalyzes the hydrolysis of a substrate yielding a chemiluminescent signal that can be measured by a NOVOstar plate-reader. This kit was provided by DiscoverRx and designed to measure only β -arrestin-2 using NMU1. Ideally the study would have examined recruitment of β -arrestin-1 and -2 by both NMU1 and NMU2 following activation with a number of different ligands. However, the only available platform was NMU1 and β -arrestin-2, although different ligands were used (hNmU-25, hNmS-33, and pNmU-8). The experiment was conducted as explained in Methods. The concentration-response curves were generated. The pEC₅₀ values for the ligands were: hNmU-25, 7.81±0.08; hNmS-33, 7.61±0.07, and, pNmU-8, 8.41±0.09, (**Figure 4.15**) indicating no significant differences between the ligands, at least for NMU1-mediated recruitment of β -arrestin-2.

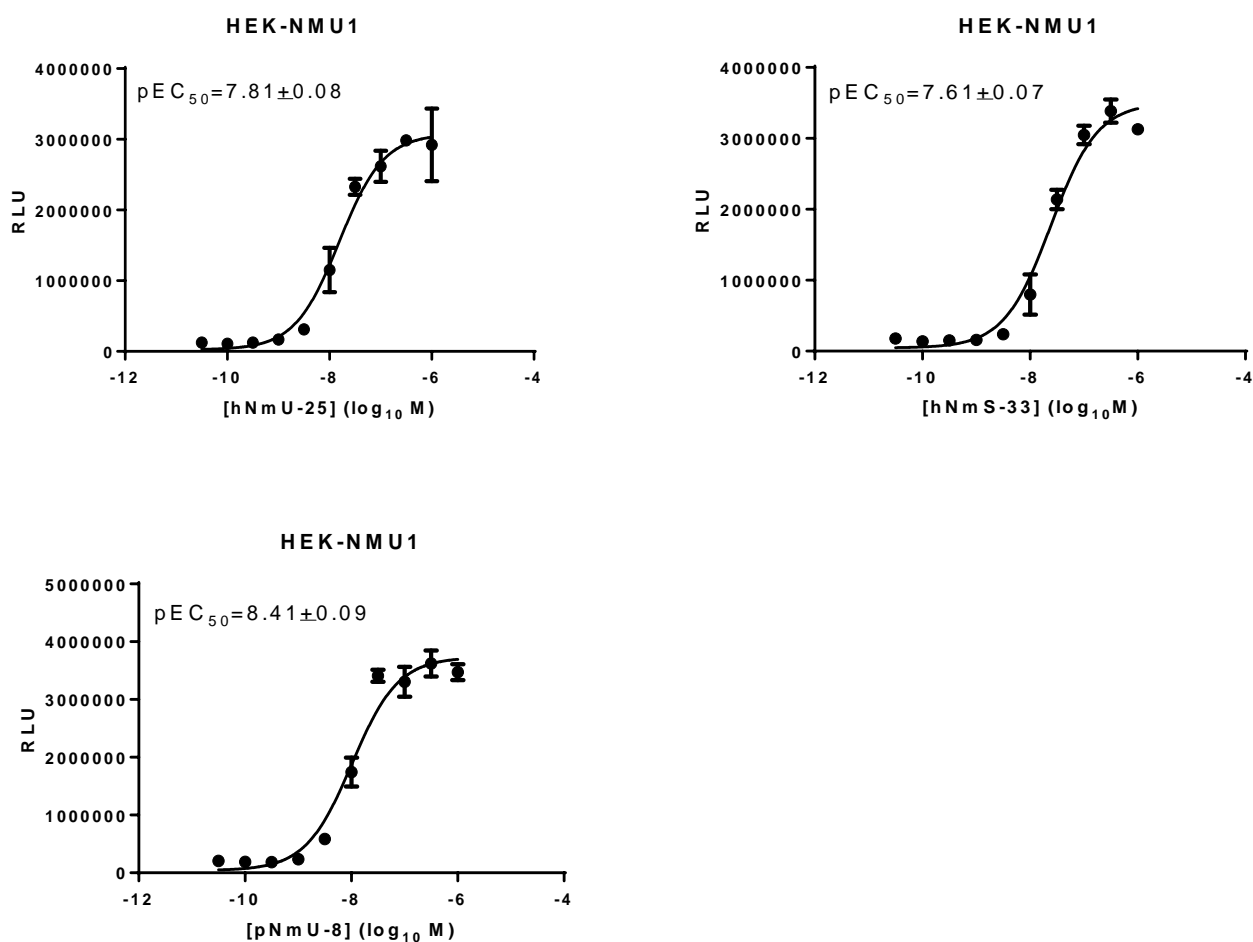


Figure 4.15 Concentration-response curves for β -arrestin-2 recruitment by activated NMU1

PathHunter eXpress cells expressing NMU1 were plated in 96 wells-plates. The cells were then incubated for 48 h at 37°C, 5% CO₂. Cells were then challenged with hNmU-25, hNmS-33, or pNmU-8. The plate was incubated for 90 minutes at 37°C, 5% CO₂. Following addition of detection reagent working solution and further incubation for 60 minutes at room temperature, chemiluminescence, (indicated as relative luminescence units (RLU)) was recorded using a NOVOstar plate reader. The pEC₅₀ values were calculated using Graph Pad Prism 6. The pEC₅₀ values for hNmU-25, hNmS-33, and pNmU-8 were 7.81± 0.08, 7.61±0.07, and 8.41±0.09, respectively. Experiments were carried out once in duplicate.

4.3 Discussion

Data in this Chapter demonstrate that hNmU-25 and hNmS-33 are equipotent on NMU-mediated ERK activation and both evoke a similar maximal degree of activation. With either ligand, ERK was activated within 5 min and this was sustained over the 3 h of the experiment when the ligand was left in the incubation medium. However, when the activating ligand was removed after 5 min of stimulation, there were clear differences in the profile of activation. Thus, in the case of NmU-25 the pERK levels returned to basal over the subsequent 2-3 h, whereas despite removal of NmS-33, pERK levels were essentially sustained. Although removal of ligand following stimulation is not a common experimental manipulation when examining the time-course of activation, it has two possible advantages. Firstly, it may be more equivalent to a physiological situation where agonists are released periodically and then rapidly removed (often by degradative pathways) and secondly it may allow examination of the impact of events such as receptor/ligand processing in the absence of potential receptor recycling and re-stimulation. The opportunity for NMU2 recycling following ligand removal was emphasized by the ability of hNmU-25 to evoke further ERK activation 3 h after the initial 5 min challenge and removal of hNmU-25.

Data in Chapter 3 demonstrated that the rate of re-sensitization of NMU2-mediated Ca^{2+} signalling following hNmU-25 was considerably faster than following hNmS-33. This may suggest that in the process of receptor internalization, re-sensitization and recycling, the nature of the ligand plays a critical role. Indeed these data would suggest that hNmS-33 retards one or more aspects of these processes compared to hNmU-25. NMU2 re-sensitization is reduced by inhibition of internalization following stimulation with either ligand. It is possible therefore that one or more aspects of signalling might be prolonged in the presence of hNmS-33 compared to hNmU-25. This could include G-protein-dependent signalling, particularly if receptor phosphorylation and/ or internalization are delayed and could potentially include G-protein-independent signalling if the life-time of the internalized ligand/receptor/complex is extended. In these experiments demonstrating that ERK signalling is more prolonged following

removal of hNmS-33 than hNmU-25, it is possible, that these differences arise from either extended G-protein-dependent signalling or extended G-protein-independent signalling. This latter possibility could arise, for example, through a slower rate of removal of hNmS-33 from the receptor within an endosomal compartment, thereby allowing sustained scaffolding of the ERK signalling complex by arrestin. Indeed the present data demonstrate that endosomal acidification is required to terminate NMU2-mediated ERK activation. This is consistent with endosomal acidification promoting ligand-receptor dissociation (Mellman *et al.*, 1986), thereby reducing any associated signalling but could also be consistent with reduced trafficking of receptor complexes through the endosomal compartment leading to, for example, reduced receptor internalization and prolonged G-protein-dependent signalling at the plasma membrane. Previous work in our laboratory (Alhosaini, 2011) and in this thesis have shown that very acidic conditions (pH 2.0) are required to remove peptide bound to NMU receptors at the cell surface, at least over a short period of time (<1 min). Although the endosomal pH may only reach pH 4.8-6.0 (Maxfield *et al.*, 1987), the ligand receptor complex may be exposed to this for considerable time. Furthermore, other influences such as ionic composition of the endosomal compartment may also play a role in promoting dissociation (Luzio *et al.*, 2007). The ability of the ECE-1 inhibitor, SM-19712, to prolong ERK activation following hNmU-25 but neither hNmS-33 nor pNmU-8 activation of NMU2 (again, in experiments in which the activating ligand was removed following a 5 min stimulation) is consistent with ECE-1 processing of hNmU-25 being an important compartment of signal termination. Taken together, these data support a model in which endosomal hNmU-25 is degraded by ECE-1, thereby reducing ligand-receptor complexes and allowing disassembly of arrestin-ERK signalling complexes to reduce G-protein-independent activation of ERK. In contrast, hNmS-33 may not be removed (degraded) by ECE-1, thereby allowing scaffolding and signalling complex to persist for longer. A similar set of circumstances have been suggested for substance P and the neurokinin 1 receptor, where endosomal ECE-1 has been suggested to disrupt the neurokinin 1 receptor/arrestin/ERK signalling complex to reduce neurokinin 1 receptor-mediated ERK activation (Cottrell *et al.*, 2009). Time-course of NMU2-mediated ERK activation in the presence and absence of ECE-1 inhibitor using a sub-maximal concentration of ligand indicated that the inhibition of ECE-1 also enhances

the pERK exposed to hNmU-25 but not hNmS-33. Interestingly, this experiment also showed that the bands are stronger following exposed to hNmS-33 compared to hNmU-25 at all times suggesting that hNmS-33 could be more potent than hNmU-25 and more studies are required to address this issue.

In the HEK-NMU2 cells, the precise mechanisms of ERK activation are unclear. There is some suggestion that for other GPCRs, the activation of ERK could be through either G-protein-dependent or arrestin-dependent (G-protein-independent) mechanisms and that both can occur in response to activation of the same receptor but with different temporal characteristics. For example, in HEK cells with recombinant expression of angiotensin II (AT₁) receptors there is a G-protein-dependent activation of ERK at 2 min but a later (10 min) β -arrestin-dependent activation (Ahn *et al.*, 2004). Similarly, parathyroid hormone (PTH) can activate ERK1/2 through the PTH receptor in two phases, an early phase (5 min) and a later (30-60 min) phase (Gesty-Palmer *et al.*, 2006). The siRNA-mediated knock-down of β -arrestin-1 and -2 left the early phase relatively unaffected but largely abolished the later phase. These data provide clear evidence that the later phase PTH receptor-mediated ERK activation is through a β -arrestin-dependent pathway but that the early phase is β -arrestin-independent and therefore likely G-protein-dependent (Gesty-Palmer *et al.*, 2006). In other situations ERK activation by these pathways may not be temporally distinct. Thus, ERK activation by both pathways peaked 2 min after stimulation in cells expressing vasopressin receptors (Ren *et al.*, 2005).

In addition to signalling through ERK it has been demonstrated that a ligand-receptor-arrestin complex might also be able to sustain more classical G-protein-dependent signalling within cells. For example, sustained cAMP signalling may result from a long-lasting PTH-PTHrP-arrestin complex (Wehbi *et al.*, 2013). In this case, β -arrestin may play a role in stabilizing a complex of the PTHrP and G $\beta\gamma$, resulting in accelerated G-protein activation and increased levels of active G α_s , thereby prolonging production of cAMP. Alternatively, the complex stabilized by β -arrestin is bypassed by re-associating the free G α -GDP to PTHrP-G $\beta\gamma$ complex to stimulate a new round of G-protein activation (Wehbi *et al.*, 2013). In the present study it is unclear if such a mechanism is

operating and if this is able to influence G-protein-dependent signalling in a ligand-dependent manner.

Given the hypothesis that ligand-receptor-arrestin interaction is responsible for the ability of hNmS-33 to sustain ERK activation compared to hNmU-25, the role of β -arrestins in ERK activation was investigated using siRNA to knockdown. Firstly, knockdown of β -arrestin-1 and -2 slowed recovery of Ca^{2+} signalling by NMU2 following desensitization with either hNmU-25 or hNmS-33, thereby identifying a role for these arrestins in recovery and by implication in recycling. Knockdown of β -arrestin-1 and -2, either individually or in combination, both enhanced and extended the duration of hNmU-25-mediated ERK activation. In contrast, individual knockdown of β -arrestin-1 or -2 had a much more limited impact on hNmS-33-mediated ERK activation. However, combined knockdown of both β -arrestin-1 and -2 enhanced the levels of pERK at least at later time points. These data suggest that β -arrestins 1/2 are not involved in driving NMU2-mediated activation of ERK. This is in contrast to the emerging paradigm that has been proposed for a number of GPCRs, in which arrestins promote G-protein-independent signalling pathways by providing sub-cellular scaffolding for signalling complexes (Lefkowitz *et al.*, 2005). It is possible that the prolonged ERK activation observed following arrestin knockdown is a consequence of enhanced and sustained G-protein activation in the presence of a reduced inhibitory feedback usually provided by arrestin binding to the phosphorylated receptor. This is consistent with a previous study (Luo *et al.*, 2008). In this study, siRNA was used to target proteins specifically involved in the agonist-dependent regulation of the endogenous M_3 mAChR in HEK-293 cells. It was found that there was differential GRK-mediated regulation of this receptor as assessed by calcium signalling and ERK activation. In addition, knockdown of either β -arrestin-1 or β -arrestin-2 resulted in enhanced signalling from the receptor with different temporal effects. The knockdown of β -arrestin-1 or arrestin-2 significantly increased carbachol-mediated calcium mobilization. Knockdown of GRK2 and the arrestins also significantly enhanced carbachol-mediated activation of extracellular signal-regulated kinases 1 and 2 (ERK1/2), whereas prolonged ERK1/2 activation was only observed with GRK2 or β -arrestin-2 knockdown.

A number of studies have examined the role of the arrestins in GPCR-mediated ERK activation with differing outcomes. In contrast to our results in which depletion of β -arrestin-2 prolonged pERK whereas depletion of β -arrestin-1 had no effect, in a recent study, it has been indicated that depletion of β -arrestin-1 prolonged pERK signal to activation of P2Y₂ in airway smooth muscle cells (ASMC), while β -arrestin-2 depletion had no effect (Morris *et al.*, 2012). In contrast, depletion of β -arrestin-2 prevented ET-1-stimulated pERK, while depletion of β -arrestin-1 was ineffective in ET-1-stimulated pERK (Morris *et al.*, 2012). In addition, oxytocin-induced generation of pERK was prevented by knocking down β -arrestin-2, while β -arrestin-1 depletion enhanced pERK responses to each ligand (Brighton *et al.*, 2011). The augmentation of oxytocin receptor-pERK signalling in the absence of β -arrestin-1 is consistent with the receptor desensitisation decrease. In contrast, the desensitisation of histamine receptors was not affected by β -arrestin-1 despite that it similarly enhanced H₁ receptor-pERK signalling. This allowed the author to suggest that the precise mechanism (s) whereby the depletion of β -arrestin-1 facilitates both receptors have not been established (Brighton *et al.*, 2011).

The present study does not allow a clear view as to which arrestin molecules are recruited by activated NMU2, nor whether the receptor belongs to the class A or class B subgroups of receptors based on arrestin recruitment and retention. Furthermore, the precise mechanisms of ERK activation over the time-courses examined in the present study are still a little unclear. It would be particularly interesting to identify if any of these processes are dependent upon the nature of the ligand. For example, the prolonged activation of ERK and the slower re-sensitisation following hNmS-33 compared to hNmU-25 might suggest that any recruited arrestin could interact with NMU2 for longer following hNmS-33. It would be particularly important, therefore, to consider some live-cell BRET and bimolecular fluorescence complementation (BiFC) (Kilpatrick *et al.*, 2010) experiments that would enable the kinetics of arrestin recruitment and retention to be explored. Similarly, it would be of great interest to explore the specific phosphorylation patterns of NMU2 in response to these two ligands.

GPCR internalisation to endosomes is proposed to be the mechanism by which G protein-coupled receptor kinase (GRK)-phosphorylated receptors are dephosphorylated

and re-sensitised. It has been suggested that β -arrestins, as GPCR trafficking molecules, might represent critical determinants for GPCR re-sensitisation. The cellular event leading to GPCR endocytosis and recycling is initiated by the agonist-promoted mobilisation of cell surface receptors to an intracellular vesicular compartment, probably endosomes (Moore *et al.*, 1995; Garland *et al.*, 1996). Moreover, receptors internalized via (CCVs) are thought to be re-sensitized in endosomes following their dephosphorylation by a membrane-associated phosphatase that exhibits specificity for G protein-coupled receptor kinase (GRK)-phosphorylated GPCRs residing in an acidified endosomal environment (Sibley *et al.*, 1986b; Krueger *et al.*, 1997). Following this dephosphorylation, the receptors can then recycle to the plasma membrane for further signalling. Therefore, whether NMU2 re-sensitization was dependent upon β -arrestins, was tested in this project. The current study indicates that combination of both β -arrestin-1 and -2 could be involved in trafficking and therefore receptor re-sensitization. This study is consistent with many other reports on a range of GPCRs, indicating that overexpression of β -arrestin 1-V53D, a dominant negative inhibitor of β_2 AR sequestration, increased the extent of agonist-induced β_2 AR phosphorylation. This in turn suggests that β -arrestins might play a role in β_2 AR re-sensitization (Ferguson *et al.*, 1996; Zhang *et al.*, 1997). Also it has been suggested that arrestins could involve in histamine H_2 receptor (H_{2r}) desensitization, internalization, and re-sensitization (Fernandez *et al.*, 2008). In this study, in COS7 transfected cells, arrestin-2 but not arrestin-1 overexpression reduced H_{2r} -evoked cAMP response and arrestin-2 knockdown abolished H_{2r} re-sensitization. Similar results were obtained in U937 cells endogenously expressing H_{2r} .

It would have been ideal here to be able to use the PathHunter™ eXpress β -arrestin Assays kit from DiscoverX to investigate the recruitment of specific arrestins to the activated NMU2, particularly in response to the different ligands. Unfortunately, NMU2 was not available and the only format was NMU1 and β -arrestin-2. These experiments with NMU1 did not identify any differences between hNmU-25 and hNmS-33 in terms of the potency or extent of β -arrestin-2 recruitment. It would have been ideal to examine both β -arrestin-1 and β -arrestin-2 and, as indicated above, examine the temporal profile of recruitment and release.

Results in this chapter highlight a key difference in the time-course of activation of ERK in response to hNmU-25 and hNmS-33. This was only apparent when cells were stimulated and the ligand removed, suggesting that differences in the internalisation, re-sensitisation and recycling occur in a ligand-dependent manner. The extended activation of ERK in response to hNmS-33 suggests that NMU2 activated by this ligand may couple to the ERK pathway for longer than when activated by hNmU-25. This may have implications for aspects such as the activation mechanism (s), the sub-cellular localisation of activated ERK and ultimately the cellular response. Some of these aspects will be explored in the subsequent chapters of this thesis.

Chapter 5

Further investigation of signalling responsible for NMU2-mediated ERK activation

5.1 Background

5.1.1 Introduction

G protein-coupled receptors (GPCRs) are the largest group of cell surface receptors. About 800 members have been identified in the human genome (Bjarnadottir *et al.*, 2006). A GPCR, as a result of responding to extracellular stimuli, changes its structural conformation and transduces this into intracellular signals. Therefore, several signalling pathways are activated by GPCRs including IP₃/PLC (phospholipase C) pathway (Chen-Izu *et al.*, 2000) and the ERK/MAPK (extracellular signal-regulated kinase) pathway (Crespo *et al.*, 1994b). NMU2 belongs to a group of receptors that signal preferentially through G α_q to activate PLC β (Brighton *et al.*, 2004b; Alhosaini, 2011). In addition, GPCRs, including NMU2, activate MAPKs (MAPK1, also called extracellular signal regulated kinases including ERK1 and ERK2), which are major cellular effectors activated by GPCRs (Eishingdrelo *et al.*, 2013). There are varieties of mechanisms by which GPCRs are able to activate ERK (see **Introduction**). This includes both G-protein-dependent and G-protein-independent pathways (Ahn *et al.*, 2004; Goldsmith *et al.*, 2007). Thus, the ERK pathway can be activated by Ras, PKC, and transactivation of receptor tyrosine kinases (RTKs) and in a G-protein-independent manner by β -arrestins (Wei *et al.*, 2003a; Leroy *et al.*, 2007). The activation of ERK via G-protein α subunits; G α_q , G α_s , G α_i and G-protein $\beta\gamma$ subunits via Ras has been investigated (Inglese *et al.*, 1995; Mochizuki *et al.*, 1999; Saini *et al.*, 2007).

β -arrestins may link receptors to ERK activation in a G protein-independent manner (Tohgo *et al.*, 2003; Wei *et al.*, 2003). It has been reported that a Class B receptor activates ERK via arrestins at endocytic vesicles (DeFea *et al.*, 2000; Luttrell *et al.*, 2001). This may be of particular functional importance as G protein-dependent activation of ERK is transient and ERK is translocated into the nucleus, whereas the G protein-independent pathway tends to be sustained and activated ERK is retained in the cytosol (Tohgo *et al.*, 2002).

It has also been highlighted that arrestins are not required for ERK activation for some GPCRs, including the D2 and D3 dopamine receptors (Beom *et al.*, 2004), the α_2 -adrenergic receptor (α_2 AR) (Wang *et al.*, 2005) and gonadotropin-releasing hormone receptor (Benard *et al.*, 2001). Moreover, it has been previously demonstrated that the (α_2 AR), which is a Class A receptor, evokes phosphorylation of ERK1/2 through G protein-dependent pathways and this process is dispensable for arrestin-mediated receptor endocytosis (Schramm *et al.*, 1999; Wang *et al.*, 2005).

A previous study has demonstrated that hNmU-25 at either NMU1 or NMU2 activates ERK1/2 via a $G\alpha_i$ -PTX-insensitive pathway when the receptors are expressed recombinantly in HEK cells (Brighton *et al.*, 2004b). The activation of mitogenic signals by GPCRs coupling to $G\alpha_{q/11}$ may be mediated by a multitude of signalling cascades. It has been confirmed that inhibition of $G\beta\gamma$ has no effect on MAP kinase activation suggesting that signals are mediated through the α -subunit of $G\alpha_{q/11}$ G-proteins (Hawes *et al.*, 1995). It should be noticed that this might be receptor-specific, since the $G\beta\gamma$ activates PLC to activate PKC leading to ERK activation. Some aspect of GPCR signalling has not been investigated due to the limited availability of suitable pharmacological tools. Exploring the role of $G\alpha_q$ has not been easy, since $G\alpha_q$ knock-out mice had lower blood pressure compared to controls (Wirth *et al.*, 2008). A most useful pharmacological agent has been the $G\alpha_q$ inhibitor YM-254890, although this is not widely available. It is a cyclic depsipeptide (i.e. a molecule that has both peptide and ester linkages in proximity in the same amino acid-containing small molecule or chain). It has been demonstrated that this peptide is a specific inhibitor of $G\alpha_{q/11}$ by inhibiting the exchange of GDP for GTP and thus preventing the activation of the G protein (Takasaki *et al.*, 2004). This inhibitor has had variable availability and is

currently not available. Structurally similar compound, UBO-QIC, has also been used to explore the role of $G\alpha_q$ in signalling (Danielle Kamato, 2015).

The mechanism (s) by which NMU2 activates ERK are unclear and a number of experimental approaches, particular using chemical inhibitors, have been employed in the chapter to investigate aspects of this.

The role of epidermal growth factor receptor (EGFR) transactivation, classical receptor tyrosine kinases (RTKs) in NMU2-induced ERK-1/-2 activation was investigated in order to provide further insight into the mechanisms underlying the NMU2 processing in ERK-1/-2 action.

5.1.2 The detection of ERK activation and distribution

It has been demonstrated that ERK substrates have been identified in different places in the cells including nucleus, plasma membrane, cytoplasm and cytoskeleton. Thus, activated ERK may play different roles dependent on where it is active in the cells. Indeed, the phosphorylated ERK1/2 mediated by the β -arrestin signalling pathway remains in cytoplasm, where they play roles in translation, apoptosis, and cross-talk with other signalling pathways (Tohgo *et al.*, 2002; Luttrell *et al.*, 2003), while the phosphorylated ERK1/2 mediated by the G-protein signalling translocate to the nucleus where they play roles in gene transcription, cell proliferation and differentiation (Chuderland *et al.*, 2008; Plotnikov *et al.*, 2011). For example, it has been demonstrated that GPCR- β -arrestin complexes are internalised and targeted to endosomes and that the subsequent β -arrestin-dependent ERK activation thus leads to the formation of cytosolic pool of ERK. This can be seen in association with early endosomes (DeFea *et al.*, 2000; Luttrell *et al.*, 2001). Because the consequences of ERK1/2 activation depends on subcellular location and duration of activation (Luttrell, 2003; McArdle, 2003; Lu *et al.*, 2006), it is important to understand the mechanisms controlling the location and duration of the ERK1/2 signal. Immunostaining is widely used to detect the distribution and localization of specific protein and has been applied to examine the subcellular distribution of ERK (Maity *et al.*, 2013).

5.1.3 The role of β -arrestins-1 and -2 in ERK activation

Agonist activation of a GPCR leads to the change of GDP for GTP on the $G\alpha$ of G-protein. The GTP-bound $G\alpha$ then dissociates from both $G\beta\gamma$ and from the receptor. Both $G\alpha$ and $G\beta\gamma$ interact with effector proteins, whereas serine and threonine residues in the intracellular loops and C-terminal of the agonist-occupied receptor is phosphorylated by GRKs (Pitcher *et al.*, 1998). β -arrestin binds and recognizes the phosphorylated residues targeting the receptor to CCPs for endocytosis (Laporte *et al.*, 1999). The internalised receptor is then dephosphorylated and the ligand is dissociated from the receptor due to the endosomal acidification. The receptor is then either recycled to the cell surface or to lysosomes for degradation (Tsao *et al.*, 2001). β -arrestins-1 and -2 were named as a consequence of their ability to hinder the G protein coupling of agonist-activated GPCRs, leading to receptor desensitization. In addition to their well-described roles in desensitization and internalization, β -arrestins can also bind GPCRs to members of the Src and MAPK families including ERK (Luttrell *et al.*, 2001; Luttrell *et al.*, 2002). It has been suggested that G-protein-dependent and -independent pathways can be separated, suggesting the opportunity that β -arrestin biased agonists may be developed (Violin *et al.*, 2007). RNA silencing technology is a powerful tool for distinguishing β -arrestin-independent activation of ERK from that initiated by G proteins.

5.2 Results

5.2.1 Investigating the role of PKC in ERK activation

PKC is involved in the activation of ERK signalling. So, the possibility of activating ERK by PKC was assessed using the PKC inhibitor, Ro-31-8220 (5 μ M). To test the ability of Ro-31-8220 to inhibit PKC, cells were challenged with the PKC activator, PDBu, in the presence and absence of Ro-31-8220. Cells were pre-incubated with KHB with or without Ro-31-8220 for 30 min followed by a 5 min challenge with PDBu (1 μ M) in the continued presence of Ro-31-8220 where appropriate. The results show that PDBu activated ERK (as judged from the levels of pERK) but in the presence of Ro-31-8220, ERK activation was completely abolished (**Figure 5.1**). In addition, the impact of the inhibitor on NMU2-mediated ERK activation was investigated. Thus, Ro-31-8220 reduced the levels of pERK at earlier time points (5 and 60 min) following stimulation of NMU2 with a maximum concentration of hNmU-25. In contrast, the inhibitor prolonged levels of pERK at later time points (90, 120 and 180 min) (**Figure 5.2; A**). When cells were stimulated by hNmS-33 (30 nM, 5min), the inhibitor reduced the pERK levels at earlier time points (5, 60 and 90 min) and no effect was observed at later time points (120 and 180 min) (**Figure 5.2; B**).

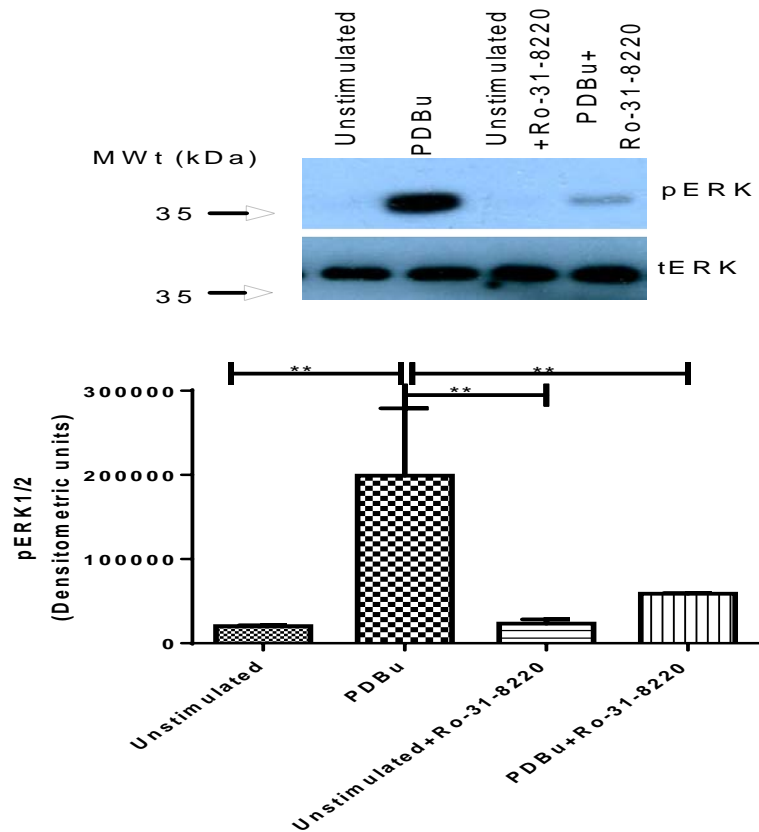


Figure 5.1 The effect of PKC inhibitor, Ro-31-8220, on PDBu-mediated activation of ERK

HEK-NMU2 cells cultured on 24-well plates for 24 h and serum-starved overnight for a further 24 h. Cells were washed with KHB and then, incubated with or without Ro-31-8220 for (30 min) and challenged (5 min) with KHB or PDBu (1 μ M) in the presence or absence of Ro-31-8220 as appropriate. Cells were washed twice with KHB and tERK and pERK determined by Western blotting and the signal density quantified using Image J software. tERK was used as a loading control. Data are representative blots or mean \pm s.e.m., n=3. Data were analysed by Bonferroni's multiple comparison test following one-way ANOVA; ** P <0.01.

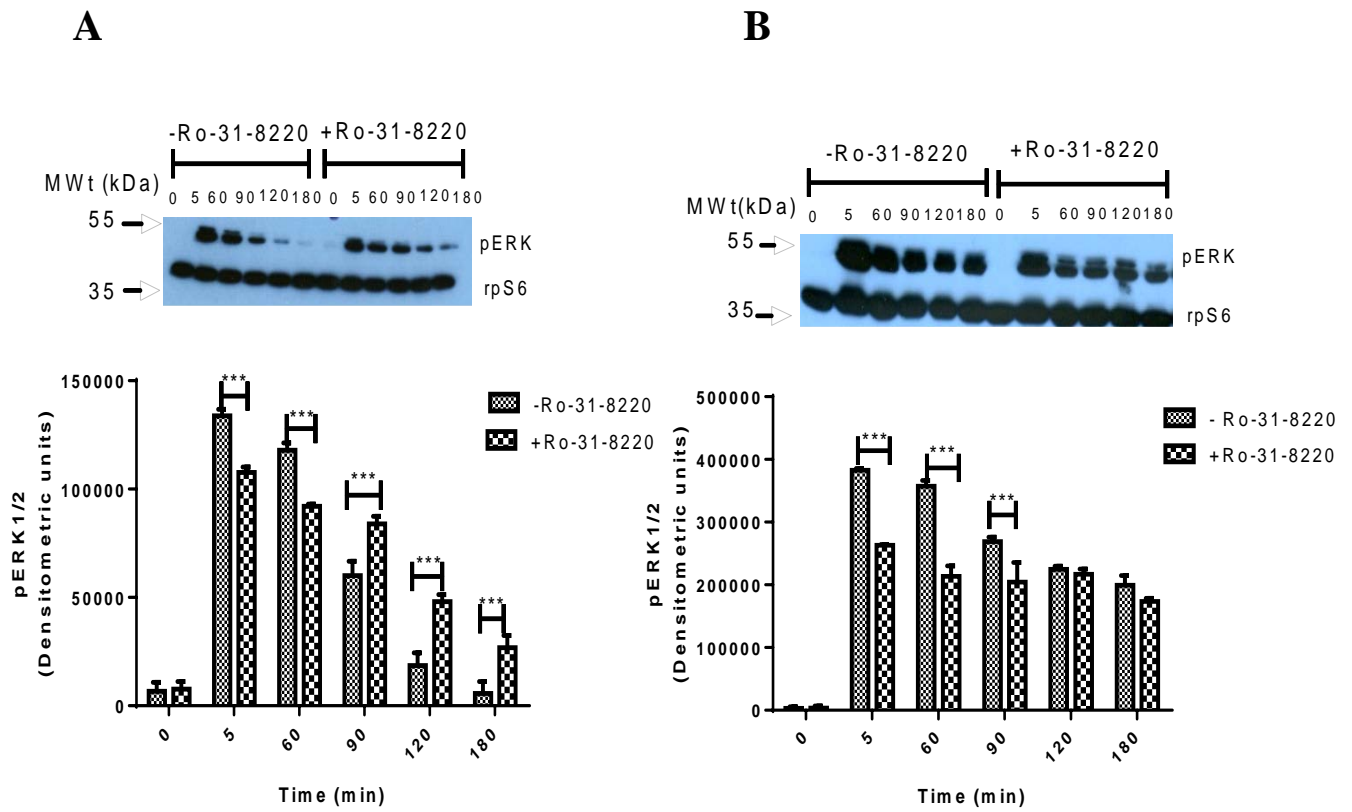


Figure 5.2 The effect of PKC inhibition on ERK activation by hNmU-25 and hNmS-33

HEK-NMU2 cells were cultured on 24-well plates for 24 h and serum-starved for a further 24 h. Cells were washed twice with KHB and then incubated with KHB without or with Ro-31-8220 (5 μ M, 30 min) and then challenged with either KHB, hNmU-25 (**A**) or hNmS-33 (**B**) (30 nM, 5 min) in the presence and absence of the inhibitor and left for the required time. Levels of pERK and rpS6 were determined by Western blotting and the signal density of each quantified using Image J software. The rpS6 was used as a loading control. Data are representative blots or mean \pm s.e.m., n=3. Data were analysed by Bonferroni's multiple comparison test following two-way ANOVA; *** P <0.001; only comparisons between \pm Ro-31-8220 at each time point were considered for clarity.

5.2.2 The role of G_{α_i} in the activation of ERK

Cells expressing NMU2 were cultured on poly-D-lysine-coated 24-well plates and G_{α_i} inhibited with pertussis toxin (PTX; 100 ng/16 h). Cells were then stimulated with either hNmU-25 or hNmS-33 (30 nM, 5 min) following which the ligand was removed and the cells allowed to recover for the required time. The results show that levels of pERK after either ligand were reduced following PTX treatment, particularly at later time points. For example, when the cells were stimulated with hNmU-25, pERK was significantly reduced at 30, 60 and 90 min. At later time points following the removal of hNmU-25, pERK levels had returned to basal and PTX had no effect (**Figure 5.3; A**). When cells were stimulated with hNmS-33, pERK was sustained for up to 3 h and PTX significantly reduced the levels at 60 and 90 min, and abolished the hNmS-33-mediated increase in pERK at 3 h (**Figure 5.3; B**).

The effect of combination of G_{α_i} inhibitor (PTX) and PKC inhibitor (Ro-31-8220) was examined. The cells were pre-incubated with or without PTX as previously and on the day of the experiment; cells were pre-incubated in KHB without or with Ro-31-8220 (5 μ M) for 30 min. The cells were then stimulated by hNmU-25 (30 nM, 5 min). The combination of Ro-31-8220 and PTX significantly reduced the levels of pERK in response to hNmU-25 (**Figure 5.4**). hNmS-33 was not used in such conditions.

Given the inhibitory effects of PTX on ERK responses to hNmU-25, its toxicity was assessed. In order to do so, the cells were pre-incubated with PTX as previously and then the cells were stimulated with PDBu (1 μ M, 5 min) (**Figure 5.5**). PDBu activates ERK via PKC and if there is any effect of PTX on cell viability, the differences in the presence and absence of PTX would be seen.

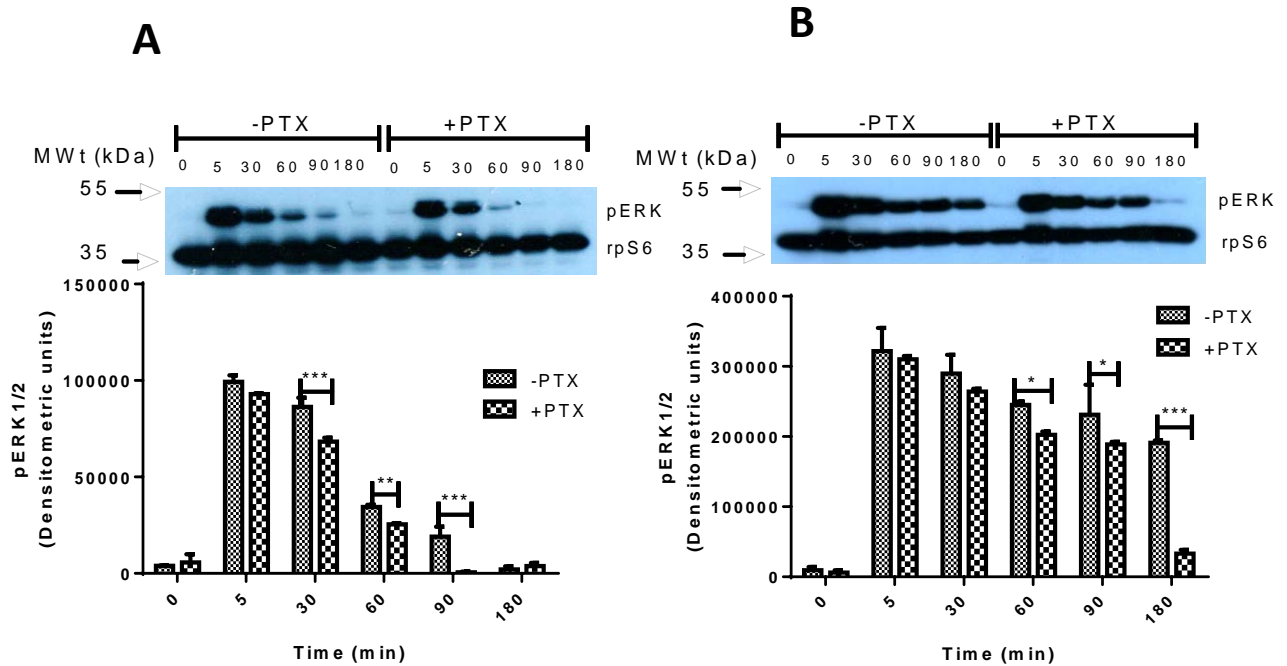


Figure 5.3 The effect of PTX on the activation of ERK by hNmU-25 and hNmS-33

HEK-NMU2 cells cultured on poly-D-lysine-coated 24-well plates for 24 h and serum-starved incubated with or without PTX (100 ng/mL) overnight. The cells were then challenged with KHB, hNmU-25 (**A**) or hNmS-33 (**B**) (30 nM, 5 min). Cells were then allowed to recover for the required times following removal the ligand. Following recovery, the levels of pERK and rpS6 were determined by Western blotting and the signal density of each quantified using Image J software. The rpS6 was used as a loading control. Data are representative blots or mean \pm s.e.m., $n=3$. Data were analysed by Bonferroni's multiple comparison test following two-way ANOVA; $*P<0.05$, $**P<0.01$, $***P<0.001$, only comparisons between \pm PTX were considered for clarity.

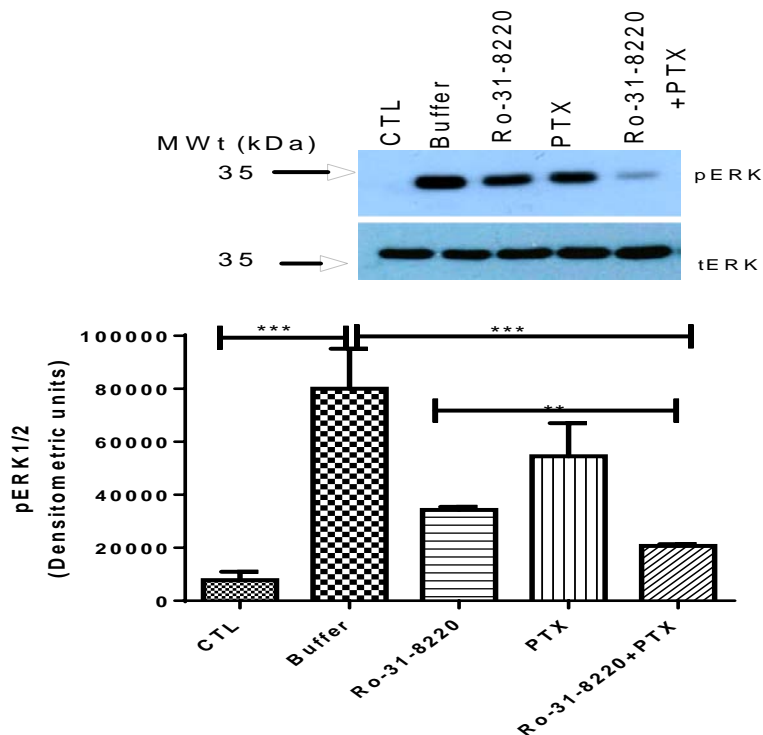


Figure 5.4 The effect of inhibition of both $G_{\alpha i}$ and PKC on ERK activation by hNmU-25

HEK-NMU2 cells cultured on 24-well plates for 24 h and then serum-starved incubated with or without PTX (100 ng/mL) overnight. On the day of the experiment, cells were then incubated with or without Ro-31-8220, 5 μ M for 30 min. Cells were then challenged with KHB or hNmU-25 (30 nM, 5 min). Cells were then allowed to recover for the 5 min following removal the ligand in the presence of Ro-31-8220. The pERK and tERK were determined by Western blotting and the signal density of each quantified using Image J software. Data are representative blots or mean \pm s.e.m., $n=3$. Data were analysed by Bonferroni's multiple comparison test following one-way ANOVA; ** $P<0.01$, *** $P<0.001$.

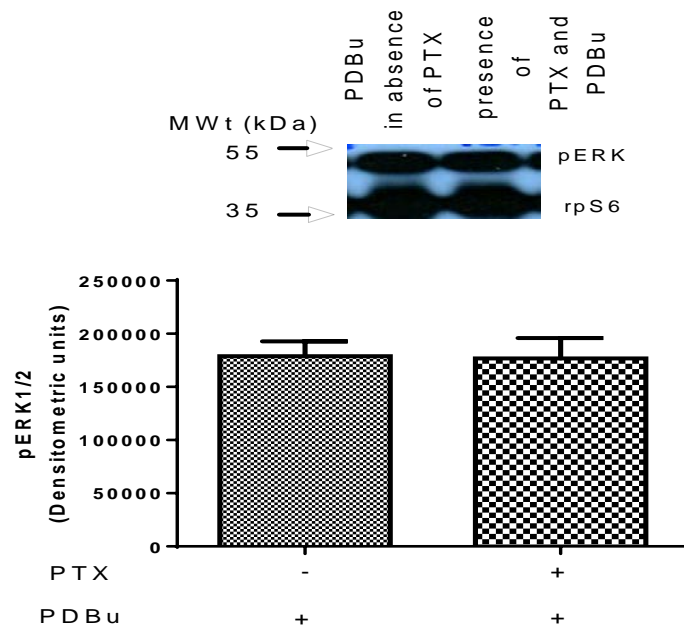


Figure 5.5 Investigation of the toxicity of PTX by assessing its impact on $G\alpha_i$ -independent activation of ERK

HEK-NMU2 cells were cultured in 24 well-plates for 24 h and then incubated without or with PTX (100 ng/mL) overnight. On the day of the experiment, cells were pre-incubated in KHB and the cells stimulated with PDBu (1 μ M, 5 min). The pERK and rpS6 were determined by Western blotting and the signal density of each quantified using Image J software. Data are representative or mean \pm s.e.m., n=3. Data were analysed by Student's unpaired *t*-test.

5.2.3 Does transactivation of RTKs play a role in NMU2-mediated ERK activation?

As transactivation of RTKs such as the EGFR could be involved in the activation of ERK by GPCRs (Kim *et al.*, 2000), EGFR was blocked by treatment with AG1478. It is a specific inhibitor of EGFR kinase (Levitzki *et al.*, 1995). It has been suggested that EGF receptors are endogenously expressed in HEK293 cells (Kramer *et al.*, 2002; Shah *et al.*, 2006). Despite that HEK293 express low endogenous levels of EGFR, these cells have epithelial morphology suggesting they are suitable for studies of EGFR, since most of tumours related to EGFR deregulation are epithelial origin (Stern *et al.*, 2007). Cells expressing NMU2 were cultured on poly-D-lysine-coated 24-well plates and EGFR inhibited with AG1478 (1 μ M) for 30 min. Cells were stimulated with either hNmU-25 (**Figure 5.6; A**), hNmS-33 (**Figure 5.6; B**) or pNmU-8 (**Figure 5.7**) (30 nM, 5 min), following which the ligand was removed and the cells allowed to recover for the required time. This inhibitor had no effect on the activation of ERK by any of the ligands.

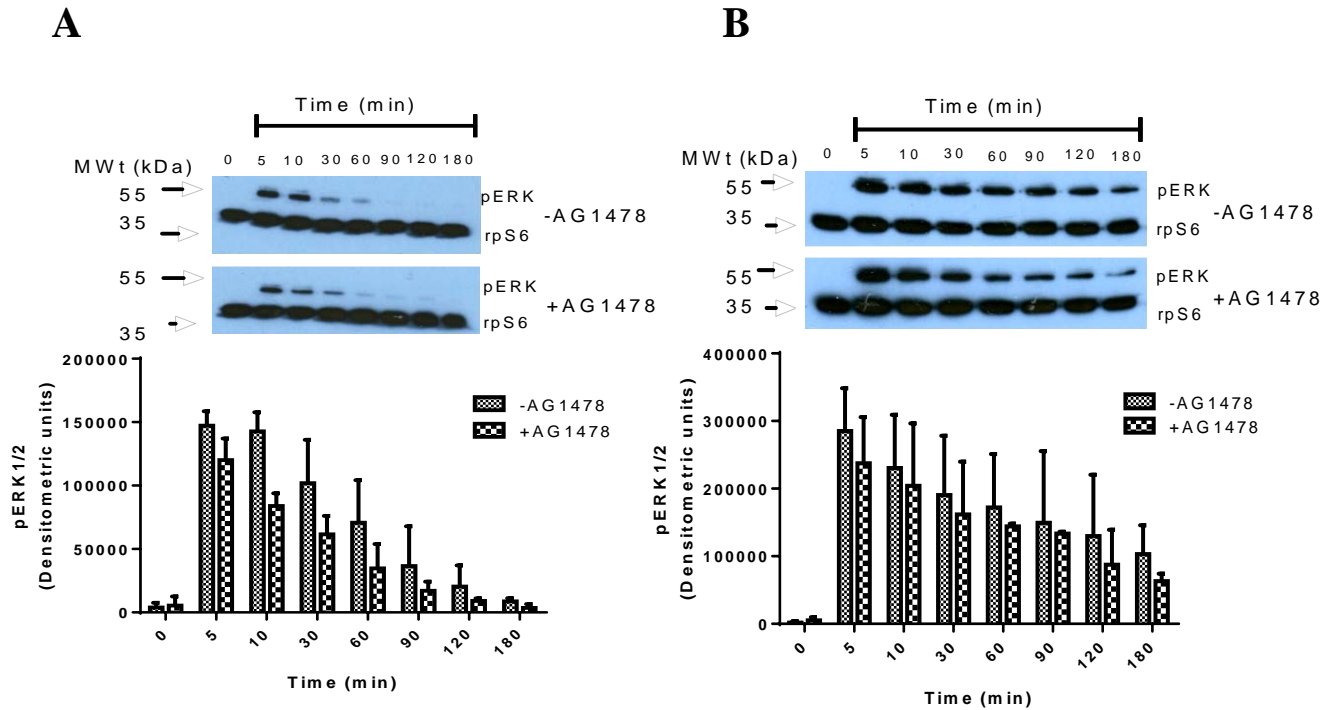


Figure 5.6 The effect of EGFR inhibition on NMU2-mediated ERK activation by either hNmU-25 or hNmS-33

HEK-NMU2 cells were cultured on 24-well plates for 24 h and then were serum-starved overnight. Cells were washed with KHB and then incubated with or without AG1478 (1 μ M) for (30 min) and challenged with KHB, hNmU-25 (**A**) or hNmS-33 (**B**) (30 nM, 5 min). The ligand was removed and the cells were allowed to recover for the required time in order to investigate the time-course of ERK activation. The pERK and rpS6 were determined by Western blotting and the signal density of each quantified using Image J software. Data are representative or means \pm s.e.m., n=3. Data were analysed by Bonferroni's multiple comparison test following two-way ANOVA. Only differences between \pm AG1478 at each time point were considered for clarity.

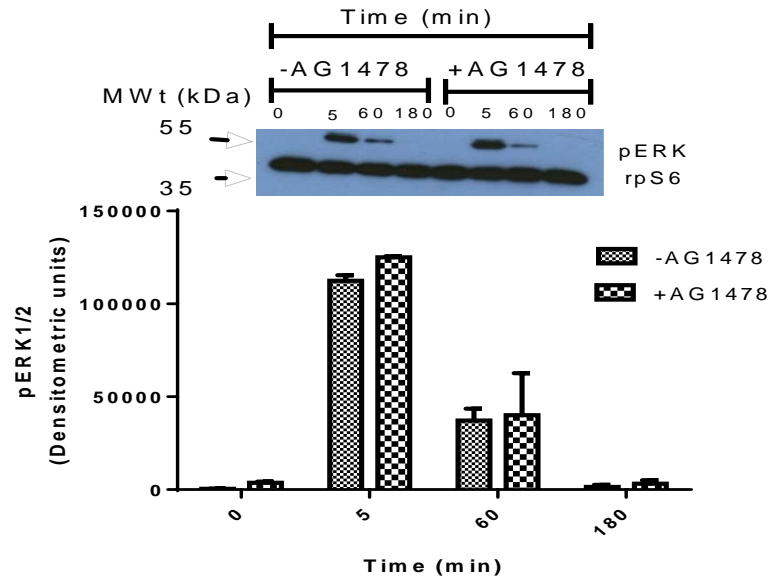


Figure 5.7 The effect of EGFR inhibition on NMU2-mediated ERK activation by pNmU-8 either in the presence and absence of the ligand

HEK-NMU2 cells were cultured on 24-well plates for 24 h and then were serum-starved overnight. Cells were washed with KHB, and then incubated with or without AG1478 (1 μ M) for 30 min and challenged with pNmU-8 (30 nM, 5 min) and the ligand was removed and the cells were allowed to recover for the required time in the presence of the inhibitor. The pERK and rpS6 were determined by Western blotting and the signal density of each quantified using Image J software. Data are representative blots or mean \pm s.e.m., n=3. Data were analysed by Bonferroni's multiple comparison test following two-way ANOVA. Only differences between \pm AG1478 at each time point were considered for clarity.

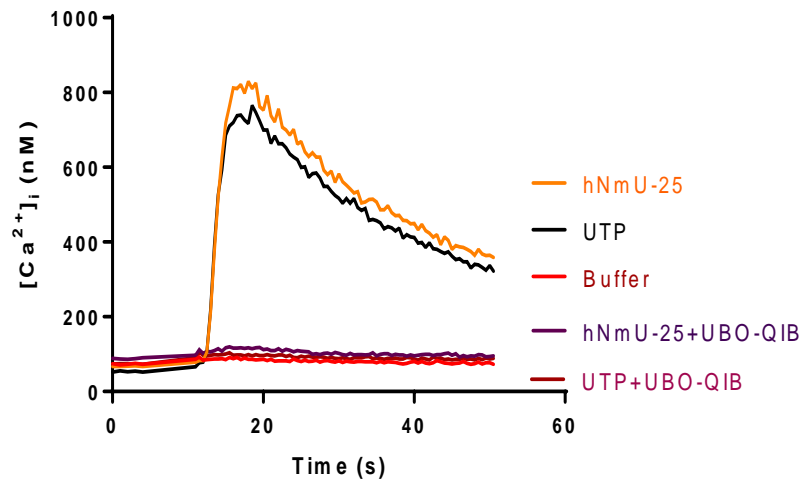
5.2.4 Activation of ERK is dependent on G_{αq} subunit

The above experiments did not reveal the pathway responsible for NMU2-mediated activation of ERK. As ERK can be activated by G_{αq} via PKC and Ca²⁺-dependent pathways, a G_{αq} inhibitor (UBO-QIB) was used kindly provided by Professor Andrew Tobin from the University of Leicester. As NMU2 activates G_{αq}, the impact of the inhibitor Ca²⁺ responses was determined. The measurement of agonist-mediated [Ca²⁺]_i was conducted using hNmU-25, hNmS-33 or UTP as an activator of G_{αq}. The cells were plated in 96 well/plates for 24 h. The cells were then loaded with fluo-4-AM in the presence and absence of the UBO-QIB (1 μM). The cells were then stimulated by hNmU-25 (30 nM), hNmS-33 (30 nM) or UTP (300 μM) (**Figure 5.8; B & C**) using a NOVOstar plate reader. HEK293 cells express at least two subtypes of P2Y receptors; including a P2Y2 receptor, which is activated by UTP. All of the agonists used caused Ca²⁺ responses. These responses were abolished by the presence of the inhibitor. The potential toxicity of the inhibitor was also evaluated. The cells were pre-incubated with KHB or the inhibitor (1 μM, 10 min). The viability of the cells were determined using two different methods either Western blotting or live/dead viability/cytotoxicity kit as described in the methods. The data indicated that this inhibitor had no effect on the viability of the cells (**Figure 5.9; A & B**), since the percentage of live cells is identical in both presence and absence of the inhibitor.

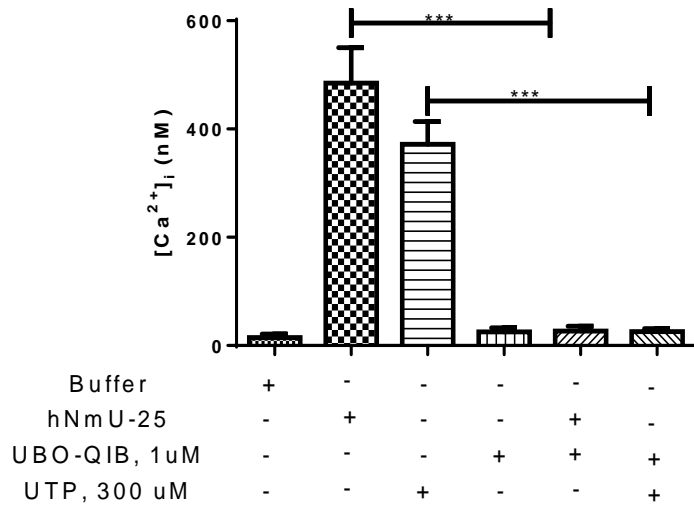
The impact of the inhibitor on pERK using Western blotting was assessed by stimulating the cells with maximum concentration of either hNmU-25 or hNmS-33 (30 nM). Following plating the cells for 24 h, the cells were then serum-starved for a further 24 h. The cells were then pre-incubated with the inhibitor (100 nM, 30 min) and the cells were then stimulated by hNmU-25 or hNmS-33 (30 nM, 5 min) in the presence and absence of the inhibitor and the ligand was removed and then allowed to recover up to 3 h. The lower concentration was effective and therefore it was used subsequently. The results revealed that this inhibitor abolished pERK activation at all-time points except at 5 min (**Figure 5.10; A & B**).

The previous results in this study have indicated that knocking down both β -arrestins-1 and -2 prolonged the activation of ERK when the cells were stimulated by either hNmU-25 or hNmS-33 (**Figures 4.8 and 4.9**). Moreover, Ca^{2+} responses were abolished by UBO-QIB, suggesting this inhibitor is specific for $\text{G}\alpha_q$. Thus, if ERK activation is dependent on $\text{G}\alpha_q$, the prolonged activation of pERK as a result of knocking down of β -arrestin-1 and -2 would be reduced. In order to confirm that ERK activation is most likely via $\text{G}\alpha_q$, a further experiment was performed using cells in which β -arrestins-1 and -2 had been knocked-down. Thus, the cells either were un-transfected or transfected with siRNA against both β -arrestins-1 and -2. The cells were then pre-incubated with the inhibitor (100 nM, 30 min) and then stimulated by hNmU-25 (**Figure 5.11; A**) or hNmS-33 (**Figure 5.11; B**) (30 nM, 5 min). The agonist-mediated increase in the levels of pERK was completely inhibited in the presence of the inhibitor except at 5 min. Combination of both $\text{G}\alpha_q$ and PKC inhibitors (100 nM and 5 μM , respectively) were used in order to investigate the activity of ERK at 5 min. The cells were pre-incubated with KHB or a combination of both inhibitors for 30 min and were then stimulated by either hNmU-25 or hNmS-33 (30 nM, 5 min). The levels of pERK were significantly reduced by UBO-QIB at this point by the combination of inhibitors (**Figure 5.12; A & B**). The inhibitor alone can be seen in (**Figure 5.10; A & B**).

A



B



C

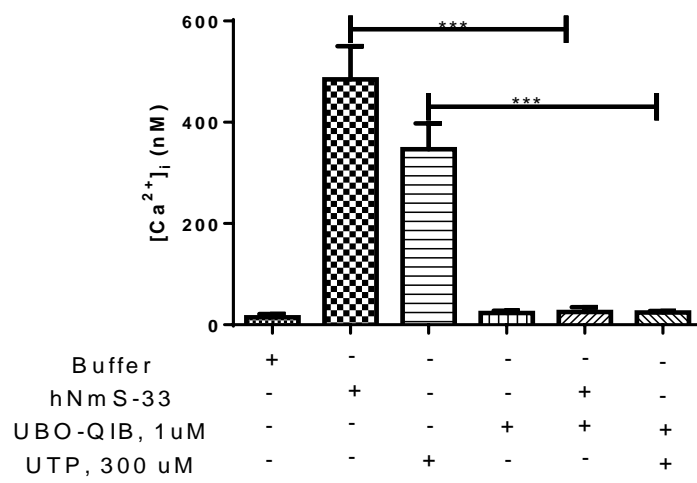


Figure 5.8 The effect of Gαq inhibition on Ca²⁺ signalling

HEK-NMU2 cells were cultured in 96 well/plates for 24 h. The cells were then loaded with fluo-4-AM in the presence or absence of the UBO-QIB (1 μM). Following loading, the cells were stimulated with either hNmU-25 (30 nM) (**B**) or hNmS-33 (**C**) (30 nM) or UTP (300 μM) in the continued absence or presence of the inhibitor. (**A**) Representative traces for three experiments. The higher traces indicate the response to ligand in the absence of the inhibitor, whereas the lower traces refer to Ca²⁺ responses in the presence of the inhibitor. Changes in cytosolic fluorescence were then monitored as an index of [Ca²⁺]_i using a NOVOstar plate reader. Data were analysed by Bonferroni's multiple comparison test following one-way ANOVA; ****P*<0.001. Data are means ± s.e.m., n=3. Significant differences between stimulated cells in the presence and absence of inhibitor were considered.

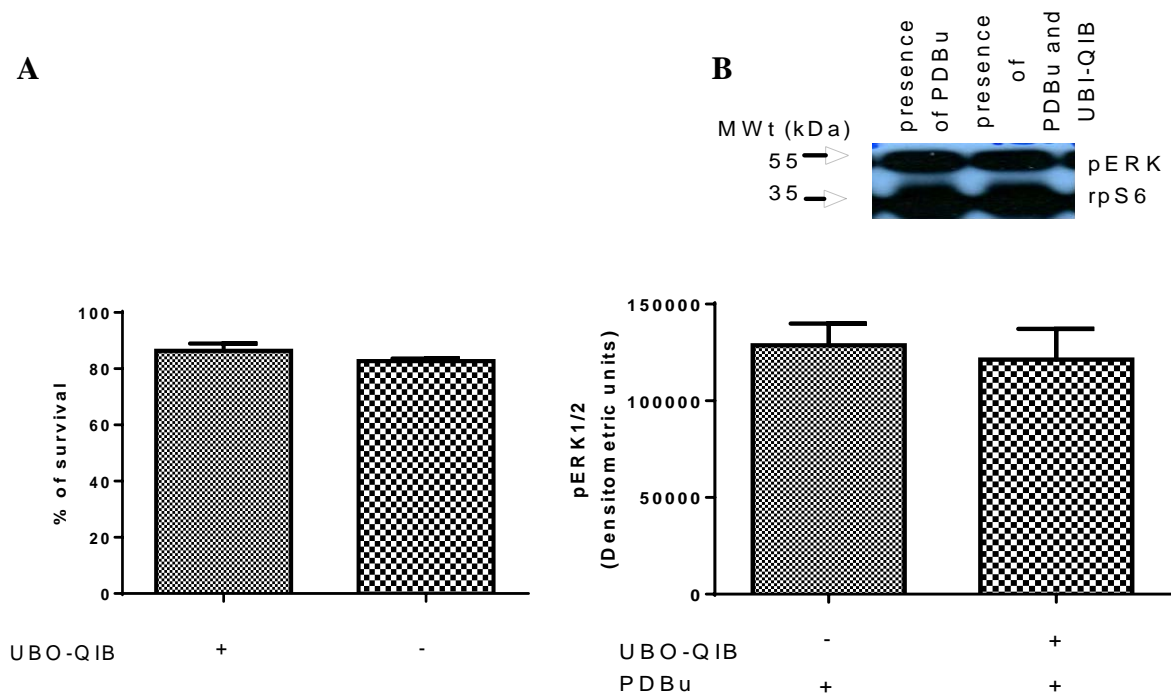


Figure 5.9 Evaluation of the potential toxicity of UBO-QIB

HEK-NMU2 cells were cultured in 24 well plates for 24 h for the live/dead viability experiment or serum-starved for a further 24 h for Western blotting. On the day of the experiment, the medium was removed and the cell were incubated with UBO-QIB for 30 min and then reagents were added as explained in the Methods and incubated at room temperature for 10 min for the kit experiment (A). For the Western blotting experiment, the cells were then stimulated by PDBu (1 μ M, 5 min) in the presence and absence of UBO-QIB. The levels of pERK and rpS6 were determined by Western blotting and the signal density of each quantified using Image J software. Data are representative or mean \pm s.e.m., n=3. Data were analysed by Student's unpaired *t*-test.

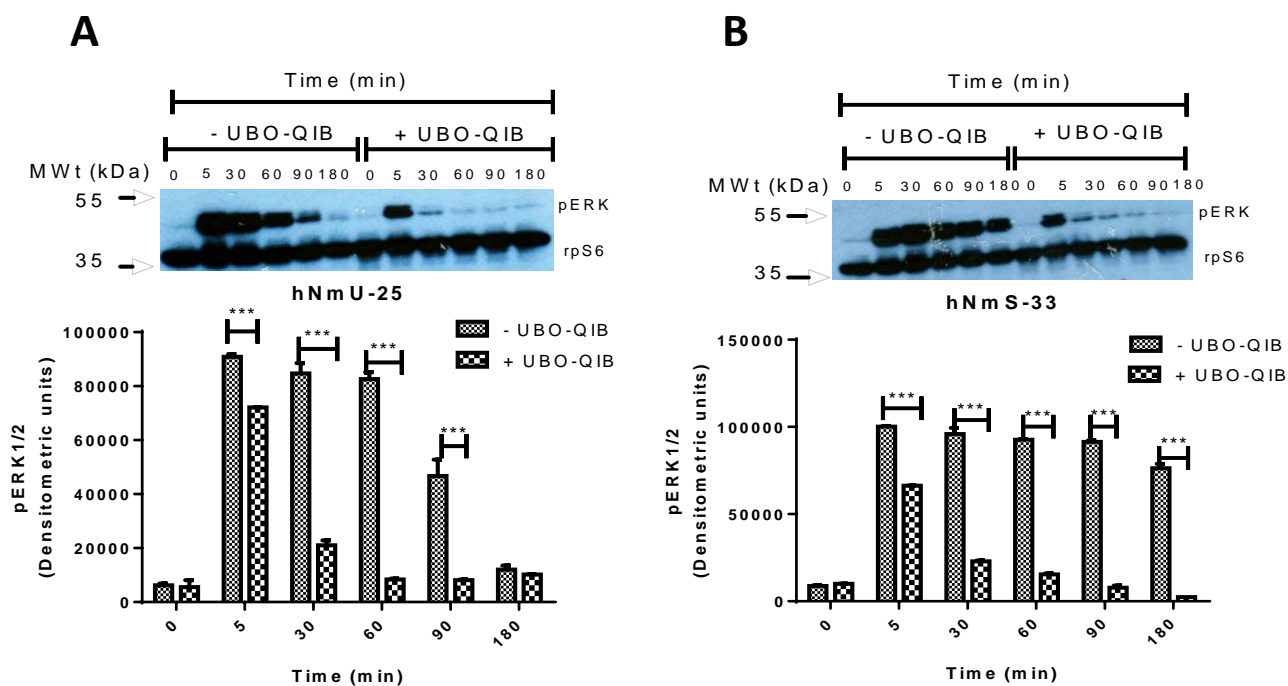


Figure 5.10 The effect of UBO-QIB on ERK activation

HEK-NMU2 cells were cultured for 24 h. The cells were then serum-starved for a further 24 h. On the day of the experiment, the cells were incubated for 30 min in KHB without or with the inhibitor (100 nM). The cells were then stimulated with either hNmU25 (**A**) or hNmS-33 (**B**) (30 nM, 5 min). The ligand was removed and the cells were allowed to recover for the required time. Data are representative or mean \pm s.e.m., $n=3$. The pERK and rpS6 were determined by Western blotting and the signal density of each quantified using Image J software. Data were analysed by Bonferroni's multiple comparison test following two-way ANOVA; $***P<0.001$. Only comparisons between \pm UBO-QIB were considered for clarity.

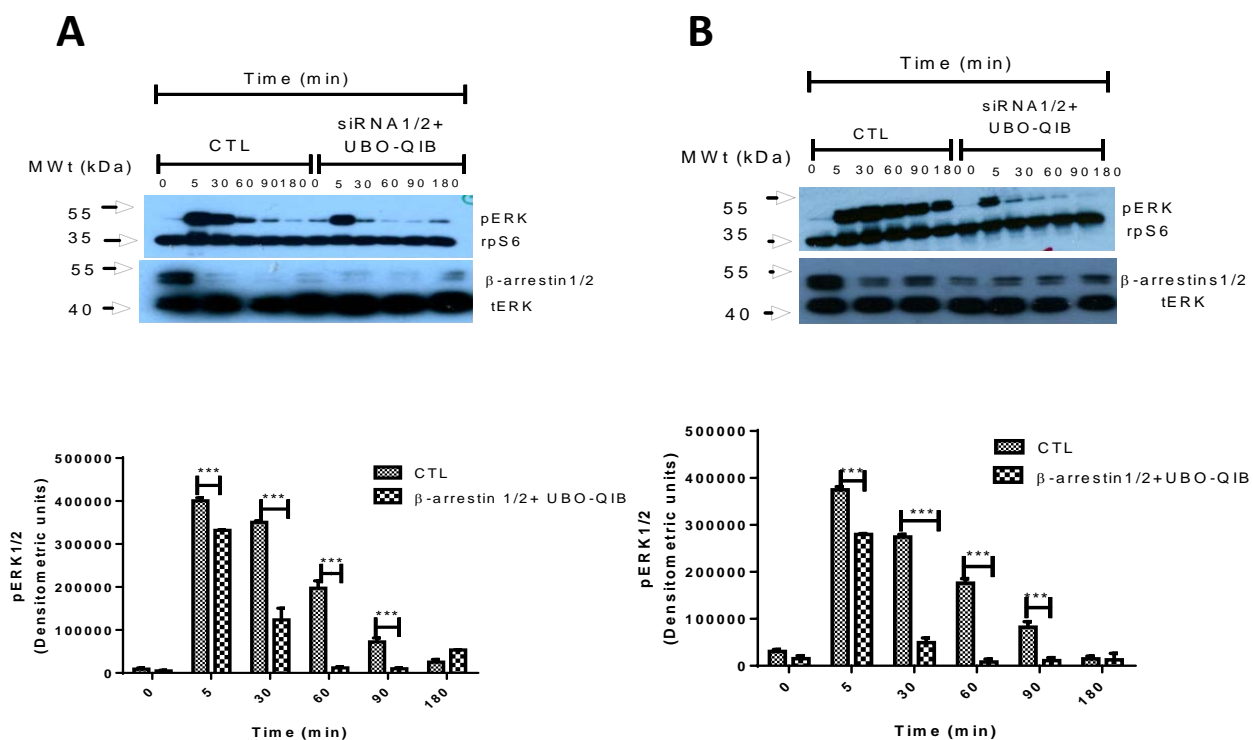


Figure 5.11 The effect of UBO-QIB and knock down of β -arrestins -1 and -2 on NMU2-mediated ERK activation

HEK-NMU2 cells were cultured for 24 h. The cells were then transfected with siRNA against β -arrestins -1 and -2 and incubated for 24 h. The cells were then serum-starved for a further 24 h. On the day of the experiment, the cells were incubated for 30 min with or without the inhibitor (transfected cells only). The cells were then stimulated with either hNmU25 (**A**) or hNmS-33 (**B**) (30 nM, 5 min) and the ligand was removed and the cells allowed recovering for the required time. The pERK, rpS6 and β -arrestin1/2, tERK were determined by Western blotting and the signal density of each quantified using Image J software. Data are representative or mean \pm s.e.m., n=3. Data were analysed by Bonferroni's multiple comparison test following two-way ANOVA; *** P <0.001. Only differences between \pm arrestin-1 and -2 + UBO-QIB were considered for clarity.

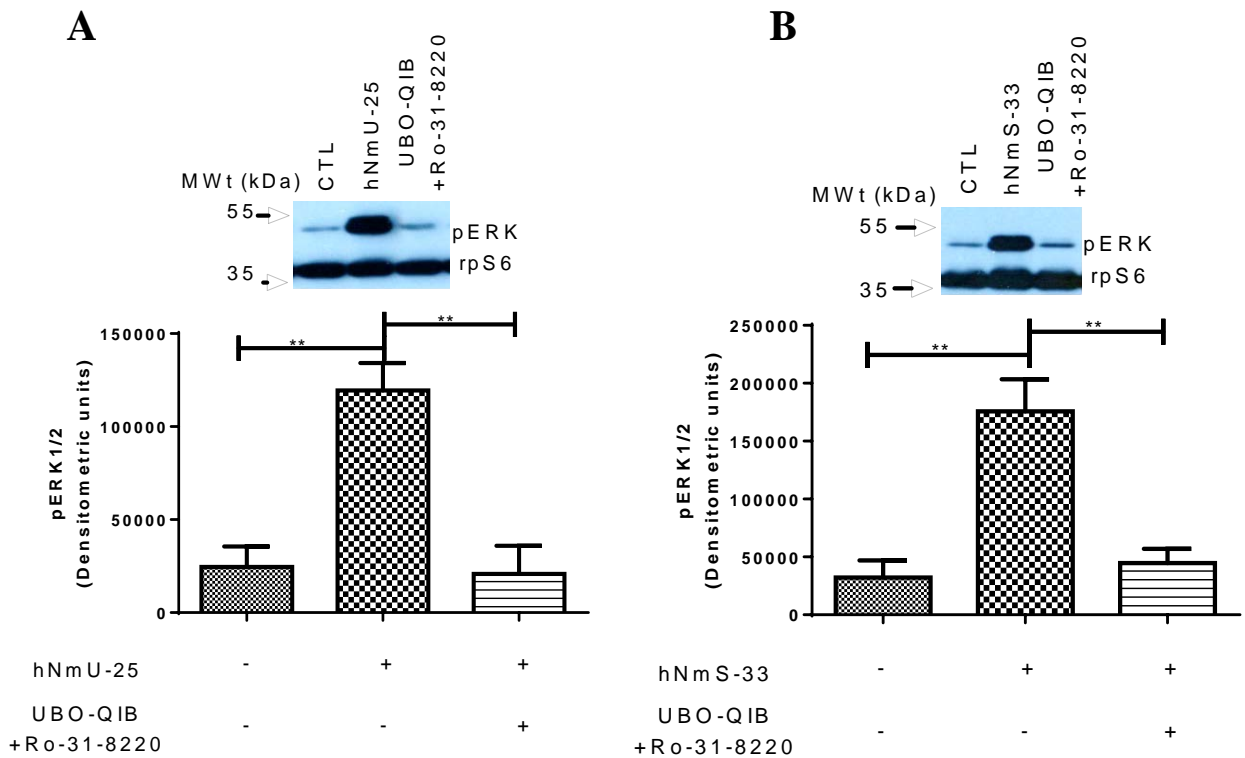


Figure 5.12 The effect of UBO-QIB and Ro-31-8220 on ERK activation at 5 min

HEK-NMU2 cells were cultured for 24 h. The cells were then serum-starved for a further 24 h. On the day of the experiment, the cells were incubated for 30 min with or without both UBO-QIB (100 nM) and Ro-31-8220 (5 μ M). The cells were then stimulated with either hNmU25 (**A**) (30 nM, 5 min) or hNmS-33 (**B**) (30 nM, 5 min). The ligand was then removed and the cells were allowed to recover for the required time. The pERK and rpS6 were determined by Western blotting and the signal density of each quantified using Image J software. Data are representative or mean \pm s.e.m., n=3, ** P <0.01; by Bonferroni's multiple comparison test following one-way ANOVA.

5.2.5 Sub-cellular localization of pERK following agonist activation of NMU2 using different ligands

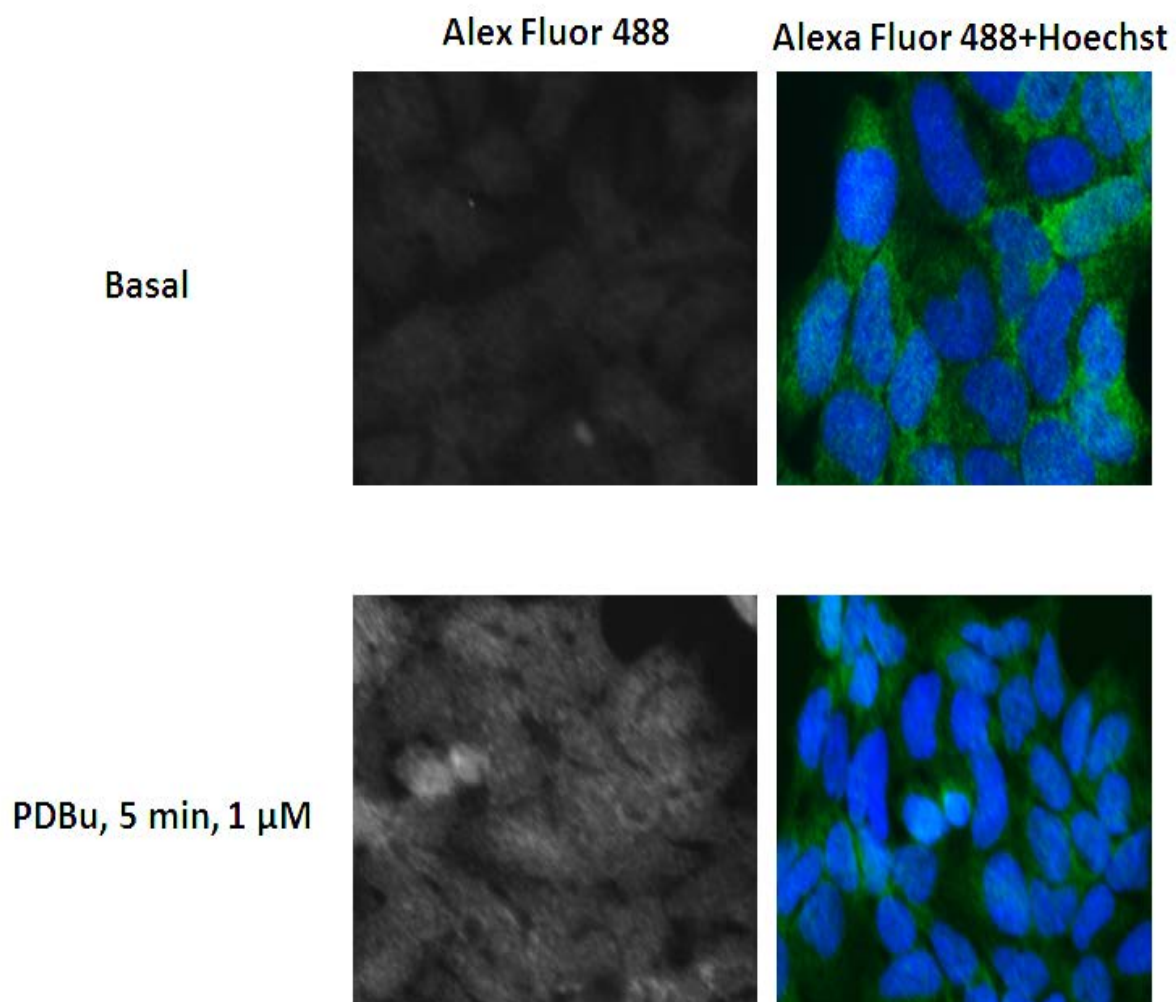
Both G-protein and β -arrestin mediated signalling pathways can lead to ERK activation. However, the subcellular distributions of activated ERK1/2 are different. For instance, the pERK mediated by the G-protein signalling pathway translocate to the nucleus, while the pERK mediated by the β -arrestin signalling pathway remain in cytoplasm (Eishingdrelo *et al.*, 2013b).

The purpose of these experiments was to investigate the distribution of ERK in response to stimulation of cells using either hNmU-25, hNmS-33 or pNmU-8.

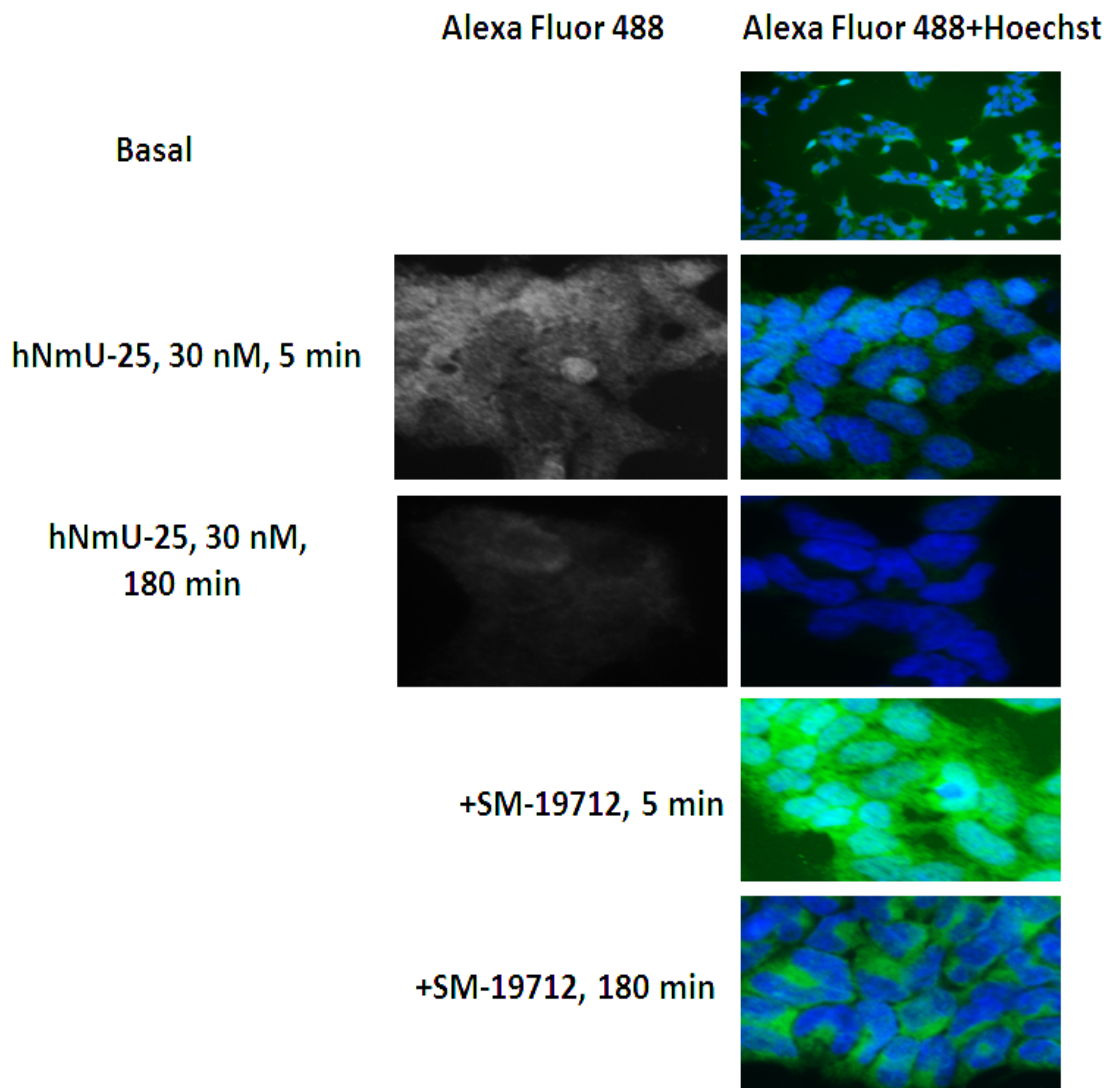
Images under basal conditions (no stimulation), indicate that pERK was absent in the cytoplasm (**Figure 5.13; A**). In cells stimulated with the activator of PKC, (PDBu, 1 μ M, 5 min), there was an increased level of pERK as indicated by the increased intensity of fluorescence that was equally distributed between the cytoplasm and nucleus. Moreover, in cells stimulated with hNmU-25, hNmS-33 or pNmU-8 (30 nM, 5 min) and allowed to recover for either 5 or 180 min), levels of pERK were again elevated in both the cytoplasm and nucleus. The background-corrected mean fluorescent intensity of the whole cell, the cytoplasm or the nucleus and the ratio of background-corrected mean fluorescent intensity of cytoplasm to nucleus were generated. Following 5 min stimulation with 30 nM of each ligand, extracellular ligand was removed and the cells were washed with KHB. At 180 min after removal of either ligand, the level of pERK and the sub-cellular distribution returned to those seen under basal conditions when the cells were stimulated with either hNmU-25 or pNmU-8 in the absence of ECE-1 inhibitor (**Figure 5.13; B & D, respectively**). However, under the same conditions but in the presence of ECE-1 inhibitor, the level of pERK was elevated at 5 min and returned to basal level at 180 min following 5 min stimulation with 30 nM of hNmU-25 and pNmU-8. In contrast, pERK was still elevated at 180 min following ligand removal when the cells were challenged with hNmS-33 in the absence of ECE-1 inhibitor and equally elevated in the presence of ECE-1 inhibitor at either 5 or 180 min

after removing the ligand (**Figure 5.13; C**). In addition, cytosolic values were used in order to construct time course. The cells were stimulated with maximum concentrations (30 nM; 5 min) of hNmU-25, hNmS-33 or pNmU-8 and then allowed to recover following ligand removal for the required time up to 3 h. The data demonstrate that the peak of pERK was at 5 min and returned to basal level following stimulation with hNmU-25 and pNmU-8. This is in contrast to hNmS-33, following which pERK was sustained up to 3 h (**Figure 5.13; E & F & G**). To study the effect of different concentrations of ligands on the subcellular distribution of pERK, cells were stimulated with either hNmU-25, hNmS-33 or pNmU-8 (0.1-100 nM, 5 min). The results indicated that the cytosolic localisation of pERK occurs in a concentration-dependent manner (**Figures; 5.14, 5.15, 5.16**).

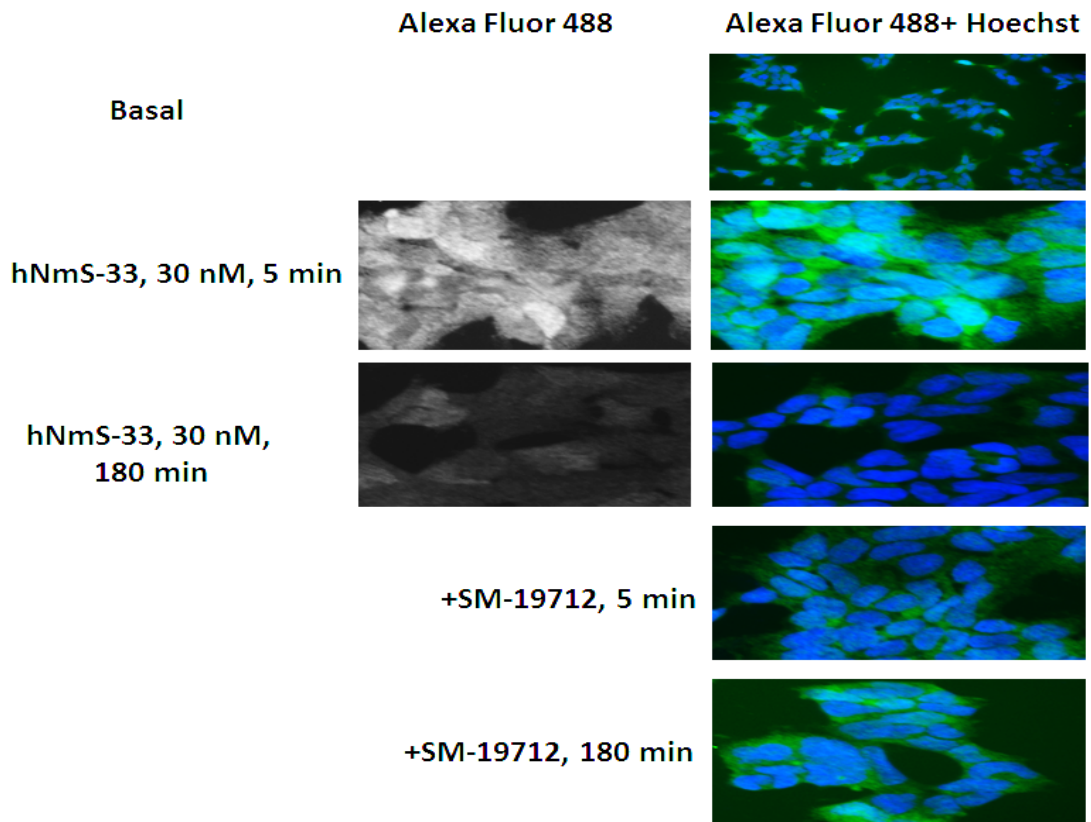
A



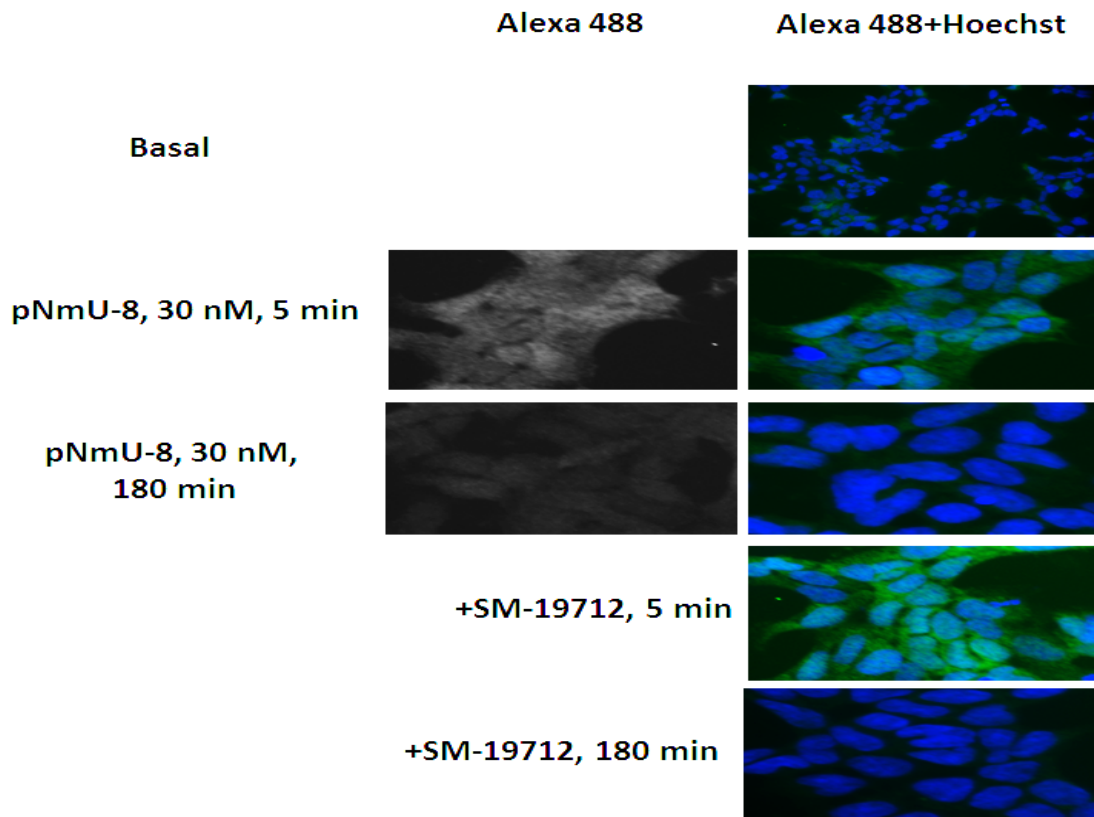
B



C



D



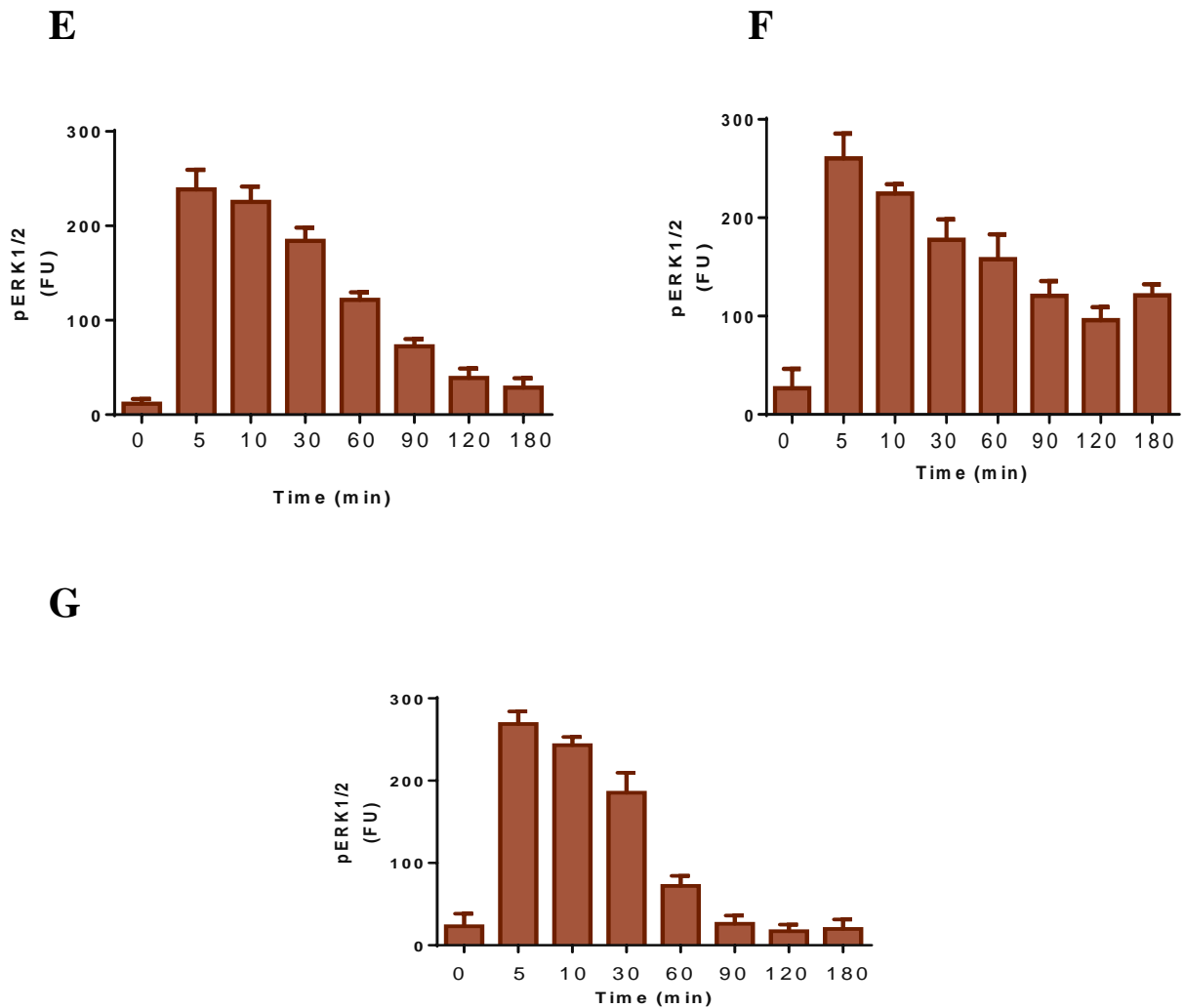


Figure 5.13 Activation and sub-cellular localisation of pERK following activation of NMU2 with hNmU-25, hNmS-33 or pNmU-8

HEK-NMU2 cells were grown in 96-well black-walled, clear bottom plates (50-80% confluence) for 24 h. Cells were then serum-starved for a further 24 h. Cells were washed and stimulated with buffer (basal), or PDBu (1 μ M, 5 min) (A) as a control, hNmU-25 (B), hNmS-33 (C), or pNmU-8 (D), (all 30 nM, 5 min). Following stimulation, the cells were allowed to recover as required (5 and 180 min). Cells were fixed and permeabilized for immunostaining with a pERK1/2 antibody and nuclear staining with Hoechst as described in Methods. Generally, 16 positions in each well (equal to at least 1,000 cells) were imaged. However, only one representative image showing staining of pERK (Alexa fluor 488) alone or merged with nuclear staining

(Alexa fluor 488 + Hoechst) and its distribution under each condition is presented here to directly compare with the quantification alongside the image. The time courses of changes in pERK for each ligand, hNmU-25 (**E**), hNmS-33 (**F**) and pNmU-8 (**G**), are shown, in which cells were stimulated (30 nM, 5 min) followed by ligand removal and recovery for the required time.

	Whole cell (FU)	Cytoplasm (FU)	Nucleus (FU)	Cytosolic/nuclear
Basal	52 \pm 3	158 \pm 6	181 \pm 4	1.35 \pm 0.05
PDBu	193 \pm 4	181 \pm 3	203 \pm 4	1.04 \pm 0.02
hNmU-25	92 \pm 5	156 \pm 3	191 \pm 8	1.30 \pm 0.03
hNmS-33	100 \pm 3	165 \pm 4	200 \pm 2	1.40 \pm 0.02
pNmU-8	95 \pm 5	160 \pm 4	190 \pm 3	1.30 \pm 0.04

Table 5.1 Analysis of images from immunostaining. The above values represent the mean fluorescent intensity of the whole cell, the cytoplasm, the nucleus and the ratio of (cytoplasmic fluorescence/nuclear fluorescence). They were generated from the cells in the three representative images (**Figure 5.13**) as described in Methods, in which cells were stimulated for 5 min by each ligand. FU = fluorescence units. Data are mean \pm s.e.m, n=3.

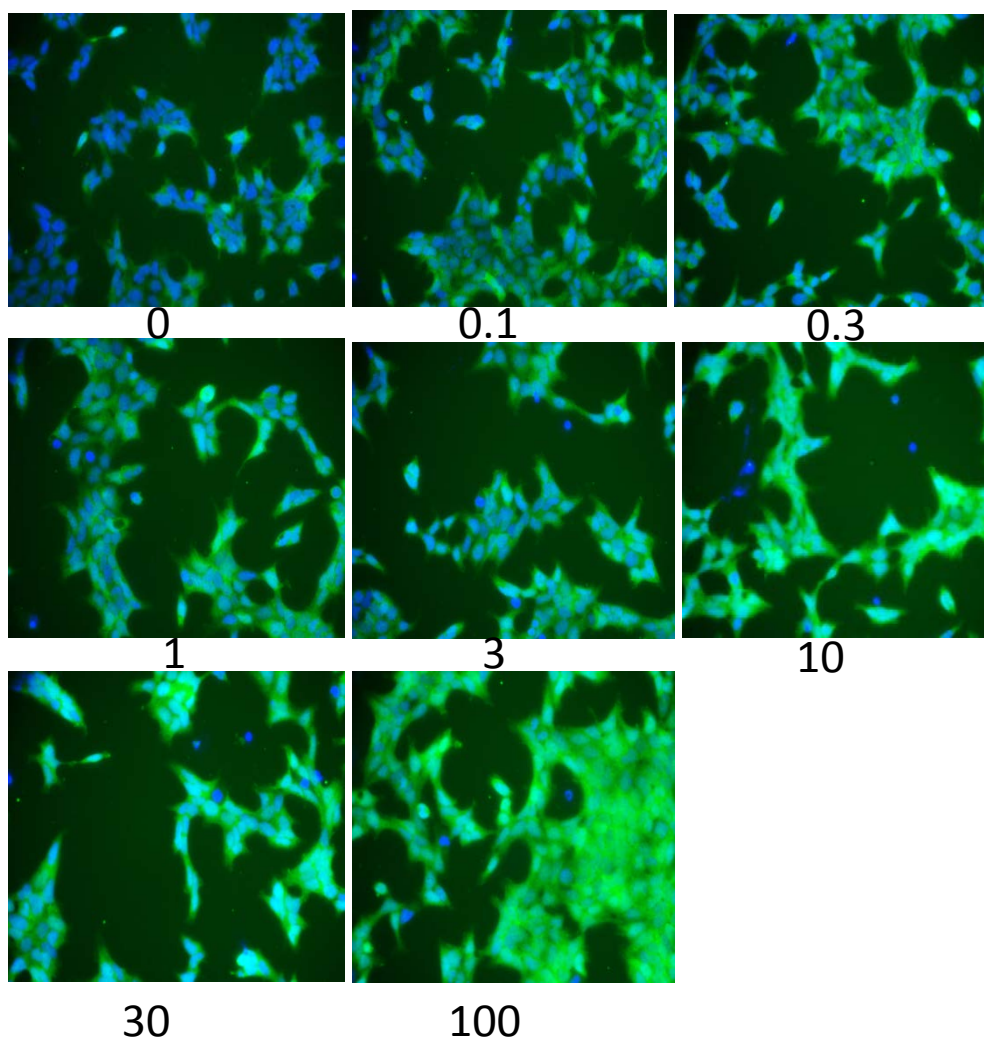


Figure 5.14 Concentration-dependent increases in pERK immunofluorescence following hNmU-25 challenge of NMU2

HEK-NMU2 cells were grown in 96-well black-walled, clear bottom plate (50-80% confluence) for 24 h. Cells were then serum-starved for 24 h before stimulation with hNmU-25 (0.1-100 nM, 5 min). The cells were then prepared for immunostaining of pERK and nuclear staining using Hoechst before imaging as described in Methods. The numbers under images show the concentration used. These images are representative of $n=3$.

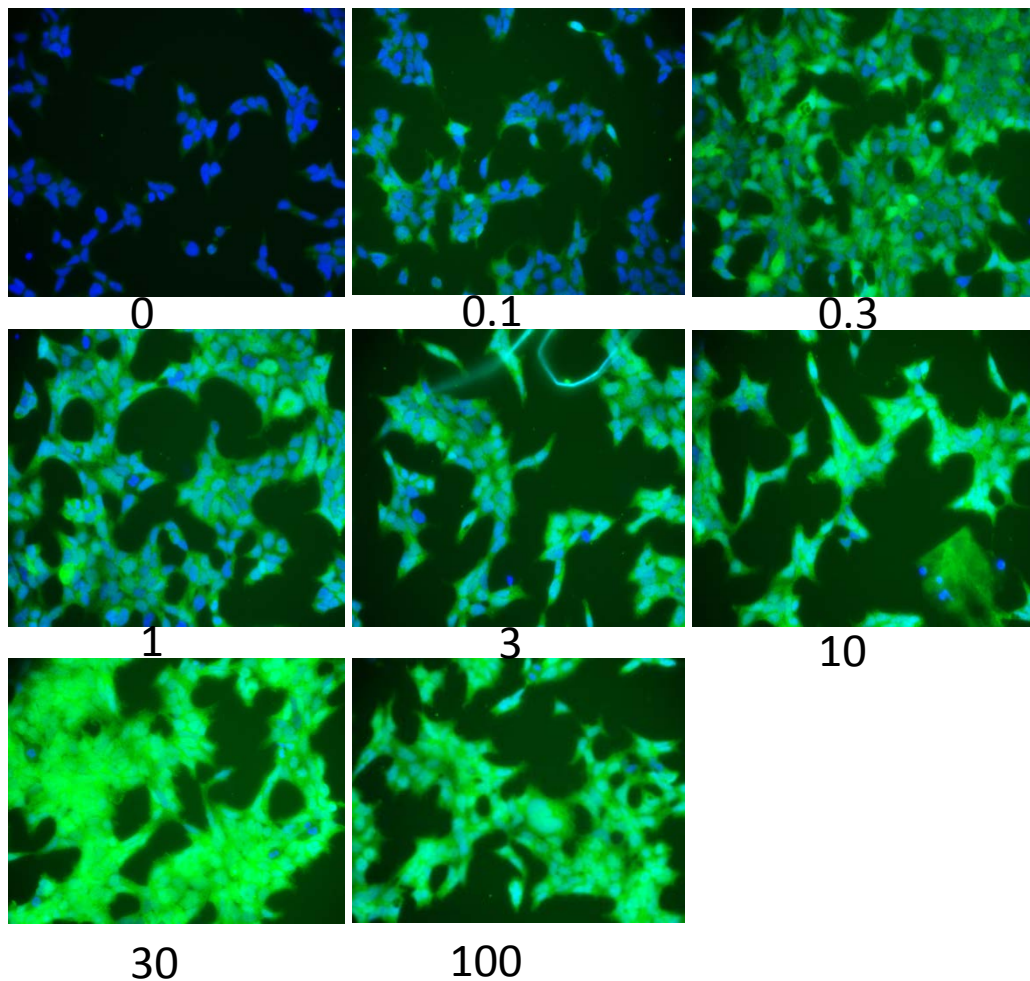


Figure 5.15 Concentration-dependent increases in pERK immunofluorescence following hNmS-33 challenge of NMU2

HEK-NMU2 cells were grown in 96-well black-walled, clear bottom plate (50-80% confluence) for 24 h. Cells were then serum-starved for 24 h before stimulation with hNmS-33 (0.1-100 nM, 5 min). The cells were then prepared for immunostaining of pERK and nuclear staining using Hoechst before imaging as described in Methods. The numbers under images show the concentration used. These images are representative of n=3.

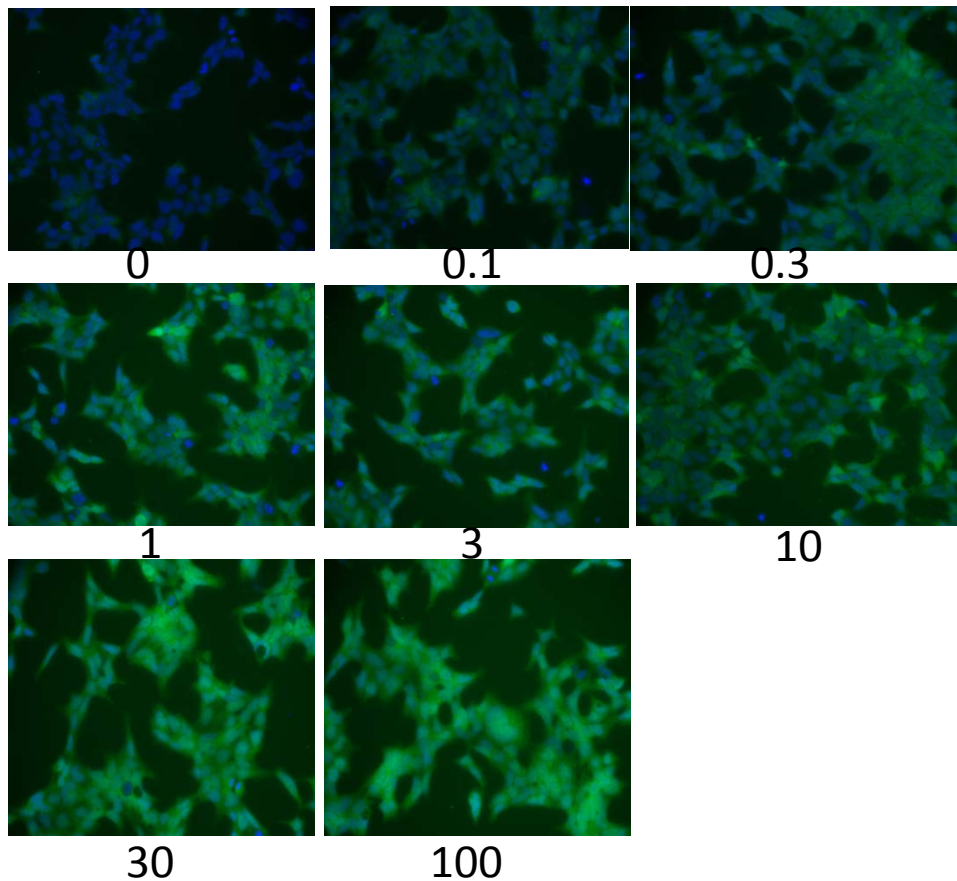


Figure 5.16 Concentration-dependent increases in pERK immunofluorescence following pNmU-8 challenge of NMU2

HEK-NMU2 cells were grown in 96-well black-walled, clear bottom plate (50-80% confluence) for 24 h. Cells were then serum-starved for 24 h before stimulation with pNmU-8 (0.1-100 nM, 5 min). The cells were then prepared for immunostaining of PERK and nuclear staining using Hoechst before imaging as described in Methods. The numbers under images show the concentration used. These images are representative of $n=3$.

5.3 Discussion

The aims of the current experiments were to investigate the pathways involved in regulating ERK activity and particularly to assess any ligand-dependent differences. The ERK pathway can be activated by different ligands including cytokines, growth factors, and GPCR ligands (Wei *et al.*, 2003a; Leroy *et al.*, 2007). It has been widely reported that ERK can be activated by both G-protein and β -arrestin mediated signalling pathways (eg. (Ahn *et al.*, 2004; Goldsmith *et al.*, 2007)). The activation of ERK cascades through G α subunits including G α_s , G α_i , and G α_q and G-protein $\beta\gamma$ subunits signalling to Ras has been extensively studied (van Biesen *et al.*, 1996a; Saini *et al.*, 2007). PKC is an important component in G-protein dependent signalling pathways leading to the activation of ERK. Pre-treatment of cells with PKC inhibitor GF109203X can abolish G-protein-dependent activation of ERK1/2 (Mochizuki *et al.*, 1999; Gesty-Palmer *et al.*, 2006). 85% sequence identity exists between ERK1 and ERK2. A wide variety of cellular processes including proliferation, differentiation, migration, survival, growth, growth arrest and apoptosis are regulated by ERK. ERK1 and 2 are activated via dual phosphorylation on Tyr 204 and Thr 202 residues by MEK, and these residues can be detected by specific antibodies for pERK1/2 (Eishingdrelo *et al.*, 2013).

ERK can also be activated by G α_q -coupled receptors in a PKC-dependent and Ras-independent manner, in a PKC and Ras-dependent manner, or in a PKC-independent but Ras-dependent manner (Gudermann *et al.*, 2000). This depends on the cell type and the receptor expression levels. On the other hand, the mechanism of activating ERK by PKC is still unclear. The reason for that is because the direct phosphorylation of Raf might not be sufficient to activate MEK and ERK (Macdonald *et al.*, 1993). However, the full activation of Raf by Ras may be facilitated by PKC through the stimulation of additional molecules involved in the Ras-Raf interaction. Moreover, G α_i and G α_s can also mediate and regulate the ERK pathway through either activation or inactivation of the GTP-binding protein Rap (Gudermann *et al.*, 2000).

Much of the evidence involving PKC in cell growth, differentiation and homeostasis has been based on the use of either tumour-promoting phorbol esters such as PDBu, which

are thought to activate PKC by mimicking DAG, and on the use of two small cell permeable inhibitors of PKC namely Ro-31-8220 (Davis *et al.*, 1989) and GF 109203X (Toullec *et al.*, 1991). Ro-31-8220 and GF109203X, are two structurally related staurosporine analogs (a natural product originally isolated from the bacterium *Streptomyces staurosporeus*) acting as ATP-competitive inhibitors of PKC. These compounds have been used extensively for studying the role of PKC in cell signalling (Nixon *et al.*, 1992). Staurosporine inhibits protein kinases through the prevention of ATP binding to the kinase. This is achieved through the stronger affinity of staurosporine to the ATP-binding site on the kinase.

So, the possibility of activating ERK by PKC was assessed using the PKC inhibitor, Ro-31-8220 (5 μ M). Because PDBu is an activator of PKC we first tested the activity of PKC inhibitor by determining its ability to inhibit PDBu-mediated activation of ERK. The data show that PDBu activated ERK (as judged from the increased level of pERK after 5 min stimulation) but in the presence of Ro-31-8220, ERK activation was completely abolished. Moreover, our results indicate that pERK is activated by PKC at early time points (cells stimulated by hNmU-25 and hNmS-33) in contrast to later time points (cells stimulated by hNmU-25) where the pERK was enhanced by adding PKC inhibitor. When cells were stimulated by hNmS-33 (30 nM, 5min), the inhibitor reduced the pERK levels at earlier time points, (5, 60 and 90 min). These results are consistent with a previous study where lipopolysaccharide (LPS) activated ERK via PKC (Chen *et al.*, 2001; Puente *et al.*, 2006). The activation of PLC β is triggered by the activation of G α_q leading to increases in [Ca²⁺]_i and PKC. PKC activation results in ERK activation (Kolch *et al.*, 1993). On the other hand, ERK activated by G α_q , under some conditions, is unaffected by inhibition of PKC (Crespo *et al.*, 1994a; Daub *et al.*, 1997).

It has been previously shown that NMU2 can be coupled to G proteins of the G $\alpha_{i/o}$ family, although their coupling to other members of the heterotrimeric G family, such a G $\alpha_q/11$ also has been described previously. The contribution of different G proteins to the stimulation of the ERK/MAPK cascade was investigated. Cells were treated with 100 ng/ml PTX; this toxin produced a partial inhibition of ERK activation after hNmU-25 or hNmS-33 addition at early times points. There was a complete inhibition at later time points when the cells were stimulated by hNmS-33 in the HEK-NMU2, indicating

that the activation of $G\alpha_i$ proteins is required for the stimulation of this pathway when the cells stimulated and the ligand was removed, suggesting that ERK could be partially activated via $G\alpha_i$ at least at later time points.

It has been observed that $G\alpha_i$ receptors activate ERK through $\beta\gamma$ -subunits in a PKC-independent but Ras-dependent manner providing the first demonstration of a role for $G\beta\gamma$ in linking G proteins to the Ras pathways (Crespo *et al.*, 1994b). $G\alpha_i$ -dependent activation of ERK involves two inhibitory pathways. The first inhibitory effect is by inhibiting AC. The second possibility is by inhibiting Rap-1 via Rap-1-GAP protein (Goldsmith *et al.*, 2007). However, the well-known signal transduction of $G\alpha_i$ is by coupling receptor to the inhibition of AC (Johnson *et al.*, 1989). This decrease in cAMP levels decreases PKA activity thereby removing the inhibitory effect of PKA on C-Raf and this in turn enhances Ras-C-Raf signalling to ERK (Radhika *et al.*, 2001). Also, it has been shown that ERK1/2 can be activated by $G\alpha_i$ involving the $\beta\gamma$ subunit including M_2 -muscarinic, D_2 dopamine and A_1 adenosine receptors (Crespo *et al.*, 1994a; Koch *et al.*, 1994). For instance, it has been established in transfected HEK293 cells that ERK1/2 could be activated by $G\alpha_i$ -coupled α_2A -adrenergic receptor in which dissociated $\beta\gamma$ stimulates PLC β resulting in IP $_3$ -mediated increase in $[Ca^{2+}]_i$ and Ca^{2+} -calmodulin-mediated activation of protein kinase tyrosine (Pyk2) kinase. This activates Src which in turn stimulates Shc adaptor protein resulting in the activation of Ras via the Ras-GEF and mSOS (Lev *et al.*, 1995; Dikic *et al.*, 1996; DellaRocca *et al.*, 1997).

The demonstration that receptors couple to multiple G-proteins suggest that multiple coupling with differential signalling is possible and this is based on two G-protein interacting with one receptor, and because the ERK was partially inhibited in the presence of PKC and $G\alpha_i$ inhibitors, the impact of both inhibitors combination was assessed (Germack *et al.*, 2004). The results revealed that ERK activation was inhibited by combining both inhibitors, suggesting that ERK activation could be mediated by two different pathways (PKC and $G\alpha_i$) without excluding the toxicity of such combination. Further studies are needed to explore this issue.

It has been reported that ligand-independent activation (transactivation) of the EGFR is a general phenomenon evoked by various $G\alpha_{q/11}$ -or $G\alpha_i$ -coupled receptor in different

cellular settings (Daub *et al.*, 1996) and that this transactivation can couple GPCR to ERK activation (Leserer *et al.*, 2000). Thus, inhibition of EGFR tyrosine kinase activity can block ERK activation via GPCRs under some circumstances, suggesting that the EGFR is an integral element of the signalling pathway (Daub *et al.*, 1996). To explore any role of transactivation in NMU2-mediated ERK activation, the inhibitor AG1478 was used in the current study (Levitzki *et al.*, 1995; D'Anneo *et al.*, 2013). It has been indicated that EGFRs are expressed in HEK cells. Thus, EGF, as a control was not used in this study and it is strongly advised to do so (See 5.2.3). Following a short (5 min) stimulation of NMU2 with either NmU, NmS or pNmU, AG1478 had no effect on the activation of ERK highlighting that transactivation is not likely to be involved in NMU2-mediated ERK activation. It has been proposed that, as the EGFR releases, it forms the inactive alternate dimer and by addition of AG1478, it accelerates EGFR untethering. On the other hand, it locks the receptor in the alternate dimer, thus reducing signalling. Also, dissociation of AG1478 allows the EGFR to adopt the back-to-back dimer (two receptors are linked by the dimerization loops so that linked ligands are positioned at opposite sites on the dimer) and participate in signalling (Gan *et al.*, 2007). Our results are in counter with a previous study using rat aortic smooth muscle cells (ASMCs) where inhibition of EGFR activity led to attenuation of UTP-stimulated ERK phosphorylation suggesting the role of transactivation in ERK activation (Morris *et al.*, 2012). This result was consistent with the idea that transactivation of the EGFR was induced by recruiting Src by P2Y₂ receptor resulting in sustained UTP-stimulated pERK, in which the phosphorylation of EGFR at Tyr-845 (Src phosphorylation site) was induced by UTP stimulation (Biscardi *et al.*, 1999). The reason for the lack of EGF receptors involvement in GPCR action in HEK 293 cells is not clear. However, it has been suggested that this could be due to the absence of agonist-induced metalloproteinase induction in such cells (Shah *et al.*, 2004).

The next experiment performed was to assess whether Ca²⁺ responses could be inhibited by Gα_q inhibitor. The measurement of agonist-mediated [Ca²⁺]_i was conducted using hNmU-25, hNmS-33 and UTP as an activator of Gα_q. It has been reported that HEK293 cells express two subtypes of P2Y receptors. P2Y₂ is activated by UTP resulting in Gα_q activation, leading to Ca²⁺ release (Schachter *et al.*, 1997).

All agonists caused a Ca^{2+} response. These responses were abolished by the presence of the inhibitor suggesting the ability of the inhibitor to inhibit Ca^{2+} signalling and therefore reassurance that $\text{G}\alpha_q$ was inhibited. Therefore, we can conclude that if the inhibitor is truly selective for $\text{G}\alpha_q$, then these data suggest that $\text{G}\alpha_q$ is the major driver of ERK activation at all-time points except at 5 min where it could be mediated by two different pathways. This data is supported by the idea that the prolonged ERK activation observed after β -arrestin-2 knockdown can be attributed to enhanced $\text{G}\alpha_q$ activity (Luo *et al.*, 2008). In addition, ERK activation could need $\text{G}\alpha_q$ activation in order to proceed to other activation mechanisms. For instance, in the absence of $\text{G}\alpha_q$ activation, other mechanisms perhaps do not work, e.g. do we still get arresting-binding and internalisation?

The earlier results in this study indicated that knocking down both β -arrestins-1 and -2 prolonged the activation of ERK when the cells were stimulated by either hNmU-25 and hNmS-33 following ligand removal. In order to confirm the effect of the $\text{G}\alpha_q$ inhibitor on the reduction in ERK activation, a further experiment was performed using cells with knockdown of both β -arrestin-1 and -2. Thus, the activation of ERK was completely inhibited in the presence of the $\text{G}\alpha_q$ except at 5 min. Combination of both $\text{G}\alpha_q$ and PKC inhibitors (100 nM and 5 μM , respectively) were used in order to investigate the activity of ERK at 5 min. The cells were pre-incubated with KHB or combination of both inhibitors for 30 min and then were stimulated by hNmU-25 and hNmS-33 (30 nM, 5 min). The levels of pERK were significantly reduced by UBO-QIB at this point. These data suggest that ERK is activated by $\text{G}\alpha_q$ at later time points, from 30 up to 180 min. In contrast, at 5 min, pERK could be mediated by two different pathways including $\text{G}\alpha_q$ and PKC. It is known that activated $\text{G}\alpha_q$ can stimulate Raf1 through PKC or by stimulating Ras by the Ca^{2+} -dependent activation of RasGEF and tyrosine kinases acting on SoS (Marinissen *et al.*, 2001). It is not clear how PKC activates the ERK pathway, since the direct phosphorylation of Raf could not be enough to stimulate MEK and ERK (MacLeod *et al.*, 1999). Indeed, it has been suggested that the full activation of Raf could be facilitated by PKC by Ras through the stimulation of additional molecules involved in the Ras-Raf interaction (Marinissen *et al.*, 2001). The potential toxicity of the combination of both inhibitors should be excluded because the

loading control rpS6 was not affected suggesting that the reduction of pERK might be due to pathway inhibition. Concentration-dependent increases in pERK immunofluorescence following either ligand challenge of NMU2 displays the pERK detectable in the cytoplasm and nucleus after 5 min of either ligand treatment, suggesting G protein-dependent ERK activation, since stimulation of G proteins activates the Raf family proteins through several convergent pathways and Raf then translocates to plasma membrane on activation (Lefkowitz *et al.*, 2005).

These results suggest that ERK activation could depend on $G\alpha_q$. In addition to PLC- IP_3 - Ca^{2+} signalling, ERK can be activated by $G\alpha_q$ via PLC-DAG-PKC mechanisms (Kolch *et al.*, 1993; Ueda *et al.*, 1996; Schonwasser *et al.*, 1998). ERK can also be activated by Ca^{2+} -calmodulin-mediated activation of Pyk2 resulting in activation of Ras and ERK1/2 (Dikic *et al.*, 1996; DellaRocca *et al.*, 1997). However, this depends on the cell types. For example, Ca^{2+} and PKC-mediated pathways can be involved in α_1 -adrenoceptor-mediated ERK activation in HEK293 cells (DellaRocca *et al.*, 1997). In contrast, PKC-C-Raf signalling can be involved in ERK activation Cos-7 and CHO cells via $G\alpha_q$ (Hawes *et al.*, 1995).

As it has been demonstrated that both G-protein and β -arrestin mediated signalling pathways can lead ERK activation. On the other hand, the subcellular distributions of activated ERK1/2 look different. For instance, pERK mediated by the β -arrestin pathway remains in the cytoplasm (Tohgo *et al.*, 2002; Luttrell, 2003). In contrast, pERK mediated by the G-protein pathway translocate to the nucleus (Chuderland *et al.*, 2008; Plotnikov *et al.*, 2011). Stimulation of numerous types of cell surface receptors leads to activation of the Raf/MEK/ERK signalling pathway (Adachi *et al.*, 2000). Raf phosphorylates only MEK, and MEK phosphorylates only ERK, whereas ERK is able to phosphorylate many substrates in nearly all cell compartments (Yoon *et al.*, 2006). ERK is primarily located in the cytoplasm of resting cells. On the other hand, overexpression results in both cytoplasmic and nuclear localization (Lenormand *et al.*, 1993). Also, it has been recognized that in the course of physiological signal transduction, ERK accumulates in the nucleus after acute stimulation of the cell (Chen *et al.*, 1992; Lenormand *et al.*, 1993). This accumulation of ERK is required for cell cycle entry. Thus, retention of ERK in the cytoplasm alters neither ERK kinase activity

nor phosphorylation of cytoplasmic substrates, whereas ERK-dependent transcription and cell proliferation are blocked (Brunet *et al.*, 1999). Some GPCR ligands can selectively determine subcellular locations of activated ERK1/2. The μ -opioid receptor (MOR) can be activated by two ligands; morphine and etorphine involving β -arrestin and G protein-dependent activation of ERK1/2 (Belcheva *et al.*, 2005; Rozenfeld *et al.*, 2007). A PKC inhibitor in contrast to etorphine that was not significantly affected, for example, could prevent morphine-induced ERK activation. Therefore, the morphine could activate ERK by a G-protein-dependent pathway whereas etorphine activates ERK by a β -arrestin-dependent pathway (Zheng *et al.*, 2008). Despite that morphine-induced ERK activation occurs via a G-protein-dependent pathway and thus should translocate to the nucleus, morphine did not induce nuclear translocation of pERK (Zheng *et al.*, 2008).

It has been shown by using HA-tagged Angiotensin II receptor type 1 (AT1aR), red fluorescent protein-tagged ERK2, and GFP- β -arrestins in HEK 293 that AT1aR, β -arrestin, and ERL all localise to endosomal vesicles after angiotensin II stimulation (Luttrell *et al.*, 2001). Therefore, the formation of stable complexes between β -arrestin and activated ERK could lead to cytosolic retention of ERK1/2. Agonist binding to receptors results in dissociation of heterotrimeric G proteins into $G\alpha$ -GTP and $G\beta\gamma$ subunits, which activate G protein effectors. One consequence of $G\beta\gamma$ subunit release is enhanced GRK-mediated phosphorylation of the agonist-occupied receptor. β -arrestins bind to both the GRK-phosphorylated receptor and to the component kinases of the ERK cascade, resulting in assembly of an ERK activation complex that is targeted into endosomal vesicles. Based on this, our data are consistent with this hypothesis, since the immunostaining experiments showed that pERK accumulates in the cytosol.

Chapter 6

Neuromedin U analogues

6.1 Introduction

A number of peptidergic systems has influenced food intake and energy homeostasis. Manipulation of several of these systems reduces food intake and body weight in preclinical models. On the other hand, in clinical trials, many of these agents did not reduce body weight due to a number of reasons, including lack of efficacy and side effects. There are different reasons for this. For example, it may be impossible to administer such an agent at the dose required to reduce body weight because of the associated side effects. The relatively wide expression of many peptidergic system components, and their associated diversity of function, makes their manipulation for the treatment of obesity full of difficulties.

There are also difficulties with the routes of administration. For instance, agents targeting CNS receptors must have a means of crossing the blood brain barrier. If a drug needs to be taken often, the route of administration becomes a patient issue. It is inconvenient and painful to have to inject a drug; orally active small molecule treatments are preferable. However, by their very nature, peptide hormones are difficult to mimic with small molecules. In particular, many gut hormone receptors require large ligands for receptor interaction, and residues essential for receptor interaction can be widely distributed throughout their secondary structure.

The effects of centrally administered NmU on feeding are considered to be mediated by NMU2 (Bechtold *et al.*, 2009; Peier *et al.*, 2009). However, a significant reduction in body weight has been shown in NMU2-deficient mice suggesting that peripheral NMU1 may also be involved (Bechtold *et al.*, 2009). In addition, peripherally administered NmU improved glucose tolerance in diet-induced obese mice. As peripherally

administered NmU is unlikely to act centrally on NMU2, this also supports a role for peripheral NMU1. Thus, the mechanism by which NmU contributes to the physiological regulation of body weight, glucose homeostasis and feeding are not entirely clear. Nevertheless, there is much interest in targeting NMU receptors for the treatment of obesity and diabetes. In order to overcome the poor pharmacokinetic properties typical of peptide hormones (e.g. the half-life of NmU after subcutaneous injection is less than 5 min), engineering of the native peptide is required (Peier *et al.*, 2011).

It has been suggested that lipidated and additionally stabilized short peptides derived from hormones could be exploited as agents for hormone-replacement therapy (Flinn *et al.*, 1996; Preza *et al.*, 2011). This may include, for example, poly ethylene glycol PEGylation which is a well-established strategy to increase the clinical efficacy of drugs and numerous examples are present of its application to peptides (Lumb *et al.*, 2007; Ortiz *et al.*, 2007; Day *et al.*, 2009). The highly hydrated shell of PEG increases the hydrodynamic radius of the conjugate and therefore decreases the rate of renal clearance and this prolongs the circulation time of the conjugate (Harris *et al.*, 2003) (**Figure 6.1**). It has also been reported that poly ethylene glycol (PEG) or human serum albumin (HAS) conjugated NmU is long-lived and has potent anorexigenic activity when administered peripherally in mice (Ingallinella *et al.*, 2012; Neuner *et al.*, 2014). Interestingly, two hexapeptide ligands; 8d and 6b have recently been designed to selectively activate NMU1 and NMU2, respectively, and these peptides in particular NMU2-specific activator 6b have potential in development of drugs reducing appetite (anorexigenic agonists) (Takayama *et al.*, 2014). Thus, the development of long-acting analogues of NmU is recommended. The unfavourable pharmacokinetic properties of NmU (the half-life of NmU after subcutaneous injection is less than 5 min) (Peier *et al.*, 2011) were improved by conjugation with PEG (Ingallinella *et al.*, 2012) or HAS (Neuner *et al.*, 2014) showing in both cases long-lasting, potent anorectic, and blood glucose-normalizing activity. Such analogues could be used in combination therapies with incretin-based therapeutic, for example.

The possibility of generating modified NmU that retained activity was tested by synthesizing a small library of truncated NmU analogues utilizing stabilization protocols, including cyclization, lipidation, introduction of α,α -disubstituted amino

acids, a *retro-inverso*-approach, and combination of these (Biron *et al.*, 2008). All peptides were synthesised as C-terminal amides using a standard fluorenylmethyloxycarbonyl (Fmoc) protocol (Fields *et al.*, 1990). Generally, lipidation was achieved by N-terminal conjugation of palmitic acid. Considering current trends in obesity treatment, the development of long-acting analogues of NmU is highly required. Such analogs could be exploited in combination therapies with, for instance, incretin-based therapeutics (s) such as semaglutide, a long-acting glucagon-like peptide 1 (GLP-1) analog that has a plasma half-life of 160 h (Monami *et al.*, 2012; Devaraj *et al.*, 2014).

In this chapter, a small library of NmU analogues, engineered by Dr. Piotr Ruchala (University of California, Los Angeles), were tested to assess concentration-response curves with the aim of selecting suitable compounds for *in vivo* testing (Micewicz *et al.*, 2015). The purpose of this study is to develop new peptidergic selective NMU2 agonists that are enzymatically stable and blood-brain-barrier (BBB) permeable.

As NmU and NmS are structurally-related neuropeptides that modulate energy homeostasis and inhibit food intake, this study aimed to see if there are differences between these neuropeptides compared to NmU analogues in terms of for example, receptor processing, including the effect of endosomal acidification and ECE-1 activity on NMU2 re-sensitisation.

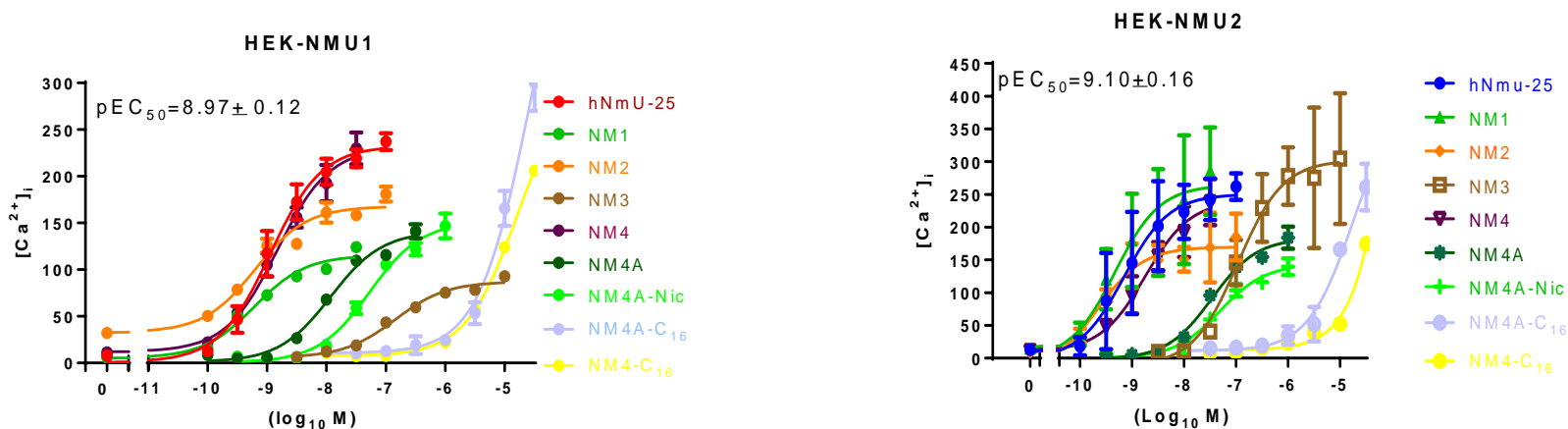
All of the analogues were tested for their abilities to mediate intracellular Ca^{2+} signalling by either NMU1 or NMU2 in HEK293 cells with stable expression of recombinant human receptors. A selection of these analogues, based on their potency, activity and availability were subsequently tested in assays assessing the effects of endosomal acidification, ECE-1 activity and β -arrestin recruitment. These analogues include NM1 and NM2, with similar pEC_{50} with hNmU-25. In addition, some inactive analogues including NM31, NM32, NM33, NM3D1, NM3D2 and NM3D3 were used to investigate their effects as antagonist for hNmU-25 (**Figure 6.1**).

6.2 Results

6.2.1 Concentration-response curves for analogues-mediated Ca^{2+} elevation in HEK-NMU1 and HEK-NMU2

Exposing either HEK-NMU1 or HEK-NMU2 to hNmU-25, NM1, NM2, NM3, NM4, NM4A, NM4A-Nic, NM7, or NM8 evoked concentration-dependent increases in fluorescence as an index of changes in $[\text{Ca}^{2+}]_i$ in populations of adherent fluo-4-loaded cells. High concentrations evoked greater and more rapid increases in $[\text{Ca}^{2+}]_i$. For instance, using a high concentration of any of the analogues led to a faster rate of increase in $[\text{Ca}^{2+}]_i$, while using a lower concentration resulted in a slower rate of increase. Following the initial peak, there was a slowly declining phase at some ligand concentrations used. This decline lasted until the end of reading (50 s). Changes in fluorescence were also calibrated as described in Methods and increases in $[\text{Ca}^{2+}]_i$ determined (**Figure 6.1**) and used to generate concentration-response curves where possible. From the concentration response curves, the pEC_{50} , E_{max} (% of maximal hNmU-25 response) and E_{max} at 10 μM and 30 μM were calculated (**Figure 6.1**). Moreover, exposing either HEK-NMU1 or HEK-NMU2 to NM6, NM10, NM11, NM4A-C16, NM31, NM32, NM33, NM34, NM35, NM15 and NM16 evoked increases in $[\text{Ca}^{2+}]_i$ in populations of adherents fluo-4-loaded cells only at high concentrations. In contrast, no increases were observed when HEK-NMU1 and HEK-NMU2 cells were exposed to NM3D1, NM3D2 or NM3D3 (**Figure 6.1 (D)**). In comparison to potency of hNmU-25, NM1 and NM2 have equal potency with $\text{pEC}_{50} = 9.24 \pm 0.12$ and 9.25 ± 0.22 for both NM1 and NM2, respectively (**Figure 6.1 (A)**). On the other hand, NM3, NM4A, and NM4A-Nic show less potency compared to hNmU-25, with $\text{pEC}_{50} = 6.85 \pm 0.08$, 7.91 ± 0.45 , and 7.32 ± 0.18 for NM3, NM4A and NM4A-Nic, respectively (**Figure 6.1 (A)**). In contrast to full agonist hNmU-25, the analogues including NM31, NM32, NM33, NM34, NM35, and NM36 started to give response at higher concentration (10 μM), and it was not possible therefore to determine the EC_{50} values for these analogues in HEK-NMU1. The results were observed using HEK-NMU2 with different EC_{50} values (**Figure 6.1 (C)**).

A1



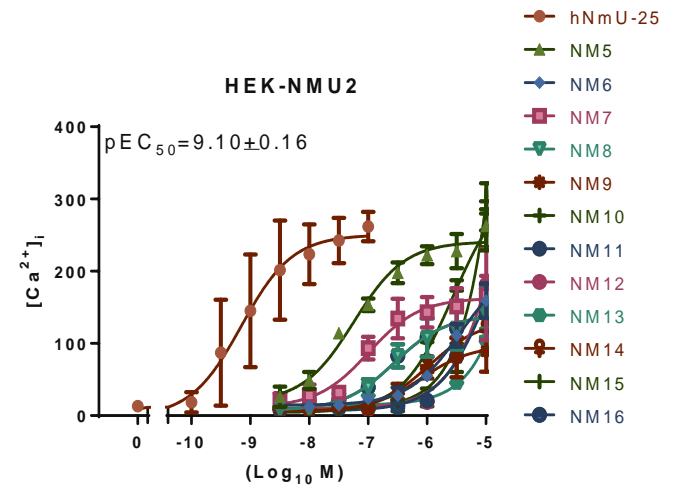
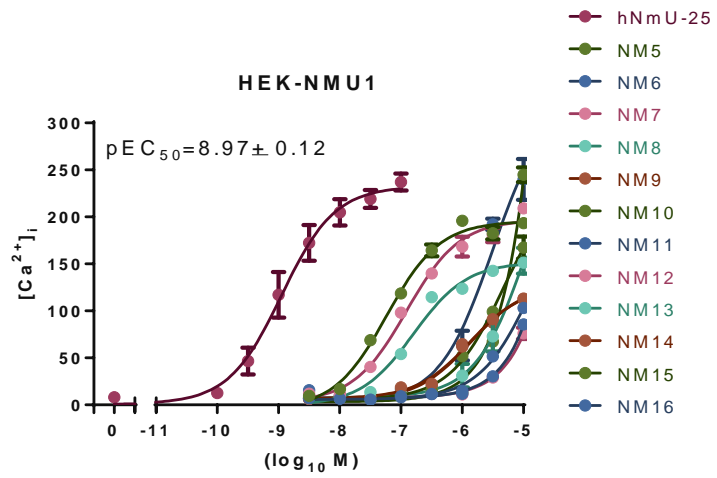
A2

Peptide	Sequence	NMU1			NMU2		
		pEC ₅₀	E _{max} (%hNmU)	E _{max} at 10 μM as %hNmU E _{max}	pEC ₅₀	E _{max} (hNmU)	E _{max} at 10 μM as %hNmU E _{max}
hNmU	FRVDEEFQSPFASQSRGY-FL-Phe-Arg-Pro-R-Asn	8.97±0.12	100		9.10±0.16	100	
NM1	Ac-FL-Phe-Arg-Pro-R-Asn	9.24±0.12	45±4.3	-	9.47±0.17	135.2±0.2	-
NM2	Aib-FL-Phe-Arg-Pro-R-Asn	9.25±0.22	66.3±0.6	-	9.67±0.19	69.9±0.2	-
NM3	Pal-Aib-FL-Phe-Arg-Pro-R-Asn	6.85±0.08	87.8±1.4	-	6.97±0.30	-	-
NM4	Pal-dPEG ₁₂ -Aib-FL-Phe-Arg-Pro-R-Asn	8.75±0.15	99.3±15.5	-	8.72±0.10	92.8±2.2	-
NM4A	Ida ^{NHPal} -Aib-FL-Phe-Arg-Pro-R-Asn	7.91±0.45	55.7±10.0	-	7.99±0.09	67.2±0.1	-
NM4A-Nic	Nic-Ida ^{NHPal} -Aib-FL-Phe-Arg-Pro-R-Asn	7.32±0.18	57.7±14.8	-	7.37±0.09	52.8±0.2	-
NM4A-C ₁₆	C ₁₆ -Ida ^{NHPal} -Aib-FL-Phe-Arg-Pro-R-Asn	~4.9 ^Δ	-	118.0±29.6 [#]	~5.0 ^Δ	-	99.6±17.9 [#]
NM4-C ₁₆	(C ₁₆) ₂ -Ahx-Aib-FL-Phe-Arg-Pro-R-Asn	~6.3 ^Δ	-	81.0±3.6 [#]	~6.1 ^Δ	-	28.4±4.3 [#]

Figure 6.1 (A) Concentration-responses curves for Ca²⁺ elevation in HEK-NMU1 and HEK-NMU2 mediated by NmU analogues and sequences and data obtained for NmU analogues (N-terminal amended analogues)

HEK-NMU1 and HEK-NMU2 cells were plated in 96-well plates for 24 h. Cells were loaded with fluo-4 then challenged with different concentrations of NmU-analogues in HEK-NMU1 and HEK-NMU2. Changes in cytosolic fluorescence were then monitored as an index of [Ca²⁺]_i using a NOVOstar plate-reader. Data were calibrated as described in Methods and maximal changes used to construct concentration-responses curves (A1). The curves were classified for clarity based on their responses compared to hNmU-25. Where they could be calculated, the pEC₅₀ values for the analogues are given in the top left hand corner of the panel. Data are mean ± s.e.m; n=4. All peptides were synthesized as C-terminal amides. Abbreviations: Ahx-6, aminohexanoic acid; Aib, aminoisobutyric acid; Ida, iminodiacetic acid, Pal, palmitic acid; NHPal, N-palmitylamide;. pEC₅₀ and E_{max} values were obtained using a calcium signalling assay where data are mean ± s.e.m, n≥4. (#) E_{max} at 30 μM as hNmU-25 E_{max}. (Δ) Approximate EC₅₀ values were derived from curves that had insufficient data points at high concentrations of ligand but which did approach the E_{max} of hNmU (A2). Modified amino acids have been highlighted for clarity.

B1



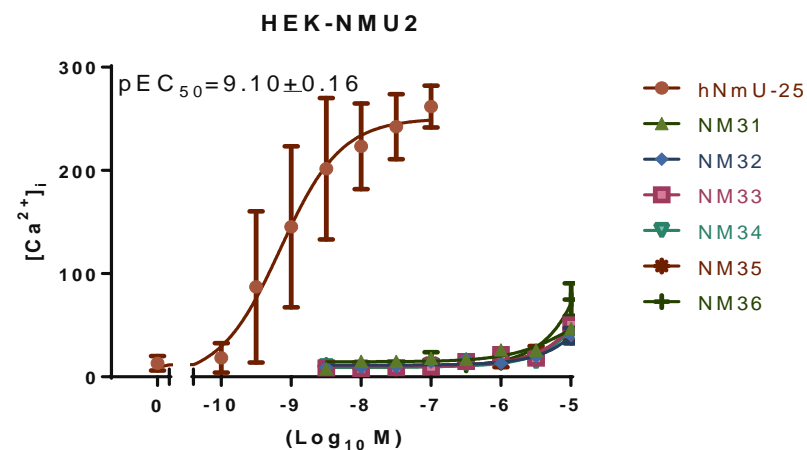
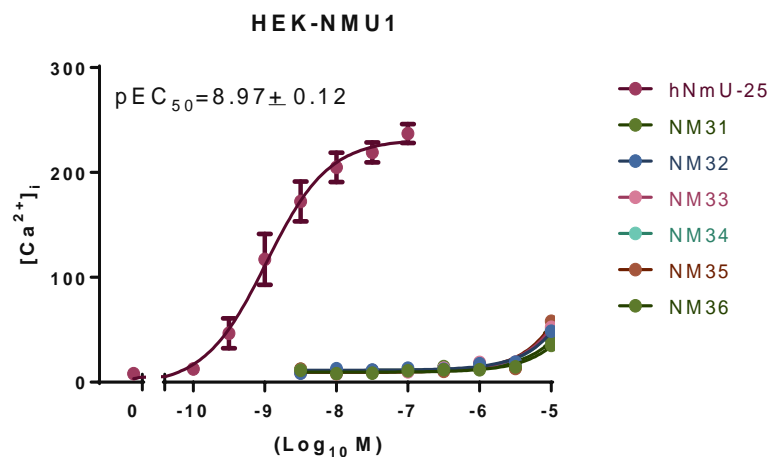
B2

Peptide	Sequence	NMU1			NMU2		
		pEC ₅₀	E _{max} (%hNmU)	E _{max} at 10 μM as %hNmU E _{max}	pEC ₅₀	E _{max} (hNmU)	E _{max} at 10 μM as %hNmU E _{max}
hNmU	FRVDEEFQSPFASQSRGY-FL-Phe-Arg-Pro-R-Asn	8.97±0.12	100		9.10±0.16	100	
NM5	Aib-FL-Phe-Arg-Pro-R-Asn-Aib	7.23±0.09	77.0±4.6	-	7.25±0.09	104.7±0.2	-
NM6	Pal-Aib-FL-Phe-Arg-Pro-R-Asn-Aib	-	-	40.6±2.2	-	-	60.7±12.1
NM7	Pal-dPEG ₁₂ Aib-FL-Phe-Arg-Pro-R-Asn-Aib	6.89±0.12	77.8±4.7	-	6.97±0.26	66.5±0.1	-
NM8	C-Ahx-dPEG ₁₂ Aib-FL-Phe-Arg-Pro-R-Asn-Ahx-C	6.79±0.50	59.8±0.5	-	6.55±0.10	53.6±0.1	-
NM9	C-Ahx-dPEG ₁₂ Aib-FL-Phe-Arg-Oic-R-Asn-Ahx-C	5.87±0.08	50.1±1.3	-	6.14±0.13	35.5±0.3	-
NM10	C-Ahx-dPEG ₁₂ Aib-FL-Phe-Arg-Tic-R-Asn-Ahx-C	~5.3 ^Δ	-	61.0±12.7	~5.6 ^Δ	-	97.8±11.8
NM11	X(C-Ahx-FL-Phe-Arg-Pro-R-Asn-Ahx-C)	-	-	33.7±0.2	-	-	60.6±11.6
NM12	X(C-Ahx-dPEG ₁₂ Aib-FL-Phe-Arg-Oic-R-Asn-Ahx-C)	-	-	30.00±6.0	-	-	70.0±6.0
NM13	X(C-Ahx-dPEG ₁₂ Aib-FL-Phe-Arg-Tic-R-Asn-Ahx-C)	-	-	60.4±13.8	-	-	39.3±8.8
NM14	PalS-X(C-Ahx-dPEG ₁₂ Aib-FL-Phe-Arg-Pro-R-Asn-Ahx-C)	5.87±0.05	50.0±3.0	-	6.00±0.09	53.1±0.3	-
NM15	PalS-X(C-Ahx-dPEG ₁₂ Aib-FL-Phe-Arg-Oic-R-Asn-Ahx-C)	~5.2 ^Δ	-	96.4±7.7	~5.2 ^Δ	-	118.4±4.8
NM16	PalS-X(C-Ahx-dPEG ₁₂ Aib-FL-Phe-Arg-Tic-R-Asn-Ahx-C)	~5.1 ^Δ	-	133.8±22.0	~5.2 ^Δ	-	126.6±10.8

Figure 6.1 (B) Concentration-responses curves for Ca²⁺ elevation in HEK-NMU1 and HEK-NMU2 mediated by NmU analogues and sequences and data obtained for NmU analogues (N-terminal and C-terminal amended analogues)

HEK-NMU1 and HEK-NMU2 cells were plated in 96-well plates for 24 h. Cells were loaded with fluo-4 then challenged with different concentrations of NmU-analogues in HEK-NMU1 and HEK-NMU2. Changes in cytosolic fluorescence were then monitored as an index of [Ca²⁺]_i using a NOVOstar plate-reader. Data were calibrated as described in Methods and maximal changes used to construct concentration-responses curves (**B1**). The curves were classified for clarity based on their responses compared to hNmU-25. Where they could be calculated, the pEC₅₀ values for the analogues are given in the top left hand corner of the panel. Data are mean ± s.e.m; n=4. All peptides were synthesized as C-terminal amides. Abbreviations: Ahx-6, aminohexanoic acid; Aib, aminoisobutyric acid; Oic, (2S,3aS,7aS)-octahydro-1H-indole-2-carboxylic acid; Tic, (3S)-1,2,3,4-tetrahydroisoquinoline-3-carboxylic acid; Pal, palmitic acid; PalS, X-3,5-bis(methyl-S-cysteinyl)-1-(methyl-S-palmityl)-benzene; X, 1,3-bis(methyl-S-cysteinyl)-benzene; NHPal, N-palmitylamide; dPEG₁₂, 40-amino-4,7,10,13,16,19,22,25,28,31,34,37-dodecaoxotetradecanoic acid. pEC₅₀ and E_{max} values were obtained using a calcium signalling assay where data are mean ± s.e.m, n ≥ 4. (#) E_{max} at 30 μM as hNmU-25 E_{max}. (^Δ) Approximate EC₅₀ values were derived from curves that had insufficient data points at high concentrations of ligand but which did approach the E_{max} of hNmU (**B2**). Modified amino acids have been highlighted for clarity.

C1



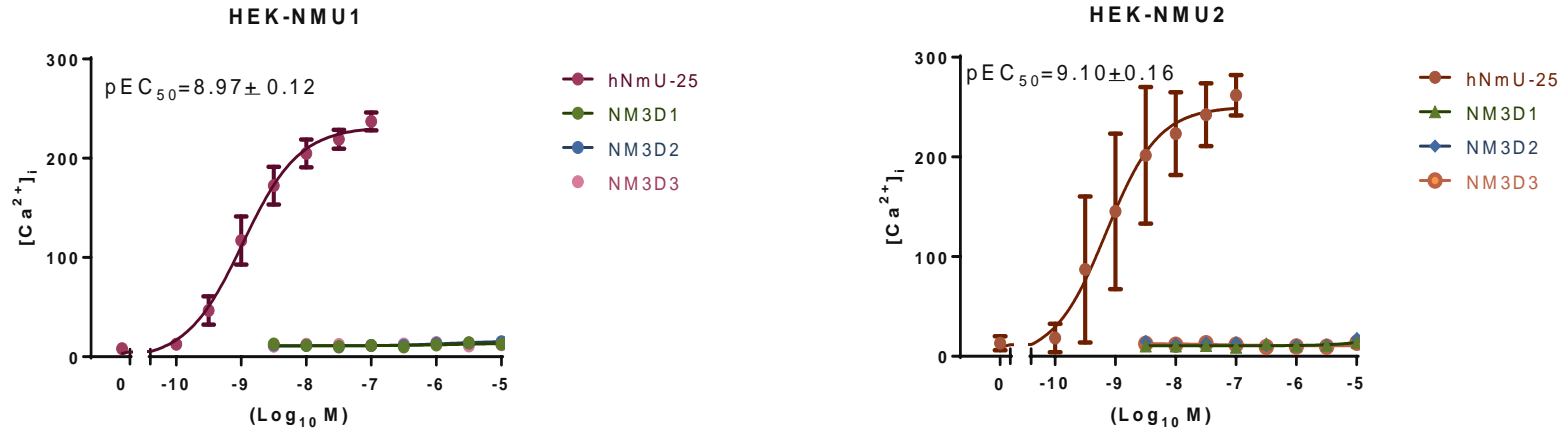
C2

Peptide	Sequence	NMU1			NMU2		
		pEC ₅₀	E _{max} (%hNmU)	E _{max} at 10 μM as %hNmU	pEC ₅₀	E _{max} (hNmU)	E _{max} at 10 μM as %hNmU
hNmU	FRVDEEFQSPFASQSRGY-FL-Phe-Arg-Pro-R-Asn	8.97±0.12	100		9.10±0.16	100	
NM31	Pal-Aib-FL-Phe-N ^{Me} R-Pro-R-N ^{Me} N	-	-	13.8±2.0	-	-	17.9±1.5
NM32	Pal-Aib-FL-N ^{Me} F-Arg-Pro-R-N ^{Me} N	-	-	19.1±1.2	-	-	15.2±3.8
NM33	Pal-Aib-FL-α ^{Me} F-Arg-Pro-R-N ^{Me} N	-	-	20.6±1.9	-	-	19.2±2.0
NM34	Pal-Aib-FL-Phe-N ^{Me} R-Pro-R-N ^{Me} N	-	-	19.6±3.2	-	-	18.4±3.2
NM35	Pal-Aib-FL-N ^{Me} F-Arg-Pro-R-N ^{Me} N	-	-	22.9±3.8	-	-	67.0±16.5
NM36	Pal-Aib-FL-α ^{Me} F-Arg-Pro-R-N ^{Me} N	-	-	15.9±6.6	-	-	28.6±7.9

Figure 6.1 (C) Concentration-responses curves for Ca²⁺ elevation in HEK-NMU1 and HEK-NMU2 mediated by NmU analogues and sequences and data obtained for NmU analogues (α -carbon-/N-methylated-variants)

HEK-NMU1 and HEK-NMU2 cells were plated in 96-well plates for 24 h. Cells were loaded with fluo-4 then challenged with different concentrations of NmU-analogues in HEK-NMU1 and HEK-NMU2. Changes in cytosolic fluorescence were then monitored as an index of $[Ca^{2+}]_i$ using a NOVOstar plate-reader. Data were calibrated as described in Methods and maximal changes used to construct concentration-responses curves (C1). The curves were classified for clarity based on their responses compared to hNmU-25. Where they could be calculated, the pEC₅₀ values for the analogues are given in the top left hand corner of the panel. Data are mean \pm s.e.m; n=4. All peptides were synthesized as C-terminal amides. Abbreviations: Ahx-6, aminohexanoic acid; Aib, aminoisobutyric acid; $\alpha^{Me}F$, α -methyl-L-phenylalanine; N^{Me}R, N ^{α} -methyl-L-arginine; N^{Me}N, N-methyl-L-asparagine; N^{Me}F, N-methyl-L-phenylalanine; Pal, palmitic acid. pEC₅₀ and E_{max} values were obtained using a calcium signalling assay where data are mean \pm s.e.m, n \geq 4. ^(#) E_{max} at 30 μ M as hNmU-25 E_{max}. ^(Δ) Approximate EC₅₀ values were derived from curves that had insufficient data points at high concentrations of ligand but which did approach the E_{max} of hNmU (C2). Modified amino acids have been highlighted for clarity.

D1



D2

Peptide	Sequence	NMU1			NMU2		
		pEC_{50}	E_{max} (%hNmU)	E_{max} at 10 μ M as %hNmU E_{max}	pEC_{50}	E_{max} (hNmU)	E_{max} at 10 μ M as %hNmU E_{max}
hNmU	FRVDEEFQSPFASQSRGY-FL-Phe-Arg-Pro-R-Asn	8.97 ± 0.12	100		9.10 ± 0.16	100	
NM3D1	CT-Ida ^{NHPal} -FL-Phe-Arg-Pro-R-Asn-NT	-	-	-	-	-	-
NM3D2	CT-Ida ^{NHPal} -Ahx-FL-Phe-Arg-Pro-R-Asn-NT	-	-	-	-	-	-
NM3D3	CT-Ida ^{NHPal} -Ahx-Aib-FL-Phe-Arg-Pro-R-Asn-NT	-	-	-	-	-	-

Figure 6.1 (D) Concentration-responses curves for Ca²⁺ elevation in HEK-NMU1 and HEK-NMU2 mediated by NmU analogues and sequences and data obtained for NmU analogues ((D)-retro-inverso-analogues)

HEK-NMU1 and HEK-NMU2 cells were plated in 96-well plates for 24 h. Cells were loaded with fluo-4 then challenged with different concentrations of NmU-analogues in HEK-NMU1 and HEK-NMU2. Changes in cytosolic fluorescence were then monitored as an index of [Ca²⁺]_i using a NOVOstar plate-reader. Data were calibrated as described in Methods and maximal changes used to construct concentration-responses curves (D1). The curves were classified for clarity based on their responses compared to hNmU-25. Where they could be calculated, the pEC₅₀ values for the analogues are given in the top left hand corner of the panel. Data are means ± s.e.m; n=4. All peptides were synthesized as C-terminal amides, NM3D1-D3 are all (D)-retro-inverso-analogues where: NT is the N-terminus and CT is the C-terminus of the peptide (s). Abbreviations: Ida, iminodiacetic acid; NHPal, N-palmitylamide. pEC₅₀ and E_{max} values were obtained using a calcium signalling assay where data are mean ± s.e.m, n≥4. ^(#) E_{max} at 30 μM as hNmU-25 E_{max}. ^(Δ) Approximate EC₅₀ values were derived from curves that had insufficient data points at high concentrations of ligand but which did approach the E_{max} of hNmU (D2). Modified amino acids have been highlighted for clarity.

6.2.2 Effect of endosomal acidification and ECE-1 on NMU2 re-sensitization following treatment with the analogues NM1 or NM2

It has been indicated earlier that the NmU analogues used here have different structures and often different potencies and E_{\max} values compared to hNmU-25 (**Figure 6.1; A, B, C, and D**). It is possible that such differences could affect receptor re-sensitisation. Furthermore, other properties of the various analogues could influence receptor re-sensitisation (e.g. different susceptibility to ECE-1 activity). Thus, effects of endosomal acidification and ECE-1 inhibitors on the recovery of NMU2, exposed to NM1 and NM2 analogues were investigated (**Figure 6.2; A & B**). HEK-NMU2 cells were stimulated with either NM1 or NM2 analogues using the maximum concentration (30 nM, 5 min), the ligands were washed off, and the cells allowed to recover for 6 h following by re-challenging using the same ligand by a NOVOstar plate-reader. The results indicated that these compounds behaved similarly to hNmU-25 in terms of affecting NMU2 re-sensitisation. Inhibition of endosomal acidification delayed recovery when the cells were stimulated using the maximum concentration of NMU1 and NM2. Moreover, inhibition of ECE-1 delayed recovery when the cells were stimulated using maximum concentration of NM1 and NM2 (**Figure 6.2; A & B**). Cells were treated with either buffer or the ECE-1 inhibitor, SM-19712 (10 μ M) for 30 min and challenged with buffer, NM1 or NM2 (30 nM, 5 min). The inhibitor concentration used here has been used previously (Murphy *et al.*, 2011). Cells were then washed with KHB and allowed to recover for 6 h. Also, monensin increased the initial response of Ca^{2+} when the cells were stimulated with either ligand.

Because the results indicated that the NMU2 recovery could be affected by ECE-1 when the cells were stimulated with NM1 and endosomal acidification when exposed to NM2, the rhECE-1 experiments were conducted using these analogues. NM1 fragments were detected when the analogues were exposed to the enzyme at either pH 5.5 or pH 7.4 and in the presence or absence of ECE-1 enzyme (**Figure 6.3**). In contrast, more NM2 fragments were detected in pH 5.5 (**Figure 6.4**). Moreover, from these fragments, the cleavage sites were identified as shown in (**Figure 6.5**). Also, it should be noticed that

some fragments are present in both absence and presence of the rhECE-1 following adding NM1, at both pH 7.4 and 5.5 (**Figure 6.3**). It can be seen from the figure that the enzyme could cleave the intact peptide in different cleavage sides. For example, the enzyme could cleave NM1 between Phe and Leu, Arg and Asn in both pH 5.5 and 7.4. Also, the enzyme could cleave NM2 between Aib and Phe, Phe and Leu, and Arg and Asn in pH 5.5 in contrast to pH 7.4 in which the enzyme cleaved NM2 between Aib and Phe, Arg and Asn.

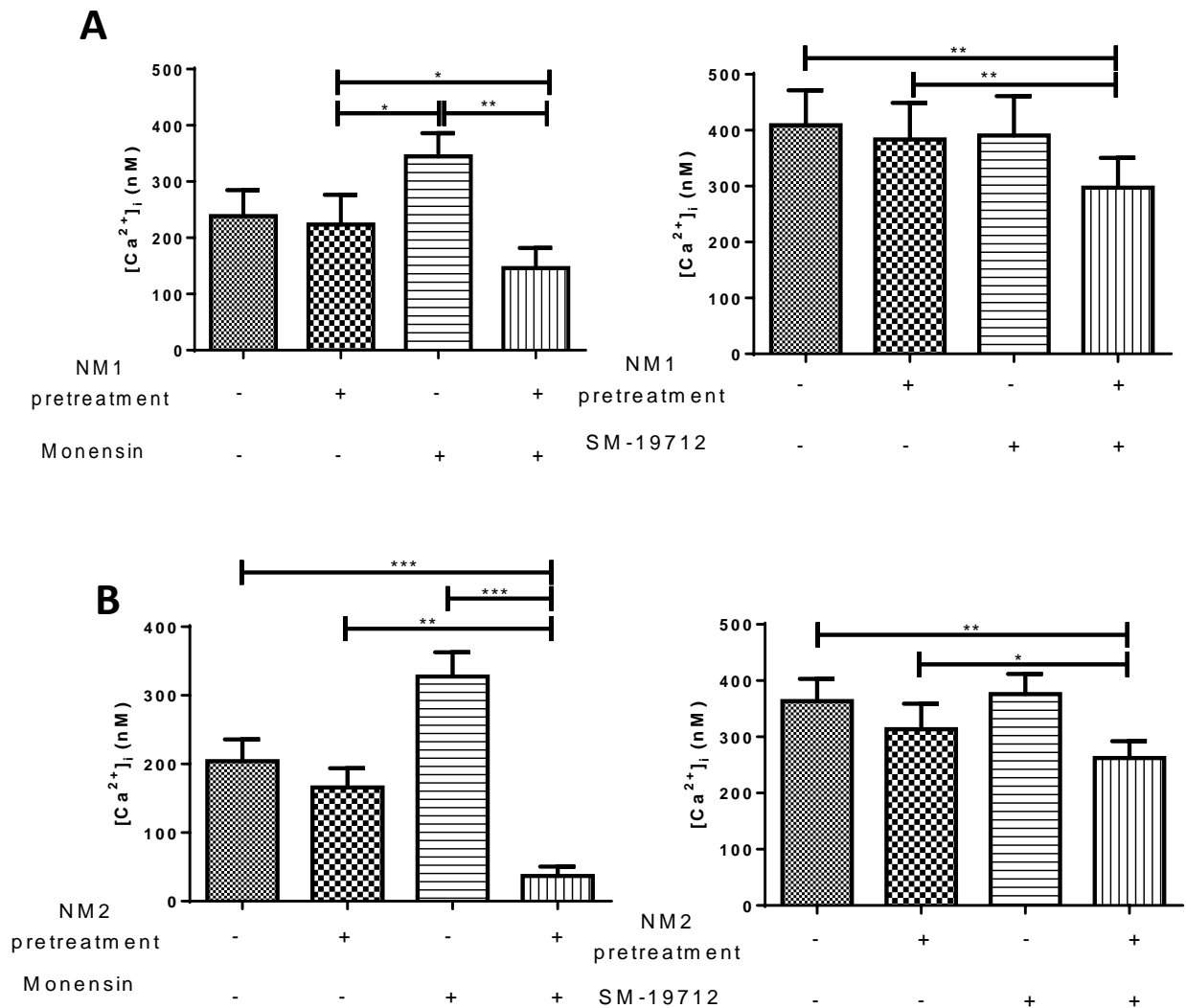


Figure 6.2 The effect of endosomal acidification and ECE-1 inhibition on NMU2 re-sensitisation following treatment with either NM1 or NM2 analogues

HEK-NMU2 cells were pre-incubated with or without inhibitors of ECE-1, SM-19712 (10 μ M) or endosomal acidification (monensin, 50 μ M), for 30 min before challenge with buffer or ligands (NM1 (**A**) or NM2 (**B**); 30 nM for 5 min). Cells were washed and allowed to recover for 6 h (in the continued presence or absence of the inhibitors) before determination of Ca^{2+} responses to the same ligand (30 nM). Data are mean \pm s.e.m., $n=3$, * $P<0.05$, ** $P<0.01$, *** $P<0.001$. The data were analysed by Bonferroni's multiple comparison test following one-way ANOVA. Significant differences between unchallenged and recovery in the presence and absence of inhibitor were considered.

		NM1				NM1			
		pH 5.5				pH 7.4			
		- Enzyme		+ Enzyme		- Enzyme		+ Enzyme	
Peptide Sequence	XIC m/z	RT	Area	RT	Area	RT	Area	RT	Area
Ac-FLFRPRN	495.7781	22.95	27106783820	22.77	33791523619	22.7	21292437132	22.9	21792887105
Ac-FLFRPR	439.2497	19.54	237283271	19.35	232961859	19.39	297700537	19.48	315143685
LFRPRN	401.2448	11.73	42495621	11.34	84552291	11.11	57034591	11.37	58793482
FRPRN	344.7028	11.74	5512101	11.34	12406123	11.09	12396553	11.37	13221642

Figure 6.3 Fragments of NM1 analogue produced by rhECE-1

NM1 (25 μ M) was added in the presence or absence of rhECE-1 (0.1 μ g) and incubated in 37°C, at either pH 5.5, MES/KOH, or 7.4, Tris-HCL for 10 min and then centrifuged 14.0 xg for 2 min using Vivacon 500 filters as described in Methods to stop the reaction and to separate the enzyme from the samples. Extracted ion chromatograms were produced for each peptide and aligned using their m/z and retention time (RT) and the peak areas (Area) integrated for comparison as described in Methods.

		NM2				NM2			
		pH 5.5				pH 7.4			
		- Enzyme		+ Enzyme		- Enzyme		+ Enzyme	
Peptide Sequence	XIC m/z	RT	Area	RT	Area	RT	Area	RT	Area
Aib-FLFRPRN	517.3019	Too Intense to Integrate							
FLFRPRN	474.7778	Too Intense to Integrate							
Aib-FLFRPR	460.7732	not detectable		23.1	499713645	19.45	5841797736	19.27	450053369
FLFRPR	418.247	not detectable		23.1	72742872	19.45	150419428	19.28	203657548
LFRPRN	401.2432	not detectable		14.74	1219244037	not detectable		not detectable	

Figure 6.4 Fragments of NM2 analogue produced by rhECE-1

NM2 (25 μ M) was added in the presence or absence of rhECE-1 (0.1 μ g) and incubated in 37°C, at either pH 5.5, MES/KOH, or pH 7.4, Tris-HCL for 10 min and then centrifuged 14.0 xg for 2 min using Vivacon 500 filters as described in Methods to stop the reaction and to separate the enzyme from the samples. Extracted ion chromatograms were produced for each peptide and aligned using their m/z and retention time (RT) and the peak areas (Area) integrated for comparison as described in Methods.

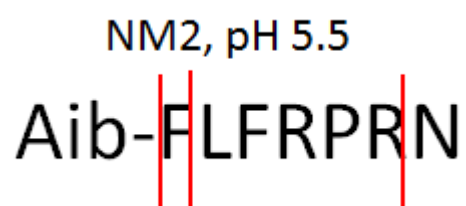


Figure 6.5 Potential cleavage sites for NmU analogues; NM2

This figure shows the cleavage sites for NM2. It represents cleavage sites in pH 5.5 at incubation for 10 min as described in Methods. The final products shown in previous figures are as a result of the activity of ECE-1 in these sites indicated by red lines.

6.2.3 Assessment of the potential antagonist activity of NmU analogues

In the current study, some analogues including NM31, NM32, NM33, NM3D1, NM3D2 and NM3D3 did not give any Ca^{2+} responses even with using a higher concentration (**Figure 6.1; C & D**). Although it is possible that these analogues simply did not interact with NMU receptor, it was possible that they had affinity but low or zero efficacy and would therefore act as antagonists. This was tested in a Ca^{2+} assay. Thus, HEK-NMU2 cells were loaded with fluo-4-AM for 45 min at 37°C. The ligands NM3D1, NM3D2 and NM3D3, NM31, NM32, and NM33 (10 μM) were added to the cells and incubated for 10 min. The cells were then stimulated with either 30 nM or 1 nM of hNmU-25 using a NOVOstar plate-reader. If these ligands were antagonist, a reduced or absent Ca^{2+} responses would be expected. However, no analogue prevented the Ca^{2+} responses stimulated with either a maximum concentration (30 nM) or EC_{50} (1 nM) of hNmU-25 suggesting these analogues are not likely to be NMU2 antagonists at least under our conditions (**Figure 6.6**).

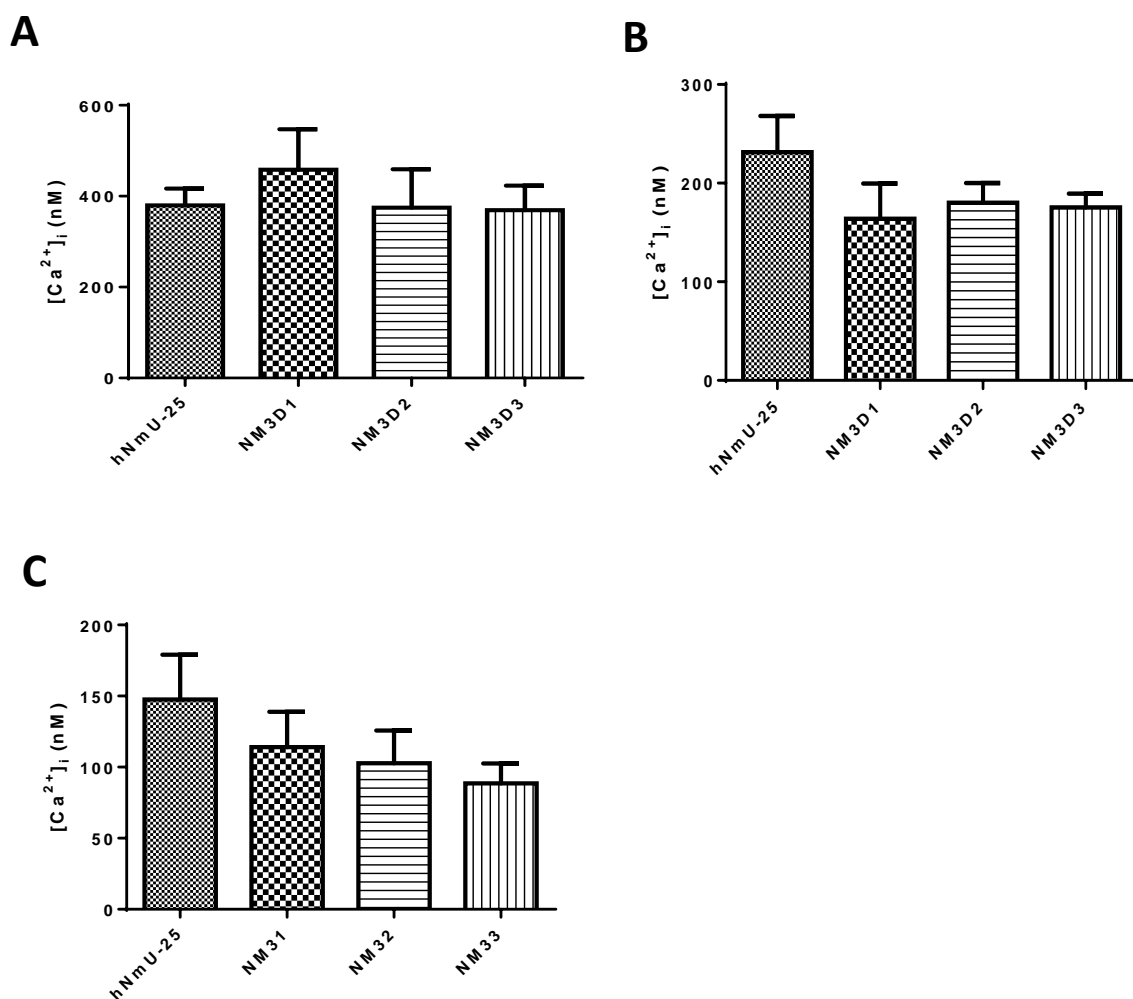


Figure 6.6 Assessment of the potential antagonist activity of NmU analogues

HEK-NMU2 cells were cultured in 96 well-plates for 24 h at 37°C. The cells were then loaded with fluo-4-AM for 45 min at 37°C. The ligands NM3D1, NM3D2 and NM3D3 (10 µM) (**A&B**) or NM31, NM32, and NM33 (10 µM) (**C**) were added to the cells and incubated for 10 min. The cells were then stimulated with either 30 nM (**A**) or 1 nM (**B&C**) of hNmU-25 using a NOVOstar plate-reader. Changes in fluorescence were monitored as an index of [Ca²⁺]_i. Data are mean ± s.e.m., n=3. The data were analysed by Bonferroni's multiple comparison test following one-way ANOVA.

6.2.4 Arrestin recruitment to NMU receptors activated by NmU analogues

The ability of the agonist-activated receptor to recruit β -arrestin-2 was determined using the DiscoverX PathHunter technology (DiscoverX) that involves enzyme complementation of fusion-tagged receptor along with an arrestin recruitment modulating sequence and β -arrestin-2 proteins. Utilization of β -arrestin recruitment allows a direct measurement of agonist binding as activated receptors act as substrates for GRKs that phosphorylate the receptor (Violin *et al.*, 2007). Thus, arrestin recruitment by activated NMU receptors was investigated as previously described (Riddy *et al.*, 2012). Ideally the study would have examined recruitment of β -arrestin-1 and -2 by both NMU1 and NMU2 following activation with a number of different ligands. However, the only available platform was NMU1 and β -arrestin-2. Different ligands were used including NM2, NM4 and NM5. These analogues were chosen due to their similar and different potency to hNmU-25. For instance, pEC₅₀ values obtained using a Ca²⁺ assay for NM2, NM4 and NM5 were 9.25 \pm 0.22, 8.75 \pm 0.15, and 7.23 \pm 0.09, respectively, whereas the pEC₅₀ value hNmU-25 in HEK-NMU1 was 8.97 \pm 0.12. The experiment was conducted once as explained in Methods to generate concentration-response curves. The pEC₅₀ values for NM2, NM4 and NM5 were 7.54 \pm 0.09, 7.11 \pm 0.08 and 5.82 \pm 0.08, respectively. These results indicated that β -arrestins are recruited to cell membrane at least by activated NMU1 receptor. However, our results indicated at least using NMU1 and β -arrestin-2; that NM5 is less efficacy that both NM2 and NM4 (**Figure 6.7**).

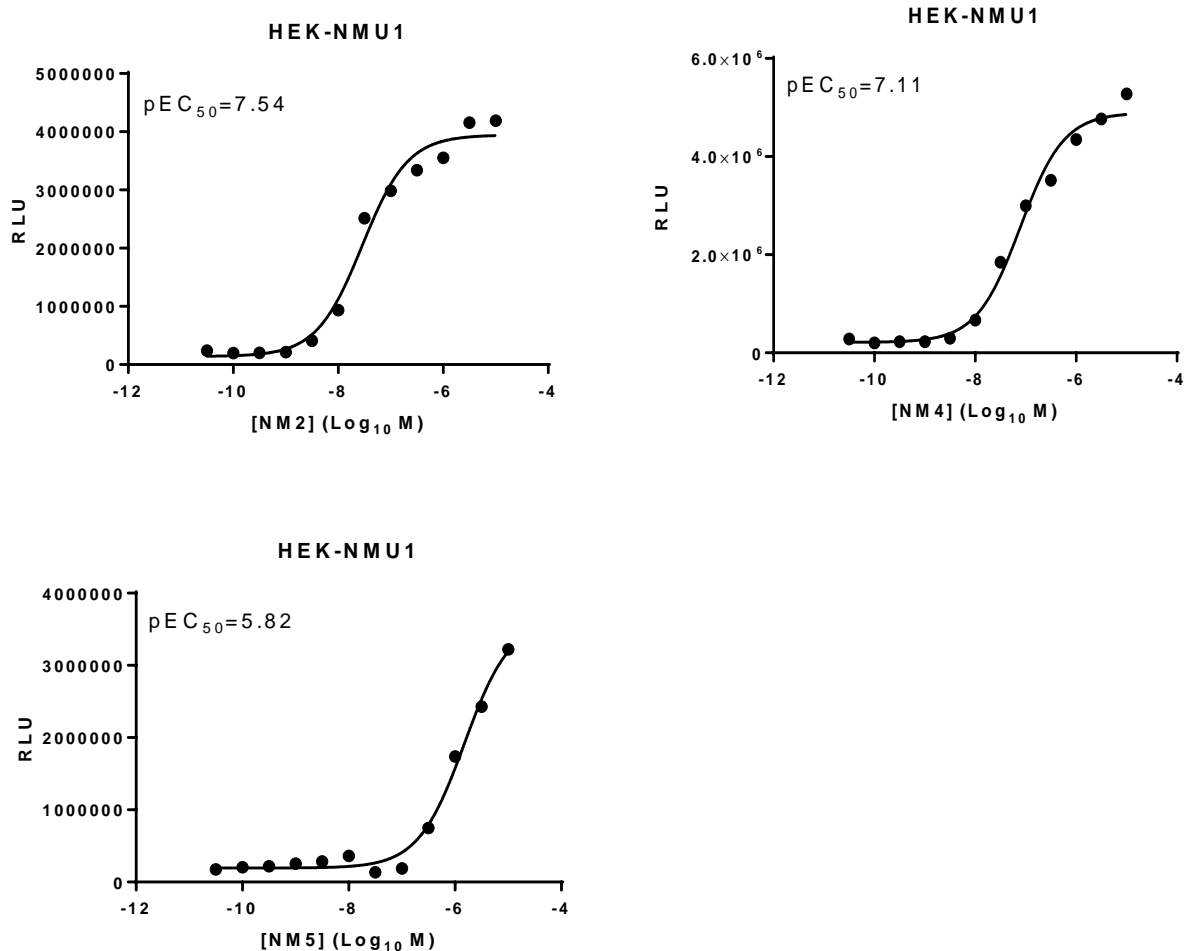


Figure 6.7 Concentration-response curves for β -arrestin-2 recruitment by activated NMU1 stimulated by different analogues

PathHunter eXpress cells expressing NMU1 were plated in 96 well-plates. The cells were then incubated for 48 h at 37°C, 5% CO₂. Cells were then challenged with NM2, NM4 or NM5. The plate was incubated for 90 minutes at 37°C, 5% CO₂. Following addition of detection reagent working solution and further incubation for 60 minutes at room temperature, chemiluminescence, indicated as relative luminescence units (RLU) was recorded using a NOVOstar plate-reader. pEC₅₀ values for all analogues were calculated using Graph Pad Prism 6. The pEC₅₀ values for NM2, NM4, and NM5 were 7.54, 7.11 and 5.82, respectively. Experiments for NM2, NM4, and NM5 were performed once with one sample.

6.3 Discussion

Obesity is a leading preventable cause of death worldwide (Boughton *et al.*, 2013). It has been suggested that lipidated and additionally stabilized short peptides derived from hormones could be exploited as therapeutic agents (Flinn *et al.*, 1996; Preza *et al.*, 2011). Therefore, to assess if NmU could be modified to generate biologically active but more stable analogues, a small library of truncated NmU analogues was synthesised by Dr. Piotr Ruchala (University of California, Los Angeles) using different stabilization protocols. All synthesized NmU-analogues (designated NMxxx) were tested using a cellular Ca^{2+} signalling assay in HEK293 cells expressing recombinant human NMU1 or NMU2. The results demonstrated that there are no differences between NMU1 and NMU2 in the action of the analogues. For example, NM1, NM2, NM4 and NM4A activated both receptors with similar potency and these potencies were similar to that of the endogenous ligand, hNmU-25. In other studies, compounds have been generated that showed some receptor sub-type selectivity (Takayama *et al.*, 2014). For example, a hexapeptide (compound 6b) activated NMU2 without significant NMU1 activation. In this study, 6b structure was as following: (3-cyclohexylpropionyl-Leu¹-Leu²-Dap³-Pro⁴-Arg⁵-Asn⁶-NH₂), while 8d structure was (3-peridonepropionyl-(2-Nal)¹-Phe²-Arg³-Pro⁴-Arg⁵-Asn⁶-NH₂). The bulky aromatic structure at residue 1 in combination with the *N*-terminal nitrogen-containing aromatic acyl moiety was suggested to be suitable for NMU1 selectivity. In the present study there was no evidence of any receptor subtype selectivity amongst the tested. Although some of the compounds tested in the present study did start to evoke Ca^{2+} responses at 10 μM (NM31-NM36), indicating very low potency, some analogues including NM3D1, NM3D2 and NM3D3 did not increase Ca^{2+} responses even at the highest concentration used (10 μM). It is unclear whether a lack of effect was a consequence of a lack of affinity or efficacy. To partially address this, compounds NM3D1-NM3D3, were screened for antagonist activity. Interestingly a previous study has reported marked decrease in agonistic activity by substitution of the corresponding D-amino acid residue for Phe², Phe⁴, Arg⁵, Pro⁶ or Asn⁸, while the replacement of Tyr¹ with the D-form enhanced activity (Hashimoto *et al.*, 1991).

In addition to assessment of potential antagonist activity, there were clear opportunities to assess a range of the synthesised ligands in other assays of signalling and receptor regulation (**as used in Chapter 3**). However, the analogues were obtained through collaboration and the desired analogues were not always available at the required times or in the required quantities.

It has been suggested that small-engineered peptides derived from NmU could be active *in vivo* and provide a useful therapeutic tool. For example, NM4 & NM7 are small peptides; with MWt \approx of approximately 1.9 kDa. They show comparative potency and intrinsic activity to hNmU/hNmS on Ca²⁺ signalling a recombinant system. These analogues were specifically engineered to extend the plasma half-life, particularly by engineering in resistance to enzymatic degradation. Moreover, such compounds are easy to synthesize in large quantities using Solid-phase peptide synthesis (SPPS) and well established protocols. In addition to having an α,α -disubstituted amino acid (aminoisobutyric acid, Aib) that may confer increased resistance to enzymatic degradation (Yamaguchi *et al.*, 2003), NM4 has similar high potency on Ca²⁺ signalling as native human peptide (hNmU) (Micewicz *et al.*, 2015). Thus, NM4 was selected by our collaborators for assessment of its *in vivo* activity. Moreover, because NM7 possesses two Aib residues that should confer greater resistance to degradation within the circulation, its *in vivo* activity was also assessed. In order to examine whether these two analogues have any *in vivo* anorectic activity, they were used in a diet-induced obese (DIO) mouse model as described previously (Peier *et al.*, 2011; Neuner *et al.*, 2014) focusing on different doses of 5344, 1603 and 534 nmol/kg body weight in addition to the discovery of a less expensive analogues including NM4A. A phospholipid-based, commercially available drug delivery system, PUREBRIGHT SL-220 (NOF America Corp., White Plains, NY) was used because it has been suggested that it is appropriate for delivery of lipidated peptides, which have limited water solubility, such as NM4 (Preza *et al.*, 2011a; Ramos *et al.*, 2012). NM4 showed significant anorectic activity in a dose-dependent manner. The C-termini of NMU ligands are presumed to play a key role in the activation of NMU1 and NMU2 (Minamino *et al.*, 1985; Mori *et al.*, 2005). In particular, structure-activity relationship studies (SAR) have demonstrated clear roles for F¹ L² F³ R⁴ P⁵ R⁶ N⁷-amide (Minamino

et al., 1985; Brighton *et al.*, 2004a). It has been shown that C-terminal amino acids residues; Pro⁴, Arg⁵, and Asn⁶-amide was important for the activation of NMU1 and NMU2 (Takayama *et al.*, 2014). In addition, it has been suggested that the stabilization of the Arg⁵-Asn⁶ bond will be critical to exert a long-lasting anorexigenic effect *in vivo* (Takayama *et al.*, 2015). For instance, R⁶ and N⁷-amide are necessary for binding and activation respectively of the avian peripheral receptor and substitution of F³ → Y results in improved bioactivity. N-terminal modifications with pyroglutamic acid, succinic acid and glutaric acid are optional and it can be used, showing improved amino peptidase resistance and increased agonistic activity in contractility assays (Sakura *et al.*, 1995). In order to increase proteolytic resistance of truncated NmU analogues, unsuccessful attempts were made introducing *retro-inverso*, α -carbon-methylated, N-methylated and cyclic analogues. *Retro-inverso* peptides are obtained by replacing the normal L-amino acid residues with the corresponding D-amino acids and reversing the direction of the peptide backbone. It was also determined that substitution of either F¹ F³ R⁴ P⁵ R⁶ or N⁷-amide with glycine or their D-amino acid counterparts results in decreased bioactivity (Hashimoto *et al.*, 1991). Our data suggested that substitution of Pros for Oic or Tic in some analogues including NM8-NM16 has an undesirable effect (low potency, compared to NmU). Moreover, the cyclization is not a viable option as it makes NM11-NM13 inactive, in comparison between analogues NM8-NM10 (linear peptides, NM11-NM13 (cyclic peptides) and NM14-NM16 (cyclic/lapidated peptides). It has also been revealed that the carboxylic acid group at the N-terminus of NmU-8 makes a major contribution to the activity (Hashimoto *et al.*, 1995). This is supported by the observation that any modifications of NmU for pharmaceutical purposes seems to be difficult since even small changes in the structure may result in significant loss of bioactivity. For instance, *retro-inverso*-analogues (NM3D1-NM3D3) and α -carbon-/N-methylated-variants (NM31-NM35) were inactive (**Figure 6.1; C**). Consistent with the published observations that underline the importance of P⁵ and N⁷-amide residues for agonistic activity at NMUs (Sakura *et al.*, 2000; Takayama *et al.*, 2014), the current study demonstrates that introduction of a lipid moiety to the cyclic analogues (NM14-NM16) seems to restore bioactivity. However, it has been shown that a viable modification is likely to be the introduction of a small α,α -disubstituted amino acid (s) (Aib) at the flanking positions of the native active sequence (e.g. FLFRPRN). In this

case, *bis*-substituted analogues (e.g. X-Aib-FLFRPRN-Aib) show decreased potency in *in vitro* assays (NM5<NM2 & NM6<NM3) and very limited activity *in vivo* (e.g. NM7) (Micewicz *et al.*, 2015). NM7 contains two Aib residues that should confer greater resistance to degradation within circulation and therefore this analogue was used as an alternative lead compound. A recent paper indicated that bond between Arg and Asn was rapidly degraded in serum by thrombin enzyme (Takayama *et al.*, 2015). Even though the impact of lipidation on full-length human NmU analogues are likely to be more diverse depending on their individual structure (Marsh DJ *et al.*, 2011). Lipidation has been utilized to modify a wide variety of peptide ligands (Zhang *et al.*, 2012). Peptide stability, prolonged half-life by facilitating binding to circulating albumin, and/or targeted excretion by the liver rather than by the kidney have been enhanced by such changes (Yuan *et al.*, 2005; Bellmann-Sickert *et al.*, 2011). Also, it has been shown that intestinal absorption by increasing the lipophilic properties of a ligand can be improved by lipidation suggesting that lipidation of peptides may increase, decrease, or have no influence on affinity (Bellmann-Sickert *et al.*, 2011).

Further, it has been suggested that Arg³ is an important residue for activity, since substituting Arg³ with Ala decreases the agonistic activity of peptides toward mouse NMU1 and NMU2 (Funes *et al.*, 2002). The PEG-free NM4A analogue, that utilized an *N*-terminal iminodiacetic acid mono-*N*-palmitoyl amide (Ida^{NHPal}), was discovered and used as it is a less expensive compared to NM4. It has been shown that it is at least 3.5 times more active than NM4 and hNmU-25 in *in vivo* testing and its anorectic effect may last up to ~20 days (Micewicz *et al.*, 2015). NM4 also contains an α,α -disubstituted amino acid (aminoisobutyric acid, Aib) that may confer increased resistance to enzymatic degradation (Yamaguchi *et al.*, 2003). It has been suggested that a key factor for the *in vivo* activity of NmU analogues may be their resistance to enzymatic proteolysis. For example, double-lipidated analogues, NM4A-C₁₆ and NM4-C₁₆, were synthesised in order to improve the pharmacokinetic properties, since plasma half-life should be increased as a result of the increased possibility/strength of hydrophobic interactions with abundant plasma proteins such as albumin (Madsen *et al.*, 2007). Plasma stability studies, as previously suggested (Eldridge *et al.*, 2014; Kang *et al.*, 2015), indicated that both NM4-C₁₆ and NM4A have significant resistance to mouse

plasma driven enzymatic degradation, compared to hNmU-25 that is quickly degraded falling to less than 1% of initial content within 4 h (Micewicz *et al.*, 2015). The low potency of many precursor peptides, including CCK and substance P, is due in part to the absence of C-terminal amidation as an affinity determinant (Eipper *et al.*, 1992). It has been suggested that membrane binding and membrane targeting of the modified proteins can be influenced by palmitoylation. Furthermore, the trafficking and function of transmembrane proteins including G-protein-coupled receptors can be regulated by palmitoylation (Resh, 2006). Thus, this is consistent with the current results in which some modified analogues with palmitoylation had lower potency compared to hNmU-25.

Following internalisation, receptors are generally trafficked to the endosomal compartment where acidification may result in ligand-receptor dissociation to allow further receptor trafficking. In order to assess the role of endosomal acidification in the re-sensitisation of NMU2 and to see whether it impacted on re-sensitisation with different ligands, monensin was used. As discussed in (**Chapter 3**) NMU2 re-sensitisation was markedly reduced by inhibition of endosomal acidification following treatment with hNmU-25 and hNmS-33. Here, the data demonstrated that re-sensitisation of NMU2-mediated Ca^{2+} responses were also significantly reduced following stimulation with NM1 or NM2. Moreover, in this experiment, following stimulation by either ligand, the cells were only allowed to recover for 6 h and it is not clear whether NMU2 recovery might differ at earlier time points to see whether small changes in amino acids could play a role in NMU2 re-sensitisation. This might be helpful in understanding the slow re-sensitisation seen following stimulation with hNmS-33. Interestingly, monensin increased the Ca^{2+} response to the first challenge of both NM1 and NM2. This is consistent with early experiments where cells were stimulated with hNmU-25 and hNmS-33; for more details of plausible explanations see (**3.4 Discussion**). The last seven amino acids (F-L-F-R-P-R-N) of NM1 and NM2 are identical to those of hNmU-25 and the potency of these analogues is also similar to that of hNmU-25 (pEC_{50} values= 9.24, 9.25 for NM1 and NM2, respectively and 8.97 for hNmU-25). This suggests these amino acids are indispensable for receptor binding and activation. This is consistent with idea that the bioactivity of NmU is mediated through

its C-terminal conserved region; FLFRPRN (Minamino *et al.*, 1985; Brighton *et al.*, 2004a).

In addition to endosomal acidification causing dissociation of the ligand-receptor complex, it has been suggested that ECE-1 activity may be required for the degradation of certain peptide ligands to allow receptor recycling and re-sensitization of signalling. It was demonstrated in an earlier chapter that inhibition of ECE-1 activity influenced NMU2 re-sensitisation following hNmU-25 but not hNmS-33 (**Chapter 3; Figure 3.15**). The effect of ECE-1 activity on the recovery of NM1- and NM2-mediated Ca^{2+} signalling in HEK-NMU2 was therefore examined. The ECE-1 inhibitor, SM-19712 inhibited recovery following desensitisation with either NM1 or NM2.

Having established that ECE-1 plays a role in the re-sensitisation of NMU2 following activation and desensitisation by some, but not all ligands, possibly through endosomal degradation, the degradation of peptide analogues by recombinant human (rhECE-1) was studied *in vitro*. Given the susceptibility of NM1- and NM2-mediated NMU2 re-sensitisation to ECE-1 inhibition, the hypothesis would be that endosomal ECE-1 degrades neuropeptides in endosomes to disrupt the peptide/receptor/ β -arrestins complex, freeing internalized receptors from β -arrestins and promoting recycling and re-sensitization. This is consistent with a previous study where ECE-1 regulated endosomal sorting of calcitonin receptor-like receptor and β -arrestins (Padilla *et al.*, 2007).

The peptide and peptide fragments present in the same samples of each of the peptide analogues analysed are shown. For NM1, the fragments identified were present at both pH 7.4 and 5.5 whether or not they had been exposed to rhECE-1, perhaps suggesting a lack of effect of rhECE-1, at least under these conditions. The reason for seeing these fragments is not clear but the data suggest that the fragments may have been present initially. Based on this, it is impossible to identify potential ECE-1-cleavage sites and further studies are required. In contrast to NM1, there were more fragments present in samples of NM2 that had been exposed to rhECE-1 than those that had not been exposed to the enzyme. This suggests some degradation of NM2 by rhECE-1, which is at least consistent with the ability of the ECE-1 inhibitor, SM-19712 to inhibit re-

sensitization (Padilla *et al.*, 2007). It can also be seen that the last amino acids that are well known to be important for the activity were conserved suggesting that this fragments could be active.

It has been reported that CGRP degradation may be promoted by endosomal acidification by enhancing ECE-1 activity or by causing CGRP dissociation from CLR/RAMP1. However, it is not clear whether receptor-associated peptide is degraded by ECE-1, since receptor-dissociated CGRP is probably degraded by ECE-1 (Roosterman *et al.*, 2007). The function of ECE-1 in endosomes is not clear. However, neuropeptides such as SP, BK, ATI, and neurotensin can be degraded by ECE-1 at an acidic endosomal pH 5.5. It has been reported that SP is degraded by ECE-1 in acidified endosomes and thus the SP/NK₁R/ β -arrestin complex is disrupted, and NK₁R recycling and re-sensitization is initiated (Roosterman *et al.*, 2007). It has been suggested that this mechanism requires that peptides are substrates for ECE-1 in acidified endosomes, and that receptors show sustained interactions with β -arrestins which are disrupted by endosomal acidification and peptide degradation (Roosterman *et al.*, 2007). It has also been demonstrated that there was no detectable degradation at up to 480 min when ATII was incubated with 83 nM rhECE-1 at pH 5.5 or 7.4, suggesting that some (CGRP, ATI, BK) but not all (ATII) vasoactive peptides are degraded by ECE-1. Furthermore, it has been reported that recycling of B₂R-V₂RCT is inhibited by SM-19712 showing sustained interaction with β -arrestins (Simaan *et al.*, 2005). Despite that ECE-1 inhibition did not affect recycling or re-sensitisation of B₂R, it has been reported that BK is degraded at pH 5.5 by ECE-1 and the B₂R agonist kallidin trafficked to endosomes containing ECE-1. It has been therefore suggested that this may be due to its low affinity interaction with β -arrestins. Taken together, current results are consistent with observations suggesting that ECE-1 promotes dissociation of GPCRs from β -arrestins in endosomes, presumably by reducing ligand-receptor interaction and thereby allowing receptors to recycle. For example, it has been shown ECE-1 inhibition/knockdown prevented CLR/RAMP1 recycling from endosomes (Roosterman *et al.*, 2007). In addition, inhibition of vacuolar H⁺-ATPase prevented CLR/RAMP1 recycling and the return of β -arrestin to the cytosol. Furthermore, ECE-1 inhibition prevented the translocation of β -arrestin from endosomes to the cytosol (Roosterman *et*

al., 2007). Thus, it has been suggested that ECE-1, by degrading CGRP in acidified endosomes, promotes dissociation of β -arrestins from CLR/RAMP1, accelerating the return of β -arrestins to the cytosol and of CLR/RAMP1 to the cell surface (Roosterman *et al.*, 2007).

Based on the final products of peptide degradation, an aim was also to determine the cleavage sites within the NM1 and NM2 analogues. The fragments were compared to the intact peptides and then the cleavages sides were identified in both conditions at either pH 5.5 or pH 7.4, so we can compare the cleavages site between each other. NM1 fragments were detected at both pH 5.5 and 7.4 either in the presence or absence of the rhECE-1. In contrast, more NM2 fragments were detected at pH 5.5 in the presence of rhECE-1, and these fragments were absent in the absence of rhECE-1 at pH 7.4. Also, it could be noticed that the recovery after 6 h in the presence of the ECE-1 inhibitor in cells stimulated with NM1 and NM2 was more than that with hNmU-25. The reason for that is not obvious. However, this could be because the inhibitor has modest effect on those analogues compared to hNmU-25. This could result from the structure of analogues and perhaps less dependence on ligand degradation for trafficking. Interestingly, following stimulation with some of the analogues (e.g. NM3) that recovery after 6 h was slower than even hNmS-33 and ECE-1 inhibitor had no effect on recovery. Although, it was not possible to assess all of the analogues, given the limited availability, there are a number that would certainly be worthy of further investigation, particularly in terms of their structure. This should include, for example, three of the potent/lipidated analogues including NM4, NM4A and NM4-C₁₆. NM4A-C₁₆ was effective in *in vivo* in a once weekly injection regimen and may be a promising start for the development of a novel anti-obesity therapeutic (Micewicz *et al.*, 2015).

In the current study, NmU analogues have been explored for agonist activity at NMU2, but it is also possible that antagonists may be of clinical use for some disorders including chronic pain, anorexia and osteoporosis. There are few reports of NMU antagonists although (R)5'(phenylaminocarbonylamino)spiro[1-azabicyclo[2.2.2]octane-3,2'(3'H)-furo[2,3-b]pyridine] (R-PSOP), has been identified as a potent and selective NMU2 antagonist (Liu *et al.*, 2009). It is likely that the binding site for the peptide agonists is well conserved between NMU1 and NMU2 given the

lack of selectivity of established agonists. Nonetheless, R-PSOP achieve more than 200-fold selectivity at NMU2 over NMU1. R-PSOP could be prevented from reaching the binding pocket by some steric effects from certain divergent residues on NMU1 (Liu *et al.*, 2009a). Although no compounds with antagonist activity were identified in the present study, at least some are likely to be partial agonists and have, therefore the potential to act as functional antagonists.

NM2, NM4 and NM5 analogues were chosen to examine β -arrestin-2 recruitment by activated NMU1. They were chosen due to their availability in addition to their similarity to hNmU-25 in terms of pEC₅₀ (NM2 and NM4) or low potency (NM5). The data obtained from PathHunter™ assay indicated that both NM2 and NM4 have the same pEC₅₀ as hNmU-25. pEC₅₀ values for NM2, NM4 and hNmU-25 were 7.54, 7.11 and 7.81, respectively. In addition, the pEC₅₀ value for NM5 was 5.82. These data reveal lower potency on arrestin recruitment than Ca²⁺ responses, which is to be expected as the Ca²⁺ response will involve amplification whereas the arrestin recruitment will be dependent on receptor phosphorylation and therefore receptor occupancy. For the analogues NM2, NM4 and NM5 analogues, the pEC₅₀ values determined in the PathHunter™ assay were significantly lower than their pEC₅₀ in the Ca²⁺ assay. These data are consistent with a previous published paper using different agonists and showed different pEC₅₀ values between these agonist using two different approach including PathHunter™ and Ca²⁺ assays and it has been suggested that a different agonist-bound receptor conformation could be measured by the PathHunter™ assay (Riddy *et al.*, 2012). It has also been indicated that low-affinity agonist compound would not be detected and it was therefore suggested that highly amplified and more traditional assays are required to identify ligands with low efficacy.

Future directions and considerations

The data presented in this thesis demonstrate that ECE-1 activity regulates re-sensitisation of NMU2-mediated signalling and aspects of NMU2-dependent signalling. It has been demonstrated that ECE-1 activity is important for the endosomal degradation of some neuropeptides such as substance P (Roosterman *et al.*, 2007b) and our data suggest that such endosomal processing of other peptide ligands may be possible. The accepted theory of receptor trafficking (**Figure 1.7**) would suggest that following internalisation, the newly formed endosomal compartment undergoes acidification over a period of ~10 min (Mellman *et al.*, 1986). The endosomal acidification (to approximately pH 5.5) (Zen *et al.*, 1992) is involved in promoting dissociation of the ligand from the receptor and this may expose the ligand to endosomally-located proteases, including ECE-1. The degradation of the ligand therefore could prevent any re-association and possibly allow the receptor to adopt a conformation that causes disassociation of the receptor- β -arrestin complex, receptor dephosphorylation and the events required for recycling.

The data in this thesis suggest that receptor recycling following internalisation is important for NMU2 re-sensitisation. Studies have demonstrated that internalization of β_2 -adrenergic receptor and angiotensin II type 1A receptor is considerably impaired in the absence of β -arrestins (Lefkowitz *et al.*, 2005; DeWire *et al.*, 2007). On the other hand, it has been observed that protease-activated receptor 1 internalization is not dependent on the presence of β -arrestins (Lefkowitz *et al.*, 2005; DeWire *et al.*, 2007). Therefore, it is highly recommended to determine whether β -arrestins isoforms are involved in NMUs internalization.

Peptide ligands of the NMU receptors co-internalise and targeting to endosomes. Following acidification the charges and their distribution on amino acids will result in conformational changes of the peptide ligand and/or the receptor thereby facilitating the dissociation of ligand-receptor complex (Mellman *et al.*, 1986) and ultimately potentially degradation by endosomally located proteases that are able to operate under these acidic conditions. Interestingly, another metalloendopeptidase, endopeptidase

24.15, interacts with the C-terminal tails of the AT₁ and bradykinin B₂ receptors at the plasma membrane and after receptor endocytosis (Shivakumar *et al.*, 2005), implying the possibility of degradation of receptor-associated peptide by endopeptidase or at least placing the enzyme in close proximity to the ligand when it dissociates from the receptor. It is possible that ECE-1 is scaffolded directly to, or alternatively in the vicinity of receptors. The acid wash has been used in order to remove cell-surface bound ligand (Widmann *et al.*, 1997; Haugh *et al.*, 1999; Li *et al.*, 2008). Our data indicated that removing bound ligand by an acid wash enhanced the rate of NMU2 re-sensitisation. Therefore, our data indicated that the presence of ligand influences NMU2 re-sensitisation, potentially by influencing receptor recycling but it is unclear if the plasma membrane receptors from which ligand has been removed subsequently internalise. It has also been indicated that the role of ECE-1 in regulating receptor recycling and re-sensitisation was not only ligand-dependent, but also dependent on the concentration of agonists. Thus, corticotropin-releasing factor (CRF) and urocortin 1 (Ucn1), for instance, are agonists for CRF1 and are also both substrates for ECE-1. ECE-1 regulates Ucn1-induced CRF1 recycling and re-sensitisation independent of the concentration of agonist whereas it influences CRF-induced CRF1 trafficking at near K_D concentration but not at higher concentrations (Hasdemir *et al.*, 2012). The mechanisms underlying this are not entirely clear but, based on the mechanisms of receptor endocytosis and post-endocytic trafficking that are dependent on the concentration of ligand (**See Chapter 3, Discussion**), it could be that high concentrations of agonist result in receptor trafficking through a different route where ECE-1 is not present or alternatively another protease(s) play(s) a more prominent role in degradation. It has been suggested that the high concentration of CRF triggers receptor trafficking through a Rab11-associated pathway whereas the pathway is unclear for the low concentration (Hasdemir *et al.*, 2012).

Data revealed that ECE-1 activity reduced ERK1/2 activation when hNmU-25 was added but then removed showing that NMU2-mediated ERK1/2 activation is regulated by ECE-1, possibly through a G protein-independent but β -arrestin dependent manner. The mechanism could be that hNmU-25 is cleaved by ECE-1 in the endosomes and the disassociation of ligand-receptor complex is facilitated reducing the binding of β -

arrestin thereby preventing its scaffolding function, specifically the recruitment of components of the MAPK signalling pathway including ERK. Furthermore, the cellular location of ERKs activated by GPCRs was shown to be dependent on the pathway that mediated their activity. For instance, ERKs activated via G protein-dependent pathway were shown to translocate to the nucleus, whereas β -arrestin-activated ERKs remained in the cytosol (Ahn *et al.*, 2004). However, it was not possible to define the sub-cellular distribution of pERK, since the immunofluorescence experiments had relatively low sensitivity compared to immunoblotting. Thus, more studies are required even using different techniques.

The results described in the present thesis are predominantly on the use the maximum concentrations of ligands, so such differences may not have been apparent. Interestingly, however, using a high, supra-maximal concentration of hNmU-25 (300 nM & 1 μ M) led to delaying the recovery after six h with hNmU-25 and the ECE-1 inhibitor had an effect on the re-sensitisation. On the other hand, using a low concentration (3 nM) prolonged pERK in the presence of ECE-1 inhibitor when the cells were stimulated with hNmU-25 but not hNmS-33. Thus, the study of using high concentration to see if there is any effect on ERK stimulation is strongly recommended. Notably, ECE-1 cleaves Ucn1 at critical residues which are responsible for ligand-receptor binding whereas the cleavage product(s) of CRF retain(s) high affinity for the receptor (Hasdemir *et al.*, 2012). There is also the possibility that when one or more of the proteolytic products has a reduced affinity for binding to the receptor, proteolysis of the released peptide-ligand from the receptor induced by the acidic pH in endosomes prevents the re-association thereby facilitating the dissociation rate and promoting recycling. On the other hand, if the product has high affinity for the receptor, ligand proteolysis in endosomes would have less impact on preventing ligand-receptor interaction and inhibition of proteolysis may, therefore, have little or no effect on either recycling or re-sensitisation. This indicates the importance of determining the ECE-1 cleavage site(s) within peptides and developing an understanding of their pharmacology. Therefore, because of rhECE-1 experiments for all ligands, the final products and the expected cleavage sides were identified. It was shown early in this thesis that NMU2 recovery was inhibited using ECE-1 inhibitor following cells

stimulation with hNmU-25 but neither hNmS-33 nor pNmU-8, suggesting the susceptibility of hNmU-25 for degradation by ECE-1 and hNmS-33 and pNmU-8 were not sensitive for SM-19712. rhECE-1 experiments, on the other hand, indicated that all ligands were degraded with some differences in terms of the numbers of fragments that were generated of each ligand. The potential cleavage sites *in vitro* might be identified; and these cleavage sites, on the other hand, may not relate to actual cleavage sites *in vivo*, suggesting that other protease could be involved.

CCX-CKR, (high affinity receptor for the chemokines) interaction with β -arrestins and G protein has been proposed (Watts *et al.*, 2013). Chemokine binding to CCX-CKR recruits G_i proteins and β -arrestin with high affinity hindering the low affinity interaction between CCX-CKR and G_{α_s} proteins. Inactive G_{α_i} protein may stay bound to CCX-CKR, whereas the chemokine-bound CCX-CKR internalizes with β -arrestin. Inhibition of G_{α_i} coupling to CCX-CKR by PTX pre-treatment did not affect β -arrestin recruitment. In contrast, it allows G_{α_s} to interact with CCX-CKR, resulting in stimulation of AC and this in turn increases cAMP levels. Because the NMUs have the ability to bind to G_{α_i} and G_{α_q} , it is strongly recommended to examine this possibility to see the effect of knocking down β -arrestins in the presence and absence of G_{α_i} inhibitor, PTX.

This study did not directly investigate GPCR/ β -arrestin interactions. Thus, in order to understand the nature of such interaction and whether, for example, the nature and temporal profile differs between the different ligands, techniques such as bioluminescence resonance energy transfer (BRET) or fluorescence resonance energy transfer (FRET) are strongly recommended to be exploited to investigate this issue.

It has been widely assumed that the production of cAMP, which is mediated by cell surface (GPCRs), and its termination take place exclusively at the plasma membrane. Recent studies have revealed that diverse GPCRs do not always follow this conventional paradigm. In the new model, GPCRs mediate G-protein signalling not only from the plasma membrane but also from endosomal membranes (Vilardaga *et al.*, 2014).

Classically, it is thought that (GPCRs) with dissociable agonists signal transiently at the cell surface and that the signalling pathway is rapidly desensitized by several mechanisms including receptor internalization. Recent studies, on the other hand, indicated that certain GPCRs continue to either stimulate or inhibit cAMP signalling or stimulate phosphoinositide signalling. In terms of persistent signalling after withdrawal of ligand, it has been recently suggested that some GPCRs including, thyrotropin receptor (TSHR), could do so via both the cAMP and inositol-1,4,5-trisphosphate pathways (Boutin *et al.*, 2012). In addition, the parathyroid hormone receptor stimulating the cAMP pathway and the sphingosine-1-phosphate receptor 1 (S1P1) receptor inhibiting the cAMP pathway, have been shown to persistently signal (Okazaki *et al.*, 2008; Mullershausen *et al.*, 2009). Because this possibility has not been examined, it is strongly recommended to study this possibility using NMUs. This in turn will help us to develop ligands that have improved efficacies for treating diseases by targeting GPCR in specific cellular location such as endosomes.

Functional selectivity (ligand bias) is the ligand-dependent selectivity for certain signal transduction pathways in the same receptor. This can be present when a receptor has several possible signal transduction pathways, in our case via $G_{\alpha q}$ and $G_{\alpha i}$. Biased ligands have been proposed to stabilize receptor conformations that are distinct from those induced by unbiased ligands and selectively change the ability of GPCR coupling to either G-proteins or β -arrestins (Reiter *et al.*, 2012). It is recommend trying these analogues to check the possibility of ligand bias using crystal structures techniques since GPCR crystal structure have shown potential structural bases for ligand bias (Wacker *et al.*, 2013). In addition to this and as mentioned early that both ligands; hNmU-25 and hNmS-33 behave differentially in terms of NMU2 re-sensitisation and ERK activation following stimulation with each ligand separately. Also, the slower recovery of NMU2 following stimulation with hNmS-33 is consistent with observations that compound 2 (a small molecule agonist of the GLP-1R) is biased for β -arrestin1 and β -arrestin2 recruitment relative to Ca^{2+} and cAMP responses (Wootten *et al.*, 2013) and it has been suggested that the reduced rate of re-sensitisation may be caused due to this matter (biased). Different functional consequences including different downstream signalling and the differential recruitment of proteins such as β -arrestin may be

generated by different kinases due to receptor phosphorylation (Tobin, 2008). Thus, hNmS-33 may expose different phosphorylation sites on the NMU2 compared to hNmU-25, and it would be worth of exploration this issue.

It has been suggested that GPCRs dimers or oligomers can be formed leading to modification of receptor function (Ferre *et al.*, 2014). Potential dimerization for class A GPCRs has been identified (Huang *et al.*, 2013). Therefore, it is a good idea to investigate such possibilities using, for example BiFC (Kilpatrick *et al.*, 2015).

References

Abassi Z, Golomb E, Keiser HR (1992). Neutral endopeptidase inhibition increases the urinary excretion and plasma levels of endothelin. *Metabolism* 41: 683-685.

Adachi M, Fukuda M, Nishida E (2000). Nuclear export of MAP kinase (ERK) involves a MAP kinase kinase (MEK)-dependent active transport mechanism. *Journal of Cell Biology* 148: 849-856.

Ahmed SI, Thompson J, Coulson JM, Woll PJ (2000). Studies on the expression of endothelin, its receptor subtypes, and converting enzymes in lung cancer and in human bronchial epithelium: 1. *American Journal of Respiratory Cell and Molecular Biology* 22: 422-431.

Ahn K, Sisneros AM, Herman SB, Pan SM, Hupe D, Lee C, *et al.* (1998). Novel selective quinazoline inhibitors of endothelin converting enzyme-1. *Biochemical and Biophysical Research Communications* 243: 184-190.

Ahn KH, Mahmoud MM, Shim JY, Kendall DA (2013). Distinct roles of β -arrestin 1 and β -arrestin 2 in ORG27569-induced biased signalling and internalization of the cannabinoid receptor 1 (CB1). *Journal of Biological Chemistry* 288: 9790-9800.

Ahn S, Shenoy SK, Wei H, Lefkowitz RJ (2004). Differential kinetic and spatial patterns of β -arrestin and G protein-mediated ERK activation by the angiotensin II receptor. *Journal of Biological Chemistry* 279: 35518-35525.

Aiyar N, Disa J, Foley JJ, Buckley PT, Wixted WE, Pullen M, *et al.* (2004). Radioligand binding and functional characterization of recombinant human NMU1 and NMU2 receptors stably expressed in clonal human embryonic kidney-293 cells. *Pharmacology* 72: 33-41.

Alexander SPH, Mathie A, Peters JA (2008). Guide to receptors and channels (GRAC). *British Journal of Pharmacology* 153: S1-S209.

Alhosaini K (2011). *Signalling, desensitization and resensitization of Neuromedin U receptors*. Unpublished PhD thesis. Leicester University.

Amsen EM, Pham N, Pak Y, Rotin D (2006). The guanine nucleotide exchange factor CNrasGEF regulates melanogenesis and cell survival in melanoma cells. *Journal of Biological Chemistry* 281: 121-128.

Anborgh PH, Seachrist JL, Dale LB, Ferguson SS (2000). Receptor/ β -arrestin complex formation and the differential trafficking and resensitization of β 2-adrenergic and angiotensin II type 1A receptors. *Journal of Molecular Endocrinology* 14: 2040-2053.

Atsuchi K, Asakawa A, Ushikai M, Ataka K, Tanaka R, Kato I, *et al.* (2010). Centrally administered Neuromedin S inhibits feeding behavior and gastroduodenal motility in mice. *Hormone and Metabolic Research* 42: 535-538.

Austin C, Lo G, Nandha KA, Meleagros L, Bloom SR (1995). Cloning and characterization of the cDNA encoding the human Neuromedin U (NMU) precursor: NMU expression in the human gastrointestinal tract. *Journal of Molecular Endocrinology* 14: 157-169.

Azarani A, Boileau G, Crine P (1998). Recombinant human endothelin-converting enzyme ECE-1b is located in an intracellular compartment when expressed in polarized madin-darby canine kidney cells. *Biochemical Journal* 333: 439-448.

Azzi M, Charest PG, Angers S, Rousseau G, Kohout T, Bouvier M, *et al.* (2003). β -arrestin-mediated activation of MAPK by inverse agonists reveals distinct active conformations for G protein-coupled receptors. *Proceedings of the National Academy of Sciences of the United States of America* 100: 11406-11411.

Beaulieu JM, Sotnikova TD, Marion S, Lefkowitz RJ, Gainetdinov RR, Caron MG (2005). An AKT/ β -arrestin 2/PP2A signalling complex mediates dopaminergic neurotransmission and behavior. *Cell* 122: 261-273.

Bechtold DA, Ivanov TR, Luckman SM (2009). Appetite-modifying actions of pro-Neuromedin U-derived peptides. *American Journal of Physiology, Endocrinology and Metabolism* 297: E545-551.

Belcheva MM, Clark AL, Haas PD, Serna JS, Hahn JW, Kiss A, et al. (2005). Mu and kappa opioid receptors activate ERK/MAPK via different protein kinase C isoforms and secondary messengers in astrocytes. *Journal of Biological Chemistry* 280: 27662-27669.

Bellmann-Sickert K, Elling CE, Madsen AN, Little PB, Lundgren K, Gerlach LO, et al. (2011). Long-acting lipidated analogue of human pancreatic polypeptide is slowly released into circulation. *Journal of Medicinal Chemistry* 54: 2658-2667.

Benard O, Naor Z, Seger R (2001). Role of dynamin, src, and ras in the protein kinase C-mediated activation of ERK by gonadotropin-releasing hormone. *Journal of Biological Chemistry* 276: 4554-4563.

Bennett VJ, Perrine SA, Simmons MA (2002). A novel mechanism of neurokinin-1 receptor resensitization. *Journal of Pharmacology and Experimental Therapeutics* 303: 1155-1162.

Benovic JL, Bouvier M, Caron MG, Lefkowitz RJ (1988). Regulation of adenylyl cyclase-coupled β -adrenergic receptors. *Annual Review of Cell Biology* 4: 405-428.

Benovic JL, DeBlasi A, Stone WC, Caron MG, Lefkowitz RJ (1989). β -adrenergic receptor kinase: Primary structure delineates a multigene family. *Science* 246: 235-240.

Benzon CR, Johnson SB, McCue DL, Li D, Green TA, Hommel JD (2014). Neuromedin U receptor 2 knockdown in the paraventricular nucleus modifies behavioral responses to obesogenic high-fat food and leads to increased body weight. *Neuroscience* 258: 270-279.

Beom S, Cheong D, Torres G, Caron MG, Kim KM (2004). Comparative studies of molecular mechanisms of dopamine D2 and D3 receptors for the activation of extracellular signal-regulated kinase. *Journal of Biological Chemistry* 279: 28304-28314.

Berridge MJ, Lipp P, Bootman MD (2000). The versatility and universality of calcium signalling. *Nature Reviews Molecular Cell Biology* 1: 11-21.

Berts A, Zhong HY, Minneman KP (1999). No role for Ca⁺⁺ or protein kinase C in α -1A adrenergic receptor activation of mitogen-activated protein kinase pathways in transfected PC₁₂ cells. *Molecular Pharmacology* 55: 296-303.

Bialojan C, Takai A (1988). Inhibitory effect of a marine-sponge toxin, okadaic acid, on protein phosphatases. Specificity and kinetics. *Biochemical Journal* 256: 283-290.

Biron E, Chatterjee J, Ovadia O, Langenegger D, Brueggen J, Hoyer D, *et al.* (2008). Improving oral bioavailability of peptides by multiple n-methylation: Somatostatin analogues. *Angewandte Chemie International Edition* 47: 2595-2599.

Biscardi JS, Maa MC, Tice DA, Cox ME, Leu TH, Parsons SJ (1999). C-Src-mediated phosphorylation of the epidermal growth factor receptor on Tyr845 and Tyr1101 is associated with modulation of receptor function. *Journal of Biological Chemistry* 274: 8335-8343.

Bjarnadottir TK, Gloriam DE, Hellstrand SH, Kristiansson H, Fredriksson R, Schioth HB (2006). Comprehensive repertoire and phylogenetic analysis of the G protein-coupled receptors in human and mouse. *Genomics* 88: 263-273.

Blais V, Fugere M, Denault JB, Klarskov K, Day R, Leduc R (2002). Processing of proendothelin-1 by members of the subtilisin-like pro-protein convertase family. *FEBS Letters* 524: 43-48.

Blaukat A, Barac A, Cross MJ, Offermanns S, Dikic I (2000). G protein-coupled receptor-mediated mitogen-activated protein kinase activation through cooperation of G α (q) and G α (i) signals. *Molecular Cell Biology* 20: 6837-6848.

Blaukat A, Pizard A, Breit A, Wernstedt C, Alhenc-Gelas F, Muller-Esterl W, *et al.* (2001). Determination of bradykinin B2 receptor in vivo phosphorylation sites and their role in receptor function. *Journal of Biological Chemistry* 276: 40431-40440.

Bockaert J, Pin JP (1999). Molecular tinkering of G protein-coupled receptors: An evolutionary success. *EMBO Journal* 18: 1723-1729.

Bode W, Gomis-Ruth FX, Stockler W (1993). Astacins, serralytins, snake venom and matrix metalloproteinases exhibit identical zinc-binding environments (HEXXHXXGXXH and Met-turn) and topologies and should be grouped into a common family, the 'metzincins'. *FEBS Letters* 331: 134-140.

Bohm SK, Grady EF, Bunnett NW (1997). Regulatory mechanisms that modulate signalling by G protein-coupled receptors. *Biochemical Journal* 322: 1-18.

Bos JL (2006). EPAC proteins: Multi-purpose cAMP targets. *Trends in Biochemical Sciences* 31: 680-686.

Boughton CK, Murphy KG (2013). Can neuropeptides treat obesity? A review of neuropeptides and their potential role in the treatment of obesity. *British journal of pharmacology* 170: 1333-1348.

Boutin A, Allen MD, Neumann S, Gershengorn MC (2012). Persistent signalling by thyrotropin-releasing hormone receptors correlates with G-protein and receptor levels. *FASEB Journal* 26: 3473-3482.

Brauner-Osborne H, Wellendorph P, Jensen AA (2007). Structure, pharmacology and therapeutic prospects of family C G protein coupled receptors. *Current Drug Targets* 8: 169-184.

Brighton P (2005). The activation and regulation of mammalian neuromedin u receptor isoforms. *Unpublished PhD thesis. Leicester University.*

Brighton PJ, Szekeres PG, Willars GB (2004a). Neuromedin U and its receptors: Structure, function, and physiological roles. *Pharmacology Reveiw* 56: 231-248.

Brighton PJ, Szekeres PG, Wise A, Willars GB (2004b). Signalling and ligand binding by recombinant Neuromedin U receptors: Evidence for dual coupling to $G\alpha/11$ and $G\alpha_i$ and an irreversible ligand-receptor interaction. *Molecular Pharmacology* 66: 1544-1556.

Brighton PJ, Wise A, Dass NB, Willars GB (2008). Paradoxical behavior of Neuromedin U in isolated smooth muscle cells and intact tissue. *Journal of Pharmacology and Experimental Therapeutics* 325: 154-164.

Brighton PJ, Rana S, Challiss RJ, Konje JC, Willets JM (2011). Arrestins differentially regulate histamine- and oxytocin-evoked phospholipase c and mitogen-activated protein kinase signalling in myometrial cells. *British Journal of Pharmacology* 162: 1603-1617.

Brooks SC, Fernandez L, Ergul A (2000). Secretion of endothelin converting enzyme-1a: The hydrophobic signal anchor domain alone is not sufficient to promote membrane localization. *Molecular and Cellular Biochemistry* 208: 45-51.

Brunet A, Roux D, Lenormand P, Dowd S, Keyse S, Pouyssegur J (1999). Nuclear translocation of p42/p44 mitogen-activated protein kinase is required for growth factor-induced gene expression and cell cycle entry. *EMBO Journal* 18: 664-674.

Burgering BM, Bos JL (1995). Regulation of Ras-mediated signalling: More than one way to skin a cat. *Trends in Biochemical Sciences* 20: 18-22.

Cabrera-Vera TM, Vanhauwe J, Thomas TO, Medkova M, Preininger A, Mazzone MR, *et al.* (2003). Insights into G protein structure, function, and regulation. *Endocrine Reviews* 24: 765-781.

Cahalan MD (2009). Stimulating store-operated Ca(2+) entry. *Nature Cell Biology* 11: 669-677.

Campfield LA, Smith FJ, Guisez Y, Devos R, Burn P (1995). Recombinant mouse OB protein: Evidence for a peripheral signal linking adiposity and central neural networks. *Science* 269: 546-549.

Carriba P, Pardo L, Parra-Damas A, Lichtenstein MP, Saura CA, Pujol A, *et al.* (2012). ATP and noradrenaline activate CREB in astrocytes via noncanonical Ca(2+) and cyclic AMP independent pathways. *Glia* 60: 1330-1344.

Carter AA, Hill SJ (2005). Characterization of isoprenaline- and salmeterol-stimulated interactions between β 2-adrenoceptors and β -arrestin 2 using β -galactosidase complementation in C₂C₁₂ cells. *Journal of Pharmacology and Experimental Therapeutics* 315: 839-848.

Castro-Obregon S, Rao RV, del Rio G, Chen SF, Poksay KS, Rabizadeh S, *et al.* (2004). Alternative, nonapoptotic programmed cell death: Mediation by arrestin 2, ERK2, and NUR77. *Journal of Biological Chemistry* 279: 17543-17553.

Chang Y, Ghansah E, Chen Y, Ye J, Weiss DS (2002). Desensitization mechanism of GABA receptors revealed by single oocyte binding and receptor function. *Journal Neuroscience* 22: 7982-7990.

Chen-Izu Y, Xiao RP, Izu LT, Cheng H, Kuschel M, Spurgeon H, *et al.* (2000). G(i)-dependent localization of β 2-adrenergic receptor signalling to l-type Ca²⁺ channels. *Biophysics Journal* 79: 2547-2556.

Chen BC, Lin WW (2001). PKC- and ERK-dependent activation of I κ B kinase by lipopolysaccharide in macrophages: Enhancement by P2Y receptor-mediated CaMK activation. *British Journal Pharmacology* 134: 1055-1065.

Chen RH, Sarnecki C, Blenis J (1992). Nuclear localization and regulation of ERK- and RSK-encoded protein kinases. *Molecular Cell Biology* 12: 915-927.

Chen T, Zhou M, Walker B, Harriot P, Mori K, Miyazato M, *et al.* (2006). Structural and functional analogs of the novel mammalian neuropeptide, Neuromedin S (NMS), in the dermal venoms of eurasian bombinid toads. *Biochemical and Biophysical Research Communications* 345: 377-384.

Chen Z, Singer WD, Sternweis PC, Sprang SR (2005). Structure of the p115RhoGEF rgRGS domain-G $\alpha_{13/i1}$ chimera complex suggests convergent evolution of a GTPase activator. *Nature Structural and Molecular Biology* 12: 191-197.

Chu C, Jin Q, Kunitake T, Kato K, Nabekura T, Nakazato M, *et al.* (2002). Cardiovascular actions of central Neuromedin U in conscious rats. *Regulatory Peptides* 105: 29-34.

Chuderland D, Konson A, Seger R (2008). Identification and characterization of a general nuclear translocation signal in signalling proteins. *Molecular Cell* 31: 850-861.

Cohen P, Klumpp S, Schelling DL (1989). An improved procedure for identifying and quantitating protein phosphatases in mammalian-tissues. *FEBS Letters* 250: 596-600.

Conlon JM, Domin J, Thim L, DiMarzo V, Morris HR, Bloom SR (1988). Primary structure of Neuromedin U from the rat. *Journal of Neurochemistry* 51: 988-991.

Conway AM, Rakhit S, Pyne S, Pyne NJ (1999). Platelet-derived-growth-factor stimulation of the p42/p44 mitogen-activated protein kinase pathway in airway smooth muscle: Role of pertussis-toxinsensitive G-proteins, c-Src tyrosine kinases and phosphoinositide 3-kinase. *Biochemical Journal* 337: 171-177.

Cook SJ, McCormick F (1993). Inhibition by camp of Ras-dependent activation of Raf. *Science* 262: 1069-1072.

Coopman K, Huang Y, Johnston N, Bradley SJ, Wilkinson GF, Willars GB (2010). Comparative effects of the endogenous agonist glucagon-like peptide-1 (GLP-1)-(7-36) amide and the small-molecule ago-allosteric agent "compound 2" at the GLP-1 receptor. *Journal of Pharmacology and Experimental Therapeutics* 334: 795-808.

Cordeaux Y, Hill SJ (2002). Mechanisms of cross-talk between G-protein-coupled receptors. *Neurosignals* 11: 45-57.

Cottrell GS, Padilla B, Pikios S, Roosterman D, Steinhoff M, Grady EF, *et al.* (2007). Post-endocytic sorting of calcitonin receptor-like receptor and receptor activity-modifying protein 1. *Journal of Biological Chemistry* 282: 12260-12271.

Cottrell GS, Padilla B, Pikios S, Roosterman D, Steinhoff M, Gehringer D, *et al.* (2006). Ubiquitin-dependent down-regulation of the neurokinin-1 receptor. *Journal of Biological Chemistry* 281: 27773-27783.

Cottrell GS, Padilla BE, Amadesi S, Poole DP, Murphy JE, Hardt M, *et al.* (2009). Endosomal endothelin-converting enzyme-1: A regulator of β -arrestin-dependent ERK signalling. *Journal of Biological Chemistry* 284: 22411-22425.

Crespo P, Xu N, Simonds WF, Gutkind JS (1994a). Ras-dependent activation of MAP kinase pathway mediated by G-protein $\beta\gamma$ subunits. *Nature* 369: 418-420.

Crespo P, Xu NZ, Daniotti JL, Troppmair J, Rapp UR, Gutkind JS (1994b). Signalling through transforming g-protein-coupled receptors in NIH 3T3 cells involves c-Raf activation - evidence for a protein kinase-C-independent pathway. *Journal of Biological Chemistry* 269: 21103-21109.

Cruz PG, Norte M, Creus AH, Fernandez JJ, Daranas AH (2013). Self-association of okadaic acid: Structural and pharmacological significance. *Marine Drugs* 11: 1866-1877.

D'Anneo A, Carlisi D, Emanuele S, Buttitta G, Di Fiore R, Vento R, *et al.* (2013). Parthenolide induces superoxide anion production by stimulating EGF receptor in MDA-MB-231 breast cancer cells. *International Journal of Oncology* 43: 1895-1900.

Kamoto D, Thach L, Bernard R, Chan V, Zheng W, Kaur H, *et al.* (2015). Structure, function, pharmacology, and therapeutic potential of the G protein, G α /q,11. *Frontiers in Cardiovascular Medicine* 2: 1-11.

Dass NB, Bassil AK, North-Laidler VJ, Morrow R, Aziz E, Tuladhar BR, *et al.* (2007). Neuromedin U can exert colon-specific, enteric nerve-mediated prokinetic activity, via a pathway involving NMU1 receptor activation. *British Journal of Pharmacology* 150: 502-508.

Daub H, Weiss FU, Wallasch C, Ullrich A (1996). Role of transactivation of the EGF receptor in signalling by G protein-coupled receptors. *Nature* 379: 557-560.

Daub H, Wallasch C, Lanckenau A, Herrlich A, Ullrich A (1997). Signal characteristics of G protein-transactivated EGF receptor. *EMBO Journal* 16: 7032-7044.

Davenport AP, Maguire JJ (2006). Endothelin. In, edn, Vol. 176/I. Berlin, Heidelberg: Springer Berlin Heidelberg. pp 295-329.

Davis PD, Hill CH, Keech E, Lawton G, Nixon JS, Sedgwick AD, *et al.* (1989). Potent selective inhibitors of protein kinase-C. *FEBS Letters* 259: 61-63.

Dawson AP (1997). Calcium signalling: How do IP₃ receptors work? *Current Biology* 7: R544-R547.

Dawson LA, Maitland NJ, Berry P, Turner AJ, Usmani BA (2006). Expression and localization of endothelin-converting enzyme-1 in human prostate cancer. *Experimental Biology and Medicine* 231: 1106-1110.

Day JW, Ottaway N, Patterson JT, Gelfanov V, Smiley D, Gidda J, *et al.* (2009). A new glucagon and GLP-1 co-agonist eliminates obesity in rodents. *Nature Chemical Biology* 5: 749-757.

DeFea KA, Zalevsky J, Thoma MS, Dery O, Mullins RD, Bunnett NW (2000). β -arrestin-dependent endocytosis of proteinase-activated receptor 2 is required for intracellular targeting of activated ERK1/2. *Journal of Cell Biology* 148: 1267-1281.

DellaRocca GJ, vanBiesen T, Daaka Y, Luttrell DK, Luttrell LM, Lefkowitz RJ (1997). Ras-dependent mitogen-activated protein kinase activation by G protein-coupled receptors - convergence of G_i - and G_q -mediated pathways on calcium/calmodulin, PYK2, and Src kinase. *Journal of Biological Chemistry* 272: 19125-19132.

Devaraj S, Maitra A (2014). Pancreatic safety of newer incretin-based therapies: Are the "-tides" finally turning? *Diabetes* 63: 2219-2221.

DeWire SM, Ahn S, Lefkowitz RJ, Shenoy SK (2007). β -arrestins and cell signalling. *Annual Reviews Physiology* 69: 483-510.

Dhillon AS, Pollock C, Steen H, Shaw PE, Mischak H, Kolch W (2002). Cyclic AMP-dependent kinase regulates Raf-1 kinase mainly by phosphorylation of serine 259. *Molecular Cell Biology* 22: 3237-3246.

Dikic I, Tokiwa G, Lev S, Courtneidge SA, Schlessinger J (1996). A role for PYK2 and Src in linking G protein-coupled receptors with MAP kinase activation. *Nature* 383: 547-550.

Domin J, Ghatei MA, Chohan P, Bloom SR (1986). Characterization of Neuromedin U like immunoreactivity in rat, porcine, guinea-pig and human tissue extracts using a specific radioimmunoassay. *Biochemical and Biophysical Research Communications* 140: 1127-1134.

Domin J, Benito-Orfila MA, Nandha KA, Aitken A, Bloom SR (1992). The purification and sequence analysis of an avian Neuromedin U. *Regulatory Peptides* 41: 1-8.

Domin J, Yiangou YG, Spokes RA, Aitken A, Parmar KB, Chrysanthou BJ, *et al.* (1989). The distribution, purification, and pharmacological action of an amphibian Neuromedin U. *Journal of Biological Chemistry* 264: 20881-20885.

Drake MT, Shenoy SK, Lefkowitz RJ (2006). Trafficking of G protein-coupled receptors. *Circulation Research* 99: 570-582.

Dumaz N, Marais R (2005). Integrating signals between camp and the Ras/Raf/MEK/ERK signalling pathways - based on the anniversary prize of the Gesellschaft für biochemie und molekularbiologie lecture delivered on 5 July 2003 at the special febs meeting in brussels. *FEBS Journal* 272: 3491-3504.

Egecioglu E, Ploj K, Xu X, Bjursell M, Salome N, Andersson N, *et al.* (2009). Central NMU signalling in body weight and energy balance regulation: Evidence from NMUR2 deletion and chronic central NMU treatment in mice. *American Journal Physiology Endocrinology Metabolsim* 297: E708-716.

Eguchi S, Frank GD, Mifune M, Inagami T (2003). Metalloprotease-dependent ErbB ligand shedding in mediating EGFR transactivation and vascular remodelling. *Biochemical Society Transactions* 31: 1198-1202.

Eguchi S, Numaguchi K, Iwasaki H, Matsumoto T, Yamakawa T, Utsunomiya H, *et al.* (1998). Calcium-dependent epidermal growth factor receptor transactivation mediates the angiotensin II-induced mitogen-activated protein kinase activation in vascular smooth muscle cells. *Journal of Biological Chemistry* 273: 8890-8896.

Eipper BA, Stoffers DA, Mains RE (1992). The biosynthesis of neuropeptides - peptide α -amidation. *Annual Reviews Neuroscience* 15: 57-85.

Eishingdrelo H, Kongsamut S (2013). Minireview: Targeting GPCR activated ERK pathways for drug discovery. *Current Chemical Genomics and Translational Medicine* 7: 9-15.

Eldridge JA, Milewski M, Stinchcomb AL, Crooks PA (2014). Synthesis and in vitro stability of amino acid prodrugs of 6- β -naltrexol for microneedle-enhanced transdermal delivery. *Bioorganic & Medicinal Chemistry Letters* 24: 5212-5215.

Erdoş EG, Skidgel RA (1989). Neutral endopeptidase 24.11 (enkephalinase) and related regulators of peptide hormones. *FASEB Journal* 3: 145-151.

Fahnoe DC, Knapp J, Johnson GD, Ahn K (2000a). Inhibitor potencies and substrate preference for endothelin-converting enzyme-1 are dramatically affected by pH. *Journal of Cardiovascular Pharmacology* 36: S22-25.

Fahnoe DC, Johnson GD, Herman SB, Ahn K (2000b). Disulfide bonds in Big ET-1 are essential for the specific cleavage at the Trp(21)-Val(22) bond by soluble endothelin converting enzyme-1 from baculovirus/insect cells. *Archives of Biochemistry and Biophysics* 373: 385-393.

Ferguson SS, Downey WE, 3rd, Colapietro AM, Barak LS, Menard L, Caron MG (1996). Role of β -arrestin in mediating agonist-promoted G protein-coupled receptor internalization. *Science* 271: 363-366.

Ferguson SSG (2001). Evolving concepts in G protein-coupled receptor endocytosis: The role in receptor desensitization and signalling. *Pharmacological Reviews* 53: 1-24.

Fernandez N, Monczor F, Baldi A, Davio C, Shayo C (2008). Histamine H₂ receptor trafficking: Role of arrestin, dynamin, and clathrin in histamine H₂ receptor internalization. *Molecular Pharmacology* 74: 1109-1118.

Ferre S, Casado V, Devi LA, Filizola M, Jockers R, Lohse MJ, *et al.* (2014). G protein-coupled receptor oligomerization revisited: Functional and pharmacological perspectives. *Pharmacological Reviews* 66: 413-434.

Fields GB, Noble RL (1990). Solid phase peptide synthesis utilizing 9-fluorenylmethoxycarbonyl amino acids. *International Journal of Peptide Research and Therapeutics* 35: 161-214.

Flinn N, Coppard S, Toth I (1996). Oral absorption studies of lipidic conjugates of thyrotropin releasing hormone (TRH) and luteinizing hormone-releasing hormone (LHRH). *International Journal of Pharmaceutics* 137: 33-39.

Fredriksson R, Lagerstrom MC, Lundin LG, Schioth HB (2003). The G protein-coupled receptors in the human genome form five main families. Phylogenetic analysis, paralogon groups, and fingerprints. *Molecular Pharmacology* 63: 1256-1272.

Fujii R, Hosoya M, Fukusumi S, Kawamata Y, Habata Y, Hinuma S, *et al.* (2000). Identification of Neuromedin U as the cognate ligand of the orphan G protein-coupled receptor FM-3. *Journal of Biological Chemistry* 275: 21068-21074.

Fujita T, Kawahara I, Quan YS, Hattori K, Takenaka K, Muranishi S, *et al.* (1998). Permeability characteristics of tetragastrins across intestinal membranes using the CACO-2 monolayer system: Comparison between acylation and application of protease inhibitors. *Pharmacological Reviews* 15: 1387-1392.

Fukuda M, Gotoh I, Adachi M, Gotoh Y, Nishida E (1997). A novel regulatory mechanism in the mitogen-activated protein (MAP) kinase cascade. Role of nuclear export signal of map kinase kinase. *Journal of Biological Chemistry* 272: 32642-32648.

Funes S, Hedrick JA, Yang S, Shan L, Bayne M, Monsma FJ, Jr., *et al.* (2002). Cloning and characterization of murine Neuromedin U receptors. *Peptides* 23: 1607-1615.

Gan HK, Walker F, Burgess AW, Rigopoulos A, Scott AM, Johns TG (2007). The epidermal growth factor receptor (EGFR) tyrosine kinase inhibitor AG1478 increases the formation of inactive untethered EGFR dimers. Implications for combination therapy with monoclonal antibody 806. *Journal of Biological Chemistry* 282: 2840-2850.

Garcia L, Garcia F, Llorens F, Unzeta M, Itarte E, Gomez N (2002). Pp1/pp2A phosphatases inhibitors okadaic acid and calyculin a block ERK5 activation by growth factors and oxidative stress. *FEBS Letters* 523: 90-94.

Garland AM, Grady EF, Lovett M, Vigna SR, Frucht MM, Krause JE, *et al.* (1996). Mechanisms of desensitization and resensitization of G protein-coupled neurokinin1 and neurokinin2 receptors. *Molecular Pharmacology* 49: 438-446.

Gartlon J, Szekeres P, Pullen M, Sarau HM, Aiyar N, Shabon U, *et al.* (2004). Localisation of NMUR1 and NMUR2 in human and rat central nervous system and effects of Neuromedin-U following central administration in rats. *Psychopharmacology (Berl)* 177: 1-14.

Germack R, Dickenson JM (2004). Characterization of ERK1/2 signalling pathways induced by adenosine receptor subtypes in newborn rat cardiomyocytes. *British Journal Pharmacology* 141: 329-339.

Gesty-Palmer D, Chen M, Reiter E, Ahn S, Nelson CD, Wang S, *et al.* (2006). Distinct β -arrestin- and G protein-dependent pathways for parathyroid hormone receptor-stimulated ERK1/2 activation. *Journal of Biological Chemistry* 281: 10856-10864.

Ghosh M, Schonbrunn A (2011). Differential temporal and spatial regulation of somatostatin receptor phosphorylation and dephosphorylation. *Journal of Biological Chemistry* 286: 13561-13573.

Gilman AG (1987). G-proteins - transducers of receptor-generated signals. *Annual Review of Biochemistry* 56: 615-649.

Goldsmith ZG, Dhanasekaran DN (2007). G-protein regulation of MAPK networks. *Oncogene* 26: 3122-3142.

Grady E, Bohm S, McConalogue K, Garland A, Ansel J, Olerud J, *et al.* (1997). Mechanisms attenuating cellular responses to neuropeptides: Extracellular degradation of ligands and desensitization of receptors. *Journal of Investigative Dermatology Symposium Proceedings* 2: 69-75.

Grady EF, Garland AM, Gamp PD, Lovett M, Payan DG, Bunnett NW (1995). Delineation of the endocytic pathway of substance P and its seven-transmembrane domain nk1 receptor. *Molecular Biological Cell* 6: 509-524.

Granados ME, Soriano E, SaavedraMolina A (1997). Use of pluronic acid F-127 with Fluo-3/AM probe to determine intracellular calcium changes elicited in bean protoplasts. *Phytochemical Analysis* 8: 204-208.

Gray JA, Sheffler DJ, Bhatnagar A, Woods JA, Hufeisen SJ, Benovic JL, *et al.* (2001). Cell-type specific effects of endocytosis inhibitors on 5-hydroxytryptamine_{2A} receptor desensitization and resensitization reveal an arrestin-, GRK2-, and GRK5-independent mode of regulation in human embryonic kidney 293 cells. *Molecular Pharmacology* 60: 1020-1030.

Gros C, Souque A, Schwartz JC, Duchier J, Cournot A, Baumer P, *et al.* (1989). Protection of atrial natriuretic factor against degradation: Diuretic and natriuretic responses after in vivo inhibition of enkephalinase (EC 3.4.24.11) by acetorphan. *Proceedings of the National Academy of Sciences of the United States of America* 86: 7580-7584.

Gschwind A, Zwick E, Prenzel N, Leserer M, Ullrich A (2001). Cell communication networks: Epidermal growth factor receptor transactivation as the paradigm for interreceptor signal transmission. *Oncogene* 20: 1594-1600.

Guan XM, Yu H, Jiang Q, Van Der Ploeg LH, Liu Q (2001). Distribution of Neuromedin U receptor subtype 2 mRNA in the rat brain. *Brain Research Gene Expression Patterns* 1: 1-4.

Gudermann T, Grosse R, Schultz G (2000). Contribution of receptor/G protein signalling to cell growth and transformation. *Naunyn-Schmiedeberg's Archives of Pharmacology* 361: 345-362.

Guo FF, Kumahara E, Saffen D (2001). A calDAG-GEFI/Rap1/B-Raf cassette couples M₁ muscarinic acetylcholine receptors to the activation of ERK1/2. *Journal of Biological Chemistry* 276: 25568-25581.

Hadjiivanova N, Flint N, Evans WH, Dix C, Cooke BA (1984). Endocytosis of β -adrenergic ligands by rat liver. Comparison of β -adrenergic receptor and adenylate cyclase distribution in endosome and plasma-membrane fractions. *Biochemical Journal* 222: 749-754.

Haigler HT, Maxfield FR, Willingham MC, Pastan I (1980). Dansylcadaverine inhibits internalization of ¹²⁵I-epidermal growth factor in BALB 3T3 cells. *Journal of Biological Chemistry* 255: 1239-1241.

Hainerova I, Torekov SS, Ek J, Finkova M, Borch-Johnsen K, Jorgensen T, *et al.* (2006). Association between Neuromedin U gene variants and overweight and obesity. *Journal of Clinical Endocrinology and Metabolism* 91: 5057-5063.

Hanada R, Teranishi H, Pearson JT, Kurokawa M, Hosoda H, Fukushima N, *et al.* (2004). Neuromedin U has a novel anorexigenic effect independent of the leptin signalling pathway. *Natur Medicine* 10: 1067-1073.

Hanada T, Date Y, Shimbara T, Sakihara S, Murakami N, Hayashi Y, *et al.* (2003). Central actions of Neuromedin U via corticotropin-releasing hormone. *Biochemical and Biophysical Research Communications* 311: 954-958.

Harris JM, Chess RB (2003). Effect of PEGylation on pharmaceuticals. *Nature reviews drug discovery* 2: 214-221.

Hasdemir B, Mahajan S, Bunnett NW, Liao M, Bhargava A (2012). Endothelin-converting enzyme-1 actions determine differential trafficking and signalling of corticotropin-releasing factor receptor 1 at high agonist concentrations. *Molecular Endocrinology* 26: 681-695.

Hashimoto T, Kurosawa K, Sakura N (1995). Structure-activity-relationships of Neuromedin-U .2. Highly potent analogs substituted or modified at the N-terminus of Neuromedin-U-8. *Chemical and Pharmaceutical Bulletin (Tokyo)* 43: 1154-1157.

Hashimoto T, Masui H, Uchida Y, Sakura N, Okimura K (1991). Agonistic and antagonistic activities of Neuromedin-U-8 analogs substituted with glycine or d-amino-acid on contractile activity of chicken CROP smooth-muscle preparations. *Chemical and Pharmaceutical Bulletin (Tokyo)* 39: 2319-2322.

Haugh JM, Schooler K, Wells A, Wiley HS, Lauffenburger DA (1999). Effect of epidermal growth factor receptor internalization on regulation of the phospholipase C- γ_1 signalling pathway. *Journal of Biological Chemistry* 274: 8958-8965.

Hawes BE, Luttrell LM, vanBiesen T, Lefkowitz RJ (1996). Phosphatidylinositol 3-kinase is an early intermediate in the G $\beta\gamma$ -mediated mitogen-activated protein kinase signalling pathway. *Journal of Biological Chemistry* 271: 12133-12136.

Hawes BE, van Biesen T, Koch WJ, Luttrell LM, Lefkowitz RJ (1995). Distinct pathways of G $_i$ - and G $_q$ -mediated mitogen-activated protein kinase activation. *Journal of Biological Chemistry* 270: 17148-17153.

Heding A, Elling CE, Schwartz TW (2002). Novel method for the study of receptor Ca $^{2+}$ signalling exemplified by the NK1 receptor. *Journal of Receptors and Signal Transduction* 22: 241-252.

Hedrick JA, Morse K, Shan L, Qiao X, Pang L, Wang S, *et al.* (2000). Identification of a human gastrointestinal tract and immune system receptor for the peptide Neuromedin U. *Molecular Pharmacology* 58: 870-875.

Higashiyama S, Nanba D (2005). ADAM-mediated ectodomain shedding of HB-EGF in receptor cross-talk. *Biochimica et Biophysica Acta-Proteins and Proteomics* 1751: 110-117.

Hilal-Dandan R, Urasawa K, Brunton LL (1992). Endothelin inhibits adenylate cyclase and stimulates phosphoinositide hydrolysis in adult cardiac myocytes. *Journal of Biological Chemistry* 267: 10620-10624.

Hilal-Dandan R, Merck DT, Lujan JP, Brunton LL (1994). Coupling of the type a endothelin receptor to multiple responses in adult rat cardiac myocytes. *Molecular Pharmacology* 45: 1183-1190.

Hoang MV, Turner AJ (1997). Novel activity of endothelin-converting enzyme: Hydrolysis of bradykinin. *Biochemical Journal* 327: 23-26.

Hökfelt T, Bartfai T, Bloom F (2003). Neuropeptides: Opportunities for drug discovery. *The Lancet Neurology* 2: 463-472.

Hosoya M, Moriya T, Kawamata Y, Ohkubo S, Fujii R, Matsui H, *et al.* (2000). Identification and functional characterization of a novel subtype of Neuromedin U receptor. *Journal of Biological Chemistry* 275: 29528-29532.

Hou Y, Delamere NA (2000). Studies on H⁺-ATPase in cultured rabbit nonpigmented ciliary epithelium. *The Journal of Membrane Biology* 173: 67-72.

Houslay MD (2006). A RSK(y) relationship with promiscuous PKA. *Science's STKE* 349: pe32.

Howard AD, Wang RP, Pong SS, Mellin TN, Strack A, Guan XM, *et al.* (2000). Identification of receptors for Neuromedin U and its role in feeding. *Nature* 406: 70-74.

Hsu SH, Luo CW (2007). Molecular dissection of G protein preference using Gas chimeras reveals novel ligand signalling of GPCRs. *American Journal of Physiology-Endocrinology and Metabolism* 293: 1021-1029.

Huang J, Chen S, Zhang JJ, Huang XY (2013). Crystal structure of oligomeric β 1-adrenergic G protein-coupled receptors in ligand-free basal state. *Nature Structure Molecular Biology* 20: 419-425.

Hunter AR, Turner AJ (2006). Expression and localization of endothelin-converting enzyme-1 isoforms in human endothelial cells. *Experimental Biology and Medicine (Maywood, N.J.)* 231: 718-725.

Huotari J, Helenius A (2011). Endosome maturation. *EMBO Journal* 30: 3481-3500.

Ida T, Mori K, Miyazato M, Murakami N, Kangawa K, Kojima M (2006). Neuromedin S is a novel anorexigenic neuropeptide. *Regulatory Peptides* 135: 130-130.

Ida T, Mori K, Miyazato M, Egi Y, Abe S, Nakahara K, *et al.* (2005). Neuromedin S is a novel anorexigenic hormone. *Endocrinology* 146: 4217-4223.

Ikegawa R, Matsumura Y, Tsukahara Y, Takaoka M, Morimoto S (1990). Phosphoramidon, a metalloproteinase inhibitor, suppresses the secretion of endothelin-1 from cultured endothelial cells by inhibiting a Big endothelin-1 converting enzyme. *Biochemical and Biophysical Research Communications* 171: 669-675.

Ingallinella P, Peier AM, Poci A, Marco AD, Desai K, Zytko K, *et al.* (2012). PEGylation of Neuromedin U yields a promising candidate for the treatment of obesity and diabetes. *Bioorganic and Medicinal Chemistry* 20: 4751-4759.

Inglese J, Koch WJ, Touhara K, Lefkowitz RJ (1995). G_{βγ} interactions with pH domains and Ras-MAPK signalling pathways. *Trends in Biochemical Sciences* 20: 151-156.

Irannejad R, von Zastrow M (2014). GPCR signalling along the endocytic pathway. *Current Opinion in Cell Biology* 27: 109-116.

Ishimaru F, Mari B, Shipp MA (1997). The type 2 CD10/neutral endopeptidase 24.11 promoter: Functional characterization and tissue-specific regulation by CBF/NF-Y isoforms. *Blood* 89: 4136-4145.

Iwasaki H, Eguchi S, Ueno H, Marumo F, Hirata Y (1999). Endothelin-mediated vascular growth requires p42/p44 mitogen-activated protein kinase and p70 s6 kinase cascades via transactivation of epidermal growth factor receptor. *Endocrinology* 140: 4659-4668.

Jacob C, Cottrell GS, Gehringer D, Schmidlin F, Grady EF, Bunnett NW (2005). C-Cbl mediates ubiquitination, degradation, and down-regulation of human protease-activated receptor 2. *Journal of Biological Chemistry* 280: 16076-16087.

Jacoby E, Bouhelal R, Gerspacher M, Seuwen K (2006). The 7TM G protein-coupled receptor target family. *Chemmedchem* 1: 760-782.

Jethwa PH, Small CJ, Smith KL, Seth A, Darch SJ, Abbott CR, *et al.* (2005). Neuromedin U has a physiological role in the regulation of food intake and partially mediates the effects of leptin. *American Journal of Physiology-Endocrinology and Metabolism* 289: E301-E305.

Jethwa PH, Smith KL, Small CJ, Abbott CR, Darch SJ, Murphy KG, *et al.* (2006). Neuromedin U partially mediates leptin-induced hypothalamo-pituitary adrenal (HPA) stimulation and has a physiological role in the regulation of the HPA axis in the rat. *Endocrinology* 147: 2886-2892.

Jiang W, Bond JS (1992). Families of metalloendopeptidases and their relationships. *FEBS letters* 312: 110-114.

Johnson EN, Appelbaum ER, Carpenter DC, Cox RF, Disa J, Foley JJ, *et al.* (2004). Neuromedin U elicits cytokine release in murine TH2-type t cell clone d10.G4.1. *Journal Immunology* 173: 7230-7238.

Johnson GL, Dhanasekaran N (1989). The G-protein family and their interaction with receptors. *Endocrine Reviews* 10: 317-331.

Jones NA, Morton MF, Prendergast CE, Powell GL, Shankley NP, Hollingsworth SJ (2006). Neuromedin U stimulates contraction of human long saphenous vein and gastrointestinal smooth muscle in vitro. *Regulatory Peptides* 136: 109-116.

Jordan JD, Carey KD, Stork PJ, Iyengar R (1999). Modulation of Rap activity by direct interaction of G α (o) with Rap1 GTPase-activating protein. *Journal of Biological Chemistry* 274: 21507-21510.

Kaczmarek P, Malendowicz LK, Pruszyńska-Oszmerek E, Wojciechowicz T, Szczepankiewicz D, Szkudelski T, *et al.* (2006). Neuromedin U receptor 1 expression in the rat endocrine pancreas and evidence suggesting Neuromedin U suppressive effect on insulin secretion from isolated rat pancreatic islets. *International Journal Molecular Medicine* 18: 951-955.

Kaczmarek P, Malendowicz LK, Fabis M, Ziolkowska A, Pruszyńska-Oszmerek E, Sassek M, *et al.* (2009). Does somatostatin confer insulinostatic effects of Neuromedin U in the rat pancreas? *Pancreas* 38: 208-212.

Kang S, Watanabe M, Jacobs JC, Yamaguchi M, Dahesh S, Nizet V, *et al.* (2015). Synthesis of mevalonate- and fluorinated mevalonate prodrugs and their in vitro human plasma stability. *European Journal Medicine Chemistry* 90: 448-461.

Kangawa K, Minamino N, Fukuda A, Matsuo H (1983). Neuromedin k: A novel mammalian tachykinin identified in porcine spinal cord. *Biochemical and Biophysical Research Communications* 114: 533-540.

Kawai T, Shibata A, Kurosawa K, Sato Y, Kato S, Ohki K, *et al.* (2006). Structure-activity relationships of Neuromedin U. V. Study on the stability of porcine Neuromedin U-8 at the C-terminal asparagine amide under mild alkaline and acidic conditions. *Chemical and Pharmaceutical Bulletin (Tokyo)* 54: 659-664.

Keeble JE (2009). Re-sensitization of neuropeptide receptors: Should we stop the recycling? *British Journal of Pharmacology* 156: 728-728.

Ketterer K, Kong B, Frank D, Giese NA, Bauer A, Hoheisel J, *et al.* (2009). Neuromedin U is overexpressed in pancreatic cancer and increases invasiveness via the hepatocyte growth factor c-MET pathway. *Cancer Letters* 277: 72-81.

Kilpatrick LE, Humphrys LJ, Holliday ND (2015). A G protein-coupled receptor dimer imaging assay reveals selectively modified pharmacology of Neuropeptide Y y1/y5 receptor heterodimers. *Molecular Pharmacology* 87: 718-732.

Kilpatrick LE, Briddon SJ, Hill SJ, Holliday ND (2010). Quantitative analysis of Neuropeptide Y receptor association with β -arrestin2 measured by bimolecular fluorescence complementation. *British Journal of Pharmacology* 160: 892-906.

Kim JH, Kim JH, Song WK, Kim JH, Chun JS (2000). Sphingosine 1-phosphate activates ERK-1/-2 by transactivating epidermal growth factor receptor in rat-2 cells. *International Union of Biochemistry and Molecular Biology Life* 50: 119-124.

King M-J (1994). Blood group antigens on human erythrocytes-distribution, structure and possible functions. *Biochimica et Biophysica Acta (BBA) - Reviews on Biomembranes* 1197: 15-44.

Klavdieva MM (1996). The history of neuropeptides III. *Frontiers in Neuroendocrinology* 17: 155-179.

Koch WJ, Hawes BE, Allen LF, Lefkowitz RJ (1994). Direct evidence that G_i -coupled receptor stimulation of mitogen-activated protein-kinase is mediated by $G\beta\gamma$ activation of p21(Ras). *Proceedings of the National Academy of Sciences of the United States of America* 91: 12706-12710.

Koenig JA, Edwardson JM (1997). Endocytosis and recycling of G protein-coupled receptors. *Trends in Pharmacology Science* 18: 276-287.

Kojima M, Haruno R, Nakazato M, Date Y, Murakami N, Hanada R, *et al.* (2000). Purification and identification of Neuromedin U as an endogenous ligand for an orphan receptor GPR66 (FM3). *Biochemical and Biophysical Research Communications* 276: 435-438.

Kolch W, Heidecker G, Kochs G, Hummel R, Vahidi H, Mischak H, *et al.* (1993). Protein kinase C α activates Raf-1 by direct phosphorylation. *Nature* 364: 249-252.

Kramer HK, Onoprishvili I, Andria ML, Hanna K, Sheinkman K, Haddad LB, *et al.* (2002). Delta opioid activation of the mitogen-activated protein kinase cascade does not require transphosphorylation of receptor tyrosine kinases. *BMC Pharmacology* 2: 5.

Kranenburg O, Verlaan I, Hordijk PL, Moolenaar WH (1997). Gi-mediated activation of the Ras/MAP kinase pathway involves a 100 KDA tyrosine-phosphorylated GRB2 SH3 binding protein, but not Src nor Shc. *EMBO Journal* 16: 3097-3105.

Krueger KM, Daaka Y, Pitcher JA, Lefkowitz RJ (1997). The role of sequestration in G protein-coupled receptor resensitization. Regulation of β_2 -adrenergic receptor dephosphorylation by vesicular acidification. *Journal of Biological Chemistry* 272: 5-8.

Kukkola PJ, Savage P, Sakane Y, Berry JC, Bilci NA, Ghai RD, *et al.* (1995). Differential structure-activity relationships of phosphoramidon analogues for inhibition of three metalloproteases: Endothelin-converting enzyme, neutral endopeptidase, and angiotensin-converting enzyme. *Journal of Cardiovascular Pharmacology* 26: S65-68.

Lalo U, Allsopp RC, Mahaut-Smith MP, Evans RJ (2010). P2X₁ receptor mobility and trafficking; regulation by receptor insertion and activation. *Journal Neurochemistry* 113: 1177-1187.

Laporte SA, Oakley RH, Zhang J, Holt JA, Ferguson SS, Caron MG, *et al.* (1999). The β_2 -adrenergic receptor/ β -arrestin complex recruits the clathrin adaptor AP-2 during endocytosis. *Proceedings of the National Academy of Sciences of the United States of America* 96: 3712-3717.

Laroche-Joubert N, Marsy S, Michelet S, Imbert-Teboul M, Doucet A (2002). Protein kinase A-independent activation of ERK and h,k-ATPase by cAMP in native kidney cells: Role of EPAC i. *Journal of Biological Chemistry* 277: 18598-18604.

Laurent M, Alain B, Eric E, Rina M, Olivier V, Pierre C, *et al.* (2003). Heterodimerization of endothelin-converting enzyme-1 isoforms regulates the subcellular distribution of this metalloprotease. *Journal of Biological Chemistry* 278: 545-555.

Lefkowitz RJ, Shenoy SK (2005). Transduction of receptor signals by β -arrestins. *Science* 308: 512-517.

Lenormand P, Sardet C, Pages G, L'Allemain G, Brunet A, Pouyssegur J (1993). Growth factors induce nuclear translocation of MAP kinases (p42MAPK and p44MAPK) but not of their activator MAP kinase kinase (p45MAPKK) in fibroblasts. *Journal of Cell Biology* 122: 1079-1088.

Leroy D, Missotten M, Waltzinger C, Martin T, Scheer A (2007). G protein-coupled receptor-mediated ERK1/2 phosphorylation: Towards a generic sensor of GPCR activation. *Journal of Receptors and Signal Transduction* 27: 83-97.

Leserer M, Gschwind A, Ullrich A (2000). Epidermal growth factor receptor signal transactivation. *International Union of Biochemistry and Molecular Biology Life* 49: 405-409.

Lev S, Moreno H, Martinez R, Canoll P, Peles E, Musacchio JM, *et al.* (1995). Protein-tyrosine kinase PYK2 involved in Ca^{2+} -induced regulation of ion-channel and map kinase functions. *Nature* 376: 737-745.

Levitzki A, Gazit A (1995). Tyrosine kinase inhibition - an approach to drug development. *Science* 267: 1782-1788.

Lewy DS, Gauss CM, Soenen DR, Boger DL (2002). Fostriecin: Chemistry and biology. *Current Medicinal Chemistry* 9: 2005-2032.

Li N, Hill KS, Elferink LA (2008). Analysis of receptor tyrosine kinase internalization using flow cytometry. *Methods in Molecular Biology* 457: 305-317.

Liu JJ, Payza K, Huang J, Liu RF, Chen TM, Coupal M, *et al.* (2009). Discovery and pharmacological characterization of a small-molecule antagonist at Neuromedin U receptor NMUR2. *Journal of Pharmacology and Experimental Therapeutics* 330: 268-275.

Lo G, Legon S, Austin C, Wallis S, Wang Z, Bloom SR (1992). Characterization of complementary DNA encoding the rat Neuromedin U precursor. *Molecular Endocrinology* 6: 1538-1544.

Lohse MJ, Benovic JL, Caron MG, Lefkowitz RJ (1990). Multiple pathways of rapid β_2 -adrenergic receptor desensitization. Delineation with specific inhibitors. *Journal of Biological Chemistry* 265: 3202-3211.

Lorenz W, Inglese J, Palczewski K, Onorato JJ, Caron MG, Lefkowitz RJ (1991). The receptor kinase family: Primary structure of rhodopsin kinase reveals similarities to the β -adrenergic receptor kinase. *Proceedings of the National Academy of Sciences of the United States of America* 88: 8715-8719.

Lu Z, Xu S (2006). ERK1/2 MAP kinases in cell survival and apoptosis. *International Union of Biochemistry and Molecular Biology Life* 58: 621-631.

Lumb KJ, DeCarr LB, Milardo LF, Mays MR, Buckholz TM, Fisk SE, *et al.* (2007). Novel selective Neuropeptide Y2 receptor PEGylated peptide agonists reduce food intake and body weight in mice. *Journal of Biological Chemistry* 50: 2264-2268.

Luo J, Busillo JM, Benovic JL (2008). M₃ muscarinic acetylcholine receptor-mediated signalling is regulated by distinct mechanisms. *Molecular Pharmacology* 74: 338-347.

Luttrell DK, Luttrell LM (2003). Signalling in time and space: G protein-coupled receptors and mitogen-activated protein kinases. *Assay and Drug Development Technologies* 1: 327-338.

Luttrell LM (2002). Activation and targeting of mitogen-activated protein kinases by G protein-coupled receptors. *Canadian Journal of Physiology and Pharmacology* 80: 375-382.

Luttrell LM (2003). 'Location, location, location': Activation and targeting of MAP kinases by G protein-coupled receptors. *Journal of Molecular Endocrinology* 30: 117-126.

Luttrell LM, Lefkowitz RJ (2002). The role of β -arrestins in the termination and transduction of G protein-coupled receptor signals. *Journal of Cell Science* 115: 455-465.

Luttrell LM, Daaka Y, Lefkowitz RJ (1999a). Regulation of tyrosine kinase cascades by G protein-coupled receptors. *Current Opinions in Cell Biology* 11: 177-183.

Luttrell LM, Hawes BE, Touhara K, van Biesen T, Koch WJ, Lefkowitz RJ (1995). Effect of cellular expression of pleckstrin homology domains on Gi-coupled receptor signalling. *Journal of Biological Chemistry* 270: 12984-12989.

Luttrell LM, Hawes BE, van Biesen T, Luttrell DK, Lansing TJ, Lefkowitz RJ (1996). Role of c-Src tyrosine kinase in G protein-coupled receptor- and $G_{\beta\gamma}$ subunit-mediated activation of mitogen-activated protein kinases. *Journal of Biological Chemistry* 271: 19443-19450.

Luttrell LM, Roudabush FL, Choy EW, Miller WE, Field ME, Pierce KL, *et al.* (2001). Activation and targeting of extracellular signal-regulated kinases by β -arrestin scaffolds. *Proceedings of the National Academy of Sciences of the United States of America* 98: 2449-2454.

Luttrell LM, Ferguson SS, Daaka Y, Miller WE, Maudsley S, Della Rocca GJ, *et al.* (1999b). β -arrestin-dependent formation of β 2 adrenergic receptor-Src protein kinase complexes. *Science* 283: 655-661.

Luzio JP, Bright NA, Pryor PR (2007). The role of calcium and other ions in sorting and delivery in the late endocytic pathway. *Biochemical Society Transactions* 35: 1088-1091.

Lyons J, Landis CA, Harsh G, Vallar L, Grunewald K, Feichtinger H, *et al.* (1990). Two G protein oncogenes in human endocrine tumors. *Science* 249: 655-659.

Macdonald SG, Crews CM, Wu L, Driller J, Clark R, Erikson RL, *et al.* (1993). Reconstitution of the Raf-1-MEK-ERK signal transduction pathway in vitro. *Molecular Cell Biology* 13: 6615-6620.

Macia E, Ehrlich M, Massol R, Boucrot E, Brunner C, Kirchhausen T (2006). Dynasore, a cell-permeable inhibitor of dynamin. *Developmental Cell* 10: 839-850.

MacLeod MJ, Dahiyat MT, Cumming A, Meiklejohn D, Shaw D, St Clair D (1999). No association between Glu/Asp polymorphism of NOS3 gene and ischemic stroke. *Neurology* 53: 418-420.

Madsen K, Knudsen LB, Agersoe H, Nielsen PF, Thogersen H, Wilken M, *et al.* (2007). Structure-activity and protraction relationship of long-acting glucagon-like peptide-1 derivatives: Importance of fatty acid length, polarity, and bulkiness. *Journal of Medical Chemistry* 50: 6126-6132.

Maity B, Sheff D, Fisher RA (2013). Immunostaining: Detection of signalling protein location in tissues, cells and subcellular compartments. *Methods in Cell Biology* 113: 81-105.

Marchese A, Paing MM, Temple BRS, Trejo J (2008). G protein-coupled receptor sorting to endosomes and lysosomes. *Annual Reviews of Pharmacology and Toxicology* 48: 601-629.

Marinissen MJ, Gutkind JS (2001). G protein-coupled receptors and signalling networks: Emerging paradigms. *Trends in Pharmacology Science* 22: 368-376.

Marsh DJ PA, Bednarek MA, Bianchi E, Ingallinella P, Peier AM, Neuromedin, U Receptor Agonists and Uses Thereof. [EP 1 999 143 B1] e--, Patent. RT (2011). Neuromedin U receptor agonists and uses thereof.

Martin NP, Lefkowitz RJ, Shenoy SK (2003). Regulation of V₂ vasopressin receptor degradation by agonist-promoted ubiquitination. *Journal of Biological Chemistry* 278: 45954-45959.

Maruyama K, Konno N, Ishiguro K, Wakasugi T, Uchiyama M, Shioda S, *et al.* (2008). Isolation and characterisation of four cDNAs encoding Neuromedin U (NMU) from the brain and gut of goldfish, and the inhibitory effect of a deduced NMU on food intake and locomotor activity. *Journal of Neuroendocrinology* 20: 71-78.

Maruyama K, Kaiya H, Miyazato M, Konno N, Wakasugi T, Uchiyama M, *et al.* (2011). Isolation and characterisation of two cDNAs encoding the Neuromedin U receptor from goldfish brain. *Journal of Neuroendocrinology* 23: 282-291.

Matsumura Y, Hisaki K, Takaoka M, Morimoto S (1990). Phosphoramidon, a metalloproteinase inhibitor, suppresses the hypertensive effect of Big endothelin-1. *European Journal of Pharmacology* 185: 103-106.

Maxfield FR, Yamashiro DJ (1987). Endosome acidification and the pathways of receptor-mediated endocytosis. *Advances in Experimental Medicine and Biology* 225: 189-198.

McArdle C (2003). G protein-coupled receptor signalling in neuroendocrine systems - foreword. *Journal of Molecular Endocrinology* 30: 85-86.

McCluskey A, Sakoff JA (2001). Small molecule inhibitors of serine/threonine protein phosphatases. *Mini Reviews in Medicine Chemistry* 1: 43-55.

Mellman I, Fuchs R, Helenius A (1986). Acidification of the endocytic and exocytic pathways. *Annual Reviews in Biochemistry* 55: 663-700.

Micewicz ED, Bahattab OS, Willars GB, Waring AJ, Navab M, Whitelegge JP, *et al.* (2015). Small lipidated anti-obesity compounds derived from Neuromedin U. *European journal of Medicinal Chemistry* 101: 616-626.

Millar RP, Newton CL (2010). The year in G protein-coupled receptor research. *Molecular Endocrinology* 24: 261-274.

Miller WE, Maudsley S, Ahn S, Khan KD, Luttrell LM, Lefkowitz RJ (2000). β -arrestin1 interacts with the catalytic domain of the tyrosine kinase c-Src. Role of β -arrestin1-dependent targeting of c-Src in receptor endocytosis. *Journal of Biological Chemistry* 275: 11312-11319.

Minamino N, Kangawa K, Matsuo H (1983). Neuromedin B: A novel bombesin-like peptide identified in porcine spinal cord. *Biochemical and Biophysical Research Communications* 114: 541-548.

Minamino N, Kangawa K, Matsuo H (1984a). Neuromedin C: A bombesin-like peptide identified in porcine spinal cord. *Biochemical and Biophysical Research Communications* 119: 14-20.

Minamino N, Kangawa K, Matsuo H (1985). Neuromedin-U-8 and Neuromedin-U-25 - novel uterus stimulating and hypertensive peptides identified in porcine spinal-cord. *Biochemical and Biophysical Research Communications* 130: 1078-1085.

Minamino N, Kangawa K, Fukuda A, Matsuo H (1984b). Neuromedin I: A novel mammalian tachykinin identified in porcine spinal cord. *Neuropeptides* 4: 157-166.

Minamino N, Kangawa K, Honzawa M, Matsuo H (1988). Isolation and structural determination of rat Neuromedin U. *Biochemical and Biophysical Research Communications* 156: 355-360.

Minelli A, Brecha NC, Karschin C, Debiasi S, Conti F (1995). GAT-1, a high-affinity GABA plasma-membrane transporter, is localized to neurons and astroglia in the cerebral-cortex. *Journal of Neuroscience* 15: 7734-7746.

Mitchell JD, Maguire JJ, Kuc RE, Davenport AP (2009). Expression and vasoconstrictor function of anorexigenic peptides Neuromedin U-25 and S in the human cardiovascular system. *Cardiovascular Research* 81: 353-361.

Mitsui H, Takuwa N, Kurokawa K, Exton JH, Takuwa Y (1997). Dependence of activated G α 12-induced G1 to S phase cell cycle progression on both Ras/mitogen-activated protein kinase and Ras/Rac1/Jun N-terminal kinase cascades in NIH₃T₃ fibroblasts. *Journal of Biological Chemistry* 272: 4904-4910.

Mochizuki N, Ohba Y, Nagashima K, Endo A, Matsuda M (2000). Activation of the ERK/MAPK pathway by an isoform of Rap1Gap associated with G α i. *Circulation* 102: 353-353.

Mochizuki N, Ohba Y, Kiyokawa E, Kurata T, Murakami T, Ozaki T, *et al.* (1999). Activation of the ERK/MAPK pathway by an isoform of Rap1Gap associated with G α i. *Nature* 400: 891-894.

Mollenhauer HH, Morre DJ, Rowe LD (1990). Alteration of intracellular traffic by monensin; mechanism, specificity and relationship to toxicity. *Biochimica et Biophysica Acta* 1031: 225-246.

Monami M, Dicembrini I, Marchionni N, Rotella CM, Mannucci E (2012). Effects of glucagon-like peptide-1 receptor agonists on body weight: A meta-analysis. *Experimental Diabetes Research*: 672658.

Moore CA, Milano SK, Benovic JL (2007). Regulation of receptor trafficking by GRKs and arrestins. *Annual Reviews Physiology* 69: 451-482.

Moore RH, Sadovnikoff N, Hoffenberg S, Liu SB, Woodford P, Angelides K, *et al.* (1995). Ligand-stimulated β ₂-adrenergic receptor internalization via the constitutive endocytic pathway into Rab5-containing endosomes. *Journal of Cell Science* 108: 2983-2991.

Mori K, Miyazato M, Ida T, Murakami N, Serino R, Ueta Y, *et al.* (2005). Identification of Neuromedin S and its possible role in the mammalian circadian oscillator system. *EMBO Journal* 24: 325-335.

Mori M, Mori K, Ida T, Sato T, Kojima M, Miyazato M, *et al.* (2012). Different distribution of Neuromedin S and its mRNA in the rat brain: NmS peptide is present not only in the hypothalamus as the mRNA, but also in the brainstem. *Frontiers in Endocrinology (Lausanne)* 3: 152.

Moriyama M, Matsukawa A, Kudoh S, Takahashi T, Sato T, Kano T, *et al.* (2006a). The neuropeptide Neuromedin U promotes Il-6 production from macrophages and endotoxin shock. *Biochemical and Biophysical Research Communications* 341: 1149-1154.

Moriyama M, Fukuyama S, Inoue H, Matsumoto T, Sato T, Tanaka K, *et al.* (2006b). The neuropeptide Neuromedin U activates eosinophils and is involved in allergen-induced eosinophilia. *American Journal of Physiology. Lung Cellular and Molecular Physiology* 290: L971-977.

Moriyama M, Sato T, Inoue H, Fukuyama S, Teranishi H, Kangawa K, *et al.* (2005). The neuropeptide Neuromedin U promotes inflammation by direct activation of mast cells. *Journal of Experimental Medicine* 202: 217-224.

Morris GE, Nelson CP, Brighton PJ, Standen NB, Challiss RA, Willets JM (2012). Arrestins 2 and 3 differentially regulate ET_A and P2Y₂ receptor-mediated cell signalling and migration in arterial smooth muscle. *American Journal of Physiology-Cell Physiology* 302: C723-734.

Moual HL, Devault A, Roques BP, Crine P, Boileau G (1991). Identification of glutamic acid 646 as a zinc-coordinating residue in endopeptidase-24.11. *Journal of Biological Chemistry* 266: 15670-15674.

Mulkey RM, Zucker RS (1992). Monensin can transport calcium across cell-membranes in a sodium independent fashion in the crayfish *procambarus-clarkii*. *Neuroscience Letters* 143: 115-118.

Muller L, Barret A, Etienne E, Meidan R, Valdenaire O, Corvol P, *et al.* (2003). Heterodimerization of endothelin-converting enzyme-1 isoforms regulates the subcellular distribution of this metalloprotease. *Journal of Biological Chemistry* 278: 545-555.

Mullershausen F, Zecri F, Cetin C, Billich A, Guerini D, Seuwen K (2009). Persistent signalling induced by FTY720-phosphate is mediated by internalized S1P1 receptors. *Nature Chemical Biology* 5: 954-954.

Mundell SJ, Barton JF, Mayo-Martin MB, Hardy AR, Poole AW (2008). Rapid resensitization of purinergic receptor function in human platelets. *Journal of Thrombosis and Haemostasis* 6: 1393-1404.

Murphy JE, Roosterman D, Cottrell GS, Padilla BE, Feld M, Brand E, *et al.* (2011). Protein phosphatase 2A mediates resensitization of the neurokinin 1 receptor. *American Journal of Physiology-cell Physiology* 301: C780-C791.

Murphy R, Turner CA, Furness JB, Parker L, Giraud A (1990). Isolation and microsequence analysis of a novel form of Neuromedin U from guinea pig small intestine. *Peptides* 11: 613-617.

Nakahara K, Katayama T, Maruyama K, Ida T, Mori K, Miyazato M, *et al.* (2010). Comparison of feeding suppression by the anorexigenic hormones Neuromedin U and Neuromedin S in rats. *Journal of Endocrinology* 207: 185-193.

Nakahara K, Hanada R, Murakami N, Teranishi H, Ohgusu H, Fukushima N, *et al.* (2004). The gut-brain peptide Neuromedin U is involved in the mammalian circadian oscillator system. *Biochemical and Biophysical Research Communications* 318: 156-161.

Nakazato M, Hanada R, Murakami N, Date Y, Mondal MS, Kojima M, *et al.* (2000). Central effects of Neuromedin U in the regulation of energy homeostasis. *Biochemical and Biophysical Research Communications* 277: 191-194.

Nandha KA, Benito-Orfila MA, Jamal H, Akinsanya KO, Bloom SR, Smith DM (1999). Effect of steroids and the estrous cycle on uterine Neuromedin U receptor expression. *Peptides* 20: 1203-1209.

Nassar-Gentina V, Rojas E, Luxoro M (1994). Rise in cytoplasmic Ca²⁺ induced by monensin in bovine medullary chromaffin cells. *Cell Calcium* 16: 475-480.

Nassel DR (2002). Neuropeptides in the nervous system of drosophila and other insects: Multiple roles as neuromodulators and neurohormones. *Progress in Neurobiology* 68: 1-84.

Nassel DR (2009). Neuropeptide signalling near and far: How localized and timed is the action of neuropeptides in brain circuits? *Invert Neuroscience* 9: 57-75.

Nelson CD, Perry SJ, Regier DS, Prescott SM, Topham MK, Lefkowitz RJ (2007). Targeting of diacylglycerol degradation to M₁ muscarinic receptors by β -arrestins. *Science* 315: 663-666.

Neuner P, Peier AM, Talamo F, Ingallinella P, Lahm A, Barbato G, *et al.* (2014). Development of a Neuromedin U-human serum albumin conjugate as a long-acting candidate for the treatment of obesity and diabetes. Comparison with the PEGylated peptide. *Journal of Peptide Science* 20: 7-19.

Niimi M, Murao K, Taminato T (2001). Central administration of Neuromedin U activates neurons in ventrobasal hypothalamus and brainstem. *Endocrine* 16: 201-206.

Nixon JS, Bishop J, Bradshaw D, Davis PD, Hill CH, Elliott LH, *et al.* (1992). The design and biological properties of potent and selective inhibitors of protein kinase C. *Biochemical Society Transactions* 20: 419-425.

Noriaki E, Masashi Y (1995). Endothelin-converting enzyme-2 is a membrane-bound, phosphoramidon-sensitive metalloprotease with acidic pH optimum. *Journal of Biological Chemistry* 270: 15262-15268.

Norum JH, Hart K, Levy FO (2003). Ras-dependent ERK activation by the human Gs-coupled serotonin receptors 5-HT_{4b} and 5-HT_{7a}. *Journal of Biological Chemistry* 278: 3098-3104.

Novak CM, Zhang M, Levine JA (2006). Neuromedin u in the paraventricular and arcuate hypothalamic nuclei increases non-exercise activity thermogenesis. *Journal of Neuroendocrinology* 18: 594-601.

O'Harte F, Bockman CS, Abel PW, Conlon JM (1991). Isolation, structural characterization and pharmacological activity of dog Neuromedin U. *Peptides* 12: 11-15.

O'Shea M, Schaffer M (1985). Neuropeptide function: The invertebrate contribution. *Annual Review of Neuroscience* 8: 171-198.

Oakley RH, Laporte SA, Holt JA, Barak LS, Caron MG (1999). Association of β -arrestin with G protein-coupled receptors during clathrin-mediated endocytosis dictates the profile of receptor resensitization. *Journal of Biological Chemistry* 274: 32248-32257.

Oakley RH, Laporte SA, Holt JA, Caron MG, Barak LS (2000). Differential affinities of visual arrestin, β -arrestin1, and β -arrestin2 for G protein-coupled receptors delineate two major classes of receptors. *Journal of Biological Chemistry* 275: 17201-17210.

Oakley RH, Laporte SA, Holt JA, Barak LS, Caron MG (2001). Molecular determinants underlying the formation of stable intracellular G protein-coupled receptor- β -arrestin complexes after receptor endocytosis. *Journal of Biological Chemistry* 276: 19452-19460.

Obara Y, Labudda K, Dillon TJ, Stork PJS (2004). PKA phosphorylation of Src mediates Rap1 activation in NGF and cAMP signalling in PC12 cells. *Journal of Cell Science* 117: 6085-6094.

Offermanns S, Wieland T, Homann D, Sandmann J, Bombien E, Spicher K, *et al.* (1994). Transfected muscarinic acetylcholine receptors selectively couple to G_i -type G proteins and $G_{q/11}$. *Molecular Pharmacology* 45: 890-898.

Ohtsu H, Dempsey PJ, Eguchi S (2006). ADAMs as mediators of EGF receptor transactivation by G protein-coupled receptors. *American Journal of Physiology-Cell Physiology* 291: C1-C10.

Okamoto A, Lovett M, Payan DG, Bunnett NW (1994). Interactions between neutral endopeptidase (EC-3.4.24.11) and the substance P (NK1) receptor expressed in mammalian-cells. *Biochemical Journal* 299: 683-693.

Okazaki M, Ferrandon S, Villardaga JP, Bouxsein ML, Potts JT, Gardella TJ (2008). Prolonged signalling at the parathyroid hormone receptor by peptide ligands targeted to a specific receptor conformation. *Proceedings of the National Academy of Sciences of the United States of America* 105: 16525-16530.

Olson BR, Drutarosky MD, Chow MS, Hruby VJ, Stricker EM, Verbalis JG (1991). Oxytocin and an oxytocin agonist administered centrally decrease food intake in rats. *Peptides* 12: 113-118.

Olson KR, Eglen RM (2007). β galactosidase complementation: A cell-based luminescent assay platform for drug discovery. *Assay and Drug Development Technologies* 5: 137-144.

Ortiz AA, Milardo LF, DeCarr LB, Buckholz TM, Mays MR, Claus TH, *et al.* (2007). A novel long-acting selective Neuropeptide Y2 receptor polyethylene glycol-conjugated peptide agonist reduces food intake and body weight and improves glucose metabolism in rodents. *Journal of Pharmacology and Experimental Therapeutics* 323: 692-700.

Ouedraogo M, Lecat S, Rochdi MD, Hachet-Haas M, Matthes H, Gicquiaux H, *et al.* (2008). Distinct motifs of Neuropeptide Y receptors differentially regulate trafficking and desensitization. *Traffic* 9: 305-324.

Pace AM, Faure M, Bourne HR (1995). G_{i2} -mediated activation of the MAP kinase cascade. *Molecular Biology of the Cell* 6: 1685-1695.

Padilla BE, Cottrell GS, Roosterman D, Pikios S, Muller L, Steinhoff M, *et al.* (2007). Endothelin-converting enzyme-1 regulates endosomal sorting of calcitonin receptor-like receptor and β -arrestins. *Journal of Cell Biology* 179: 981-997.

Palmer TM, Benovic JL, Stiles GL (1995). Agonist-dependent phosphorylation and desensitization of the rat A_3 adenosine receptor. Evidence for a G protein-coupled receptor kinase-mediated mechanism. *Journal of Biological Chemistry* 270: 29607-29613.

Park KS, Li Y, Zhang Y, Gerbes AL, Liu H, Swain MG, *et al.* (2003). Effects of the neutral endopeptidase inhibitor thiorphan on cardiovascular and renal function in cirrhotic rats. *British journal of Pharmacology* 139: 81-88.

Patel TB (2004). Single transmembrane spanning heterotrimeric G protein-coupled receptors and their signalling cascades. *Pharmacological Reviews* 56: 371-385.

Pearson GW, Earnest S, Cobb MH (2006). Cyclic AMP selectively uncouples mitogen-activated protein kinase cascades from activating signals. *Molecular and Cellular Biology* 26: 3039-3047.

Peier A, Kosinski J, Cox-York K, Qian Y, Desai K, Feng Y, *et al.* (2009). The antiobesity effects of centrally administered Neuromedin U and Neuromedin S are mediated predominantly by the Neuromedin U receptor 2 (NMUR2). *Endocrinology* 150: 3101-3109.

Peier AM, Desai K, Hubert J, Du X, Yang L, Qian Y, *et al.* (2011). Effects of peripherally administered Neuromedin U on energy and glucose homeostasis. *Endocrinology* 152: 2644-2654.

Pelayo JC, Poole DP, Steinhoff M, Cottrell GS, Bunnett NW (2011). Endothelin-converting enzyme-1 regulates trafficking and signalling of the neurokinin 1 receptor in endosomes of myenteric neurones. *Journal of Physiology* 589: 5213-5230.

Perlman JH, Wang W, Nussenzveig DR, Gershengorn MC (1995). A disulfide bond between conserved extracellular cysteines in the thyrotropin-releasing-hormone receptor is critical for binding. *Journal of Biological Chemistry* 270: 24682-24685.

Perry SJ, Baillie GS, Kohout TA, McPhee I, Magiera MM, Ang KL, *et al.* (2002). Targeting of cyclic AMP degradation to β_2 -adrenergic receptors by β -arrestins. *Science* 298: 834-836.

Pierce KL, Premont RT, Lefkowitz RJ (2002). Seven-transmembrane receptors. *Nature Reviews Molecular Cell Biology* 3: 639-650.

Pitcher JA, Freedman NJ, Lefkowitz RJ (1998). G protein-coupled receptor kinases. *Annual Review of Biochemistry* 67: 653-692.

Pitcher JA, Payne ES, Csontos C, DePaoli-Roach AA, Lefkowitz RJ (1995). The G protein-coupled receptor phosphatase: A protein phosphatase type 2A with a distinct subcellular distribution and substrate specificity. *Proceedings of the National Academy of Sciences of the United States of America* 92: 8343-8347.

Plotnikov A, Chuderland D, Karamansha Y, Livnah O, Seger R (2011). Nuclear extracellular signal-regulated kinase 1 and 2 translocation is mediated by casein kinase 2 and accelerated by autophosphorylation. *Molecular and Cellular Biology* 31: 3515-3530.

Pollok-Kopp B, Schwarze K, Baradari VK, Oppermann M (2003). Analysis of ligand-stimulated CC chemokine receptor 5 (CCR5) phosphorylation in intact cells using phosphosite-specific antibodies. *Journal of Biological Chemistry* 278: 2190-2198.

Praefcke GJ, McMahon HT (2004). The dynamin superfamily: Universal membrane tubulation and fission molecules? *Nature Reviews in Molecular Cell Biology* 5: 133-147.

Prendergast CE, Morton MF, Figueroa KW, Wu X, Shankley NP (2006). Species-dependent smooth muscle contraction to Neuromedin U and determination of the receptor subtypes mediating contraction using NMU1 receptor knockout mice. *British Journal of Pharmacology* 147: 886-896.

Prenzel N, Zwick E, Daub H, Leserer M, Abraham R, Wallasch C, *et al.* (1999). EGF receptor transactivation by G protein-coupled receptors requires metalloproteinase cleavage of prohb-EGF. *Nature* 402: 884-888.

Preza GC, Ruchala P, Pinon R, Ramos E, Qiao B, Peralta MA, *et al.* (2011). Minihepcidins are rationally designed small peptides that mimic hepcidin activity in mice and may be useful for the treatment of iron overload. *Journal of Clinical Investigation* 121: 4880-4888.

Puente LG, He JS, Ostergaard HL (2006). A novel PKC regulates ERK activation and degranulation of cytotoxic T lymphocytes: Plasticity in PKC regulation of ERK. *European Journal of Immunology* 36: 1009-1018.

Raddatz R, Wilson AE, Artymyshyn R, Bonini JA, Borowsky B, Boteju LW, *et al.* (2000). Identification and characterization of two Neuromedin U receptors differentially expressed in peripheral tissues and the central nervous system. *Journal of Biological Chemistry* 275: 32452-32459.

Radhika V, Dhanasekaran N (2001). Transforming G proteins. *Oncogene* 20: 1607-1614.

Rahman N, Buck J, Levin LR (2013). pH sensing via bicarbonate-regulated "soluble" adenylyl cyclase (sAC). *Frontiers in Physiology* 4: 343.

Ramos E, Ruchala P, Goodnough JB, Kautz L, Preza GC, Nemeth E, *et al.* (2012). Minihepcidins prevent iron overload in a hepcidin-deficient mouse model of severe hemochromatosis. *Blood* 120: 3829-3836.

Raote I, Bhattacharyya S, Panicker MM (2013). Functional selectivity in serotonin receptor 2A (5-HT_{2A}) endocytosis, recycling, and phosphorylation. *Molecular Pharmacology* 83: 42-50.

Rashid AJ, O'Dowd BF, George SR (2004). Minireview: Diversity and complexity of signalling through peptidergic G protein-coupled receptors. *Endocrinology* 145: 2645-2652.

Reiter E, Ahn S, Shukla AK, Lefkowitz RJ (2012). Molecular mechanism of β -arrestin-biased agonism at seven-transmembrane receptors. *Annual Review of Pharmacology and Toxicology* 52: 179-197.

Ren XR, Reiter E, Ahn S, Kim J, Chen W, Lefkowitz RJ (2005). Different G protein-coupled receptor kinases govern G protein and β -arrestin-mediated signalling of V₂ vasopressin receptor. *Proceedings of the National Academy of Sciences of the United States of America* 102: 1448-1453.

Resh MD (2006). Palmitoylation of ligands, receptors, and intracellular signalling molecules. *Science STKE* 359: re14.

Rhee MH, Nevo I, Levy R, Vogel Z (2000). Role of the highly conserved Asp-Arg-Tyr motif in signal transduction of the CB₂ cannabinoid receptor. *FEBS Letters* 466: 300-304.

Riddy DM, Stamp C, Sykes DA, Charlton SJ, Dowling MR (2012). Reassessment of the pharmacology of sphingosine-1-phosphate S1P3 receptor ligands using the discoverx pathhunter (TM) and Ca²⁺release functional assays. *British Journal of Pharmacology* 167: 868-880.

Rinaman L, Baker EA, Hoffman GE, Stricker EM, Verbalis JG (1998). Medullary c-Fos activation in rats after ingestion of a satiating meal. *American Journal of Physiology* 275: R262-268.

Rink R, Arkema-Meter A, Baudoin I, Post E, Kuipers A, Nelemans SA, *et al.* (2010). To protect peptide pharmaceuticals against peptidases. *Journal of Pharmacological and Toxicological Methods* 61: 210-218.

Roosterman D, Cottrell GS, Schmidlin F, Steinhoff M, Bunnett NW (2004). Recycling and resensitization of the neurokinin 1 receptor. Influence of agonist concentration and Rab GTPases. *Journal of Biological Chemistry* 279: 30670-30679.

Roosterman D, Cottrell GS, Padilla BE, Muller L, Eckman CB, Bunnett NW, *et al.* (2007). Endothelin-converting enzyme 1 degrades neuropeptides in endosomes to control receptor recycling. *Proceedings of the National Academy of Sciences of the United States of America* 104: 11838-11843.

Roosterman D, Kempkes C, Cottrell GS, Padilla BE, Bunnett NW, Turck CW, *et al.* (2008). Endothelin-converting enzyme-1 degrades internalized somatostatin-14. *Endocrinology* 149: 2200-2207.

Roques BP, Noble F, Dauge V, Fourniezasuski MC, Beaumont A (1993). Neutral endopeptidase-24.11 - structure, inhibition, and experimental and clinical-pharmacology. *Pharmacological Reviews* 45: 87-146.

Rose RH, Briddon SJ, Holliday ND (2010). Bimolecular fluorescence complementation: Lighting up seven transmembrane domain receptor signalling networks. *British Journal Pharmacology* 159: 738-750.

Rovati GE, Capra V (2014). The dry motif at work: The P2Y₁₂ receptor case. *Journal of Thrombosis and Haemostasis* 12: 713-715.

Rovati GE, Capra V, Neubig RR (2007). The highly conserved DRY motif of class A G protein-coupled receptors: Beyond the ground state. *Molecular Pharmacology* 71: 959-964.

Roy S, Wyse B, Hancock JF (2002). H-Ras signalling and K-Ras signalling are differentially dependent on endocytosis. *Molecular and Cellular Biology* 22: 5128-5140.

Rozenfeld R, Devi LA (2007). Receptor heterodimerization leads to a switch in signalling: β -arrestin2-mediated ERK activation by μ - δ opioid receptor heterodimers. *FASEB Journal* 21: 2455-2465.

Rozengurt E (2011). Neurokinin 1 receptor desensitization and resensitization: Is it all happening at the membrane? Focus on "protein phosphatase 2a mediates resensitization of the neurokinin 1 receptor". *American Journal of Physiology-Cell Physiology* 301: C772-C774.

Rucinski M, Ziolkowska A, Neri G, Trejter M, Zemleduch T, Tyczewska M, *et al.* (2007). Expression of Neuromedins S and U and their receptors in the hypothalamus and endocrine glands of the rat. *International Journal of Molecular Medicine* 20: 255-259.

Saini DK, Kalyanaraman V, Chisari M, Gautam N (2007). A family of G protein $\beta\gamma$ subunits translocate reversibly from the plasma membrane to endomembranes on receptor activation. *Journal of Biological Chemistry* 282: 24099-24108.

Sakamoto T, Mori K, Nakahara K, Miyazato M, Kangawa K, Sameshima H, *et al.* (2007). Neuromedin S exerts an antidiuretic action in rats. *Biochemical and Biophysical Research Communications* 361: 457-461.

Sakamoto T, Mori K, Miyazato M, Kangawa K, Sameshima H, Nakahara K, *et al.* (2008). Involvement of neuromedin s in the oxytocin release response to suckling stimulus. *Biochemical and Biophysical Research Communications* 375: 49-53.

Sakamoto T, Nakahara K, Maruyama K, Katayama T, Mori K, Miyazato M, *et al.* (2011). Neuromedin S regulates cardiovascular function through the sympathetic nervous system in mice. *Peptides* 32: 1020-1026.

Sakura N, Kurosawa K, Hashimoto T (1995). Structure-activity-relationships of Neuromedin-U .1. Contractile activity of dog Neuromedin-U-related peptides on isolated chicken crop smooth-muscle. *Chemical and Pharmaceutical Bulletin (Tokyo)* 43: 1148-1153.

Sakura N, Kurosawa K, Hashimoto T (2000). Structure-activity relationships of neuromedin u. Iv. Absolute requirement of the arginine residue at position 7 of dog Neuromedin U-8 for contractile activity. *Chemical and Pharmaceutical Bulletin (Tokyo)* 48: 1166-1170.

Sato S, Hanada R, Kimura A, Abe T, Matsumoto T, Iwasaki M, *et al.* (2007). Central control of bone remodeling by Neuromedin U. *Nature Medicine* 13: 1234-1240.

Savarese TM, Wang CD, Fraser CM (1992). Site-directed mutagenesis of the rat M1 muscarinic acetylcholine receptor. Role of conserved cysteines in receptor function. *Journal of Biological Chemistry* 267: 11439-11448.

Sawamura T, Kimura S, Shinmi O, Sugita Y, Kobayashi M, Mitsui Y, *et al.* (1990). Characterization of endothelin converting enzyme activities in soluble fraction of bovine cultured endothelial cells. *Biochemical and Biophysical Research Communications* 169: 1138-1144.

Schachter JB, Sromek SM, Nicholas RA, Harden TK (1997). HEK293 human embryonic kidney cells endogenously express the P2Y₁ and P2Y₂ receptors. *Neuropharmacology* 36: 1181-1187.

Schafer B, Gschwind A, Ullrich A (2004). Multiple G protein-coupled receptor signals converge on the epidermal growth factor receptor to promote migration and invasion. *Oncogene* 23: 991-999.

Scheer A, Costa T, Fanelli F, De Benedetti PG, Mhaouty-Kodja S, Abuin L, *et al.* (2000). Mutational analysis of the highly conserved arginine within the Glu/Asp-Arg-Tyr motif of the α_{1b} -adrenergic receptor: Effects on receptor isomerization and activation. *Molecular Pharmacology* 57: 219-231.

Scheerer P, Park JH, Hildebrand PW, Kim YJ, Krauss N, Choe HW, *et al.* (2008). Crystal structure of opsin in its G-protein-interacting conformation. *Nature* 455: 497-502.

Schmidlin F, Dery O, DeFea KO, Slice L, Patierno S, Sternini C, *et al.* (2001). Dynamin and Rab5a-dependent trafficking and signalling of the neurokinin 1 receptor. *Journal of Biological Chemistry* 276: 25427-25437.

Schmidt M, Kroger B, Jacob E, Seulberger H, Subkowski T, Otter R, *et al.* (1994). Molecular characterization of human and bovine endothelin converting enzyme (ECE-1). *FEBS Letters* 356: 238-243.

Schonwasser DC, Marais RM, Marshall CJ, Parker PJ (1998). Activation of the mitogen-activated protein kinase/extracellular signal-regulated kinase pathway by conventional, novel, and atypical protein kinase C isotypes. *Molecular and Cellular Biology* 18: 790-798.

Schramm NL, Limbird LE (1999). Stimulation of mitogen-activated protein kinase by G protein-coupled α_2 -adrenergic receptors does not require agonist-elicited endocytosis. *Journal of Biological Chemistry* 274: 24935-24940.

Schwartz JC, Gros C, Lecomte JM, Bralet J (1990). Enkephalinase (EC 3.4.24.11) inhibitors: Protection of endogenous ANF against inactivation and potential therapeutic applications. *Life Science* 47: 1279-1297.

Schweizer A, Valdenaire O, Nelböck P, Deuschle U, Dumas Milne Edwards JB, Stumpf JG, *et al.* (1997). Human endothelin-converting enzyme (ECE-1): Three isoforms with distinct subcellular localizations. *The Biochemical Journal* 328 : 871-877.

Seachrist JL, Ferguson SSG (2003). Regulation of G protein-coupled receptor endocytosis and trafficking by Rab gtpases. *Life Science* 74: 225-235.

Shah BH, Neithardt A, Chu DB, Shah FB, Catt KJ (2006). Role of EGF receptor transactivation in phosphoinositide 3-kinase-dependent activation of MAP kinase by GPCRs. *Journal of Cellular Physiology* 206: 47-57.

Shah BH, Yesilkaya A, Olivares-Reyes JA, Chen HD, Hunyady L, Catt KJ (2004). Differential pathways of angiotensin II-induced extracellularly regulated kinase 1/2 phosphorylation in specific cell types: Role of heparin-binding epidermal growth factor. *Molecular Endocrinology* 18: 2035-2048.

Shan LX, Qiao XD, Crona JH, Behan J, Wang S, Laz T, *et al.* (2000). Identification of a novel Neuromedin U receptor subtype expressed in the central nervous system. *Journal of Biological Chemistry* 275: 39482-39486.

Sharman JL, Mpamhanga CP, Spedding M, Germain P, Staels B, Dacquet C, *et al.* (2011). IUPHAR-DB: New receptors and tools for easy searching and visualization of pharmacological data. *Nucleic Acids Research* 39: D534-D538.

Shetzline SE, Rallapalli R, Dowd KJ, Zou S, Nakata Y, Swider CR, *et al.* (2004). Neuromedin U: A Myb-regulated autocrine growth factor for human myeloid leukemias. *Blood* 104: 1833-1840.

Shimada K, Takahashi M, Ikeda M, Tanzawa K (1995). Identification and characterization of two isoforms of an endothelin-converting enzyme-1. *FEBS Letters* 371: 140-144.

Shivakumar BR, Wang Z, Hammond TG, Harris RC (2005). Ep24.15 interacts with the angiotensin II type I receptor and bradykinin B₂ receptor. *Cell Biochemistry and Function* 23: 195-204.

Shousha S, Nakahara K, Miyazato M, Kangawa K, Murakami N (2005). Endogenous Neuromedin U has anorectic effects in the Japanese quail. *General and Comparative Endocrinology* 140: 156-163.

Sibley DR, Lefkowitz RJ (1985). Molecular mechanisms of receptor desensitization using the β -adrenergic receptor-coupled adenylate cyclase system as a model. *Nature* 317: 124-129.

Sibley DR, Strasser RH, Benovic JL, Daniel K, Lefkowitz RJ (1986). Phosphorylation/dephosphorylation of the β -adrenergic receptor regulates its functional coupling to adenylate cyclase and subcellular distribution. *Proceedings of the National Academy of Sciences of the United States of America* 83: 9408-9412.

Simaan M, Bedard-Goulet S, Fessart D, Gratton JP, Laporte SA (2005). Dissociation of β -arrestin from internalized bradykinin B₂ receptor is necessary for receptor recycling and resensitization. *Cell Signal* 17: 1074-1083.

Skidgel RA, Engelbrecht S, Johnson AR, Erdos EG (1984). Hydrolysis of substance P and neurotensin by converting enzyme and neutral endopeptidase. *Peptides* 5: 769-776.

Soltoff SP (1998). Related adhesion focal tyrosine kinase and the epidermal growth factor receptor mediate the stimulation of mitogen-activated protein kinase by the G protein-coupled P2Y₂ receptor. Phorbol ester or [Ca²⁺]_i elevation can substitute for receptor activation. *Journal of Biological Chemistry* 273: 23110-23117.

Stern KA, Smit GDV, Place TL, Winistorfer S, Piper RC, Lill NL (2007). Epidermal growth factor receptor fate is controlled by HRS tyrosine phosphorylation sites that regulate HRS degradation. *Molecular and Cellular Biology* 27: 888-898.

Stevens RC, Cherezov V, Katritch V, Abagyan R, Kuhn P, Rosen H, *et al.* (2013). The GPCR network: A large-scale collaboration to determine human GPCR structure and function. *Nature Reviews Drug Discovery* 12: 25-34.

Stork PJS, Schmitt JM (2002). Crosstalk between cAMP and MAP kinase signalling in the regulation of cell proliferation. *Trends in Cell Biology* 12: 258-266.

Strader CD, Fong TM, Tota MR, Underwood D, Dixon RA (1994). Structure and function of G protein-coupled receptors. *Annual Review of Biochemistry* 63: 101-132.

Szekeres PG, Muir AI, Spinage LD, Miller JE, Butler SI, Smith A, *et al.* (2000). Neuromedin U is a potent agonist at the orphan G protein-coupled receptor FM3. *Journal of Biological Chemistry* 275: 20247-20250.

Takai A, Murata M, Torigoe K, Isobe M, Mieskes G, Yasumoto T (1992). Inhibitory effect of okadaic acid derivatives on protein phosphatases. A study on structure-affinity relationship. *Biochemical Journal* 284: 539-544.

Takasaki J, Saito T, Taniguchi M, Kawasaki T, Moritani Y, Hayashi K, *et al.* (2004). A novel Gαq/11-selective inhibitor. *Journal of Biological Chemistry* 279: 47438-47445.

Takayama K, Taguchi A, Yakushiji F, Hayashi Y (2015). Identification of a degrading enzyme in human serum that hydrolyzes a C-terminal core sequence of Neuromedin U. Accepted article, *doi: 10.1002/bip.22770*.

Takayama K, Mori K, Taketa K, Taguchi A, Yakushiji F, Minamino N, *et al.* (2014). Discovery of selective hexapeptide agonists to human Neuromedin U receptors types 1 and 2. *Journal of Medicinal Chemistry* 57: 6583-6593.

Takayama K, Mori K, Sohma Y, Taketa K, Taguchi A, Yakushiji F, *et al.* (2015). Discovery of potent hexapeptide agonists to human Neuromedin U receptor 1 and identification of their serum metabolites. *ACS Medicinal Chemistry Letters* 6: 302-307.

Tan CP, McKee KK, Liu Q, Palyha OC, Feighner SD, Hreniuk DL, *et al.* (1998). Cloning and characterization of a human and murine T-cell orphan G protein-coupled receptor similar to the growth hormone secretagogue and neurotensin receptors. *Genomics* 52: 223-229.

Tan Y, Xiao PG, Koizumi S, Conlon JM, Rennard SI, Mayhan WG, *et al.* (1992). Role of peptidases in bradykinin-induced increase in vascular-permeability *in vivo*. *Circulation Research* 70: 952-959.

Tang WJ, Gilman AG (1991). Type-specific regulation of adenylyl cyclase by G protein $\beta\gamma$ subunits. *Science* 254: 1500-1503.

Tang WJ, Gilman AG (1992). Adenylyl cyclases. *Cell* 70: 869-872.

Tobin AB (2008). G-protein-coupled receptor phosphorylation: Where, when and by whom. *British Journal of Pharmacology* 153: S167-S176.

Tohgo A, Choy EW, Gesty-Palmer D, Pierce KL, Laporte S, Oakley RH, *et al.* (2003). The stability of the G protein-coupled receptor- β -arrestin interaction determines the mechanism and functional consequence of ERK activation. *Journal of Biological Chemistry* 278: 6258-6267.

Tohgo AK, Pierce KL, Choy EW, Lefkowitz RJ, Luttrell LM (2002). β -arrestin scaffolding of the ERK cascade enhances cytosolic ERK activity but inhibits ERK-mediated transcription following angiotensin AT_{1A} receptor stimulation. *Journal of Biological Chemistry* 277: 9429-9436.

Tong J, Du GG, Chen SR, MacLennan DH (1999). HEK-293 cells possess a carbachol- and thapsigargin-sensitive intracellular Ca²⁺ store that is responsive to stop-flow medium changes and insensitive to caffeine and ryanodine. *Biochemical Journal* 343: 39-44.

Toullec D, Pianetti P, Coste H, Bellevergue P, Grandperret T, Ajakane M, *et al.* (1991). The bisindolylmaleimide GF-109203x is a potent and selective inhibitor of protein-kinase-C. *Journal of Biological Chemistry* 266: 15771-15781.

Trejter M, Neri G, Rucinski M, Majchrzak M, Nussdorfer GG, Malendowicz LK (2008). Neuromedin-U stimulates enucleation-induced adrenocortical regeneration in the rat. *International Journal of Molecular Medicine* 21: 683-687.

Tsao P, Cao T, von Zastrow M (2001). Role of endocytosis in mediating downregulation of G protein-coupled receptors. *Trends in Pharmacological Sciences* 22: 91-96.

Tsygankova OM, Kupperman E, Wen W, Meinkoth JL (2000). Cyclic AMP activates Ras. *Oncogene* 19: 3609-3615.

Turner AJ, Murphy LJ (1996). Molecular pharmacology of endothelin converting enzymes. *Biochemical Pharmacology* 51: 91-102.

Turner AJ, Isaac RE, Coates D (2001). The neprilysin (NEP) family of zinc metalloendopeptidases: Genomics and Function. *Bioessays* 23: 261-269.

Ueda Y, Hirai S, Osada S, Suzuki A, Mizuno K, Ohno S (1996). Protein kinase C activates the MEK-ERK pathway in a manner independent of Ras and dependent on Raf. *Journal of Biological Chemistry* 271: 23512-23519.

Umekawa K, Hasegawa H, Tsutsumi Y, Sato K, Matsumura Y, Ohashi N (2000). Pharmacological characterization of a novel sulfonylureid-pyrazole derivative, SM-19712, a potent nonpeptidic inhibitor of endothelin converting enzyme. *Japanese Journal of Pharmacology* 84: 7-15.

Valdenaire O, Lepailleur-Enouf D, Egidy G, Thouard A, Barret A, Vranckx R, *et al.* (1999). A fourth isoform of endothelin-converting enzyme (ECE-1) is generated from an additional promoter molecular cloning and characterization. *European Journal of Biochemistry* 264: 341-349.

Valentin-Hansen L, Groenen M, Nygaard R, Frimurer TM, Holliday ND, Schwartz TW (2012). The arginine of the DRY motif in transmembrane segment III functions as a balancing micro-switch in the activation of the β_2 -adrenergic receptor. *Journal of Biological Chemistry* 287: 31973-31982.

Van Biesen T, Luttrell LM, Hawes BE, Lefkowitz RJ (1996a). Mitogenic signalling via G protein-coupled receptors. *Endocrine Reviews* 17: 698-714.

Van Biesen T, Hawes BE, Raymond JR, Luttrell LM, Koch WJ, Lefkowitz RJ (1996b). G_o-protein α -subunits activate mitogen-activated protein kinase via a novel protein kinase C-dependent mechanism. *Journal of Biological Chemistry* 271: 1266-1269.

Vemulapalli S, Chiu PJ, Chintala M, Bernardino V (1993). Attenuation of ischemic acute renal failure by phosphoramidon in rats. *Pharmacology* 47: 188-193.

Vigna SR (1999). Phosphorylation and desensitization of the neurokinin-1 receptor expressed in epithelial cells. *Journal of Neurochemistry* 73: 1925-1932.

Vigo E, Roa J, Lopez M, Castellano JM, Fernandez-Fernandez R, Navarro VM, et al. (2007). Neuromedin S as novel putative regulator of luteinizing hormone secretion. *Endocrinology* 148: 813-823.

Villardaga JP, Jean-Alphonse FG, Gardella TJ (2014). Endosomal generation of cAMP in GPCR signalling. *Nature Chemical Biology* 10: 700-706.

Violin JD, Lefkowitz RJ (2007). β -arrestin-biased ligands at seven-transmembrane receptors. *Trends in Pharmacological Science* 28: 416-422.

Volmat V, Pouyssegur J (2001). Spatiotemporal regulation of the p42/p44 MAPK pathway. *Biology of the Cell* 93: 71-79.

Von Kriegsheim A, Pitt A, Grindlay GJ, Kolch W, Dhillon AS (2006). Regulation of the Raf-MEK-ERK pathway by protein phosphatase 5. *Nature Cell Biology* 8: 1011-U1102.

Voyno-Yasenetskaya TA, Faure MP, Ahn NG, Bourne HR (1996). G α 12 and G α 13 regulate extracellular signal-regulated kinase and c-Jun kinase pathways by different mechanisms in COS-7 cells. *Journal of Biological Chemistry* 271: 21081-21087.

Wacker D, Wang C, Katritch V, Han GW, Huang XP, Vardy E, *et al.* (2013). Structural features for functional selectivity at serotonin receptors. *Science* 340: 615-619.

Walsh AH, Cheng AY, Honkanen RE (1997). Fostriecin, an antitumor antibiotic with inhibitory activity against serine/threonine protein phosphatases types 1 (PP1) and 2A (PP2A), is highly selective for PP2A. *FEBS Letters* 416: 230-234.

Wan Y, Huang XY (1998). Analysis of the Gs/mitogen-activated protein kinase pathway in mutant S49 cells. *Journal of Biological Chemistry* 273: 14533-14537.

Wang F, Zhang Y, Jiang X, Zhang L, Gong S, Liu C, *et al.* (2011). Neuromedin U inhibits t-type Ca²⁺ channel currents and decreases membrane excitability in small dorsal root ganglia neurons in mice. *Cell Calcium* 49: 12-22.

Wang Q, Zhao JL, Brady AE, Feng J, Allen PB, Lefkowitz RJ, *et al.* (2004). Spinophilin blocks arrestin actions in vitro and in vivo at G protein-coupled receptors. *Science* 304: 1940-1944.

Wang YJ, Zhou YX, Szabo K, Haft CR, Trejo J (2002). Down-regulation of protease-activated receptor-1 is regulated by sorting nexin 1. *Molecular Biology of the Cell* 13: 1965-1976.

Wang ZP, Dillon TJ, Pokala V, Mishra S, Labudda K, Hunter B, *et al.* (2006). Rap1-mediated activation of extracellular signal-regulated kinases by cyclic AMP is dependent on the mode of Rap1 activation. *Molecular and Cellular Biology* 26: 2130-2145.

Waters CM, Connell MC, Pyne S, Pyne NJ (2005). C-Src is involved in regulating signal transmission from PDGF receptor-GPCRs complexes in mammalian cells. *Cell Signal* 17: 263-277.

Watts AO, Verkaar F, van der Lee MM, Timmerman CA, Kuijper M, van Offenbeek J, *et al.* (2013). β -arrestin recruitment and G protein signalling by the atypical human chemokine decoy receptor CCX-CKR. *Journal of Biological Chemistry* 288: 7169-7181.

Wehbi VL, Stevenson HP, Feinstein TN, Calero G, Romero G, Vilardaga JP (2013). Noncanonical GPCR signalling arising from a PTH receptor-arrestin-G $\beta\gamma$ complex. *Proceedings of the National Academy of Sciences of the United States of America* 110: 1530-1535.

Wehrman TS, Casipit CL, Gewertz NM, Blau HM (2005). Enzymatic detection of protein translocation. *Nature Methods* 2: 521-527.

Wei H, Ahn S, Shenoy SK, Karnik SS, Hunyady L, Luttrell LM, *et al.* (2003). Independent β -arrestin 2 and G protein-mediated pathways for angiotensin II activation of extracellular signal-regulated kinases 1 and 2. *Proceedings of the National Academy of Sciences of the United States of America* 100: 10782-10787.

Weissman JT, Ma JN, Essex A, Gao Y, Burstein ES (2004). G protein-coupled receptor-mediated activation of Rap GTPases: Characterization of a novel G α i regulated pathway. *Oncogene* 23: 241-249.

Westfall TD, McCafferty GP, Pullen M, Gruver S, Sulpizio AC, Aiyar VN, *et al.* (2002). Characterization of Neuromedin U effects in canine smooth muscle. *Journal of Pharmacology and Experimental Therapeutics* 301: 987-992.

Widmann C, Dolci W, Thorens B (1997). Internalization and homologous desensitization of the GLP-1 receptor depend on phosphorylation of the receptor carboxyl tail at the same three sites. *Molecular Endocrinology* 11: 1094-1102.

Wilbanks AM, Laporte SA, Bohn LM, Barak LS, Caron MG (2002). Apparent loss-of-function mutant GPCRs revealed as constitutively desensitized receptors. *Biochemistry* 41: 11981-11989.

Wirth A, Benyo Z, Lukasova M, Leutgeb B, Wettschureck N, Gorbey S, *et al.* (2008). G12-G13-LARG-mediated signalling in vascular smooth muscle is required for salt-induced hypertension. *Nature Medicine* 14: 64-68.

Wootten D, Savage EE, Willard FS, Bueno AB, Sloop KW, Christopoulos A, *et al.* (2013). Differential activation and modulation of the glucagon-like peptide-1 receptor by small molecule ligands. *Molecular Pharmacology* 83: 822-834.

Wren AM, Small CJ, Abbott CR, Jethwa PH, Kennedy AR, Murphy KG, *et al.* (2002). Hypothalamic actions of Neuromedin U. *Endocrinology* 143: 4227-4234.

Wu J, Dent P, Jelinek T, Wolfman A, Weber MJ, Sturgill TW (1993). Inhibition of the EGF-activated MAP kinase signalling pathway by adenosine 3',5'-monophosphate. *Science* 262: 1065-1069.

Wunderlich L, Farago A, Buday L (1999). Characterization of interactions of NCK with SOS and dynamin. *Cell Signal* 11: 25-29.

Xu D, Emoto N, Giaid A, Slaughter C, Kaw S, Dewit D, *et al.* (1994). ECE-1 - a membrane-bound metalloprotease that catalyzes the proteolytic activation of Big endothelin-1. *Cell* 78: 473-485.

Yamaguchi H, Kodama H, Osada S, Kato F, Jelokhani-Niaraki M, Kondo M (2003). Effect of α,α -dialkyl amino acids on the protease resistance of peptides. *Bioscience Biotechnology and Biochemistry* 67: 2269-2272.

Yamasaki-Mann M, Demuro A, Parker I (2009). cADPR stimulates SERCA activity in xenopus oocytes. *Cell calcium* 45: 293-299.

Yanagisawa M, Kurihara H, Kimura S, Tomobe Y, Kobayashi M, Mitsui Y, *et al.* (1988). A novel potent vasoconstrictor peptide produced by vascular endothelial cells. *Nature* 332: 411-415.

Yang G, Su J, Yao Y, Lei Z, Zhang G, Liu Y, *et al.* (2012). Distribution of Neuromedin S and its receptor NMU2R in pigs. *Research in Veterinary Science* 92: 180-186.

Yang SD, Fong YL, Benovic JL, Sibley DR, Caron MG, Lefkowitz RJ (1988). Dephosphorylation of the β_2 -adrenergic receptor and rhodopsin by latent phosphatase 2. *Journal of Biological Chemistry* 263: 8856-8858.

Yoon S, Seger R (2006). The extracellular signal-regulated kinase: Multiple substrates regulate diverse cellular functions. *Growth Factors* 24: 21-44.

Yu R, Hinkle PM (1997). Effect of cell type on the subcellular localization of the thyrotropin-releasing hormone receptor. *Molecular Pharmacology* 51: 785-793.

Yuan LY, Wang J, Shen WC (2005). Reversible lipidization prolongs the pharmacological effect, plasma duration, and liver retention of octreotide. *Pharmaceutical research* 22: 220-227.

Zen K, Biwersi J, Periasamy N, Verkman AS (1992). Second messengers regulate endosomal acidification in swiss 3T3 fibroblasts. *Journal of Cell Biology* 119: 99-110.

Zeng H, Gragerov A, Hohmann JG, Pavlova MN, Schimpf BA, Xu H, *et al.* (2006). Neuromedin U receptor 2-deficient mice display differential responses in sensory perception, stress, and feeding. *Molecular and Cellular Biology* 26: 9352-9363.

Zhang J, Barak LS, Winkler KE, Caron MG, Ferguson SS (1997). A central role for β -arrestins and clathrin-coated vesicle-mediated endocytosis in β_2 -adrenergic receptor resensitization. Differential regulation of receptor resensitization in two distinct cell types. *Journal of Biological Chemistry* 272: 27005-27014.

Zhang J, Ferguson SS, Law PY, Barak LS, Caron MG (1999). Agonist-specific regulation of δ -opioid receptor trafficking by G protein-coupled receptor kinase and β -arrestin. *Journal of Receptors and Signal Transduction* 19: 301-313.

Zhang L, Bulaj G (2012). Converting peptides into drug leads by lipidation. *Current Medicinal Chemistry* 19: 1602-1618.

Zhang Y, Skolnick J (2004). Automated structure prediction of weakly homologous proteins on a genomic scale'. *Proceedings of the National Academy of Sciences of the United States of America* 101: 7594-7599.

Zhang Y, DeVries ME, Skolnick J (2006). Structure modeling of all identified G protein-coupled receptors in the human genome. *PLoS Computational Biology* 2: 88-99.

Zhang Y, Jiang D, Zhang J, Wang F, Jiang X, Tao J (2010). Activation of Neuromedin U type 1 receptor inhibits l-type Ca²⁺ channel currents via phosphatidylinositol 3-kinase-dependent protein kinase C epsilon pathway in mouse hippocampal neurons. *Cell Signal* 22: 1660-1668.

Zheng H, Loh HH, Law PY (2008). β -arrestin-dependent mu-opioid receptor-activated extracellular signal-regulated kinases (ERKs) translocate to nucleus in contrast to G protein-dependent ERK activation. *Molecular Pharmacology* 73: 178-190.

Zhong M, Yang M, Sanborn BM (2003). Extracellular signal-regulated kinase 1/2 activation by myometrial oxytocin receptor involves $G\alpha_q$ $\beta\gamma$ and epidermal growth factor receptor tyrosine kinase activation. *Endocrinology* 144: 2947-2956.

Zhong Q, Lazar CS, Tronchere H, Sato T, Meerloo T, Yeo M, *et al.* (2002). Endosomal localization and function of sorting nexin 1. *Proceedings of the National Academy of Sciences of the United States of America* 99: 6767-6772.

Zhu X, Jiang M, Birnbaumer L (1998). Receptor-activated Ca²⁺ influx via human TRP3 stably expressed in human embryonic kidney (HEK)293 cells. Evidence for a non-capacitative Ca²⁺ entry. *Journal of Biological Chemistry* 273: 133-142.

Ziolkowska A, Macchi C, Trejter M, Rucinski M, Nowak M, Nussdorfer GG, *et al.* (2008). Effects of Neuromedin-U on immature rat adrenocortical cells: In vitro and in vivo studies. *International Journal of Molecular Medicine* 21: 303-307.

Zolnierowicz S (2000). Type 2A protein phosphatase, the complex regulator of numerous signalling pathways. *Biochemical Pharmacology* 60: 1225-1235.

Zwick E, Daub H, Aoki N, Yamaguchi-Aoki Y, Tinhofer I, Maly K, *et al.* (1997). Critical role of calcium- dependent epidermal growth factor receptor transactivation in PC12 cell membrane depolarization and bradykinin signalling. *Journal of Biological Chemistry* 272: 24767-24770.